Performance of Narrow Tillage Tools with

Inertial and Strain Rate Effects

A Thesis submitted to the College of Graduate Studies and Research

in Partial Fulfillment of the Requirements of the Degree of Doctor of Philosophy

in the Department of Agricultural and Bioresource Engineering

University of Saskatchewan

by

Uriel Aparecido Rosa

March 1997

Canada

UNIVERSITY OF SASKATCHEWAN
COLLEGE OF GRADUATE STUDIES AND RESEARCH

Saskatoon

CERTIFICATION OF THESIS WORK

We, the undersigned, certify that **Uriel A. ROSA,** candidate for the degree of Doctor of Philosophy has presented a thesis with the following title: *"Performance of Narrow Tillage Tools With Inertial and Strain Rate Effects"* We consider that the thesis is acceptable in form and content, and that a satisfactory knowledge of the field covered by the thesis was demonstrated by the candidate through an oral examination held on March 10, 1997.

External Examiner: Dr. S.K. Upadhyaya
University of California

Internal Examiners:

for D. Wulfsohn

Abstract

Conservation tillage practices have replaced traditional plowing and conventional seedbed tillage in some dry areas in Western Canada and the USA. The planter or seed drill is an important piece of equipment used in crop production systems. Because of time constraints and large cropped areas, high-speed seeding operations are desirable. However, the increased draft and power requirements associated with high operating speeds are major factors limiting the speeds at which it is feasible to use tillage tools.

Dynamic effects on soil-tool cutting forces are important when operating at elevated speeds. The rate-dependent behaviour of narrow tillage tools was investigated in this study. A 9-m long linear monorail system was developed to carry narrow tools through a linear soil bin at high speeds. Steady-state speeds from 0.5 to 10.0 m/s over 1 to 3 m were attained using this system.

The performance of tools with rectangular, triangular and elliptical cross sections were studied. Experimental measurements showed a linear increase of draft with increasing operating speed, for all tool shapes. Power input per operating depth and soil pulverization also increased with an increase in tool speed. Elliptical, triangular and flat tool shapes presented the lowest to highest draft requirements, respectively.

A hypoelastic soil constitutive relationship with variable Young's modulus and Poisson's ratio was developed to describe the dynamic soil-tool cutting problem. Inertial effects were initially included in the stiffness matrix; however, doing this introduced numerical oscillations, even for small tool displacements (< 1 mm) and therefore this

model was abandoned. As a next step, lumped viscous components were incorporated in the equation of motion (i.e., outside of the stiffness matrix). This reduced the oscillating problem by adding more damping to the system. However, oscillations still occurred at larger tool displacements (1-10 mm) after soil failure started. Using this model, it was possible to simulate tool performance up to the early stages when soil failure started.

A reference tool procedure was proposed to estimate the dynamic soil parameter in the soil model. The procedure used the flat tool as a reference tool and solved the soil constitutive formulation using a finite element numerical scheme in an inverse method to determine the set of damping coefficients. Static model parameters were determined using conventional triaxial compression tests. The determined parameters were than used along with the mathematical model to predict the performance of the triangular tool. Predictions of triangular tool draft produced correct trends but overestimated experimental data. Draft was overpredicted by less than 1% at 2.8 m/s but by 25% at 8.4 m/s tool speed.

Future work should focus on the reference tool concept to predict all soil parameters for the dynamic model. This approach would avoid the need for lab tests using disturbed soil samples and would provide further opportunities for practical application of this technique. A shallow reference tool can be used in the field at different tool speeds to determine parameters of a dynamic soil model. The model would then be used to predict draft forces for other narrow tools running at the same operating depth. Although the topic presented in this thesis is very promising, more studies are required.

Acknowledgments

Dedication

This work is dedicated to my wife Fernanda and my son Gabriel for their love and encouragement.

Table of Contents

List of Figures

List of Tables

List of Symbols

a	parameter determined from triaxial tests (kPa^{-1})
a_l	dimensionless parameter used in the variable Poisson's ratio expression (equation 3.41)
$a_{0...7}$	constants used in the Newmark integration method
A	area (m^2)
A'	soil-metal parameter (equation 2.37)
A_0	initial specimen cross sectional area (m^2)
AN	dynamic soil constant multiplying strain rate difference ($kPa \cdot s$)
b	parameter determined from triaxial tests (kPa^{-1})
b_l	dimensionless parameter used in the variable Poisson's ratio expression (equation 3.41)
B_1 , B_2	geometry-dependent factors
B_s	coefficient of the modified Duncan and Chang soil model (kPa)
B	strain-displacement matrix operator
$\mathbf{B}_L$	linear strain displacement transformation matrix
$\mathbf{B}_{NL}$	non-linear strain displacement transformation matrix
c	soil cohesion (kPa)
C'	soil-metal parameter (equation 2.37)
$C_{1...4}$	soil parameters (equation 2.36)

C_a	soil-metal adhesion (kPa)
C_i^d	dynamic cone index (kPa)
C_{ijkl}	material response function (kPa)
C	constitutive matrix
$_tC$	incremental material property matrix at time t [$F \cdot L^{-2}$]
C_l	damping lumped matrix (kN·s/m)
D	depth of operation (m)
d	tool depth (m)
H	draft (N)
E	Young's modulus of elasticity (kPa)
E_i	initial tangent modulus (kPa)
E_{ij}	Green-Lagrange strain tensor
E_S	tangent modulus with strain rate formulation (kPa)
E_d	input energy rate per operating depth $\left(\dfrac{W}{m}\right)$
E_t	tangent modulus for any stress condition (kPa)
$E(t-s)$	infinitesimal strain tensor
f	yield function
f_i	body force vector [$F \cdot L^{-3}$]
f_p	soil-metal shear effect [$F \cdot L^{-2}$]
$f_s(\sigma_{ij}, h) = 0$	static yield surface
F	vector of nodal point forces equivalent to the element stresses (N)

$\left(\mathbf{F}^{n} - \mathbf{R} \right)$ unbalanced force vector [F]

G Modulus of rigidity [$F \cdot L^{-2}$]

GF_{tool} geometrical tool factor

H_i vertical distances measured from the trace of furrow profile (mm)

h_k interpolation function corresponding to nodal point k

h hardening parameter

I index (equation 2.48)

I_1 first invariant of the stress tensor, σ_{ii} , [$F \cdot L^{-2}$]

$I_1^{'}$ first invariant of the strain tensor, ε_{ii}

J_2 second deviatoric stress invariant [$F \cdot L^{-2}$]

$\mathbf{J}$ Jacobian matrix

K modulus number

K' bulk modulus (kPa)

K_f material parameter used in equation 2.33, (kPa)

$\mathbf{K}$ stiffness matrix [$F \cdot L^{-1}$]

$\overline{\mathbf{K}}$ stiffness matrix including linear and nonlinear effects [$F \cdot L^{-1}$]

$\hat{\mathbf{K}}$ effective stiffness matrix [$F \cdot L^{-1}$]

$\mathbf{K}_L$ linear part of the stiffness matrix [$F \cdot L^{-1}$]

$\mathbf{K}_{NL}$ nonlinear part of the stiffness matrix [$F \cdot L^{-1}$]

$\mathbf{K}_T^0$ initial tangent stiffness matrix [$F \cdot L^{-1}$]

$\mathbf{K}_T^n$ n^{th} tangent stiffness matrix [$F \cdot L^{-1}$]

l	length of specimen during loading (m)
l_0	initial length of specimen [L]
LDL^T	triangularized matrix of the effective stiffness matrix
M	mass matrix (kg)
n	soil exponent (equation 2.23)
n_i	direction cosines of a unit outward normal to dA
N_k	interpolation function corresponding to nodal point k
n'	number of measurements
N	shape function matrix
P	axial load (N)
Δp	pressure change in the chamber during loading (kPa)
p_a	atmospheric pressure (kPa)
P_W	power per unit operating depth $\left(\dfrac{W}{m}\right)$
r'	natural coordinate [L]
R_f	failure ratio (equation 2.24)
r_i	coordinates of the element in the local system [L]
R_i	index quantifying soil disturbance
R	vector of externally applied nodal point loads [F]
$\overline{R}$	total external load vector [F]
$\hat{R}$	effective load matrix [F]
R_0	initial load vector [F]

$\Delta \mathbf{R_0}$	incremental load matrix (N)
$\mathbf{R_b}$	load vector related to body forces [F]
$\mathbf{R_c}$	load vector related to concentrated forces [F]
$\mathbf{R_i}$	load vector related to element inertial forces [F]
$\mathbf{R_s}$	load vector related to surface forces [F]
s	natural coordinate [L]
S	operating speed (m/s)
s'	time (s)
SF	swelling factor
s_i	coordinates of the element in the local system [L]
S_{ij}	2nd Piola-Kirchhoff stress tensor [$F \cdot L^{-2}$]
Sm	mobilized stress strength of the soil
SSF	soil strength factor
t	time [T]
t'	natural coordinate [L]
t_i	coordinates of the element in the local system [L]
t_k	surface force vector [$F \cdot L^{-2}$]
TGF	tine geometrical factor
$\mathbf{T}(t)$	stress tensor [$F \cdot L^{-2}$]
u_i	displacement tensor [L]
u_i^k	displacement at nodal point k with corresponding i direction [L]
$\mathbf{u}$	displacement vector [L]

$\Delta \mathbf{u}$	vector of displacement increment [L]
$\Delta(\Delta \mathbf{u})$	vector of increment of displacement increment [L]
$\dot{\mathbf{u}}$	velocity vector [L·T^{-1}]
$\ddot{\mathbf{u}}$	acceleration vector [L·T^{-2}]
$\mathbf{u_0}$	initial displacement vector [L]
v	instantaneous current speed (m/s)
V	element domain [L^3]
$\Delta V'$	volume change in soil sample during loading (m^3)
v_0	initial set sliding speed (m/s)
V_0'	total volume of air in sample, line and test chamber before loading (m^3)
$\|V\|_2$	Euclidean vector norm
V_b	soil volume before cut (m^3)
V_f	soil volume after cut (m^3)
V_{lo}	element local domain [L^3]
w	tool width (m)
x_1, x_2, x_3	Cartesian coordinates [L]
$^{t+\Delta t}x_l$	coordinates of the body in relation to the axis 1 at configuration t+Δt [L]
x_i	coordinates in the i direction [L]
x_i^k	coordinate at nodal point k with corresponding i direction [L]
$\mathbf{x}$	particle coordinates vector (L)
α	constant in Newmark's integration scheme

$\overset{\cdot}{\alpha}$	material parameter (equation 2.33)
$\alpha_{0..11}$	response coefficients used in equation 2.12.
β	scaling factor
δ	constant of Newmark's integration scheme
$\overset{\cdot}{\delta}$	interface friction angle
$\overset{\cdot}{\delta}$	variation (for instance, $\delta^{\cdot}u_k$ is a variation in the displacement components)
δ_{ij}	Kronecker's delta
$\Delta\varepsilon_t$	incremental strain value in the axial direction
$\Delta\varepsilon_r$	incremental strain value in the radial direction
Δt	time intervals [T]
ε	strain
$\overset{\cdot}{\varepsilon}$	strain rate $[T^{-1}]$
$\overset{\cdot}{\varepsilon}_0$	reference strain rate (T^{-1})
ε_a	true axial strain
ε_{ij}	strain tensor
$\overset{\cdot}{\varepsilon}_{ij}$	total strain rate tensor (T^{-1})
ε_{ij}^e	elastic strain tensor
$\overset{\cdot}{\varepsilon}_{ij}^e$	elastic strain rate tensor (T^{-1})
ε_{ij}^p	plastic strain tensor

$\dot{\varepsilon}_{ij}^{vp}$	viscoplastic strain rate tensor (T^{-1})
ε_r	radial strain
ε_v	volumetric strain
ϕ	soil angle of internal friction
Φ	stress relaxation function
ϕ_a	soil-metal parameter
γ	viscosity $[T^{-1}]$
$\dot{\gamma}$	shear rate $[T^{-1}]$
γ_b	unit density before cut (N / m^3)
γ_f	unit density after cut (N / m^3)
η_{ij}	nonlinear component of the Green-Lagrange strain tensor
λ	Lame's constant $[F{\cdot}L^{-2}]$
μ	material damping $(F{\cdot}T/L)$
ν	Poisson's ratio
ρ	soil bulk density $[M{\cdot}L^{-3}]$
σ	normal stress $[F{\cdot}L^{-2}]$
σ_0	dynamic stress at base strain rate (kPa)
σ_1	major principal stress (kPa)
σ_3	minor principal stress (kPa)
$(\sigma_1 - \sigma_3)_f$	deviatoric stress at failure (kPa)
$(\sigma_1 - \sigma_3)_{f0}$	Mohr-Coulomb failure criteria at a reference strain rate, $\dot{\varepsilon}_0$ (kPa)

$(\sigma_1 - \sigma_3)_{ult}$	ultimate deviatoric stress (kPa)
σ_a	true axial stress (kPa)
σ_{ij}	components of stress tensor (kPa)
$\dot{\sigma}_{ij}$	components of stress rate tensor (kPa·s^{-1})
σ_n	normal stress (kPa)
τ	soil shear stress (kPa)
$\tau^{\prime}$	instantaneous time (s)
τ_0	soil parameter related to the static component of shear strength (kPa)
τ_1	soil parameter related to the dynamic component of shear strength (kPa·s/m)
τ_{ij}	Cauchy's stress tensor (kPa)
τ_f	soil shear strength (kPa)
Ω	linear transformations of the space of symmetric tensors
$\Psi(\varepsilon)$	stress state material parameter (kPa)
Ψ	unit matrix

CHAPTER ONE

INTRODUCTION

1.1   Conservation Tillage Systems

Agricultural crop production systems require proper soil conditioning for adequate plant establishment and growth. Tillage, which is defined as the physical manipulation of soil, is the operation commonly used to transform soil structure according to plant needs. Tillage tools are used to perform such operations. These tools are mechanical devices used to apply forces to the soil to cause some desired effects such as pulverization, cutting, inversion or movement of soil (Gill and Vanden Berg 1968).

The design and operation of tillage tools involve economic and energetic aspects, as well as environmental aspects;

- tillage operations are expensive practices, even though various tool designs and shapes can be manufactured at relatively low cost,

- tillage is traditionally performed at low speeds due to the high forces involved in cutting and turning soil,

- one hectare of land cultivated to a depth of 100 mm has an estimated mass of 1 Gg,

- the time spent tilling is substantial because of machinery's slow working rates,

- capital investments in machinery acquisitions are also high due to the heavy nature of the task.

The cost of energy for producing crops is becoming more important. Efficient operation of tractors and implements is a problem faced by most farmers. Manufacturers need data to assist in the development of more efficient tillage systems (Grisso et al. 1994). There is potential for energy savings by redefining current tillage systems or by redesigning its actual components.

The world is becoming more conscious about environmental damages due to modern farming practices. The degree of soil manipulation varies according to economical and technological aspects. Excessive harrowing accelerates decomposition of crop residues, pulverizes surface aggregates and can increase wind and water erosion. Tillage, beyond that needed for satisfactory weed control on summer fallow, does not increase crop yields (Johnson 1977). Soil conservation programs have been given priorities by governmental research centres. Johnson (1977) stated that conservation tillage research must be given priority in the design of equipment and systems for mechanically handling and retaining crop residue on the land, and for seed and fertilizer placement. The goal of conservation tillage is to provide very little tillage - just that necessary for crops' needs.

Trends in conservation tillage equipment

Many changes in tillage and planting equipment have occurred over the past 15 years. Conservation tillage practices have replaced moldboard plowing and conventional seedbed tillage on a large portion of cropped areas in the North American Prairies. The planter or drill has become a very important piece of equipment used in crop production (Harrigan and Rotz 1994). Furrow openers of a combined seed and fertilizer drill are

2

required to place the seed and fertilizer in the seedbed with the minimum expenditure of energy. Soil disturbance caused by the opener should be the minimum possible to avoid soil water losses and aggravated weed problems (Darmora and Pandey 1995).

Today's soil tillage and seeding practices in the great plains of North America incorporate the use of wide equipment. At the same time, there is a limitation in increasing the power unit. While width of current equipment has already reached an extreme value, the power delivered from tractors could be easily increased. However, the adoption of larger and consequently heavier driving units would cause more compaction of soil. With these limitations, an alternative way of increasing capacity of farm equipment is to increase the speed of operation.

In Saskatchewan, the cultivator has become part of every farmer's operation and is used for weed control. Recently, with the introduction of air seeders, the cultivator is also being used for seeding and deep banding of fertilizer. No-till drills have been introduced for seeding directly into the soil with a minimum of soil disturbance. No-till drills usually use either disc-openers or hoe-openers (University of Saskatchewan 1987). Soil openers are of major importance in conservation tillage equipment. Adequate opener design and proper operation for a wide range of operating speeds is a major goal guiding the present study.

Modeling of soil-tool interaction

Models of soil-tool interaction can be used in the new tool shape designs intended to minimize draft, energy and soil disturbance during tillage.

3

The first problem to be addressed is understanding the behaviour of tillage tools interacting with soil. The field of soil dynamics has been addressing related subjects since the early 1900's. Soil dynamics is defined as the branch of knowledge that considers the motion of soil. More specifically, soil dynamics, a phase of soil science and mechanics concerned with soils in motion, may be defined as the relation between forces applied to the soil and the resultant soil reaction (Gill and Vanden Berg 1968).

When a mechanical device passes through the soil, irreversible and transient phenomena may occur, even when the device is driven at a steady speed (Shibusawa 1992). Soil manipulation, including tillage, planting, and fertilization, is generally a dynamic process in which strain-rate effects on soil stress-strain relations should be considered in analytical modeling (Shen and Kushwaha 1995a). Quasi-static modeling of soil-tool interaction can be acceptable for the low speed range of agricultural operations; however, as the speed is increased, dynamic components have to be incorporated in analytical models. Simplifications in the theory are usually made due to the difficulty in formulating and solving 'real' problems, considering the nonlinearities and dynamics involved. Soil failure around a narrow tillage tool is a three-dimensional problem (McKyes 1985). Because of the complexity, only a few investigators have considered the three-dimensional case and even fewer have considered the dynamic behaviour of the soil (Xie and Zhang 1985). The development of computers and numerical solution methods such as the finite element method make analyses of such complex problems feasible.

Strain-rate effects

Rate effects on the force response of tillage tools such as moldboard plows have been known to be significant since the early 1900's (Wismer and Luth 1972). The power requirement increases rapidly with speed, and soil shattering is usually greater at higher speeds (Scott and Yule 1993). The resistance of a tool also increases with increased speed. The effect of tool speed on forces can be significant. Draft, associated with speed, is a major factor limiting increases in speed of operation. Tool shapes also affect the tool draft. A better design of a tool shape can reduce draft requirements, and high working rates would lead to a reduction in number of operations required to produce a seedbed because of increased soil pulverization.

Draft is an important parameter for measurement and evaluation of implement performance (Grisso et al. 1994). Rational design must be based on a knowledge of tool performance and soil parameters (Stafford 1984). For efficient tillage, both must be considered with the aim of minimizing specific resistance, i.e., draft per unit area of soil disturbance (Godwin et al. 1984). Quantification of force response relations for the soil cutting process can be used by the equipment designer for improving cutting element design, and for mathematically simulating whole vehicle performance (Wismer and Luth 1972). Traditional tools have been designed in the light of empirical experimentation based on low speed tests and quasi-static theory of soil cutting. Experimental results cannot be directly extrapolated for use with high speed tools because the results would be unrealistic.

5

Narrow tillage tools are the main components of conservation tillage equipment. Literature regarding dynamic behaviour of narrow tillage tools is scarce. A better understanding of soil dynamic behaviour will help in the design of new tool shapes which will reduce tool draft and energy demand over a wide speed range. At the same time, narrow tools disturb less soil, ideally only the minimum necessary to establish a crop. Measurement of draft and energy requirements of tools tested over a wide range of speeds should indicate optimum working speeds.

1.2 Objectives

The objectives of this study are as follows:

1) To design, construct and test an experimental setup to measure narrow tool performance, including tool reaction forces and corresponding instantaneous speeds over a large operating speed range.

2) To develop a model to predict dynamic soil behaviour which incorporates dynamic rate effects and to implement a finite element solution of the model to analyze soil-tool interaction over a large range of speeds.

3) To compare predictions of draft of narrow tillage tools with experimental data obtained using the developed equipment (1).

CHAPTER 2

LITERATURE REVIEW

2.1 Soil Openers

Designs for reduced draft requirements and consequently energy expenditures are some of the main concerns for soil manipulations produced by soil openers. Accessories such as coulters, depth control wheels, press wheels and covering devices, contribute to low drafts in general. Therefore, greater importance must be attributed to soil openers. A brief overview on current soil-opener design is presented in this section.

Under prairie conditions, soils are usually shallow. In general, soil openers are narrow tools. Narrow tools disturb considerably more soil than the extent of their width. For this reason, soil openers present three dimensional effects.

Seeding of cereals is normally performed either by conventional practices on a previously tilled field, or by conservation tillage systems on undisturbed soil (Kushwaha and Foster 1993). Pre-seeding tillage operations typically use cultivators. Seeding operations use disc openers or hoe openers. Air seeders use forced air flow to distribute seed and fertilizer to cultivator shanks, hoes or discs (University of Saskatchewan 1987).

Disc openers are appropriate for trash conditions and heavy clay fields. They have been very popular. Opened furrows are quite regular in shape with small soil disturbance. However, acquisition and maintenance costs are usually high because of moving parts, a great number of items present in the final unit assemblage, and manufacturing of elaborate

shapes. Disc units present heavy construction, adjustable frames for disc angle adjustments, individual disc gangs, gauge wheels for improved depth control, disc bearing gangs and expensive high carbon discs usually manufactured smooth or in notched shapes. Disc damage and replacement are expensive compared to replacing shovels or hoe openers. Gang bearing bolts must be tightened periodically to reduce disc damage in rocky conditions.

Cultivator categories include heavy duty, intermediate and field cultivators. Heavy duty cultivators or chisel plows are employed for operations such as breaking of new lands using operating speeds in the range of 6-8 km/h. Crumbling increases with speed (Koolen and Kuipers 1983). It is also used for deep banding of fertilizers and seeding. Field cultivators have relatively narrowly spaced shanks and are used for secondary tillage. Operating depth reaches the arable layer for chisel plows and half of it for field cultivators. Arable layers of 100 mm are typical in the prairies. Intermediate cultivators combine field and heavy duty cultivators with narrow shank spacing.

Hoe openers and cultivators have simple design with low manufacturing costs. Depth control is adequate, but furrow shapes are not quite regular when compared with disc openers. Soil disturbance is usually greater than the soil disturbance caused by disc drills. Seed scattering is also greater for these type of tools than for discs. Operating speeds average 2.2 m/s (University of Saskatchewan 1987).

Rigid openers work fine under light trash conditions. They present a low-cost and simplified design. In direct stubble seeding, however, trash clogging becomes a problem. Coulters are used to deal with the trash. Other types of accessories are also used for

furrow covering and depth control. Coulters cut trash ahead of tool openers. After seed and fertilizers have been placed, covering devices close the furrow. Press wheels pack soil against the seed for optimum germination conditions.

Conservation tillage includes no-till drills. Heavy shanks open a soil slice on previously unprepared soil. Very little tillage and seeding operations are performed at the same time. These systems do not require any prior seedbed preparation. Fertilizer banding and seeding are done in one operation. Soil water losses and soil manipulation are minimized. Conservapak® (Conservapack, Indian Head, SK) is one example of a no-till drill conservation system (Figure 2.1).

Air seeders are versatile. They can perform conventional or conservation tillage practices during seeding operations. All previously referred tillage tools can be used on air seeders and are considered to be narrow tools.

2.2   Performance of Tillage Tools

2.2.1 Draft-speed relationship

Historically, the moldboard plow has been dominant in agriculture. For this reason ample literature on draft-speed relationships for the moldboard plow is available. It is known that its draft increases with speed (Gill and Vanden Berg 1968; Stafford 1979). This relationship is usually of a quadratic form, but depending upon soil type, it can vary between linear and quadratic. A large component of moldboard draft is due to the movement of large masses of soil. Such forces are commonly referred to as 'inertial' forces.
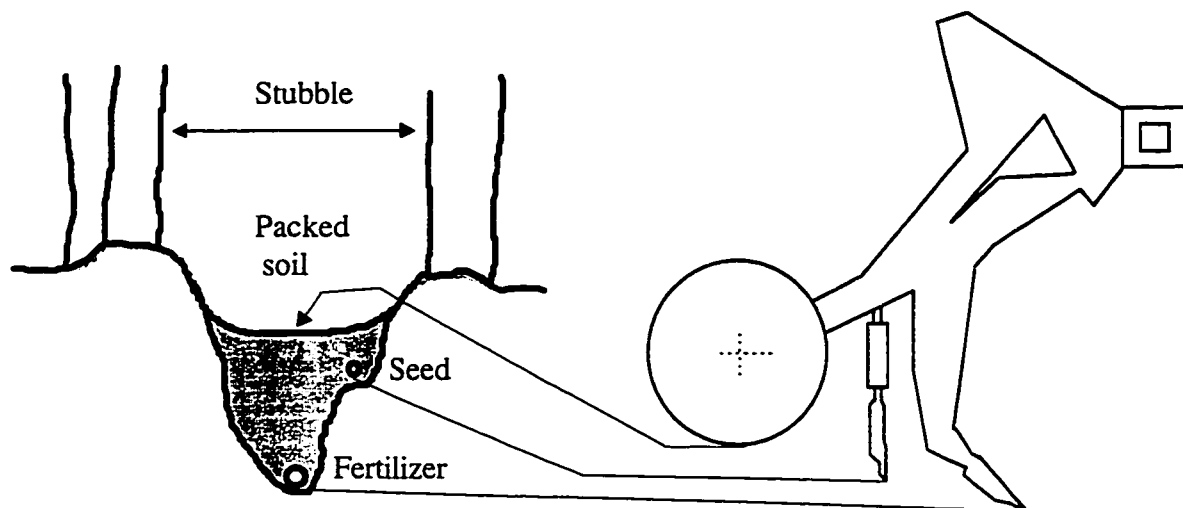
Figure 2.1 **Simultaneous tillage and seeding operations performed using a no-till drill conservation system - Conservapak™ (Saskatchewan Prairie Care 1991).**

Since the late 1970's, the use of chisel plows has increased in importance. Chisel plows represent a class of narrow tools. The amount of soil displaced by narrow tools is considerably lower than that disturbed by moldboard plows. Inertial effects are not expected to be as significant for narrow tools as for wide tools, although, they may still be important. Instead, strain rate effects are mostly responsible for changes in soil strength with speed (Stafford 1979).

Olson and Weber (1965) used high speed movies and an instrumented soil bin to study the effect of speed on two artificial soils in front of simple wide tools. Tested speeds ranged from 0.2 to 1.1 m/s. Increase of draft with speed was observed in the experiments, but the causes for the increase were not fully explained. Stress-strain properties and viscoelastic properties of the soil were identified as important factors. Acceleration of the soil was not considered a significant factor to increase tool draft with increase in speed.

McKyes (1985) gives a general explanation for the dynamic effects of tillage tools, based on the literature and practical experience. Considerable dynamic effects on soil can be produced by cutting tools operating at high speeds. Two mechanisms in particular affect the draft required to move soil. Inertial forces have remarkable importance for sandy soils, or so called frictional soils. In clay soils the draft required is not too sensitive to inertial forces, but shear strength increases substantially with increasing shear rates.

Dynamic interactions between soil and narrow tools are still not well understood. Most of the published data are from experiments performed at relatively low speeds, up to 3 m/s. Much attention has been dedicated over the years to identify and understand basic principles of soil cutting by narrow tools. Three works in particular provide basic

information from which basic guidelines on dynamic aspects of soil-tool interactions can be drawn, namely, Payne (1956), Wismer and Luth (1972) and Stafford (1979).

Payne (1956) recognized the effect of speed on draft. Drafts of a flat vertical tool, 25 mm wide, were obtained in clay, clay loam and sandy loam soils (Figure 2.2). Drafts measured at speeds of 2.7 m/s increased more than 20% in comparison with drafts at 0.2 m/s. The strengthening of soil with speed was observed for all three soils. The data also seem to present a linear draft-speed relationship.

Wismer and Luth (1972) tried to isolate effects of inertial and non-inertial components on pure frictional and pure cohesive soils. Chisel plow measurements on a sandy silt soil in the field presented a linear draft-speed relationship. The maximum investigated speed was 4.0 m/s. Inertial effects were shown to be not so noticeable for the chisel plow as for the moldboard plow. A linearly increasing draft-speed relationship of the 3-m wide chisel plow working on a sandy silt soil is shown in Figure 2.3.

Soil cutting forces increased with speed, and soil water content highly affected the form of the draft-speed relationship in the study by Stafford (1979). The plastic limit appears to be an approximate boundary which defines two different soil behaviours. Below the plastic limit an increasing draft-speed relationship is predominant. Above the plastic limit a reduction seems to occur on the rate of increase of draft with speed. Asymptotic relationships occurred for soils with high water contents. The maximum investigated speed was 5.0 m/s.
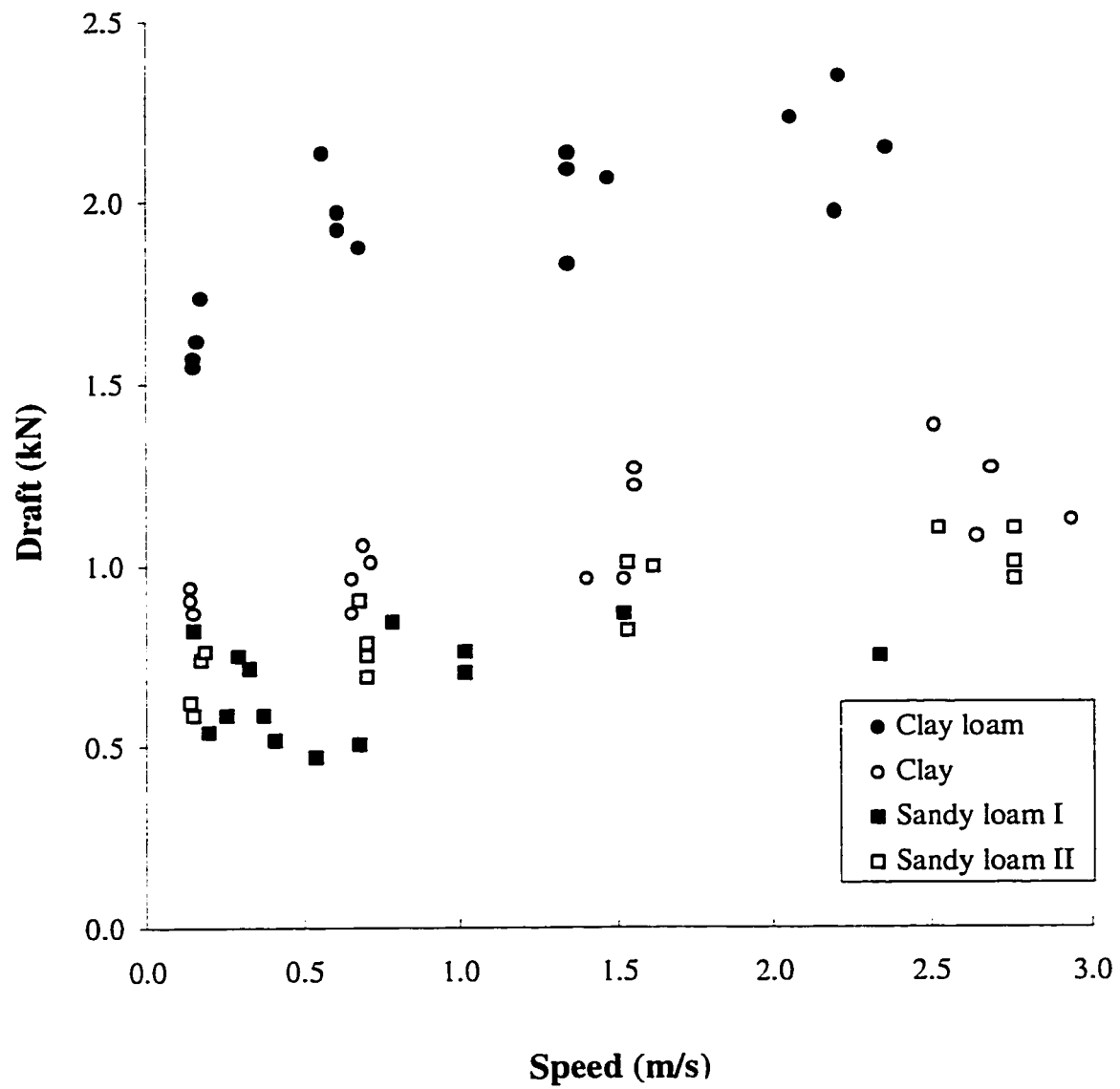
Figure 2.2   Draft versus speed relationship showing influence of speed on draft of a 25 mm wide flat vertical tool (adapted from Payne 1956).

The chart shows data points with the equation label:

Draft=19.37+2.41*Speed
0.2 m depth
10 chisels
Sandy silt

Axis labels: Draft (kN) on y-axis, Speed (m/s) on x-axis.
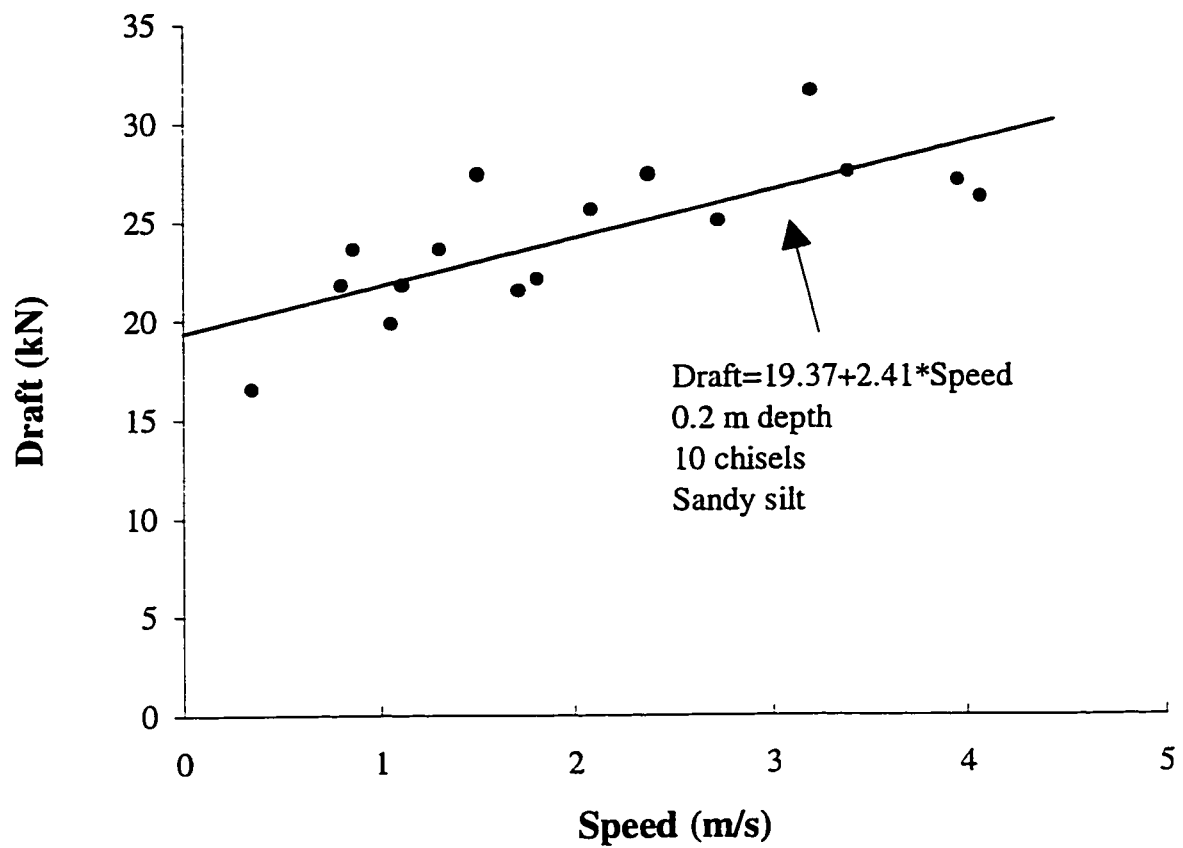
Figure 2.3　Draft versus speed relationship of a 3 m wide chisel plow working on a sandy silt soil field (after Wismer and Luth 1972).

Measurements of tool draft in situ result in highly scattered data. Despite the difficulties faced in the field, data are still valuable if analysis makes use of proper statistical tools and care is taken in doing the experiments. Ground unevenness, terrain non-uniformity, and variable soil water content are among many factors that make field data difficult to collect and interpret. Particularly at high speeds, depth of tool operation must be carefully controlled and monitored because draft is very sensitive to tool depth.

Draft-speed data for narrow tools are scarce in the literature. ASAE Standards D497 (1993) groups equipment and relates standard required draft according to speed of operation in the commercial range (~ 1 to 3 m/s). It is a valuable source of information for decision-making on aspects of management and practical design. To understand the behaviour of soil-tool interactions, however, more specific and accurate determinations are necessary.

Linke and Kushwaha (1992) conducted field tests on vertical narrow tools in the field. Data with speeds up to 18 m/s were obtained. It was concluded that draft either decreased or remained constant above a certain speed range. However, highly scattered data typical of field tests were obtained. Draft variations were almost 100% for speeds slightly lower than 8.4 m/s. The sensitivity of the draft to depth variations large. At a shallow working depth of 50 mm, for instance, a ± 5 mm variation in depth (i.e., 10% variation) is very difficult to maintain under field conditions, especially at high operating speeds.

Wheeler and Godwin (1994) presented laboratory data for narrow tools working in frictional and cohesive soils at speeds up to 5.6 m/s. Wheeler and Godwin (1996) showed

measurements of narrow tools running at speeds up to near 4.2 m/s in cohesive field soils (Figure 2.4). In both their studies, draft increased as speed increased.

2.2.2 Soil bin measurements

Soil bin experimentation is very common, mainly because of difficulties in the interpretation of field measurements. Even though there is an extra investment involved with soil bin facilities, variables can be more easily controlled, which facilitates data analysis. Draft versus speed relationships for narrow tools working in soil bins are also scarce.

Early soil bin measurements were usually obtained for wide tools because basic principles were easier to isolate and understand. Narrow tools present pronounced side effects that complicate the analysis. Work done by Siemens et al. (1965) represents such a basic kind of work. Rowe and Barnes (1961) also considered the dynamic case of flat wide blades moving in a clay and in a sandy clay soil at speeds from 0.2 to 0.8 m/s. The heavier clay soil showed pronounced draft increases with speed; however, the increase in draft was much smaller for the sandy clay. They concluded that soil shear strength became larger as the rate of shear increased.

Xie and Zhang (1985), in one of the first studies to incorporate dynamic effects in the numerical analysis of tool draft, presented graphs of draft versus speed for a wide tool. Data from their work showed draft increasing with speed for a black loam as well as for a sandy loam soil. Tool speed of operation reached a maximum of 1.4 m/s. The
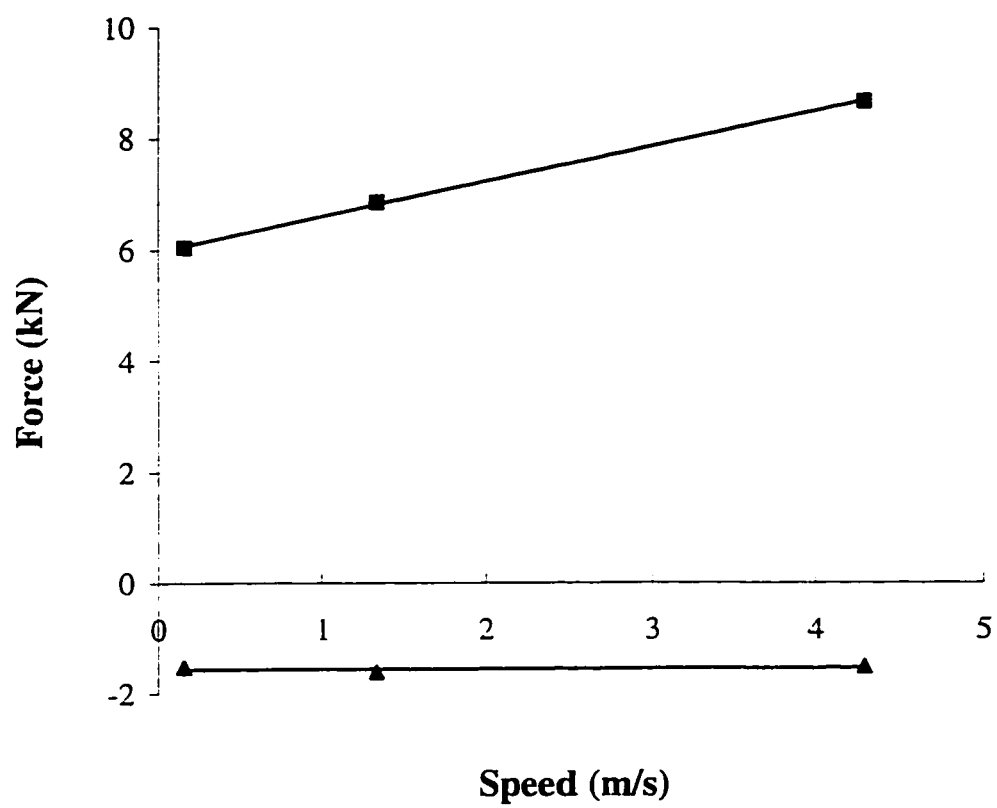
Figure 2.4 **Effect of speed on forces of narrow tools working in a cohesive soil (■ horizontal force, ▲ vertical force), (after Wheeler and Godwin 1996).**

clay loam soil showed more pronounced increases in draft with speed in comparison with results for the sandy loam soil. The latter produced little increase in draft with speed.

Stafford (1979, 1984) described soil bin force measurement equipment and presented data results. Measured speeds were up to 5 m/s. Water contents ranged from 12.6% to 48.9%. Rare and valuable experimental data were presented in these papers. Two sample cases of vertical narrow tools are shown in Figures 2.5 and 2.6, working on sandy clay loam and clay soils, respectively. There is a noticeable influence of water content on the draft-speed relationship. A linearly increasing draft-speed relationship was obtained for a low water content of 12.6% (Figure 2.5). For the higher water content (16.0%), increase in draft with speed was reduced and the curve leveled off. The same trend is observed in Figure 2.6, in which the draft tends to level off with speed at higher water contents (28.8, 38.7 and 48.9%). The only difference was that for soil at 18.2% water content, the increase in draft showed a polynomial form.

Zeng and Yao (1992) measured horizontal and vertical forces for a 40 mm wide tool working at a depth of 160 mm in a loam soil. Soil water content was 13% and soil bulk density was 1.28 Mg/m^3. The tool rake angle was 70° and speeds were up to 2.6 m/s. Experimental and simulated data showed horizontal tool forces increasing with speed. Vertical tool forces also increased with speed, but force values were small.

2.2.3 Energy requirements

Tillage operations demand a considerable amount of energy to deform and fail soil. Energy is transferred into the soil. Energy requirements of tillage equipment are usually
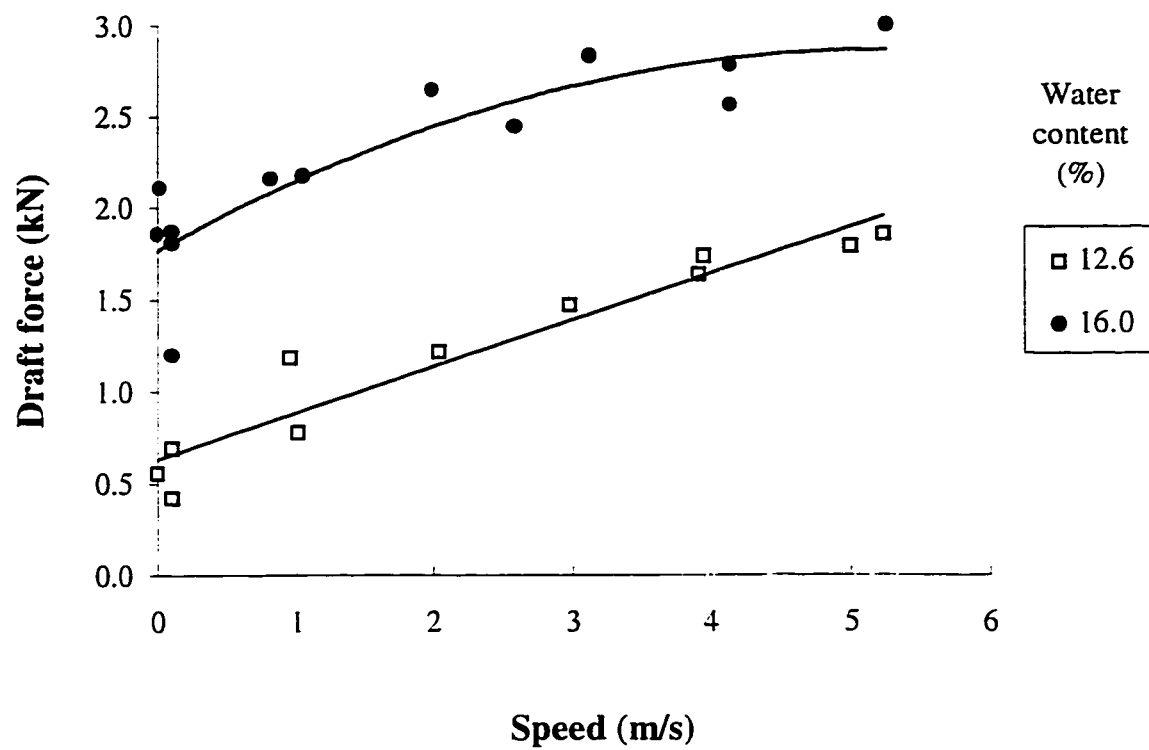
Figure 2.5   Mean draft of a vertical narrow tool (40 mm wide, 150 mm deep) in a sandy clay loam soil at water contents 12.6% and 16.0% (after Stafford 1979).
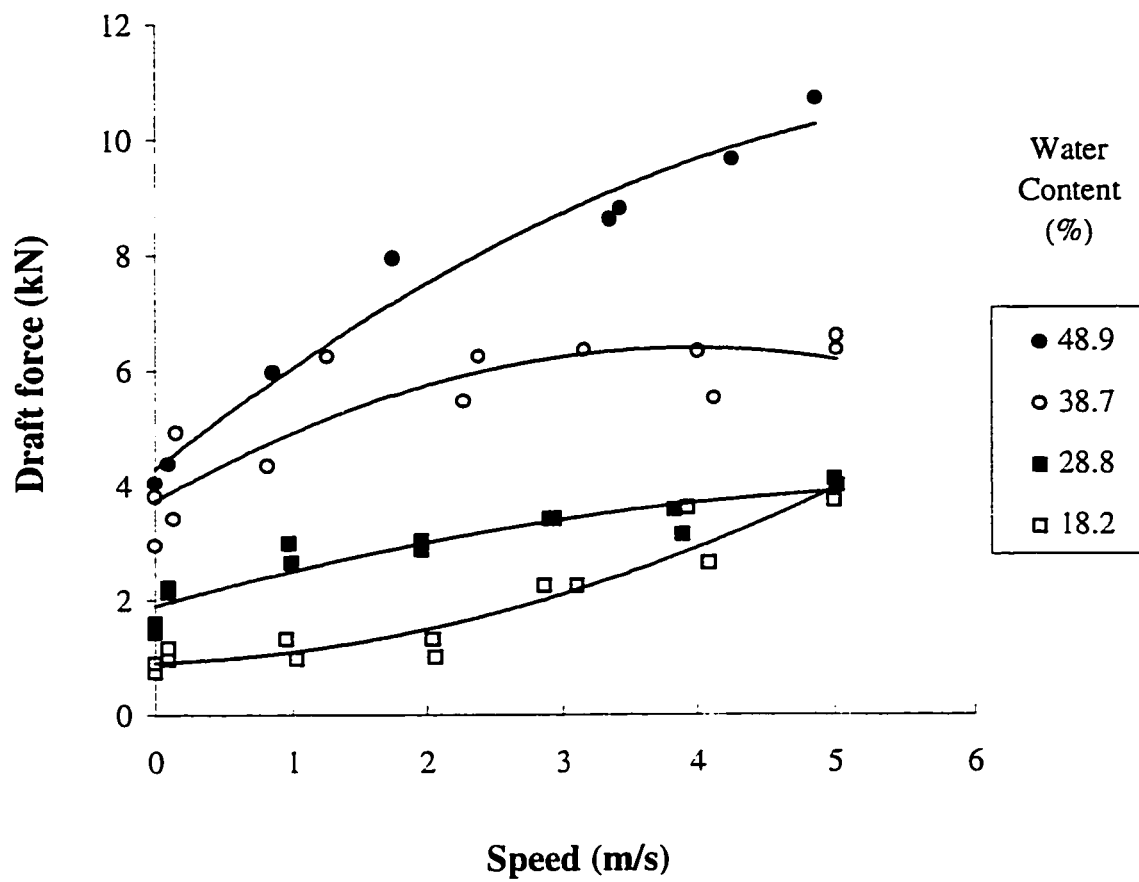
Figure 2.6 Mean draft of a vertical narrow tool (40 mm wide and 150 mm deep) in a clay soil at water contents of 18.2%. 28.8%, 38.7% and 48.9% (after Stafford 1979).

expressed in terms of unit area or volume of manipulated soil (Panwar and Siemens 1972). This section deals with soil input energy, and the following section with soil changes resulting from this action, i.e., soil disturbance and pulverization.

McKyes (1985) and Chancellor (1994) demonstrated the convenience of presenting data in terms of energy per unit volume, since it has the same units as draft per unit area. Tool draft divided by tool furrow cross sectional area represents the energy required to cut a volume of soil:

$$\frac{energy(N.m)}{volume(m^3)} = \frac{force(N)}{area(m^2)} \frac{length(m)}{length(m)}$$

Darmora and Pandey (1995) used the energy rate per depth of operation as an index of performance for soil openers:

$$E_d = \frac{H \cdot S}{D} \tag{2.1}$$

where,

E_d = input energy rate per unit operating depth $\left(\dfrac{W}{m}\right)$.

H = draft force (N),

S = operating speed (m/s),

D = depth of operation (m).

Soil water content and bulk density considerably affect the amount of energy required to fail soil in unconfined compression. These two quantities define a specific soil structure. In Panwar and Siemens' (1972) investigations, stress-strain curves for low water content samples had peaks at low strains and the soil tended to fail in a brittle mode.

At a high water content (28.1%) there was no occurrence of a definite peak and soil failed plastically. At a low water content (16.5%), low energy levels were obtained, and although failure strength was high, the failure strain was small. At the high water content, the increase in failure strain (~ 210%) more than overcame the decrease in failure strength (~ 55%). Increased levels of energy per unit volume (twelve-fold increase) were obtained with increase in soil bulk density (1.2 to 1.4 Mg/m^3) and water content (16.5 to 28.1%).

An increase in energy due to an increase in confining stress was reported by Chancellor (1994). A clay loam soil with confining pressure of 74 kPa presented a ten-fold increase in energy per unit volume of soil when compared with unconfined soil. It was concluded that this energy increase was due to increases in both failure stress and failure strain. A four-hundred fold increase in energy was also noted as compared to soil failure in tension.

Chancellor (1994) also reported investigations by Aref et al. (1975) on triaxial tests, and used partitioning of energy to analyze relaxation tests in confined compression. The proportion of recovered energy increased with increased soil water content. It was also pointed out that the energy transferred to surroundings was important in terms of predicting volumetric and shear strains on the sample.

Dynamic effects relating rates of strain and energy have also been reported in the literature. Niyamapa and Salokhe (1992) measured energy necessary to break soil specimens in quasi-static and dynamic triaxial tests. For the quasi-static case, failure energy per unit volume for a silty loam soil presented a minimum value at the lowest water content and increased rapidly with increases in water content. Higher bulk density (1.3

Mg/m^3) specimens required considerably more energy to fail than lower bulk density (1.2 Mg/m^3) for similar water contents. Under dynamic tests (speeds up to 6 m/s), failure energy for silty loam and sandy loam soils showed rapid increases with speed up to approximately 5 m/s, and then decreased (Figure 2.7).

Care must be taken in interpreting dynamic triaxial tests. Characteristics of the load cell might overlap with soil response itself. Energy transferred to surroundings might take place in a very different manner than in field conditions, particularly for high strain rates. Difficulties in interpretation of dynamic triaxial tests might explain the rare number of publications relating energy requirements and strain rates from triaxial tests.

Another aspect related to energy was presented in the work of Russian academicians on high speed tillage during the 1960's and translated by the USDA at Auburn, AL. Hendrick and Gill (1973) tried to analyze the Russian work. The existence of operating velocities above which the energy required to cut soil would decrease was suggested. The main aspects of some of these papers are summarized in the following.

Katsygin (1961, 1964) noted that with an increase in operating speed, an additional "dynamic" resistance originates and the expenditure of energy is increased. A concentration of energy will increase in the soil media so that both stresses and soil crushing will increase. Since soil deformation requires some time to manifest, a reduction of the deformed zone in front of the tool and increases in stress would occur. Therefore, draft and crumbling of the soil slice would increase.
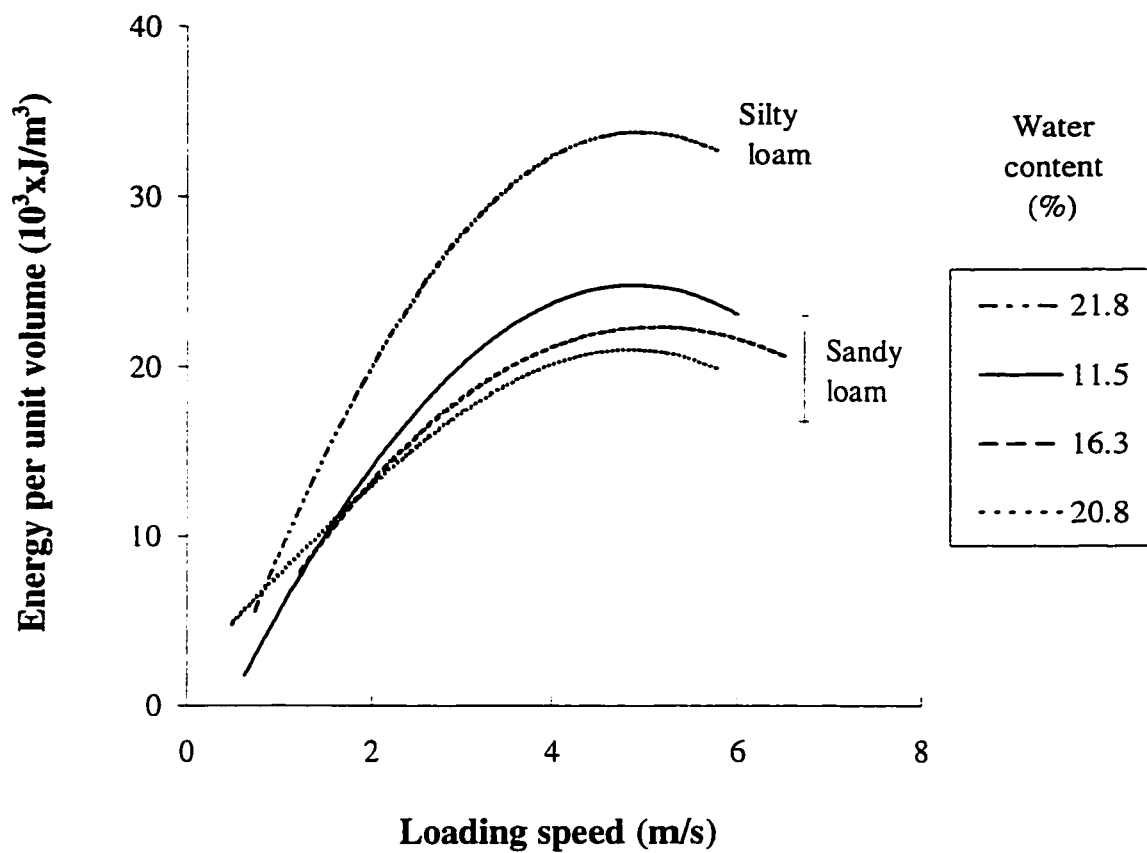
Figure 2.7   Failure energy per unit volume for a silty loam soil submitted to
dynamic triaxial tests (after Niyamapa and Salokhe 1992).

Azyamova (1963) reported that for operating speeds greater than 2.8 to 3.3 m/s the linear nature of shear stress vs. speed ceases, and an intense increase in shear or normal stress occurs. This was explained by the excessive concentration of energy in front of the narrow tool (which cannot distribute to the soil uniformly in short intervals of time).

Vetrov and Stanevski (1969) conducted studies with simple inclined blades, 50 mm wide, at cutting speeds between 0 and 10 m/s (details not reported). Although the main study was concerned with draft, energy requirements were obtained from this study too. It was concluded that increase in draft is less rapid at speeds below a speed of plastic soil deformation, which they termed the 'critical speed'. At speeds of cutting greater than critical, the narrow tool is subjected all the time to undisturbed soil so that the character of soil disturbance is changed. It was reported that the force for cutting soil with the narrow tool increases proportionally to the speed of cutting, while above the critical speed it doubles in comparison with the draft measured at a very low speed.

2.2.4 Soil disturbance

One objective of tillage is to break down soil structure. Tillage tools disturb and pulverize soil particles. The extent of soil disturbance and pulverization depends on soil properties and amount of energy input to the soil.

2.2.4.1 Disturbed area

Soil disturbance can be evaluated by measuring the soil cross-sectional area affected by the tool pass. Disturbed area can be measured using roughness meters. Soil roughness meters are able to measure soil disturbance and geometry of the seeding

furrow. They generally consist of a number of long pins with small cross sections. The use of roughness meters is a reliable and inexpensive technique. The only requirement is that the needle spacing be small enough to record abrupt surface variations. Specific draft, which is the draft per disturbed area ratio, may also be evaluated. This ratio has the same value as the ratio energy per volume of soil. It is an important parameter in the design of soil tools.

Tessier et al. (1989) measured soil disturbance produced by soil openers using roughness meters. No method has been adopted, in standard form, to quantify the soil disturbance. Visual observation and comparison of disturbed areas among different soil tools also have been used. Reported results in the field indicated hoe type furrow openers disturbed more than twice the soil surface disturbed by disc type openers. Effects of operating speed were not reported in this study.

McKyes and Desir (1984) measured disturbed soil areas of narrow tools on different soil conditions at speeds of 1.4 m/s. Failure area was calculated by means of passive earth pressure and it was assumed that the shape of the soil failure wedges was determined by soil weight and strength. Predicted and measured disturbed areas indicated reasonable agreement.

Tessier et al. (1989) and Darmora and Pandey (1995) used an index, R_i , to quantify soil disturbance:

$$R_i = \left[\frac{\sum H_i^2}{n'-1} \right]^{0.5}$$
(2.2)

where:

H_i = residual highs measured from the trace of furrow profile (mm),

n' = number of measurements.

Low values of R_i indicate low soil disturbance.

In tests with simple cultivation implements (speeds up to 2.7 m/s), Payne (1956) could not note any difference on the area of soil disturbed for various speeds. It was noted, however, that soil adjacent to the tine seemed to be more disrupted at higher speeds.

In the tests of Vetrov and Stanevski (1969) with simple blades, tests with different speeds (up to 10 m/s) produced little change in the shape of the soil cut. The soil cross section remained trapezoidal, and the relative dimensions were approximately constant.

2.2.4.2 Quality of tillage

Level of soil pulverization can be quantified by determining the change in surface area of the soil particles. Alternatively, relative loosening of soil can also be used to quantify the quality of tillage. The quality of work inside the disturbed area can be evaluated through the determination of particle surface per volume of soil; in the case of relative loosening of soil, by measuring soil densities before and after the process of cut. These parameters, indicate the energy effectively transferred to the soil.

Gill and Vanden Berg (1968) observed that soil break up is important for plant growth. A fine clod structure and a slight compaction is desirable to provide good contact between soil and seed and give conditions for germination (Sitkei 1985). However,

28

describing the amount of soil breakup does not directly describe plant's growth needs. It is still useful to evaluate performance of tools and compare soil conditions.

The amount of soil breakup can be determined by sieving and classifying soil particles. Mean weight diameter (MWD) is an index used to quantify the effects of soil pulverization. A soil sample is passed through different sieve meshes and retained fractions weighed. Soil mean diameter is computed according to cumulative mass contribution of clods retained in each diameter range. The resultant mean diameter is called the mean weight diameter (Gill and Vanden Berg 1968). Mean weight diameter can be used to compare soil structures before and after a tillage operation. However, there are many initial soil conditions in which the soil cannot be separated and sieved. The soil may be a continuous mass more like one clod soil block. In these cases only final soil conditions are classified and compared. This method has been useful to quantify impact effects on soil structures processed by rotary tillers.

Table 2.1 presents the effect of speed on the amount of soil breakup produced by a chisel tool. It shows that as the speed of operation increased, the average size of clods decreased. Therefore, the amount of soil breakup increased with speed.

Another index which has been used in mining excavations, the swelling factor, can also be used to help quantify the quality of work (McKyes 1985). Swelling factor indicates soil expansion based on soil densities prior to and after soil work, and is defined as:

$$SF = \left(\frac{V_f}{V_b} - 1\right)100\% = \frac{\gamma_b - \gamma_f}{\gamma_f}100\% \tag{2.3}$$

where:

Table 2.1 Size of clods produced by chisel tool in relation to operating speed (Gill and Vanden Berg 1968).

Soil type	Tillage tool speed (m/s)	Clods greater than 19.2 mm in diameter (%)
Silty clay loam	0.8	31.7
	1.1	30.8
	1.4	28.2
Silt loam	1.4	8.3
	1.7	5.8
	1.9	5.3

V_f = soil volume after cut (m^3),

V_b = soil volume before cut (m^3),

γ_b = unit density before cut (N / m^3),

γ_f = unit density after cut (N / m^3).

Even in cases where soil has a structure of one clod, density can still be measured before tillage and the soil loosening quantified. Changes in soil density mainly depend upon initial soil density, water content and tillage tool geometry. Soil water content and tool speeds are two of the factors that affect soil loosening.

Narrow tools pulverize more soil than wide ones; however, they require more energy per volume to cut soil. The increase in energy does not increase soil breakup proportionally (McKyes 1985). For environmental purposes, soil structure and bulk densities are two important factors that would be, in some cases, even more important than the energy spent in tillage machinery.

Sitkei (1985) investigated soil clod breakup for seedbed preparation purposes. Under dry conditions, difficulties arise in breaking clods down to desirable levels. Several implement passes and high energy may be required to reach this aim. There was a lack of clod support to allow energy transfer from the tool. Impact duration was studied. Test results indicated that there was a critical tool velocity for clod breakage. Experiments in a soil bin showed that clay loam clods tended to be broken only when tine tool velocity was higher than the critical velocity. Therefore, soil pulverization would increase above this critical tool velocity. Maximum tool velocity was 5.5 m/s. From experimental tests with velocities from 3.1 to 3.6 m/s, breakable clod weights decreased only slightly. Second passes were less efficient in breaking clods.

Other methods are being developed to evaluate soil structures. Stafford and Ambler (1990) analyzed black and white pictures of soil on a moving camera mounted to the rear of a seedbed cultivator. An image analysis processing unit was required. Zuo et al. (1995) used fiber optics sensors on the go, to correlate the analog electrical signal from the sensor to soil structure. Both of these studies reported some success, but indicated that further research is needed to develop these methods.

2.3 General Theory of Material Behaviour

Truesdell and Noll (1965) tried to unify all theories of material behaviour in continuum mechanics. Earlier attempts at the beginning of this century were not successful (Eringen 1962). The main open problem of continuum mechanics, as described by Truesdell and Noll (1965) still persists; that is, to formulate a general theory of material behaviour for all classes of materials. As suggested in their treatise, a unified theory might

be only possible after a formulation of a unified theory of mechanics, thermodynamics and electromagnetism.

Modern continuum mechanics had a great expansion in the late 1950's and 1960's (Malvern 1969). The modern continuum mechanics are in essence theories of theories, establishing possible forms that individual theories can take. Continuum mechanics had traditionally been studied in separate branches. Now, there is a unified treatment of the general principles and constitutive theory. The theory is divided in three parts: 1) general principles applicable to all materials, 2) constitutive equations which define particular idealized materials, and 3) specialized theories built on the foundations of general principles and equations, applicable to specific problems (Malvern 1969).

General principles are presented in the book by Malvern (1969). The most substantial improvement came from the formulation of very general principles, restricting different forms of constitutive equations. Both nonlinear constitutive equations and some widely used linear theories were affected by the new theoretical considerations. Two Encyclopedia of Physics treatises "The classical field theories" by Truesdell and Toupin (1960) and "The non-linear field theories of mechanics" by Truesdell and Noll (1965) presented extensive literature reviews, with references extending back to the 17th century.

The general principles, combined with constitutive equations, can for example be used to formulate a complete theory of linearized elasticity. The nonlinear theory of elasticity is so mathematically complex, that severe restrictions such as infinitesimal displacements and velocities were introduced to linearize the theory (Fung 1977). The

basic equations are as follows, representing field equations of linearized isotropic elasticity in material coordinates (Malvern 1969).

The three equations of motion, six equations of Hook's law, and six geometric equations from definition of strain in the material coordinates, respectively, are represented by the following well known equations:

$$\frac{\partial \sigma_{ij}}{\partial x_j} + \rho b_i = \rho \frac{\partial^2 u_i}{\partial t^2} \tag{2.4}$$

$$\sigma_{ij} = \lambda \varepsilon_{kk} \delta_{ij} + 2G \varepsilon_{ij} \tag{2.5}$$

$$\varepsilon_{ij} = \frac{1}{2} \left(\frac{\partial u_i}{\partial x_j} + \frac{\partial u_j}{\partial x_i} \right) \tag{2.6}$$

where b denotes the body force per unit mass [F·M^{-1}] and ρ denotes the mass per unit volume [M·L^{-3}]. The Lame constants are denoted by λ [F·L^{-2}] and G [F·L^{-2}]. The u_i are displacements [L], x_j are particle coordinates [L], ε strains [L/L], σ_{ij} are stresses [F·L^{-2}] and δ is the Kronecker delta.

Based on Truesdell and Noll's work, Haupt (1993) presented a comprehensive review of the mathematical modeling of material behaviour in continuum mechanics. The objective of the theory of material behaviour is the mathematical modeling to represent material properties. Classical theories of continuum mechanics (Haupt 1993) include: linear elasticity; hydrodynamics; Fuler and Navier Stokes equations; linear viscoelasticity; Boltzmann's principle of superposition; classical theory of plasticity; and the theory of material behaviour.

Constitutive equations form a distinct mark of a particular theory. The classical theories can be understood as asymptotic approximations of one far more general constitutive model. To solve initial boundary value problems, the universal balance equation of continuum mechanics must be completed by convenient assumptions about individual material behaviour. Material properties relations might be represented by stress-strain relations, material symmetry, and kinematics constraints. In continuum mechanics a constitutive equation is a relation between state variables; for example, strain and stress tensors. Figure 2.8 summarizes four different classes of the whole variety of material behaviour. This behaviour can be recognized from experiments. The behaviour can be rate-dependent or rate-independent, with hysteresis or without. These four different categories of material behaviour motivated four classes of mathematical models, namely, elasticity, plasticity, viscoelasticity and viscoplasticity.

These classes will be explained in sequence and only cases with potential applications to the present problem will be referred to here. For instance, hyperelasticity will not be mentioned in the elastic case, only hypoelasticity.

2.3.1 Hypoelasticity

Elasticity is a theory that models rate independent material behaviour without hysteresis. A new class of elasticity is hypoelasticity. This theory was first introduced by Truesdell (1955). Hypoelasticity theory has been presented by Eringen (1962), Gudehus (1977b), and Chen and Saleb (1982). The term "hypo" means elastic in a lower sense or in an incremental sense (Chen 1984). It is intended to explain the behaviour of materials with

Rate independent

without hysteresis   with hysteresis

Rate dependent

without static hysteresis   with static hysteresis
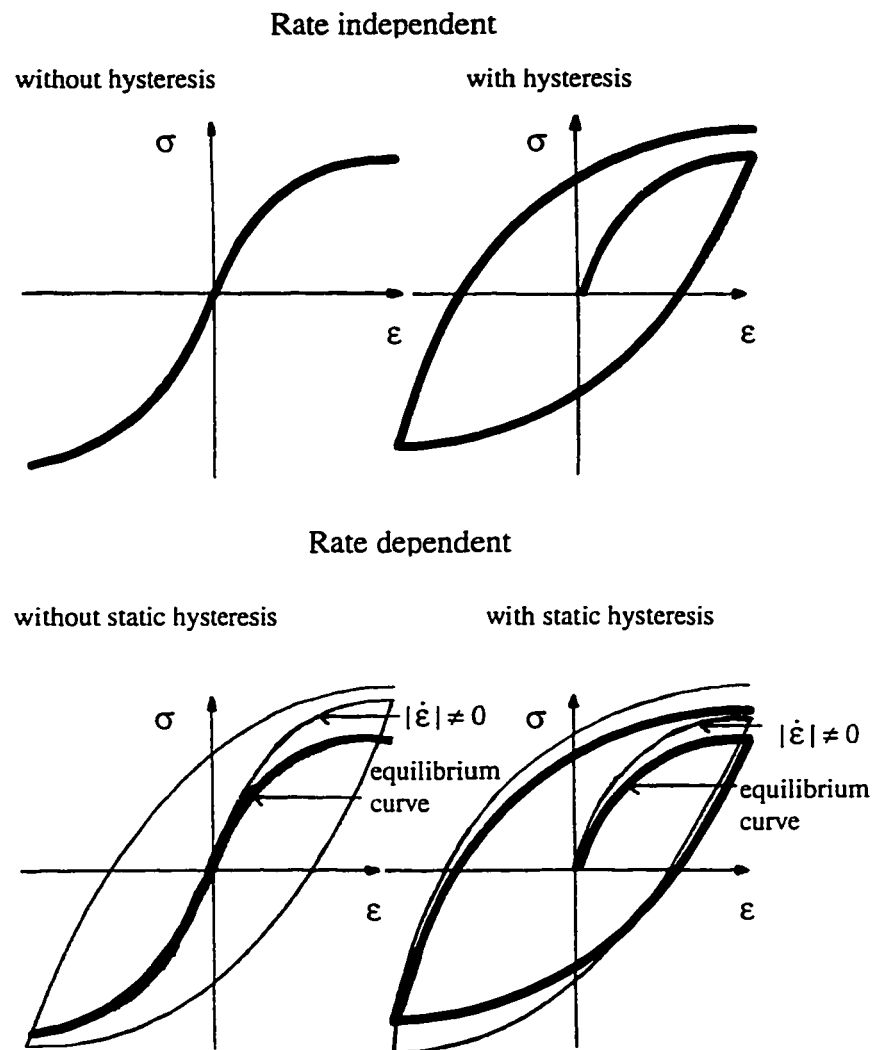
Figure 2.8   Classes of material behaviour (after Haupt 1993).

short memory (Eringen 1962). Hypoelasticity is also powerful because it is formulated in the incremental form, which provides advantages for computational implementation. Incremental constitutive models are intended to represent a class of behaviour where the state of stress depends on the current state of strain and on the stress path as well (Chen and Saleb 1982).

Two types of constitutive equations could be classified as hypoelastic materials: (1) the hyperbolic Duncan and Chang (1970) is a simplified form of hypoelastic model; and, (2) the variable moduli, which separates hydrostatic and deviatoric stresses, constitutes a more advanced model. These two constitutive relationships introduce an additional (strain) rate relationship to the original rate-independent elasticity theory. Hypoelasticity is path dependent and can also model plastic behaviour in a smooth manner. The mechanical state of the material, however, is independent of the rate of deformation (Antmam 1995). Although hypoelasticity theory is formulated in incremental form in a rate type relationship, the final equations are strain rate and time independent.

A general form of constitutive law can be represented as:

$$f(\sigma, \dot{\sigma}, \varepsilon, \dot{\varepsilon}) = 0 \tag{2.7}$$

where:

σ = stress ($F \cdot L^{-2}$),

$\dot{\sigma}$ = stress rate ($F \cdot L^{-2} \cdot T^{-1}$),

ε = strain ($L \cdot L^{-1}$),

$\dot{\varepsilon}$ = strain rate ($L/L \cdot T^{-1}$).

The incremental stress and strain tensors are linearly related through variable material response moduli, which are functions of stress and strain states; for instance:

$$\dot{\sigma}_{ij} = C_{ijkl}(\sigma_{mn})\dot{\varepsilon}_{kl} \tag{2.8}$$

The material response function, C_{ijkl}, describes instantaneous behaviour directly in terms of time rates of σ_{ij} (i.e., $\dot{\sigma}_{ij}$). The incremental stress-strain relationship is adequate for mathematical representation of materials with limited memory. Integration of equation 2.8 shows the stress dependence of the model:

$$\sigma_{ij} = \int_0^t C_{ijkl}(\sigma_{mn})\frac{\partial \varepsilon_{kl}}{\partial \tau'}d\tau' + \sigma_{ij}^0 \tag{2.9}$$

where σ_{ij}^0 denotes initial stress and τ' denotes instantaneous time (s). When $C_{ijkl}(\sigma_{mn})$ is a constant, the model degenerates to hyperelasticity. When $\det|C_{ijkl}(\sigma_{mn})| = 0$, material instability or failure occurs. A drawback mentioned by Chen and Baladi (1985) is that when tangential modulus of elasticity and Poisson's ratio, E_t and v, are used, the behaviour near failure cannot be adequately described.

Equation 2.7 represents a form homogeneous in time. Therefore, time could be removed from the equation. The rate then would simply be an incremental value. An anisotropic material will be represented by the general relationship:

$$\dot{\sigma}_{ij} = f_{ij}(\sigma_{kl}, \dot{\varepsilon}_{kl}) \tag{2.10}$$

If all terms have the same dimension in time, then the incremental equation holds:

$$\dot{\sigma}_{ij} = C_{ijkl}\dot{\varepsilon}_{kl} \tag{2.11}$$

For an isotropic hypoelastic material the general equation is expressed as:

$$\dot{\sigma}_{ij} = \alpha_0 \dot{\varepsilon}_{kk} \delta_{ij} + \alpha_1 \dot{\varepsilon}_{ij} + \alpha_2 \dot{\varepsilon}_{kk} \sigma_{ij}$$
$$+ \alpha_3 \sigma_{mn} \dot{\varepsilon}_{nm} \delta_{ij} + \alpha_4 \left(\sigma_{im} \dot{\varepsilon}_{mj} + \dot{\varepsilon}_{im} \sigma_{mj} \right)$$
$$+ \alpha_5 \dot{\varepsilon}_{kk} \sigma_{im} \sigma_{mj} + \alpha_6 \sigma_{mn} \dot{\varepsilon}_{nm} \sigma_{ij}$$
$$+ \alpha_7 \sigma_{mn} \sigma_{nk} \dot{\varepsilon}_{km} \delta_{ij} + \alpha_8 \left(\sigma_{im} \sigma_{mk} \dot{\varepsilon}_{kj} + \dot{\varepsilon}_{im} \sigma_{mk} \sigma_{kj} \right) \qquad (2.12)$$
$$+ \alpha_9 \sigma_{mn} \dot{\varepsilon}_{nm} \sigma_{ik} \sigma_{kj} + \alpha_{10} \sigma_{mn} \sigma_{nk} \dot{\varepsilon}_{km} \sigma_{ij}$$
$$+ \alpha_{11} \sigma_{mn} \sigma_{nk} \dot{\varepsilon}_{km} \sigma_{ir} \sigma_{rj}$$

where the α_{ij} are response coefficients.

The hypoelastic models are quite general and the theory of incremental elasticity can be considered a special case (Desai and Siriwardane 1984). The great advantage of hypoelasticity in relation to plasticity is that hypoelasticity is smooth during all paths, unlike classical plasticity that requires a defined yielding. Moreover, when equation 2.12 is assumed independent of stress, a grade zero hypoelastic model is obtained which represents exactly the generalized Hook's law in incremental form (with only two independent constants). When the equations on the right hand side are assumed linear functions of stress then it is called a grade one hypoelastic material and seven parameters are required. Model parameters are usually determined by curve fitting data from laboratory tests. Grade two hypoelasticity requires eighteen parameters.

2.3.2 Viscoelasticity

The theory of viscoelasticity models rate-dependent material behaviour without equilibrium hysteresis. A general theory of viscoelasticity was formulated by Coleman and Noll (1961). Due to the complexity of the general theory of viscoelasticity it is not considered here. The classical linear theory of viscoelasticity was first introduced by L.

Boltzmann in 1874 (Coleman and Noll 1961). A good review of viscoelasticity is presented by Lee (1962). The basic assumption of the linear theory of viscoelasticity is a constitutive equation relating stress tensor at time t, $\mathbf{T}(t)$, to the history of the infinitesimal strain tensor $\mathbf{E}(t-s')$, $0 \le s' < \infty$. If $\mathbf{E}(t-s')$ is small in magnitude for all s', then:

$$\mathbf{T}(t) = \Omega\{\mathbf{E}(t)\} + \Phi(0)\{\mathbf{E}(t)\} + \int_0^\infty \dot{\Phi}(s')\{\mathbf{E}(t-s')\}ds' \qquad (2.13)$$

where:

$$\dot{\Phi}(s') = \frac{d\Phi(s')}{ds'}; \qquad (2.14)$$

$$\lim_{s' \to \infty} \Phi(s') = 0. \qquad (2.15)$$

The stress relaxation function, Φ, is a function of time. For an isotropic material $\Phi(t)$ is completely determined by two scalar-valued functions of time; the stress relaxation functions for shear and dilatation. The $\Phi(s')\{\}$ (for each s') and $\Omega\{\}$ are linear transformations of the space of symmetric tensors in itself. The parameter Ω characterizes the "linear equilibrium stress-strain law" of infinitesimal elasticity and is determined from the two Lame's constants for an isotropic solid. The classic linear theory (equations 2.13 to 2.15) refer to infinitesimal viscoelasticity because they are applicable only for small strains.

The theory of infinitesimal viscoelasticity is justified on the assumption that at the microscopic level, matter can be regarded as composed of linear viscous elements ("dash-pots") and linear elastic elements ("springs") connected together in an intricate network. The material to which the theories are applied are not really composed of microscopic springs and dash-pots, this is simply a mathematical idealization of material behaviour.

Since any function can be represented by piecewise linear functions over small neighborhoods, for small deformations the stress can be expressed by a linear function of the deformation history, as expressed by equations 2.13-2.15 (Coleman and Noll 1961).

Oida (1984) presents an example of an infinitesimal viscoelastic application - a two dimensional finite element analysis of soil modeled as linear time dependent viscoelastic material. A sinkage analysis of a wheel on a sandy loam soil was satisfactorily calculated based on viscoelastic soil properties in the infinitesimal analysis. A rheological three-element solid model (two dimensional) was used for the soil constitutive relationship. To obtain viscoelastic soil parameters, relaxation curves were used from soil compression tests. Volumetric strain of soil was not predicted.

2.3.3 Viscoplasticity

Every material shows more or less pronounced viscous properties. It can be said that these effects are even more intensified when materials reach a plastic state. Viscoplasticity simultaneously describes rheology and plastic effects. Rheology is concerned with deformation of materials. The viscous properties of materials introduce a time dependence of the state of the stress and strain. The plasticity properties make these states of stress dependent on loading path. Thus, we obtain a dependence on load history and time state. Figure 2.9 exemplifies dynamic stress-strain curves for work hardening and stress sensitive material (Perzina 1966).
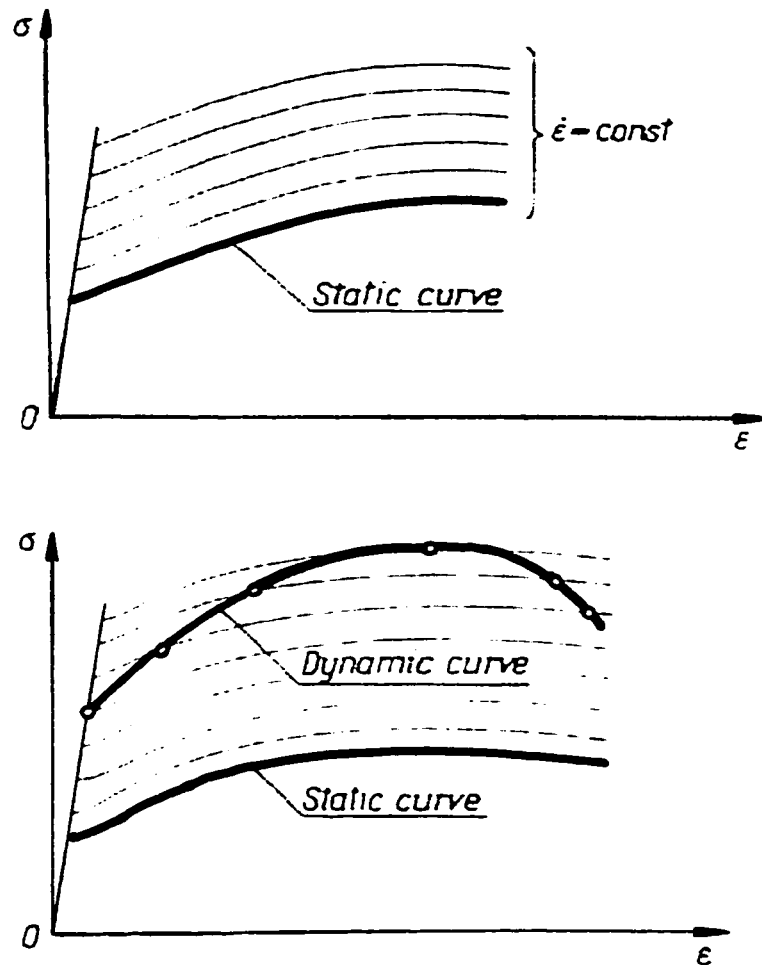
Figure 2.9   Dynamic stress-strain curves for work hardening (bottom) and

stress-sensitive materials (top) (Perzina 1966).

The most general constitutive model of material behaviour is the viscoplastic one. This model represents rate dependent material behaviour including equilibrium hysteresis. The classical rate independent plasticity is a limiting case of classical viscoplasticity. In viscoplasticity, when the viscosity terms reduce to zero, the strain rate becomes infinite, reducing the theory to the theory of plasticity (Lubliner 1990).

Viscoplasticity formulation for small strains is widely accepted in the literature. The following presentation is similar to that given in Baladi and Rohani (1984), and in Perzina (1966) as cited by Desai and Zhang (1987).

The total strain is decomposed in elastic and plastic parts:

$$\varepsilon_{ij} = \varepsilon_{ij}^e + \varepsilon_{ij}^p \tag{2.16}$$

where the total strain rate $\dot{\varepsilon}_{ij}$ can also be resolved into elastic and inelastic parts (Perzina 1966):

$$\dot{\varepsilon}_{ij} = \dot{\varepsilon}_{ij}^e + \dot{\varepsilon}_{ij}^{vp} \tag{2.17}$$

where:

$\dot{\varepsilon}_{ij}^e$ = elastic strain rate ($L/L \cdot T^{-1}$),

$\dot{\varepsilon}_{ij}^{vp}$ = viscoplastic strain rate ($L/L \cdot T^{-1}$).

The term $\dot{\varepsilon}_{ij}^{vp}$ combines viscous and plastic effects. The viscoplastic material model does not include viscous properties in the elastic region, simplifying the choice of yield criteria. The initial static yield criterion does not differ from the known inviscid theory of plasticity.

An elastic relation is used in the elastic range.

$$\dot{\varepsilon}_{ij}^e = C_{ijkl}(\sigma_{mn})\dot{\sigma}_{kl} \tag{2.18}$$

where:

C_{ijkl} = material response function ($F^{-1} \cdot L^2$),

$\dot{\sigma}_{kl}$ = components of stress rate tensor ($F \cdot L^{-2} \cdot T^{-1}$),

σ_{mn} = components of stress tensor ($F \cdot L^{-2}$).

The essential difference between viscoplasticity and the model of rate-independent plasticity is the flow rule. The inelastic strain rate depends on the 'distance' of the instantaneous yield surface from the static yield surface. Inside the static yield surface only purely elastic response occurs. The flow rule for a work-hardening and rate-sensitive plastic material may be written as:

$$\dot{\varepsilon}_{ij}^{vp} = \gamma \left\langle g(\frac{f_S}{\beta}) \right\rangle \frac{\partial f_S}{\partial \sigma_{ij}} \qquad (2.19)$$

where:

$$\left\langle g(\frac{f_S}{\beta}) \right\rangle = \begin{cases} g(\frac{f_S}{\beta}) & \text{for} \quad f_S > 0 \\ \\ 0 & \text{for} \quad f_S \leq 0 \end{cases}$$

$f_S(\sigma_{ij}, h) = 0$ = static yield surface ($F \cdot L^{-2}$),

γ = viscosity (T^{-1}),

h = hardening parameter ($F \cdot L^{-2}$),

β = scaling factor, ($F \cdot L^{-2}$).

The static yield surface $f_S = 0$ may expand or contract as h increases or decreases, respectively (Figure 2.10). For very low rates of deformation equation 2.19 reduces to the relation for inviscid plasticity.

Baladi and Rohani's (1984) model gives reasonable predictions of dynamic behaviour. The main drawback is the large number of parameters needed, i.e., sixteen. Figure 2.11 shows typical dynamic responses on triaxial tests for stress-strain responses and failure envelopes. The figure illustrates the growth of the failure envelope as the "strength of the material increases with increasing rate of deformation".

Viscoplastic problems have also been treated by Zienkiewicz (1977). An assumption of no viscoelastic strain in the elastic range is usually used to simplify the problem.

2.4 Models of Soil Cutting

2.4.1 Rate-independent models

2.4.1.1 Passive earth pressure theory

Classical theories of soil cutting have assumed soil behaviour to be independent of strain rates. Changes in soil strength are not substantial in the low range of tillage operating speeds. Models to predict soil-tool interactions began to appear in literature in the 1960's (e.g., Hettiaratchi and Reece 1967; Godwin and Spoor 1977; McKyes and Ali 1977; Perumpral et al. 1983). Terzaghi's (1943) theory of passive earth pressure was used for the prediction of the failure zone ahead of the tool, and soil forces were obtained from slip-line theory. In these models, soil was assumed to behave as a rigid-plastic material so

Subsequent dynamic
loading surface

Initial yield surface

σ_{ij}

$\dot{\varepsilon}_{ij}^{vp}$

O
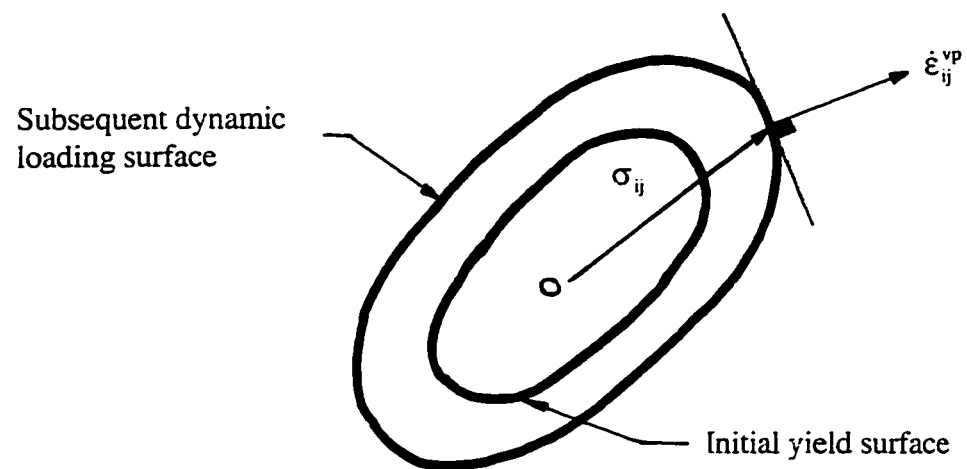
Figure 2.10 **Dynamic load surface and strain rate vector (after Baladi and Rohani 1984).**

Dynamic stress-strain curves

$$\frac{d\varepsilon}{dt} = C > B$$

Stress difference, $\sigma_1 - \sigma_3$

$$\frac{d\varepsilon}{dt} = B > A$$

$$\frac{d\varepsilon}{dt} = A$$

Static stress-strain curve
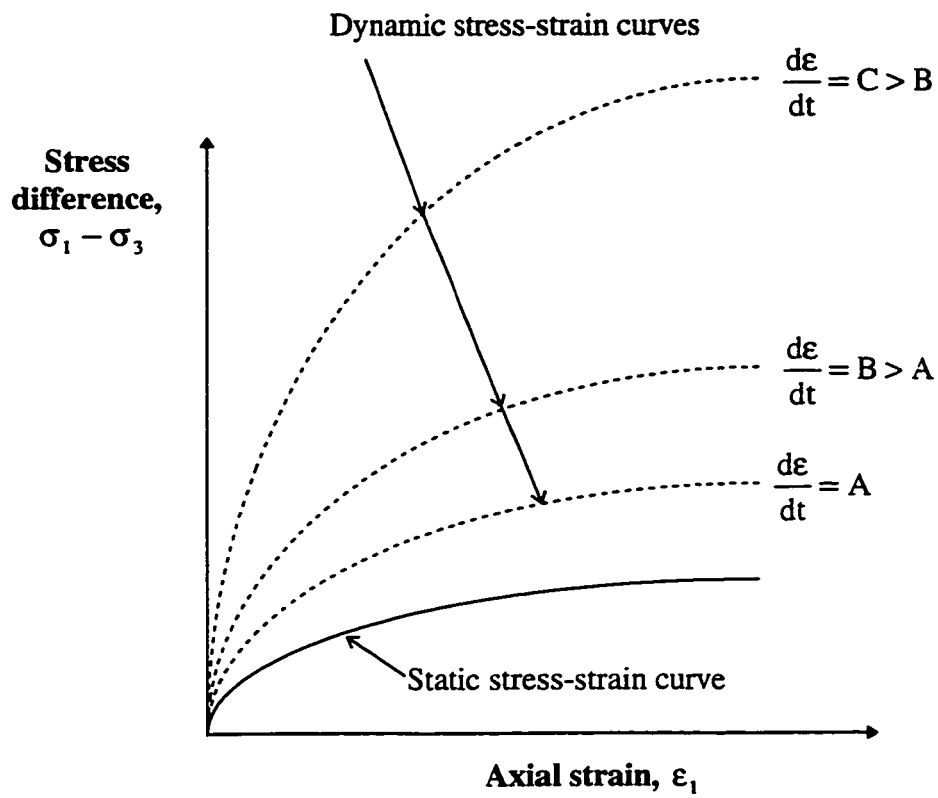
Axial strain, ε_1

Figure 2.11   Typical stress-strain curves and failure envelopes for different strain rates from an axisymmetric triaxial test (after Baladi and Rohani 1984).

that failure is immediately reached upon load application. The validity of these models has been generally proved by comparisons between theoretical experiments results (Grisso and Perumpral 1985). The models are simple and fast to use, but their application is limited to fairly simple tool geometries. Furthermore, analysis is limited to soil loads, and shear behaviour of soil just prior to and failure is not dealt with (Hettiarachi and O'Callaghan 1980).

Studies using the theory of passive earth pressure have also provided basic knowledge of soil cutting by narrow tools. It has been analytically formulated and experimentally demonstrated that a narrow tool disturbs a wider soil zone than that defined by its width. A model for side effects of a narrow tool and a centre wedge which is formed in front of the tool was presented by Payne (1956). Soil angle of internal friction and geometrical parameters greatly influenced the size of the wedge crescents.

2.4.1.2 Nonlinear elastic and elastoplastic models

Since the early 1970's, the application of finite element methods to solve material behaviour models based upon continuum mechanics have become increasingly popular, mainly due to increasing power and availability of computers. The introduction of finite element methods made it possible to model complex tool shapes in comparison with passive earth pressure models; however, accurate results are strongly dependent on the use of an appropriate soil constitutive relationship. Two categories of soil constitutive relationships, non-linear elastic and elastoplastic, have found widespread application in soil mechanics (Chi et al. 1993c; Wang and Gee-Clough 1993).

In the nonlinear-elastic constitutive models, the behaviour of a nonlinear material is considered as piecewise linear elastic behaviour. These models work well for simple loading and unloading situations, but not for more generalized stress paths. Hooke's law in incremental form is usually employed. Parameters of the material, K (bulk modulus) and G (shear modulus), or E (Young's modulus) and v (Poisson's ratio) are revised at every increment along its stress-strain curve. Thus, nonlinear models are approximated by quasi-linear models with nonlinear effects included in two basic material parameters.

Yong and Hanna (1977) were the first to apply finite element analysis to simulate two dimensional soil cutting (Gee-Clough et al. 1994). A wide blade was used for cutting a clay soil. Experiments were performed at blade speeds of 0.4 mm/s. They used an incremental loading procedure, with interpolations on the stress-strain curve and a hyperbolic type stress-strain relationship. Nodal coordinates were updated at the end of every increment to accommodate large deformations. Strain rate components were obtained by dividing incremental strains by the time increment.

Gee-Clough et al. (1994) used a finite element method to simulate cutting of wet soil. Wide blades with rake angles of 25° to 125° were used in a nearly purely cohesive Bangkok clay soil. The hyperbolic relationship was used to model soil behaviour. A good agreement between predicted and experimental forces was reported. The incremental method was adopted with material and geometrical nonlinearities, simultaneously solved in the same load increment. Deformations from 48 mm to 60 mm were imposed on the soil to reach failure.

A nonlinear elastoplastic soil model was proposed by Duncan and Chang (1970). The Mohr-Coulomb failure criteria was adopted as the failure criterion. The Duncan and Chang (1970) model was based on studies conducted by Kondner and coworkers (Upadhyaya 1994). Kondner (1963) proposed the following hyperbolic stress-strain relationship for soils.

$$(\sigma_1 - \sigma_3) = \frac{\varepsilon}{a + b\varepsilon} \qquad (2.20)$$

where:

σ_1 = major principal stress (kPa),

σ_3 = minor principal stress (kPa),

ε = axial strain in σ_1 direction,

a, b = soil parameters determined from triaxial tests (kPa^{-1}).

Figure 2.12 shows the determination of parameters 'a' and 'b' from a stress-strain plot, where:

$$a = \frac{1}{E_i} \qquad (2.21)$$

$$b = \frac{1}{(\sigma_1 - \sigma_3)_{ult}} \qquad (2.22)$$

E_i = initial tangent modulus (kPa),

$(\sigma_1 - \sigma_3)_{ult}$ = ultimate deviatoric stress (kPa).

The initial tangent modulus is expressed as:

$$E_i = Kp_a (\frac{\sigma_3}{p_a})^n \qquad (2.23)$$
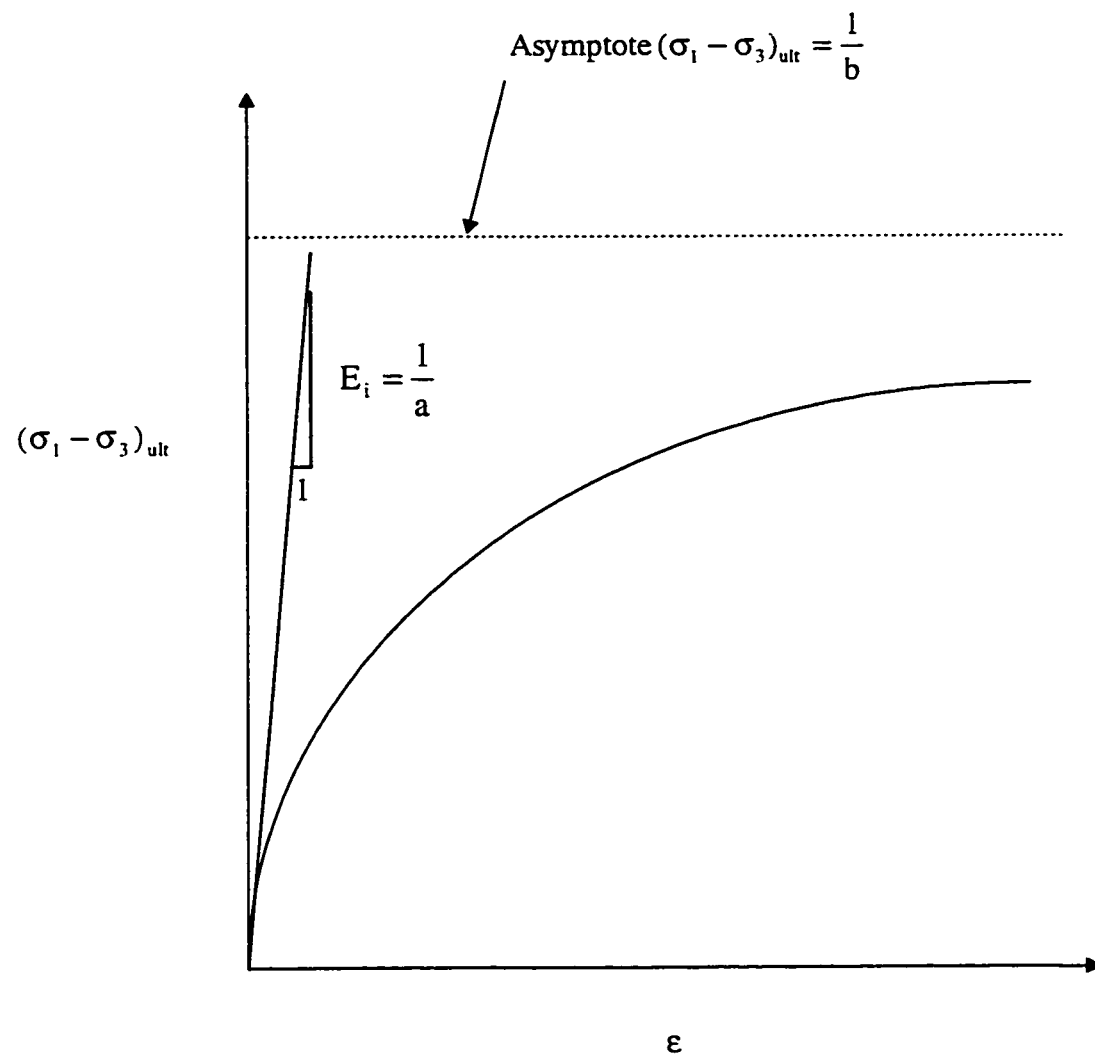
Figure 2.12 Determination of parameters 'a' and 'b' from a stress-strain plot (after Duncan and Chang 1970).

where:

p_a = atmospheric pressure (kPa),

K   = modulus number,

n   = exponent.

The ultimate compressive strength of the soil is usually higher than the deviatoric stress at failure by a small amount. A failure ratio R_f can be defined as:

$$R_f = \frac{(\sigma_1 - \sigma_3)_f}{(\sigma_1 - \sigma_3)_{ult}}$$
(2.24)

where:

$(\sigma_1 - \sigma_3)_f$ = deviatoric stress at failure (kPa).

An expression for the tangent modulus E_t was obtained as follows (Duncan and Chang 1970):

$$E_t = \left[1 - \frac{R_f(1 - \sin\phi)(\sigma_1 - \sigma_3)}{2c\cos\phi + 2\sigma_3\sin\phi} \right]^2 Kp_a \left(\frac{\sigma_3}{p_a} \right)^n$$
(2.25)

where:

E_t = tangent modulus for any stress condition (kPa).

The hyperbolic model provides a mathematical form to relate stress and strain through the use of a variable Young's modulus (and Poisson's ratio). Five parameters K, n, c, ϕ, and R_f are used to determine the instantaneous value of soil Young's modulus of elasticity according to the current element stress state. These parameters are normally obtained from conventional triaxial tests.

Chi (1989) and Chi and Kushwaha (1990) used the Duncan and Chang (1970) hyperbolic stress-strain model to analyze soil failure of narrow tillage tools. A non-linear, three dimensional, finite element program was written in FORTRAN to calculate soil forces and predict zones of soil failure. Tetrahedral constant strain elements were adopted because of their simplicity. The program analysis routine included the total load divided into small tool displacement increments. The Poisson's ratio was maintained constant during the analysis. The tangent modulus was recalculated for every displacement increment. Nodal coordinates (updated Lagrangian) were also updated after the end of each displacement increment. Tool loading continued to be applied, up to when the force reaction on the tool began to stay constant. Most soil in front of the tool had failed at this point. Results of the finite element model for a flat tool at different rake angles compared to soil bin data showed reasonably good agreement. For a triangular blade with 60° rake angle, a remarkable decrease in draft with displacement occurred after failure.

Subsequently, Chi et al. (1993a, 1993b) modified the Duncan and Chang (1970) model by assuming a variable Poisson's ratio for the compressive loading process before soil failure. After failure, a constant Poisson's ratio close to 0.5 was assumed. Eight node rectangular brick elements were used in the analysis. The modification produced a better prediction of volumetric strain. The modified expression for Poisson's ratio assumed a linear relationship with the ratio of the actual deviatoric stress and deviatoric stress at failure:

$$v = a_1 + b_1 \frac{\sigma_1 - \sigma_3}{(\sigma_1 - \sigma_3)_f} \qquad (2.26)$$

where:

ν = Poisson's ratio,

a_1, b_1 = dimensionless parameters.

Note that equation 2.26 can also be expressed as a function of mobilized stress strength S_m of the soil:

$$\nu = a_1 + b_1 S_m \tag{2.27}$$

The Mohr-Coulomb failure criterion is written as:

$$\tau_f = c + \sigma_n \tan \phi \tag{2.28}$$

where:

τ_f = soil shear strength (kPa),

σ_n = normal stress (kPa),

c = cohesion of the soil (kPa),

ϕ = angle of internal friction of the soil (deg).

By substitution of the Mohr-Coulomb failure criterion in equation 2.26, the following equation is obtained:

$$\nu = a_1 + b_1 \frac{(1 - \sin \phi)(\sigma_1 - \sigma_3)}{2c \cos \phi + 2\sigma_3 \sin \phi} \tag{2.29}$$

Chi et al. (1993c) studied the behaviour of undisturbed samples of clay and a gravely-clay loam soil under laboratory conditions. Two nonlinear elastic and two elastoplastic soil models were evaluated, namely: a) Duncan and Chang (1970) with variable Poisson's ratio (Chi et al. 1993a, 1993b); b) Bayley et al.'s (1984) hyperbolic model; c) Cam Clay model (Roscoe et al. 1958; Schofield and Wroth 1968); and, d) Cap model (Drucker et al. 1955). The hyperbolic model, which incorporated variable Poisson's

ratio, best reproduced test data on triaxial and hydrostatic tests. The comparisons were done only on simple stress paths in the laboratory. These models need to be verified under field conditions.

Including a variable Poisson's ratio requires two additional parameters, a_1 and b_1, and considering unloading and reloading requires an additional two parameters, K and n, for a total of ten soil parameters. On the other hand, the elastoplastic models perform reasonably well with only six parameters (Chi et al. 1993c). Thus, there is a trade off between accuracy and complexity of model when chosen a constitutive model.

The Cam clay model (a simple critical-state model with a single yield surface) is one of the simplest elastoplastic models available. Roscoe et al. (1958) and Schofield and Roth (1968) pioneered this work on saturated clays at the University of Cambridge. Wroth and Houlsby (1980) further modified the relationships of the consolidation and swelling lines in terms of specific volume and mean normal pressure. Kirby (1989) measured critical-state lines and yield surfaces for sampled unsaturated field soils. Although, some significant differences in relation to saturated soil behaviour occur, it is possible to use the model for unsaturated soils. The Cam clay model has attracted much attention because of its efficiency. Only five soil parameters, which all have well defined physical meanings, are necessary to describe elastic and plastic soil deformation (Chi et al. 1993c). A generalized constitutive relationship for this model is described in Desai and Siriwardane (1984).

Critical-state theory relates the states of stress of a soil to its specific volume. Based on soil triaxial tests, hydrostatic and deviatoric stresses can be measured for various

specimens with different specific volumes. Historically, variable names p and q have been used to denote hydrostatic and deviatoric stresses, respectively. State surfaces and a critical-state line are defined. Soil behaviour is elastic for stress states within the state surface. When stresses increase and reach state surfaces soil hardening or softening occurs, as in classical plasticity theory. When the critical-state line is reached, soil flows with no volume change.

Utilization of this model has been extended by agricultural engineers to tillage and traction of unsaturated soils. Mechanical behaviour of wide and narrow tools has been analyzed in the context of the critical-state soil mechanics. (Hettiarachi and O'Callaghan 1980; Hettiarachi 1987; Mojlaj et al. 1992; Wulfsohn 1994). Some criticism of the theory has also been made. Laboratory tests are excessively time consuming. Hettiarachi and O'Callaghan (1980), point out the major obstacle to critical state implementation is the lack of knowledge of the relationship between stress components in all but the simplest soil-implement relations. This is a general concern and applies not just for critical state models. However, such limitations can be overcome by implementing the method in finite element formulations (Wulfsohn 1994). Britto and Gunn (1987) implemented the finite element formulation for saturated soils in FORTRAN computer code; which led to the development of a commercially available code, CRISP-90. Practical implementation of critical-state theory in agricultural soils requires development of simple techniques to measure critical-state parameters in situ (Wulfsohn 1994). This is an objective for all constitutive models.

An elastoplastic hardening cap model was used in the investigation of a subsoiler using three-dimensional finite element analysis by Araya and Gao (1995). Two types of subsoilers with various rake angles were investigated: a soil breaker subsoiler type aimed to produce maximum soil disturbance, and an injector type intended to produce minimum soil disturbance. The experimental study was conducted in a mobile soil bin. Analysis was conducted with a commercial finite element program. ADINA. One subroutine program was written to solve the approximate equations representing the problem. When soil is in elastic state, stress-strain relationship is given by:

$$d\sigma_{ij} = \lambda d\epsilon_{ii}\delta_{ij} + 2Gd\epsilon_{ij} \qquad (2.30)$$

$$\lambda = \frac{2Gv}{1-2v}$$

where:

σ_{ij} = stress tensor (kPa),

ϵ_{ij} = strain tensor (m/m),

δ_{ij} = Kronecker's delta,

G = modulus of rigidity (kPa).

When the material reaches plastic state, the strain tensor consists of elastic and plastic incremental strain components:

$$d\epsilon_{ij} = d\epsilon_{ij}^{e} + d\epsilon_{ij}^{p} \qquad (2.31)$$

where:

ϵ_{ij} = strain tensor,

e = elastic superscript,

56

p   = plastic superscript.

The plastic strain tensor is expressed by Drucker-Prager strain-hardening law:

$$d\varepsilon^p_{ij} = \lambda_{ij} \frac{\partial f}{\partial \sigma_{ij}} \qquad (2.32)$$

Yield criterion is determined by:

$$f = \alpha' I_1 + J_2^{1/2} - K_f \qquad (2.33)$$

where:

σ = compressive stress (kPa),

f   = Yield function (kPa),

α' = material parameter,

K_f = material parameter (kPa),

I_1 = first stress invariant (kPa),

J_2 = second deviatoric stress invariant (kPa).

Results indicated good agreement between experimental and predicted forward soil rupture distances. However, predicted sideways soil rupture distances were larger than experimental measurements, and predicted upward soil movements were smaller than experimental measurements. Draft requirements from finite element predictions differed from soil bin tests. For the pan breaker, predicted draft was 1.6 times the experimental value. However, it was pointed out that degree of compaction in the soil bin was not the same as that for the soil of the triaxial tests.

Desai and co-workers have presented a remarkable analysis and guidelines for the solution of the general nonlinear three dimensional soil-structure interaction using a finite

57

element method (Desai and Phan 1980; Desai et al. 1981; Desai et al. 1982). The analysis also included a narrow tool pushed into the soil with analytical and experimental comparisons. The formulation presented allowed consistent definitions of stress, stress rate and constitutive laws in the incremental analysis and used Lagrangian and Eulerian approaches for geometrical nonlinearities. The soil element formulations incorporated various constitutive laws for geologic materials. Six different constitutive laws based on Von Mises, Mohr-Coulomb, Drucker-Prager, critical state, capp and viscoplastic criteria were incorporated in the computer code. Laboratory tests were developed to obtain model parameters. Cap models were found to be the most suitable to model soil behaviour among the studied models, based on laboratory data (Desai et al. 1981).

In agricultural applications, soil deformations are usually large. Two principal nonlinearities are involved in numerical soil-tool modeling. First is the material nonlinearity, which is related to soil behaviour, and second is the geometric nonlinearity which is caused by large displacements. An incremental numerical procedure is often used to solve soil-tool interaction with updated Lagrange. To deal with geometric and material nonlinearities within each load step and iteration, (Desai and Phan 1980) suggested use of the original Newton-Raphson method rather than the modified Newton-Raphson method (constant initial stiffness matrix within load steps) for convenience and to save computation time.

Liu and Hou (1985) reported the analysis of a continuous cutting of soil by narrow blades. The three-dimensional nonlinear finite element method used incorporated large displacements and a new elastoplastic mechanical model. The yield function was modeled

as a series of ellipses and the hardening function required six coefficients which had to be experimentally determined. A satisfactory agreement of results with soil bin test data was also reported.

2.4.2 Rate-dependent models

When a wider range of tillage operating speeds is to be investigated, changes in soil strength with strain rate cannot be neglected.

Swick and Perumpral (1988) modified the Perumpral et al. (1983) quasi-static model to incorporate dynamic effects. Model formulation included soil shear rate effects, soil inertial forces and soil-metal friction parameters. Based on earlier results they reported that soil shear strength and soil-metal friction increased with increasing shear rates. The dynamic model formulation gave reasonable predictions for the narrow tools tested (Swick and Perumpral 1988). Shear rates for both soil strength and soil-metal friction tests were obtained using a shear box at different displacement rates in the range of 0.08-21.2 mm/s. Maximum tested tool speed reached 1.2 m/s. Results indicated, however, that acceleration forces accounted for a large portion of the increase in tool force, contradicting the findings of others (e.g., Rowe and Barnes 1961; Siemens 1965; Wismer and Luth 1972).

McKyes (1985) proposed a dynamic model which included an inertial component in its formulation. The inertial forces involved in continuously accelerating new masses of soil as the tool travels are the most important mechanisms in frictional soils when operating speeds increase. Similarly, the strain rate dependent components are the most

important mechanisms for cohesive soils. Inertial forces were incorporated in the wedge analysis of a soil cutting. The model resulted in reasonable predictions when compared with respect to the experimental draft of flat tools cutting sand reported by Luth and Wismer (1971) and the maximum verified speed was about 3 m/s. Predictions presented approximately 25% error with respect to the measured draft at a speed of 2.5 m/s.

Chi (1989) suggested a mathematical model to include dynamic effects in the original formulation of the nonlinear elastic model. Inertial components were added in the general equation of equilibrium of the soil as:

$$\frac{\partial \sigma_{ij}}{\partial x_j} - f_i = \rho \frac{\partial^2 u_i}{\partial t^2} \tag{2.34}$$

where:

f_i = body force vector (kN/m^3),

u_i = displacement vector of soil element (m),

ρ = soil density (kg/m^3),

t = time (s),

x_j = particle coordinates (m).

For an incremental procedure the acceleration force term can be written as follows:

$$\frac{\partial^2 u}{\partial t^2} = \frac{\partial}{\partial t}\left(\frac{\partial u}{\partial t}\right) = \frac{\partial}{\partial t}\left(\frac{\Delta u}{\Delta t}\right) \tag{2.35}$$

where:

Δu = vector of displacement increment (m).

For solution of the dynamic equations in time a Newmark integration method (Newmark 1959) can be adopted. Bathe (1982) presented the procedure to solve dynamic cases.

Zeng and Yao (1992) developed a soil cutting model to predict forces on wide and narrow tools. The model incorporated shear rate effects on soil shear strength, soil-metal friction and soil inertial effects. Comparison between prediction and experimental values indicated that results were acceptable. Some important features of this model were as follows: a) soil-metal friction and shear strength were not affected by shear rate; b) the model is not applicable for soils that flow plastically; rather, a limiting stress condition of Coulomb material is assumed at failure; c) shear rates were incorporated as:

$$\ln \tau = C_1 + C_2 \ln \dot{\gamma} + C_3 \ln(1 + C_4 \sigma_n) \tag{2.36}$$

where:

C_1, C_2, C_3, C_4 = soil parameters,

τ = shear stress (kPa),

$\dot{\gamma}$ = shear rate (s^{-1}),

σ_n = normal stress pressure (kPa).

and, d) soil-metal effects of shear rates were incorporated by the following normalized equation:

$$f_p = C' + A' \ln\left(1 + \frac{v}{v_0}\right) + \sigma_n \tan\phi_a \tag{2.37}$$

where:

C', A', ϕ_a = soil-metal parameters,

61

v_0 = initial set sliding speed (m/s),

v = current speed of soil along soil-tool interface (m/s),

f_p = soil-metal shear (kPa).

Davis and Mullenger (1978) proposed a theoretical rate-type constitutive relationship for the critical state soil mechanics, opening the possibility of incorporation of dynamic effects in critical-state models. However, theoretical aspects and a fast and practical determination of soil parameters remain to be solved.

Xie and Zhang (1985) investigated a soil-tool dynamic system using an elastoplastic cap model with incorporated strain rate effects. The model was implemented in a three-dimensional finite element program. A true triaxial test device and a dynamic shear device were used to obtain soil parameters. An updated Lagrangian approach was used to deal with large deformations. Predictions seemed to follow experimental data quite well. Maximum speed range was 1.4 m/s.

Shen and Kushwaha proposed a model for the solution of the dynamic cutting problem for agricultural tool operations (Shen and Kushwaha 1995b). A nonlinear elastic soil constitutive relationship, the Duncan and Chang (1970) formulation, was adopted. Strain rate effects were incorporated in the tangent modulus of elasticity E_t. Based on Qun and Shen's (1988) work on rheological properties of wet soils, an equation was proposed to modify the Mohr-Coulomb failure criterion and incorporate rate effects as follows:

$$(\sigma_1 - \sigma_3)_f = (\sigma_1 - \sigma_3)_{f0} + B_s \ln\left(\frac{\dot{\varepsilon}}{\dot{\varepsilon}_0}\right) \qquad \text{for } \dot{\varepsilon} > \dot{\varepsilon}_0$$

$$(\sigma_1 - \sigma_3)_f = (\sigma_1 - \sigma_3)_{f0} \qquad \text{for } \dot{\varepsilon} \leq \dot{\varepsilon}_0$$

(2.38)

with,

$$(\sigma_1 - \sigma_3)_{f0} = \frac{2c\cos\phi + 2\sigma_3 \sin\phi}{1 - \sin\phi}$$

(2.39)

where:

$(\sigma_1 - \sigma_3)_{f0}$ = Mohr-Coulomb failure criteria at a reference strain rate $\dot{\varepsilon}_0$ (kPa),

$\dot{\varepsilon}$ = current strain rate of a soil element (s^{-1}),

$\dot{\varepsilon}_0$ = reference strain rate (s^{-1}),

B_s = coefficient of the modified Duncan and Chang model for soil (kPa).

After substitution of equation 2.38 in the original equation for E_t (equation 2.25) the final expression for E_s is as follows:

$$E_s = Kp_a \left(\frac{\sigma_3}{p_a}\right)^n \left[1 - \frac{R_f(1 - \sin\phi)(\sigma_1 - \sigma_3)}{2c\cos\phi + 2\sigma_3 \sin\phi + B_s(1 - \sin\phi)\ln(\frac{\dot{\varepsilon}}{\dot{\varepsilon}_0})}\right]^2 \text{ for } \dot{\varepsilon} > \dot{\varepsilon}_0$$

$$E_s = Kp_a \left(\frac{\sigma_3}{p_a}\right)^n \left[1 - \frac{R_f(1 - \sin\phi)(\sigma_1 - \sigma_3)}{2c\cos\phi + 2\sigma_3 \sin\phi}\right]^2 \text{ for } \dot{\varepsilon} \leq \dot{\varepsilon}_0$$

(2.40)

Kushwaha and Shen (1995) reportedly used the Newton-Raphson method to solve for material nonlinearity, and an updated Lagrangian method for geometric nonlinearities. They reported the use of an incremental and iterative algorithm to solve the dynamic equilibrium equation (Shen and Kushwaha 1995b). Soil parameters were obtained from a series of quasi-static and fast triaxial tests.

63

2.5 Soil Parameters

Material parameters have to be identified for any application of constitutive material modeling. The values of these parameters must be determined experimentally (Haupt 1993). Idealizations and simplifying assumptions are required to obtain experimental identification of material parameters. Specimens are usually assumed to develop homogeneous states of stress and strain; however, this is not always a reasonable assumption. The material test specimen is seen as an 'operator' which associates an output process to each input process. Frequently, the input/output processes can also be conveniently presented by stress-strain curves.

2.5.1 Dynamic soil properties

Gill and Vanden Berg (1968) defined dynamic properties of soil as properties which manifest through movement of soil. Movement has to occur for these properties to be determined. However, it does not necessarily have to be time-dependent. Relations relating applied soil forces and deformations might be considered as dynamic soil properties. It is difficult to study dynamic reactions because measurements must be done during the action. Moreover, placement of equipment into a soil mass may alter soil reactions.

The crux in soil dynamics is to identify and measure idealized soil mechanics parameters. Therefore, dynamic parameters have to be measured in order to develop soil-machine system descriptions and relationships.

Mathematical relations can describe relations between stresses and strains. Appropriate stress-strain mathematical relationships are a first step in describing soil reactions due to tillage tool forces. For example, the simple linear elastic isotropic theory describing stress-strain relations can relate stress to strain using only two parameters. These two parameters measure the nature of the material and can be considered dynamic properties of the material. In the same way, the basic Duncan and Chang (1970) model has six parameters.

In other words, dynamic properties of soil can only be determined if a suitable stress-strain relation, which in turn determines soil parameters, is identified. For instance, c and ϕ are dynamic soil parameters determined experimentally on the assumption that the Mohr-Coulomb relationship describes soil failure data. Thus, they are not real physical properties of the soil as has been frequently stated, but curve-fitting parameters.

Chancellor (1994) reported many advances in measuring soil dynamic properties since the Gill and Vanden Berg (1968) publication. Over the last 25 years, there has been a remarkable improvement in equipment and instrumentation.

When rigid bodies of soil move or have contact with tool surfaces, the analysis is simplified. Properties like friction, adhesion and abrasion can be more easily determined.

Separating properties into static and dynamic components is one way to characterize soil. A dynamic property originates from the response of applied forces to soil, which include movements. Static properties are defined as those that exist even when forces are not acting on the body. Static properties do not have to remain constant when

the body is moving in the same way dynamic properties do not have to change when the body is moving.

Some dynamic properties might not be readily mathematically modeled. In such cases a rough description of these phenomena in an empirical form is adopted. An example is the measurement of shattering or rupture of soil, often called pulverization. The mean weight diameter method (MWD) is a common empirical way to characterize the soil structure. For such cases more development is needed in the theoretical aspects.

Hassan and Chancellor (1970) measured viscoplastic characteristics of saturated clays. They found linear relationships between stress and strain rates. Highest measured strain rate values were about 2 s⁻¹. The viscosity term was defined as the slope of the stress-strain rate graph.

Kocker and Summers (1988) were able to identify dynamic parameters of one-dimensional second order viscoelastic model using cylindrical soil samples. One end was vibrated at sonic frequencies and accelerometers were placed on the ends of the samples.

Remarkable advances have been made in the formulation of new constitutive relationships for soil and the solution of differential equations by numerical methods (commonly, the finite element method) to determine model parameters. Making use of numerical tools such as response surface methodology and finite element methods, a method called "inverse method" has been used in engineering to determine model material properties. Upadhyaya (1993) and Rubinstein and Upadhyaya (1994) used this approach to identify in-situ soil properties. First, a mathematical soil relationship is assumed and a response surface is generated through orthogonal regression and a finite element solution

technique. Soil field data are then measured and used to match the response surface through the use of optimization algorithms. Model parameters are "calibrated" in this way. This procedure overcomes the drawback of using remolded samples in laboratory tests which present some differences from field cemented soils. Therefore, in-situ soil properties can be accessed. The idea is to create a response surface once and then simply use it.

2.5.2 High speed triaxial tests

Many problems in engineering practice require the knowledge of soil properties of dynamically loaded soils. The primary intention of fast triaxial tests is to apply a load at similar rate to that a soil element would encounter during applications such as tillage. It follows then that strain rates should reach levels on the same order of magnitude as the soil dynamically loaded by a tool at fast speed of operation.

There are, however, a few difficulties associated with fast triaxial testing:

i) To reach fast and constant speed of soil specimen loading for a short specimen, usually no longer than 100 to 150 mm, will require development of the specific equipment.

ii) With the shock wave blast imposed upon the specimen, a homogeneous stress and strain distribution cannot be expected inside the specimen (as an illustration, for a rapid axial load of a brass rod, more deformation occurs close to the application of the ram than in the rest of the specimen, due to viscoplastic effects).

iii) Remolded soils in triaxial cells do not behave the same as in situ soils for quasi-static tests. For dynamic cases the differences might be enlarged. The energy and confining conditions imposed upon the specimen boundary from pressurized air or water, is far different than that imposed by surrounding soil mass. Different mechanisms act in real soils and in triaxial cells (Chancellor and Upadhyaya 1994). It would be of value if these mechanisms could be incorporated in triaxial cells. It is, therefore, not likely that fast triaxial cells will represent soil behaviour as it behaves in the field, unless sophisticated analytical corrections are made to interpret fast soil triaxial tests. However, a soil model has to be assumed in anticipation for such an analysis. No studies have been reported to support the correlation of the use of fast triaxial cell tests with agricultural field tests.

Das (1993) conducted static and dynamic unconsolidated undrained triaxial tests for saturated clay soils. The experimental results of an axially loaded soil specimen showed increases in deviatoric stress with increased axial strain rates (Figure 2.13).

Yong and Japp (1968) studied clay soil specimens under impulsive loading undergoing large strain deformations. Their primary objective was to determine material parameters and material behaviour. It appeared that loading rate was too high for the specimen to deform in response. Therefore, a moving shock front was created and changed strength of the material. This triaxial test study paid special attention to transverse and longitudinal inertial effects, to the formulation of a flow law and to the dynamic yielding. Corrections were made to account for the mass of the loading cap and acceleration sensitivity of the force transducer. A uniform strain field was assumed. Compressed air was the confined medium, used to avoid pressure drop due to volume variation during the entry of the loading piston. Results were analyzed in terms of total

$\sigma_1 - \sigma_3$
(kPa)

200

Water content = 33.5 ± 0.2 %

$\sigma_3 = 96$ kPa

150

$\dot{\varepsilon} = 314$ % / s
and 426 % / s

128 % / s

53.6 % / s

100

14.4 % / s

4.76 % / s

0.033 % / s

50

0

0   4   8   12

Strain, ε (%)
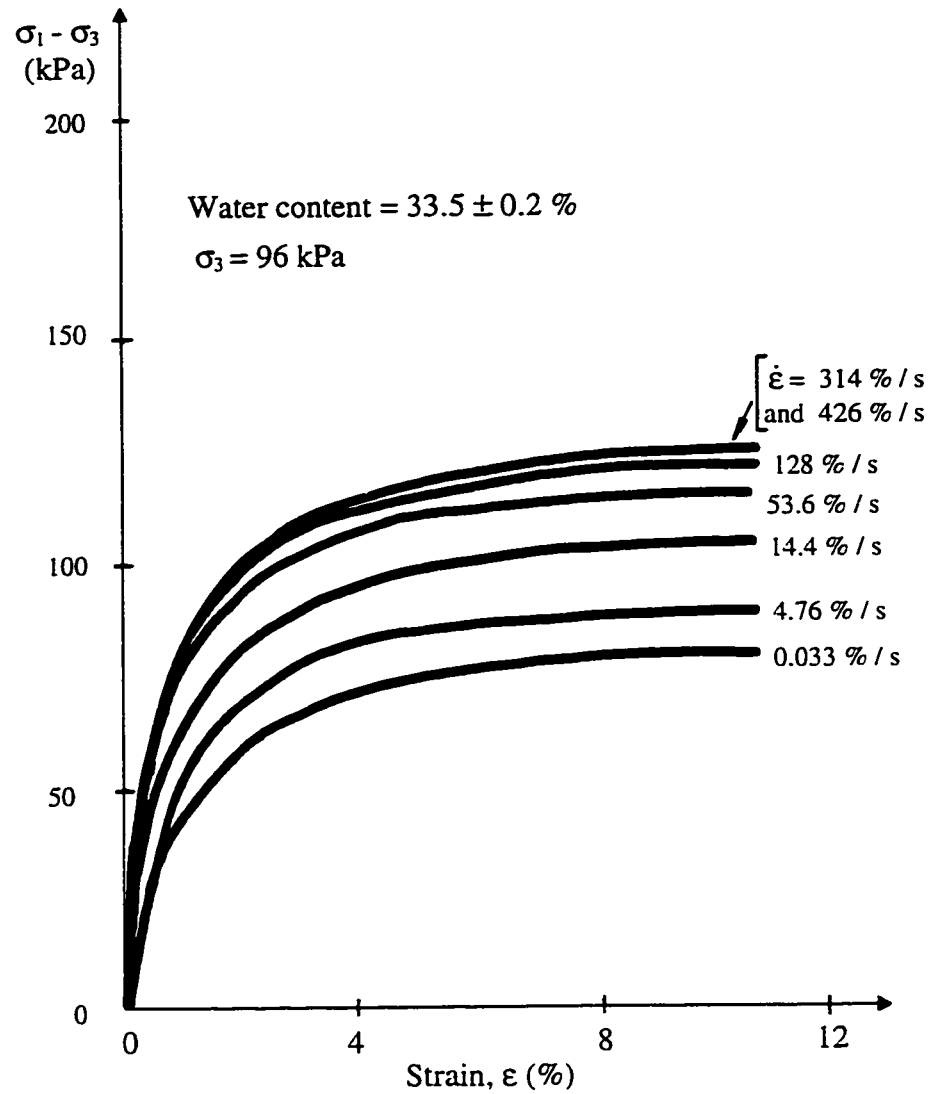
Figure 2.13 **Static and dynamic unconsolidated undrained triaxial tests for**

saturated clay soils (after Das 1993).

stresses only, due to short term of failure and large hydrodynamic lag in pore pressure measurement. They also mentioned that the system performed adequately for loading velocities in excess of 0.25 m/s and the machine was capable of delivering uniform loading velocities of up to approximately 12.7 m/s. Strain rates were in the range of 1 to 20 s^{-1}.

Many simplifying assumptions were made: body forces were neglected; soil remains saturated; velocity fields at quasi-static case, with negligible inertia, could represent dynamic situations; perfect plastic material flow (no variation of volume, which is reasonable for a wet clay); circumferencial specimen velocity equals zero; and, isotropy. Large displacements (Eulerian strains) were considered in the formulation.

Test results showed increased strain rates produced increasing deviatoric stresses (Figure 2.14). A strain rate $\dot{\varepsilon}_0$ was taken as a reference. The graph showed deviatoric stresses had linear relationship with logarithm of the ratio between actual strain ratio and the reference one. The instantaneous dynamic stress, $\sigma(\varepsilon,\dot{\varepsilon})$, was given as:

$$\sigma(\varepsilon,\dot{\varepsilon}) = \sigma_0(\varepsilon,\dot{\varepsilon}_0) + \Psi(\varepsilon)\log(\frac{\dot{\varepsilon}}{\dot{\varepsilon}_0})$$
(2.41)

where:

$\sigma(\varepsilon,\dot{\varepsilon})$ = instantaneous dynamic stress (kPa),

$\sigma_0(\varepsilon,\dot{\varepsilon}_0)$ = base value for dynamic stress, at base strain rate (kPa),

$\Psi(\varepsilon)$ = stress state parameter dependent on material (kPa),

$\dot{\varepsilon},\dot{\varepsilon}_0$ = strain rate and reference strain rate, respectively (s^{-1}).
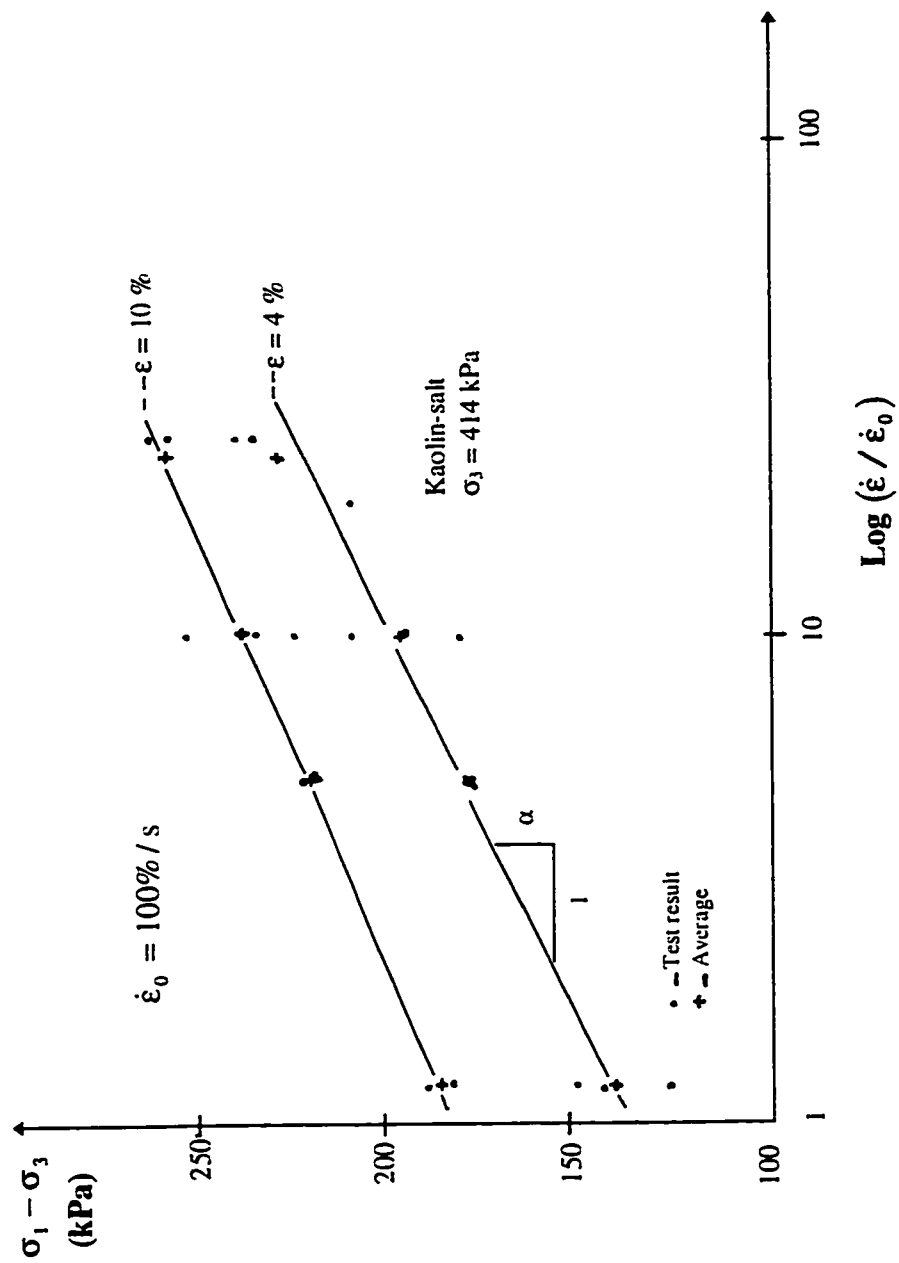
Figure 2.14 Increased strain rates produced by increasing deviatoric stresses, obtained from high speed triaxial tests for wet clay soils (after Yong and Japp 1968).

71

The calculated velocity of shock wave front indicated a region of instability when the velocity of loading approached this velocity. This velocity was about 0.38 m/s for the oil base clay used by Yong and Japp (1968) (Figure 2.15).

High speed compression tests have been reported by Kawamura (1985), but no details of experiments were supplied. Breaking stresses increased with logarithm of speed up to a maximum of 1 to 3 m/s.

Niyamapa and Salokhe (1992) conducted triaxial experiments in unsaturated soils under undrained conditions. Speed of loading was from 0.35 to 6.2 m/s. Pressurized air was used to produce a confining pressure. Forces at lower and upper parts of the specimen were measured. For the high speed test the stress was not transmitted at once to all parts of the test specimen. They noted that the peak axial stress at the lower force transducer appeared at 7.8% axial strain, but at 11.6% strain at the upper transducer.

Change in mode of soil failure from brittle to plastic flow at 4.4 m/s for the sandy loam and 5.7 m/s for the silty loam was reported by Niyamapa and Salokhe (1992). The energy per volume used to break soil specimens at different water contents increased rapidly with speed up to 4.5 m/s and then decreased. The energy for breaking sandy loam soil decreased with increase in water content; however, the energy for breaking sandy loam soil at 20.8% water content at 4.8 m/s was 87% higher than the quasi-static test at similar conditions. General shear mode of failure and fragmentation were observed in the brittle case. Fragmentation refers to soil specimen failure at numerous slip planes. Under high speed, small cracks and fluidization were also observed.
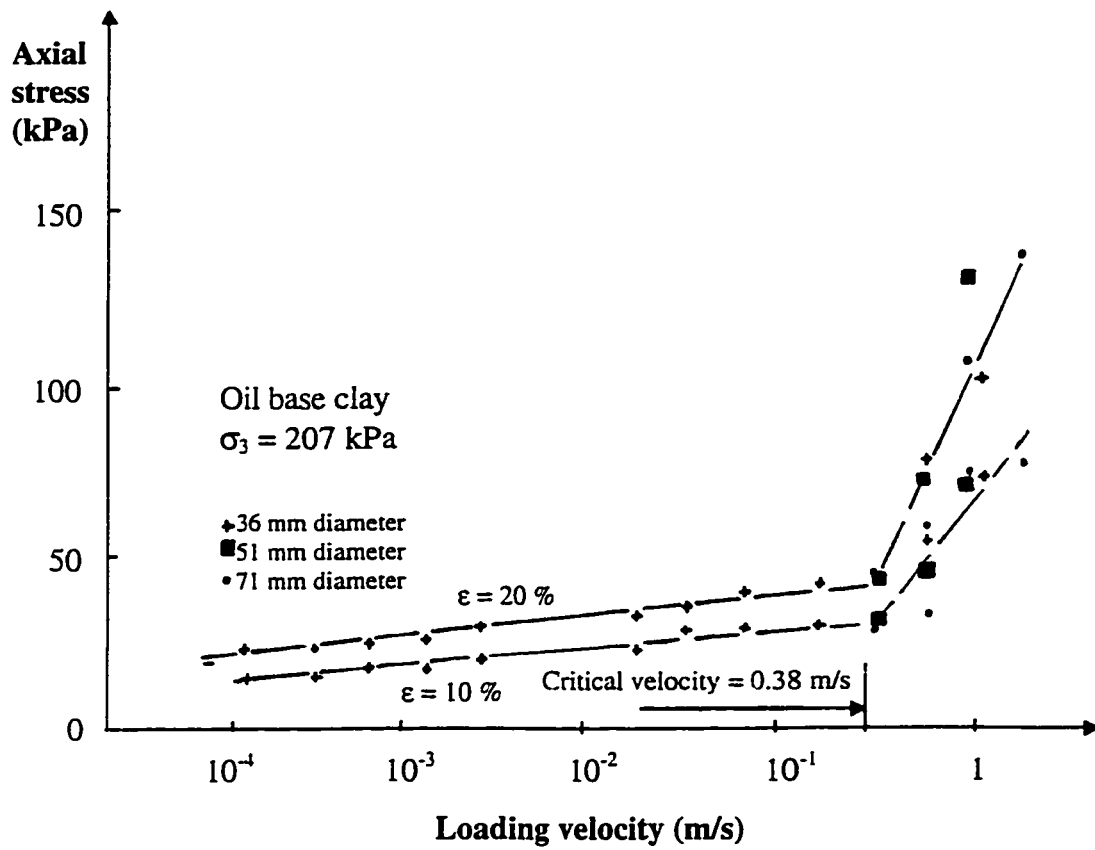
Figure 2.15   **Calculated velocity of a shock wave indicates a region of instability**

when the velocity of loading approaches a critical velocity, obtained

from high speed triaxial tests for wet clay soils (after Yong and Japp

1968)

Shen and Kushwaha (1995b) proposed an equation similar to equation 2.41:

$$(\sigma_1 - \sigma_3)_f = (\sigma_1 - \sigma_3)_{f0} + B_s \ln(\frac{\dot{\varepsilon}}{\dot{\varepsilon}_0}) \qquad (2.42)$$

where:

B_s = strain-rate dependent coefficient of maximum stress difference (kPa).

Triaxial tests of specimens under displacement rates from 0.002 mm/s up to 12 mm/s were performed (Shen and Kushwaha 1995b). Pressurized water was used to provide the confining pressure.

2.5.3 Standard reference tool concept

The development of reference tillage tools to determine a dynamic soil strength parameter was suggested by Upadhyaya (1984). The standard reference tool concept is meant to characterize dynamic soil conditions based on a standard tillage tool acting as an analog device. Standard reference tools have been developed to predict draft implement requirements in any soil condition based on reference tillage tools run at a desired location (Glancey and Upadhyaya 1990).

Glancey et al. (1996) predicted draft requirements of an implement based on standard tillage tool drafts obtained in a particular soil condition. The standard reference tool acted as an analog device to characterize dynamic conditions of the soil. Configurations of standard tools used for prediction did not significantly affect draft prediction. The prediction procedure required testing in many soil conditions. Three implements were used, namely, a subsoiler, moldboard plow and chisel plow.

Upadhyaya (1984) used dimensional analysis and mechanics to develop a prediction equation for tillage tool draft. The expression of draft also included a 'dynamic cone index' and speed of operation. A reference tool was proposed to measure dynamic cone index. The developed equation can be expressed as:

$$\left(\frac{H}{C_i^d w^2}\right) = \left(\frac{d}{w}\right)\left[B_1 + B_2\left(\frac{\rho S^2}{C_i^d}\right)\right]$$

(2.43)

Where: H is the draft [F], C_i^d dynamic cone index [F·L^{-2}], d depth of operation [L], w width [L], S speed [L·T^{-1}], ρ bulk density [M·L^{-3}], and B_1 and B_2 are geometry-dependent factors.

Applying equation 2.43 to a reference tool of width w and rake angle α yields:

$$\left(\frac{H}{wd}\right)^r = B_1^r C_i^d + B_2^r \rho S^2$$

where the superscript r stands for reference implement. Defining $B_1^r \equiv 1.0$ gives:

$$\left(\frac{H}{wd}\right)^r = C_i^d + B_2^r \rho S^2$$

(2.44)

For a selected implement (other than the reference tool):

$$\left(\frac{H}{wd}\right)^r = B_1 C_i^d + B_2 \rho S^2$$

(2.45)

Eliminating C_i^d from equations 2.44 and 2.45 results in:

$$\left(\frac{H}{wd}\right) = B_1\left(\frac{H}{wd}\right)^r + \left(B_2 - B_2^r\right)\rho S^2 = B_1\left(\frac{H}{wd}\right)^r + B_2' \rho S^2$$

(2.46)

where $B_2' = B_2 - B_2^r$. Equation 2.46 can be used to estimate the specific draft of a desired tool based on the measurement of the specific draft of the reference tool at a specific

speed of operation. Thus, the specific draft of a reference tool at the adopted operating speed is used as an indicator of the dynamic cone index of the soil.

Desbiolles et al. (1994a) developed a methodology based upon empirical prediction relationships of draft forces of primary tillage tools obtained by Godwin and Spoor (1977). A standard tine was used as a reference tool, and based upon calculated indices the actual field tool draft was predicted. The reference tool used was a simple $45°$ rake angle, 70 mm wide tine, working at 0.44 m/s. The methodology was based on a draft force of a standard-tine, H^r:

$$H^r = SSF \times TGF \tag{2.47}$$

where:

SSF   = soil strength factor,

TGF   = tine geometrical factor.

The 70 mm wide tine was used as a measuring device to measure the soil strength factor of the soil at a desirable depth. The tine geometrical factor was theoretically determined. An index I, assumed constant for a specified depth, related predicted and standard tine draft:

Predicted tool draft = I x Standard-tine draft

where:

$$I = \frac{GF_{tool}}{TGF} \tag{2.48}$$

GF_{tool} = geometrical tool factor.

The tine geometrical factor TGF can be determined theoretically for the standard-tine based on Godwin and Spoor (1977). A novel approach was achieved to empirically

predict tool draft based on a standard tool concept used as reference. The tool indirectly estimated soil strength. Results showed fairly good correlation, in the order of errors of 20%, for full tillage implements. In contrast, an extended study by Desbiolles et al. (1994b) in which a cone penetrometer was used instead of a standard tool, produced poorer predictions. Although satisfactory for sandy loam soils (predictions within 20%), predictions errors for clay soils were on the order of 40%.

2.6 Summary of Literature

Soil openers are widely employed on dry land tillage equipment in the prairies. Conservation tillage practices use openers intended to produce very little soil disturbance. In general, such openers are narrow tools and there has been increasing interest in their performance.

While quasi-static mechanics for prediction of soil-tool performance are well developed, the science of soil-tool dynamic performance has not progressed much. Typically, tool performance data show draft increasing with increases in speed. Wet soils may show draft leveling off with speed. Failure energy per unit soil volume also increases up to certain speeds. Soil disturbance and pulverization are also reported to increase with increase in tool speed.

A general unified theory of material behaviour which could be used to model soil behaviour is not currently available. Instead, specialized theories for various materials have been developed. Models of dynamic soil behaviour have involved: i) incorporating dynamic components, i.e., inertial and strain rate effects, in the formulation of a hypoelastic material; ii) viscoelasticity; and, iii) viscoplasticity.

Hypoelasticity represents one of the simplest theories available to be implemented in a computer code. However, numerical instabilities may occur once soil behaviour approaches failure. The nonlinear elastic soil model proposed by Duncan and Chang (1970), which represents a simple form of hypoelasticity, incorporates a Mohr-Coulomb failure criterion. Incorporation of dynamic components in this model can be readily facilitated. The more specialized theories of viscoelasticity and viscoplasticity increase the degree of difficulty in modeling soil.

Care must be taken when interpreting high speed triaxial test data. Energy transferred to specimen surroundings might be expressed in a different form than behaviour in the field. Soil parameters can be obtained in situ by using standard reference tools. Standard reference tools are used as analog devices to characterize undisturbed dynamic soil parameters. One advantage of this approach is that high speed triaxial tests can be avoided and soil in-situ conditions can be tested.

CHAPTER 3

MATHEMATICAL MODEL DEVELOPMENT

This chapter describes the development of a mathematical model of soil being cut by a tool running at a constant speed. The first step, as in any evaluation of soil-tool interaction, is the mathematical idealization of the system. A general equation developed from continuum mechanics principles is introduced to represent the problem. The equation is nonlinear and capable of representing large displacements, large strains and material nonlinearities. To solve the equation, it is linearized and an approximate solution is developed using the finite element method in an incremental procedure. In the procedure, the total load is applied in increments. Large displacements are implemented using an updated Lagrangian method, and material nonlinearities are used iteratively in a modified Newton-Raphson method.

The soil constitutive relationship, which will contribute to the finite element stiffness matrices, is for a hypoelastic material with strain rate effects incorporated in its formulation. Appropriate assembling matrices are derived for the implementation of the finite element method solution. Eight node isoparametric elements are used to discretize the continuum. Applied body forces include inertia forces in the dynamic analysis. A numerical time integration scheme is required for the dynamic analysis. Newmark's constant-average-acceleration (unconditionally stable) scheme is adopted in this study. Damping effects are also considered. Mass matrices are implemented in a lumped form.

The solution is implemented using a FORTRAN computer code. The computational algorithm, including flow charts and the program structure, is described.

3.1 Soil Narrow Tool Idealization

To make a mathematical solution of soil-tool interaction possible, some idealizations of the soil-tool system are necessary. The following assumptions were made:

1) The tool is narrow, rigid, and working at a constant depth in the soil with a constant velocity (Figure 3.1). According to quasi-static theory, valid for low speeds of operation, side effects are significant for the draft evaluation of a narrow tool and so cannot be neglected. This means that a three-dimensional model must be considered.

2) The physical symmetry of tools used in this study can be used to simplify the numerical solution using the finite element method. A symmetric mesh discretization reduces the number of elements by half and the degrees of freedom by almost a half. This means that computation time and memory are significantly reduced. Final draft prediction must be doubled when comparing the computational solution with experimental tool data.

3) Since the tool stiffness is many orders of magnitude greater than soil stiffness, for a given force tool deflections are negligible in comparison to soil deformation. Thus, representation of tool solid elements need not be included in the analysis. Instead, tool shape and reactions can be modeled by rigid prescribed displacement nodes in the finite element analysis.
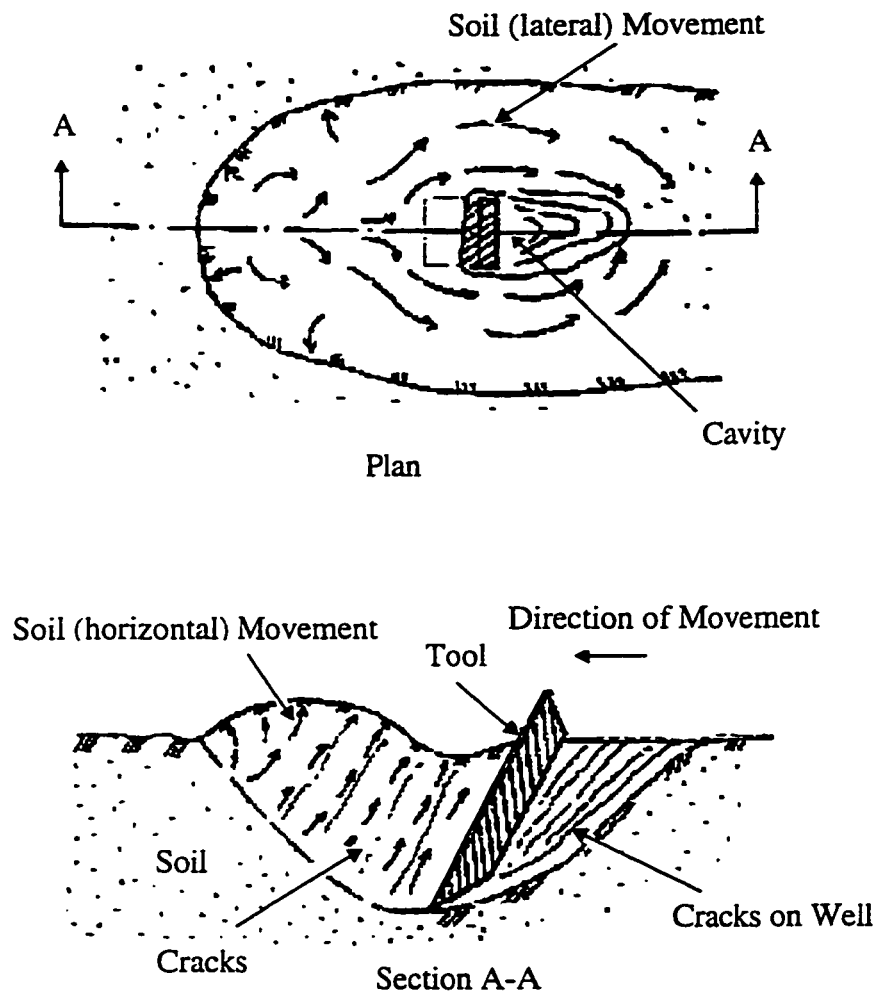
Figure 3.1   Soil tool idealization (after Desai and Phan 1980).

4) A 'smooth' surface is expected to better represent the soil-tool surface than a 'rough' interface. Precise modeling of the soil-tool surface would require the formulation of interface elements and the determination of interface properties under static and dynamic cases, substantially increasing the work in determining model parameters. Alternatively, contact or gap elements may be used to even further refine analysis and improve predictions (Byrne 1987). In this study, however, the soil-tool interface is assumed to be either a totally smooth or a totally rough surface, to simulate the extreme cases.

5) The soil is idealized as an isotropic and homogeneous continuum. Soil particles are idealized as lumped masses. The soil constitutive relationship is non-linear and with strain rate dependency. Thus, the effect of different tool operating velocities on tool reactions may be investigated.

6) Soil body forces are neglected since it is assumed that shallow soil would produce negligible contribution to draft when compared to inertial and strain rate effects or soil stiffness contributions. Inertial forces are considered in the model development.

3.2 Governing Equations

In this section nomenclature and general continuum mechanics equations that represent the cutting problem are introduced. Then, an approximate finite element solution and matrices are derived. Appendix A presents a review of tensors and the tensor notation used in this section.

The motion of a body in a Cartesian system of coordinates is illustrated in Figure 3.2. Assume that all static and kinematic solutions are available for time 0 to time t, and the solution for t+Δt is required.

Nomenclature

The notation uses left superscripts to refer to the body configuration in time and right subscripts to indicate the coordinate axis. For instance, $^{t+\Delta t}x_l$ refers to the coordinates of the body in relation to the axis 1 at time t+Δt. A left subscript indicates the configuration with respect to which the quantity is measured (Bathe et al. 1975). The notation for displacements is similar; for instance, when the quantity is related to some reference (see below).

Some definitions for strains and stresses are now introduced:

The Green-Lagrange strain tensor is defined by (Kardestuncer and Norrie 1987):

$$E_{ij} = \frac{1}{2}(u_{i,j} + u_{j,i} + u_{k,i}u_{k,j}) \qquad (3.1)$$

When displacements and their gradients are infinitesimal, the strain tensor (equation 3.1) may be approximated as:

$$\varepsilon_{ij} = \frac{1}{2}(u_{i,j} + u_{j,i}) \qquad (3.2)$$

The tensor ε_{ij} is referred to as Cauchy's infinitesimal strain tensor. Cauchy's stresses τ_{ij} are defined by :

$$df_i = (dA)n_j\tau_{ji} \qquad (3.3)$$
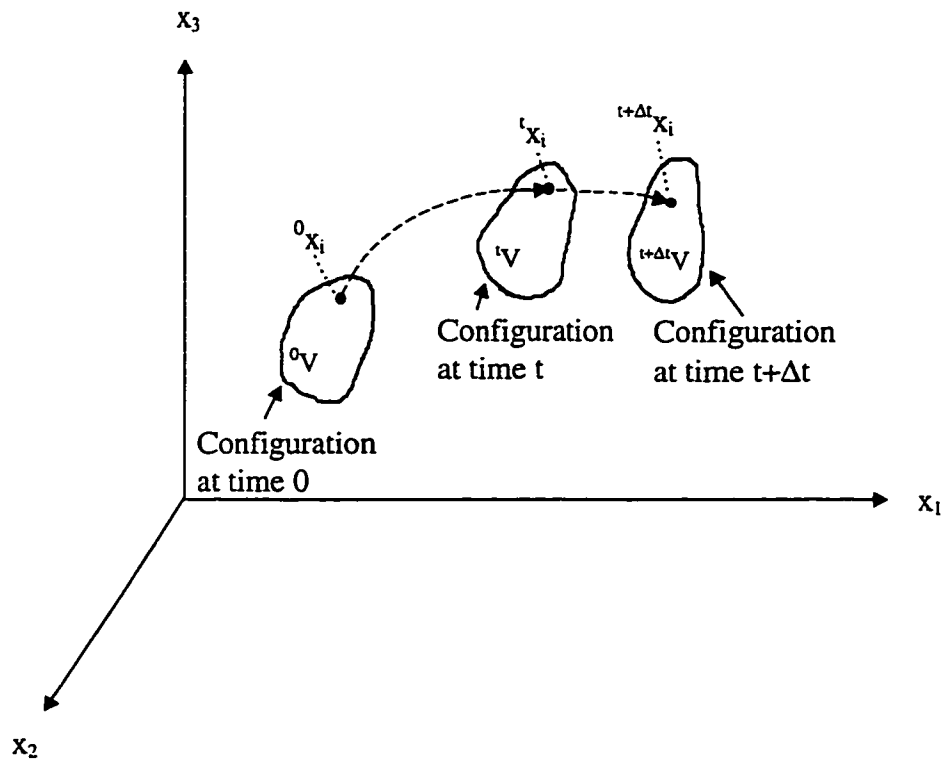
Figure 3.2 **Motion of a body in the Cartesian system of coordinates (after Bathe et al. 1975).** A consistent notation is used for coordinates, displacements, strains, stresses and applied forces. A left superscript indicates the configuration in time in which the quantity occurs; a left subscript indicates with respect to which configuration in time the quantity is measured (not shown); and the right subscript refers to the coordinate axis.

where dA is a differential area in a deformed body, n_j the direction cosines of a unit outward normal to dA, and df_i a differential force acting on this area. The Cauchy stress and strain thus simply refer to the stress or strain of the body at a particular configuration (Figure 3.2).

In contrast, the 2nd Piola-Kirchhoff stress tensor, S_{ij}, corresponds to the configuration $(t + \Delta t)$ of a deformed body in relation to a reference configuration t :

$$ {}^{t+\Delta t}_{t}S_{ij} = \frac{{}^{t}\rho}{{}^{t+\Delta t}\rho} \, {}_{t+\Delta t}x_{i,s} \, {}^{t+\Delta t}\tau_{sr} \, {}_{t+\Delta t}x_{j,r} \tag{3.4} $$

where:

$^{t}\rho, {}^{t+\Delta t}\rho$ = mass density at a configuration t and $(t + \Delta t)$, respectively (kg/m^3),

^{t}x = Cartesian coordinate at configuration t (m),

$^{t+\Delta t}\tau_{sr}$ = Cauchy's stress tensor at configuration $(t + \Delta t)$, i.e., the stress if the reference configuration is the current configuration (kPa).

For example, using the above conventions, the Cauchy infinitesimal strain tensor components referred to configuration $(t + \Delta t)$ are denoted by ${}_{t+\Delta t}\varepsilon_{ij}$, while the Green-Lagrange strain tensor at $(t + \Delta t)$ with reference to time t is denoted by ${}^{t+\Delta t}_{t}E_{ij}$. For infinitesimal strains, the Cauchy and Green-Lagrange strains are identical. The reference configuration used for applied forces, and for both 2nd Piola-Kirchhoff and Green-Lagrange strains, is typically time t as denoted by the left subscripts in equation 3.4.

Large deformations

The soil cutting problem with a narrow tool involves large soil displacements. General formulations which incorporate large displacements, large strains and material nonlinearities are presented by Bathe et al. (1975) and Desai and Phan (1980). In the present study an updated Lagrangian or Eulerian configuration is developed to analyze large deformations.

The formulation follows an incremental procedure. Once all discrete time points 0, Δt, $2\Delta t$, ..., t have known solutions, the principal of virtual work is used to solve for unknown static and kinematic variables, such as displacements, velocities and accelerations in the $t+\Delta t$ configuration. The objective is to evaluate the equilibrium positions of the body at discrete points 0, Δt,...,t , $t+\Delta t$... where Δt is an increment in time. The equilibrium of the body in the $t+\Delta t$ configuration is expressed as:

$$\int_{t+\Delta t_V} {}^{t+\Delta t}\tau_{ij}\, \delta^{\bullet}{}_{t+\Delta t}\varepsilon_{ij}\, ({}^{t+\Delta t}dV) = \int_{t+\Delta t_A} {}^{t+\Delta t}_{t+\Delta t}t_k\, \delta^{\bullet}u_k\, ({}^{t+\Delta t}dA)$$

$$\hspace{3cm} (3.5)$$

$$+ \int_{t+\Delta t_V} {}^{t+\Delta t}\rho\, {}^{t+\Delta t}_{t+\Delta t}f_k\, \delta^{\bullet}u_k\, ({}^{t+\Delta t}dV)$$

where $\delta^{\bullet}u_k$ is a variation in the current displacement components ${}^{t+\Delta t}u_k$, $\delta^{\bullet}{}_{t+\Delta t}\varepsilon_{ij}$ are the variations in strains, and

ρ $\quad$ = mass density $[M{\cdot}L^{-3}]$,

t_k $\quad$ = surface force vector $[F{\cdot}L^{-2}]$,

A $\quad$ = boundary surface of the element $[L^2]$,

V $\quad$ = element domain $[L^3]$,

86

f_k = body force vector [F·M^{-1}].

Loading is assumed independent of the configuration of the soil body. Incremental stress is decomposed as,

$$\substack{t+\Delta t \\ t}S_{ij} = {}^t\tau_{i,j} + {}_tS_{ij} \tag{3.6}$$

The constitutive relationship can be written:

$${}_tS_{ij} = {}_tC_{ijrs}\,E_{rs} \tag{3.7}$$

where:

C_{ijrs} = incremental constitutive (4th order) tensor.

Substituting equation 3.7 in equation 3.6 yields a nonlinear equation in the incremental displacements u_i:

$$\int_{{}^tV} {}_tC_{ijrs}\,E_{rs}\,\delta^{\bullet}E_{ij}\,({}^tdV) + \int_{{}^tV} {}^t\tau_{ij}\,\delta^{\bullet}{}_t\eta_{ij}\,({}^tdV) = \int_{t+\Delta t A} {}^{t+\Delta t}_{t+\Delta t}t_k\,\delta^{\bullet}u_k\,({}^{t+\Delta t}dA)$$
$$+ \int_{t+\Delta t V} {}^{t+\Delta t}\rho\,{}^{t+\Delta t}_{t+\Delta t}f_k\,\delta^{\bullet}u_k\,({}^{t+\Delta t}dV) \tag{3.8}$$
$$- \int_{{}^tV} {}^t\tau_{ij}\,\delta^{\bullet}{}_t\varepsilon_{ij}\,({}^tdV)$$

where; ${}^tV$ is the element domain in the configuration at time t, and $\eta_{ij} = \dfrac{1}{2}{}_tu_{k,i}\,u_{k,j}$.

Equation 3.8 is valid for large deformations.

Linearization of equilibrium equations

Equation 3.8 is nonlinear in displacement increments and cannot be solved directly; however, this equation can be linearized using the equality ${}_tE_{ij} = {}_t\varepsilon_{ij}$ for infinitesimal

strains, and $\delta^* {}_t E_{ij} = \delta^* {}_t \varepsilon_{ij}$ (where $\delta^* {}_t \varepsilon_{ij}$ is a variation in the current strain components).

This yields a constitutive relation in incremental form:

$${}_t S_{ij} = {}_t C_{ijrs} \varepsilon_{rs} \tag{3.9}$$

The approximate equilibrium equation to be solved is then:

$$\int_{{}^t V} C_{ijrs} \, \varepsilon_{rs} \, \delta^* \varepsilon_{ij} \, ({}^t dV) + \int_{{}^t V} {}^t \tau_{ij} \, \delta^* {}_t \eta_{ij} \, ({}^t dV) = \int_{{}^{t+\Delta t} A} {}^{t+\Delta t}_{t+\Delta t} t_k \, \delta^* u_k \, ({}^{t+\Delta t} dA)$$

$$+ \int_{{}^{t+\Delta t} V} {}^{t+\Delta t} \rho \, {}^{t+\Delta t}_{t+\Delta t} f_k \, \delta^* u_k \, ({}^{t+\Delta t} dV)$$

$$- \int_{{}^t V} {}^t \tau_{ij} \, \delta^* {}_t \varepsilon_{ij} \, ({}^t dV)$$

$$\tag{3.10}$$

Equation 3.10 is linear in terms of the incremental displacements. It is the basic equation used for the finite element analysis using small incremental strains in finite element methods (small discrete elements) for large deformations.

3.2.1 Finite element solution

In this section, the main focus is given to the presentation of matrices corresponding to a single isoparametric element in the local system of coordinates (i.e., in the element domain). Attention is also given to basic aspects of transformation of equations to the global domain to calculate volume integrations and strain displacement matrices. The objective is to develop stiffness matrices and load vectors to implement in a finite element solution of equation 3.10. The final assemblage of the stiffness and load vectors follow standard procedures for assembly of structure matrices, which can be

obtained in text books such as Zienkiewicz (1977), Bathe (1982) and others. For small strains, E_{ij} and ε_{ij} represent the same value, thus from now on we assume $E \equiv \varepsilon$.

Element domain formulations

A solution of equation 3.10 is developed here using a finite element method to obtain appropriate matrices. Eight node isoparametric elements are adopted for the continuum discretization (Figure 3.3). Any point in the isoparametric element can be expressed in terms of coordinate and displacement components at the nodes using the same interpolation functions. Thus, the coordinates at any point in the element can be expressed as:

$$x_i = \sum_{k=1}^{8} N_k \,^{t+\Delta t}x_i^k \tag{3.11}$$

where:

$^{t+\Delta t}x_i^k$ = coordinate at nodal point k with corresponding i direction, at

           configuration $t + \Delta t$ in the global system,

k   = nodal point,

N_k = interpolation function corresponding to nodal point k.

The shape function matrix for the current element is expressed as,

$$N = \begin{bmatrix} N_1 & 0 & 0 & N_2 & 0 & 0 & \dots & N_8 & 0 & 0 \\ 0 & N_1 & 0 & 0 & N_2 & 0 & \dots & 0 & N_8 & 0 \\ 0 & 0 & N_1 & 0 & 0 & N_2 & \dots & 0 & 0 & N_8 \end{bmatrix} \tag{3.12}$$

In global x_1 x_2 x_3 domain

In local r' s' t' domain
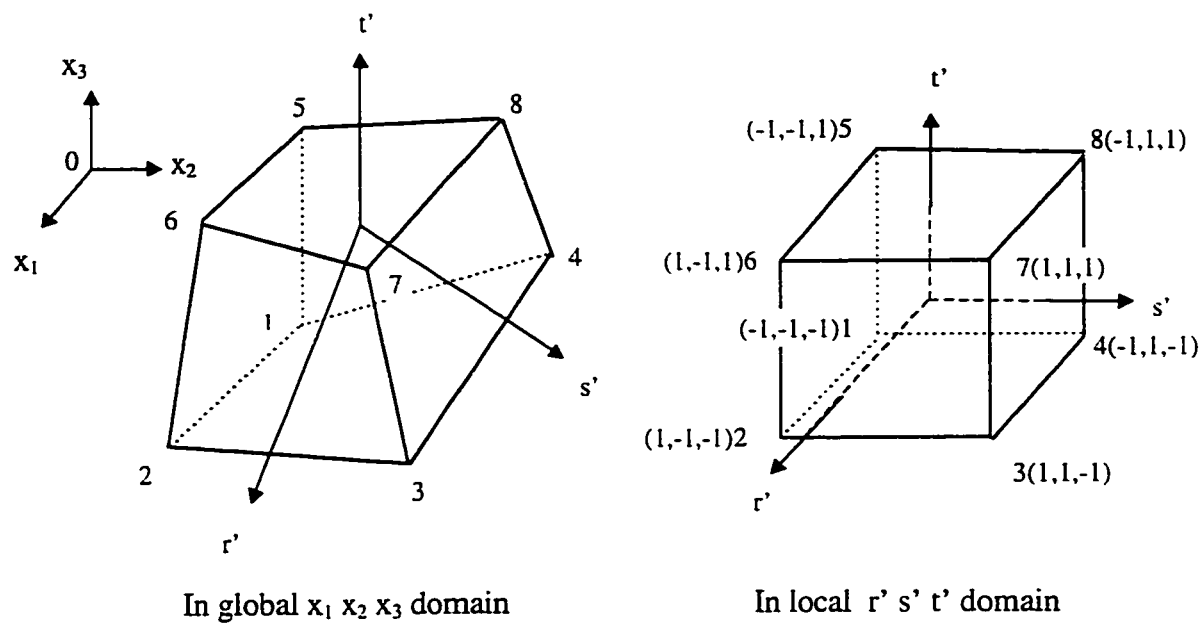
Figure 3.3 **Eight node isoparametric solid elements used for the three-dimensional finite element solution (after Rao 1982).**

where the shape functions N_j are obtained as (Desai and Abel 1972):

$$N_j(r',s',t') = \frac{1}{8}(1 + r'r_j')(1 + s's_j')(1 + t't_j') \quad j = 1 \text{ to } 8 \qquad (3.13)$$

where (r',s',t') are natural coordinates and (r_i',s_i',t_i') are natural coordinates of the hexahedron nodes in the local system (Rao 1982), (Figure 3.3).

The displacements **u** at any point in the element can also be expressed using interpolation functions, that is:

$$u_i = \sum_{k=1}^{8} N_k \,^{t+\Delta t} u_i^k \qquad (3.14)$$

where:

$^{t+\Delta t} u_i^k$ = displacement at nodal point k with corresponding i direction at

configuration $t + \Delta t$.

To evaluate the stiffness matrix of an element and the vector of nodal point forces the strain-displacement transformation matrix needs to be calculated. Strain-displacement relationships are obtained for any point in the element. In the following expression for strain components only first-order linear terms are retained and second order terms are neglected.

$$\begin{Bmatrix} \varepsilon_{11} \\ \varepsilon_{22} \\ \varepsilon_{33} \\ \varepsilon_{12} \\ \varepsilon_{23} \\ \varepsilon_{13} \end{Bmatrix} = \begin{Bmatrix} u_{1,1} \\ u_{2,2} \\ u_{3,3} \\ 0.5(u_{1,2} + u_{2,1}) \\ 0.5(u_{2,3} + u_{3,2}) \\ 0.5(u_{1,3} + u_{3,1}) \end{Bmatrix} \qquad (3.15)$$

The strain matrix ε is represented as:

$$\varepsilon = \mathbf{B}\,\mathbf{u} \qquad\qquad (3.16)$$

where the matrix $\mathbf{B}$, namely, the strain-displacement transformation matrix, is an operator which is completely defined once the shape function $\mathbf{N}$ is defined:

$$\mathbf{B} = \begin{bmatrix} \mathbf{B}_1 \mathbf{B}_2 ... \mathbf{B}_8 \end{bmatrix}, \qquad\qquad (3.17)$$

and,

$$\mathbf{B}_j = \begin{bmatrix}
\dfrac{\partial N_j}{\partial x_1} & 0 & 0 \\[2mm]
0 & \dfrac{\partial Nj}{\partial x_2} & 0 \\[2mm]
0 & 0 & \dfrac{\partial Nj}{\partial x_3} \\[2mm]
\dfrac{\partial Nj}{\partial x_2} & \dfrac{\partial Nj}{\partial x_1} & 0 \\[2mm]
0 & \dfrac{\partial Nj}{\partial x_3} & \dfrac{\partial Nj}{\partial x_2} \\[2mm]
\dfrac{\partial Nj}{\partial x_3} & 0 & \dfrac{\partial Nj}{\partial x_1}
\end{bmatrix}, \quad j = 1 \text{ to } 8. \qquad\qquad (3.18)$$

To evaluate derivatives of the shape functions it is necessary to establish a transformation relationship from global to local coordinates. This is accomplished using the Jacobian matrix, which is also used in the numerical integration scheme (Siriwardane 1980). The Jacobian matrix $\mathbf{J}$ is calculated as:

$$\mathbf{J} = \begin{bmatrix}
\dfrac{\partial x_1}{\partial r'} & \dfrac{\partial x_2}{\partial r'} & \dfrac{\partial x_3}{\partial r'} \\[2mm]
\dfrac{\partial x_1}{\partial s'} & \dfrac{\partial x_2}{\partial s'} & \dfrac{\partial x_3}{\partial s'} \\[2mm]
\dfrac{\partial x_1}{\partial t'} & \dfrac{\partial x_2}{\partial t'} & \dfrac{\partial x_3}{\partial t'}
\end{bmatrix} = \begin{bmatrix}
\displaystyle\sum_{i=1}^{8}\left(\dfrac{\partial N_i}{\partial r'}x_1^i\right) & \displaystyle\sum_{i=1}^{8}\left(\dfrac{\partial N_i}{\partial r'}x_2^i\right) & \displaystyle\sum_{i=1}^{8}\left(\dfrac{\partial N_i}{\partial r'}x_3^i\right) \\[4mm]
\displaystyle\sum_{i=1}^{8}\left(\dfrac{\partial N_i}{\partial s'}x_1^i\right) & \displaystyle\sum_{i=1}^{8}\left(\dfrac{\partial N_i}{\partial s'}x_2^i\right) & \displaystyle\sum_{i=1}^{8}\left(\dfrac{\partial N_i}{\partial s'}x_3^i\right) \\[4mm]
\displaystyle\sum_{i=1}^{8}\left(\dfrac{\partial N_i}{\partial t'}x_1^i\right) & \displaystyle\sum_{i=1}^{8}\left(\dfrac{\partial N_i}{\partial t'}x_2^i\right) & \displaystyle\sum_{i=1}^{8}\left(\dfrac{\partial N_i}{\partial t'}x_3^i\right)
\end{bmatrix},$$

$$\qquad\qquad (3.19)$$

Now, substituting equations 3.11, 3.14 and 3.16 in equation 3.10 results in:

$$\left({}_t^t\mathbf{K}_L + {}_t^t\mathbf{K}_{NL} \right)\mathbf{u} = {}^{t+\Delta t}\mathbf{R} - {}_t^t\mathbf{F} \tag{3.20}$$

where:

${}_t^t\mathbf{K}_L$ = linear strain stiffness matrix in configuration at time t (referred to configuration at time t),

$$= {}_t^t\mathbf{K}_L = \int_{{}^t V} {}_t^t\mathbf{B}_L^T \, {}_t\mathbf{C}_t^t \, \mathbf{B}_L \; {}^t dV \tag{3.21}$$

${}_t^t\mathbf{K}_{NL}$ = non-linear strain stiffness matrix in configuration at time t (referred to configuration at time t),

$$= {}_t^t\mathbf{K}_{NL} = \int_{{}^t V} {}_t^t\mathbf{B}_{NL}^T \; {}^t\tau \, {}_t^t\mathbf{B}_{NL} \; {}^t dV \tag{3.22}$$

${}^{t+\Delta t}\mathbf{R}$ = vector of externally applied nodal point loads (element surface and body forces) at time $t + \Delta t$,

${}_t^t\mathbf{F}$ = vector of nodal point forces equivalent to the element stresses at time t.

$$= {}_t^t\mathbf{F} = \int_{{}^t V} {}_t^t\mathbf{B}_L^T \; {}^t\hat{\tau} \; {}^t dV \tag{3.23}$$

${}_t^t\mathbf{B}_L$ = linear strain displacement transformation matrix (defined below),

${}_t^t\mathbf{B}_{NL}$ = non-linear strain displacement transformation matrix,

${}_t\mathbf{C}$ = incremental material property matrix at time t,

${}^t\tau$ = matrix of Cauchy stress with configuration at time t,

${}^t\hat{\tau}$ = vector of Cauchy stress with configuration at time t,

$$= [\tau_{11}, \tau_{22}, \tau_{33}, \tau_{12}, \tau_{23}, \tau_{31}]^T .$$

The $_t^t K_L u$, $_t^t K_{NL} u$ and $_t^t F$ matrices were obtained from finite element representations

of $\int_{^tV} C_{ijrs} \, \varepsilon_{rs} \, \delta^* \varepsilon_{ij} \, (^tdV)$, $\int_{^tV} {}^t\tau_{ij} \, \delta^*_t\eta_{ij} \, (^tdV)$ and $\int_{^tV} {}^t\tau_{ij} \, \delta^*_t\varepsilon_{ij} \, (^tdV)$, respectively.

As noted above, the nonlinear part of the stiffness matrix (i.e., K_{NL}) is neglected

in this thesis since increments of loads are small. Instead, K_L is updated at the beginning

of each load step. Britto and Gunn (1987) used the small displacement, small strain

approach in the Crisp program. Updated coordinates of nodal points were used. This is a

first approximation of an updated Lagrangian formulation. The first order updated

Lagrangian approach is also described by Cook (1981).

The linear stiffness matrix K_L can be calculated using numerical integration. A

two-point Gaussian quadrature scheme is used for numerical integration. It should be

noted that the components of matrix B are functions of the natural coordinates r', s' and

t', so that the volume integration is evaluated over the natural coordinate volume. The

differential volume dV is evaluated in terms of natural coordinates. Generally,

$$dV = \det J \, dr' \, ds' \, dt' \tag{3.24}$$

The numerical integration requires the use of weighting factors calculated at sampling

points (i.e., the Gauss points) for optimum accuracy. The procedure is well explained in

Zienkiewicz (1977).

In the local domain, K_L is calculated for every element as:

$$K_L = \iiint_{V_{to}} B^T C B \det J \, dr \, ds \, dt \tag{3.25}$$

where:

C = constitutive matrix,

V_{lo} = element local domain.

Dynamic solution

Equation 3.20 represents a static solution, e.g., it has no time dependent terms. The dynamic solution is expressed by:

$$\left({}_t^t \mathbf{K}_L + {}_t^t \mathbf{K}_{NL} \right) \mathbf{u} = {}^{t+\Delta t} \mathbf{R} - {}_t^t \mathbf{F} - \mathbf{M}^{t+\Delta t} \ddot{\mathbf{u}} \qquad (3.26)$$

where:

${}^{t+\Delta t} \ddot{\mathbf{u}}$ = vector of element nodal points accelerations at configuration t+Δt,

$\mathbf{M}$ = time independent mass matrix, calculated at configuration 0.

In the dynamic solution (equation 3.26) the applied body forces include inertia forces. Damping is not considered. Mass of the body is assumed to be preserved. Thus, the mass matrix is evaluated using the initial configuration, before time integration, at time t = 0 as reference (Bathe 1982). For a three-dimensional solution, eight node isoparametric solid elements, brick or hexahedron are used (Figure 3.3), (Rao 1982).

The mass matrix $\mathbf{M}$ can usually be calculated using consistent or lumped formulation (Desai and Abel 1972). The lumped formulation is adopted here due to its simplicity. In this procedure, masses are placed at nodal points in directions of the assumed displacement degrees of freedom, on the assumption that material behaves like a rigid body. Thus, there is an implicit assumption of no interaction between nodal masses. Consequently, there is no coupling between element displacements and the lumped matrix, resulting in a purely diagonal mass matrix. The lumped mass matrix can be obtained by

dividing the total element mass equally among the element nodes:

$$\mathbf{M} = \int_v \rho \Psi^T \Psi dV \tag{3.27}$$

where:

ρ = material density (M/L^{-3}),

Ψ = matrix of functions Ψ_i which have unit value over the region tributary to

    node i, and zero elsewhere.

The volume differential is calculated using equation 3.24.

3.3 Finite Element Implementation

Implementation of the finite element solution presented above requires the solution of the dynamic transient problem, which involves time, as well as geometric and material nonlinearities.

Nonlinearity is simply a failure of a material to respond proportionally to the excitation magnitude (Desai and Siriwardane 1984). Many factors can generate nonlinearities. The most common are nonlinearities due to geometry (large displacements), and material nonlinearities (nonlinear stress-strain behaviour). Both of these are factors in this analysis.

The procedure developed in this thesis can accommodate all three cases in an incremental solution using the same algorithm. The dynamic solution uses the Newmark direct integration method to solve the dynamic equation 3.26 with respect to time. An incremental scheme is combined with a material geometric nonlinearity solution scheme

and an updated Lagrangian scheme (Eulerian). To accommodate material nonlinearity, a modified Newton-Raphson method is used iteratively within each incremental load.

In the incremental procedure the total load is divided and applied in load increments. In the basic incremental procedure (Desai and Abel 1972) the load matrix $\mathbf{R}$ and total displacement matrix $\mathbf{u}$ are defined by:

$$\mathbf{R} = \mathbf{R}_0 + \sum_{j=1}^{M} \Delta \mathbf{R} \tag{3.28}$$

$$\mathbf{u} = \mathbf{u}_0 + \sum_{j=1}^{M} \Delta \mathbf{u} \tag{3.29}$$

where:

$\mathbf{R}_0, \Delta \mathbf{R}$ = initial and incremental load matrices, respectively,

$\mathbf{u}_0, \Delta \mathbf{u}$ = initial and incremental displacement vectors, respectively.

3.3.1 Material nonlinearity

The main reason for material nonlinearity is caused by the stress history of the material. Soil physical characteristics change during loading. Material stiffness changes with loading changes, and these changes are usually nonlinear for soils. Thus, the constitutive matrix $\mathbf{C}$ must be reevaluated at each incremental load step.

Nonlinearity can also be caused by the type of loading, e.g., dynamic, rate of loading and loading path. In the present case, the latter two cases apply. To solve material nonlinearity problems some iterative techniques are available, for example, direct iteration, Newton-Raphson method, modified Newton-Raphson method, and others. The modified

Newton-Raphson method is used due to its simplicity, although convergence is slower compared with the Newton-Raphson method.

Figure 3.4 illustrates the basic scheme of the modified Newton-Raphson method. At the first iteration the tangential stiffness matrix, K_T^0, of the system is known, as is the imposed load, R. Thus, a displacement u^0 is calculated by solving the following system of equations for the first step (Zienckiewickz 1977):

$$\Delta u^n = -\left(K_T^0\right)^{-1}\left(F^n - R\right) \tag{3.30}$$

where:

n   = iteration number,

K_T^0 = initial tangent stiffness matrix,

$\left(F^n - R\right)$ = unbalanced force vector,

F^n = internal reaction forces at n iteration.

Second and subsequent iterations are reached maintaining the same initial calculated stiffness K_T^0, such that $K_T^n = K_T^0$. Thus a new system of equations has to be solved at every iteration. However, the stiffness remains constant. A new unbalanced load vector is solved at every iteration. The process is completed when the unbalanced vector is small compared with a preselected tolerance, say 1% based on the Euclidian vector norm (Dhatt and Touzot 1984). Alternatively, displacements can be used to check convergence,

$conv.criter. = \dfrac{\left\|\Delta(\Delta u)\right\|_2}{\left\|\Delta u\right\|_2}$. The process is supposed to converge less rapidly than in the full
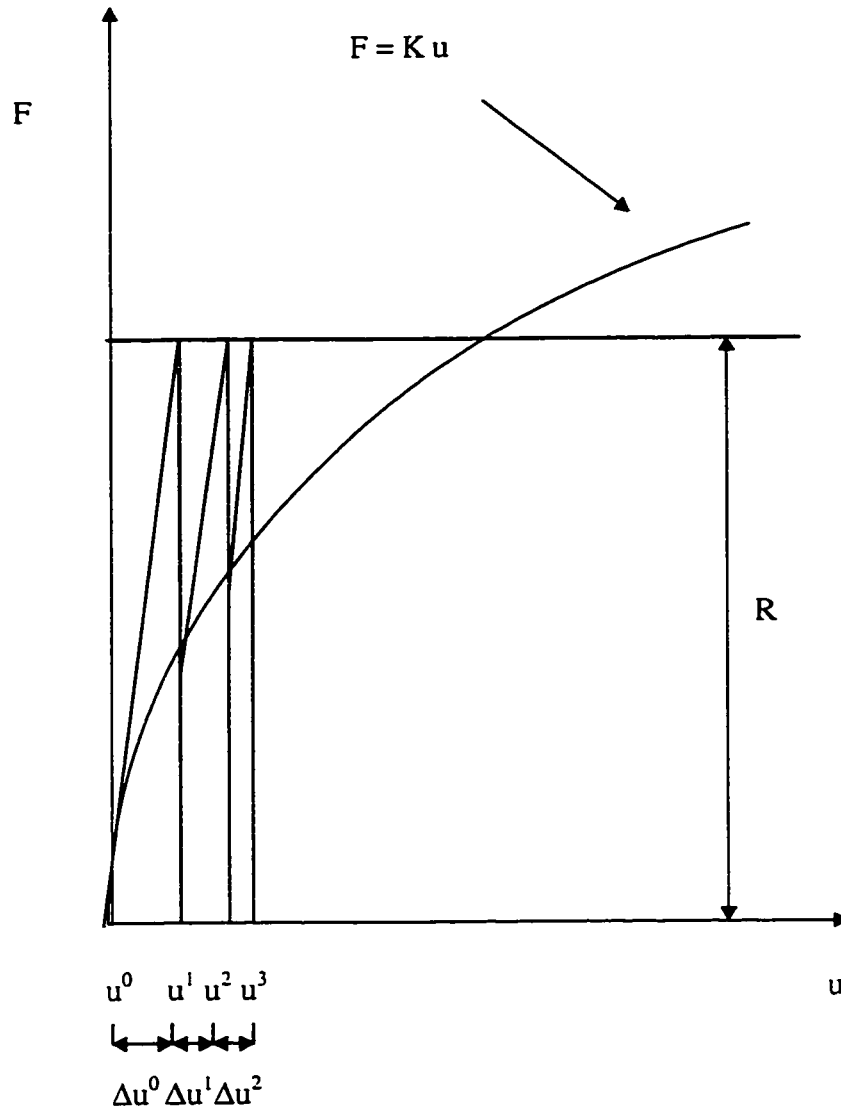
Figure 3.4 **Basic scheme of the modified Newton-Raphson method (after Zienckiewickz 1977).** The u^n indicate displacements at the nth iteration, F^n is the internal reaction force at the nth iteration and **R** is the total load (including both surface and body element forces).

Newton-Raphson method. However, the modified method is simpler to implement in a computer program.

3.3.2 Transient analysis

A dynamic analysis requires a numerical time integration of the finite element equations of motion (e.g., equation 3.26). Equation 3.26 is of the form,

$$\mathbf{M\ddot{u}} + \mathbf{\overline{K}u} = \mathbf{\overline{R}} \tag{3.31}$$

$$\mathbf{\overline{R}} = \mathbf{R_b} + \mathbf{R_s} - \mathbf{R_i} + \mathbf{R_c} \tag{3.32}$$

where:

$\mathbf{\overline{R}}$ = external load vector,

$\mathbf{\overline{K}}$ = stiffness matrix including linear and nonlinear effects,

$\mathbf{R_b}$ = load vector related to body forces,

$\mathbf{R_s}$ = load vector related to surface forces,

$\mathbf{R_i}$ = load vector related to element inertial forces,

$\mathbf{R_c}$ = load vector related to concentrated nodal forces.

Direct integration means that equation 3.31 is satisfied at discrete time intervals Δt, (Δt = total time T / n equal time intervals), and a variation of displacements, velocities and accelerations are assumed within each time interval. The integration scheme gives an approximate solution at times 0, Δt, 2Δt, ..., t , t+Δt, ... T.

The solution of the equilibrium equation 3.31 governing the linear dynamic response, might use one of the four direct integration methods: central difference method, the Houboult method, the Wilson θ method and the Newmark method (Bathe 1982;

Newmark 1959). The Newmark method is adopted here due to its stability and effectiveness. It is applied for each incremental load step. Table 3.1 outlines the complete Newmark scheme in which damping effects are also included. The damping coefficient was neglected in equation 3.31.

The Newmark integration scheme can be classified as an extension of the linear acceleration method (Bathe 1982). Figure 3.5 illustrates the Newmark constant-average acceleration scheme.

The basic equations of Newmark's method are given by:

$$^{t+\Delta t}\dot{u} = {}^{t}\dot{u} + \left[(1-\delta)^{t}\ddot{u} + \delta^{t+\Delta t}\ddot{u}\right]\Delta t \tag{3.33}$$

$$^{t+\Delta t}u = {}^{t}u + {}^{t}\dot{u}\Delta t + \left[\left(\frac{1}{2}-\alpha\right)^{t}\ddot{u} + \alpha^{t+\Delta t}\ddot{u}\right]\Delta t^{2} \tag{3.34}$$

The α and δ are constants (Table 3.1). When $\alpha = \frac{1}{2}$ and $\delta = \frac{1}{4}$ the method is unconditionally stable; this is the constant average acceleration method. Equation 3.31 is assumed to be satisfied at times t and t+Δt.

$$M^{t+\Delta t}\ddot{u} + \overline{K}^{t+\Delta t}u = {}^{t+\Delta t}\overline{R} \tag{3.35}$$

The $^{t+\Delta t}\ddot{u}$ in equation 3.34 is solved in terms of $^{t+\Delta t}u$ and substituted into equation 3.33. Thus, $^{t+\Delta t}\ddot{u}$ and $^{t+\Delta t}\dot{u}$ are obtained as functions of $^{t+\Delta t}u$. These two relations are substituted in 3.35 to solve for $^{t+\Delta t}u$. Then, using 3.32 and 3.33, $^{t+\Delta t}\ddot{u}$ and $^{t+\Delta t}\dot{u}$ can also be calculated.

It should be noted that the Newmark's integration method is used once at every load step to solve for displacements, velocities and accelerations. The material nonlinearity

Table 3.1   **Step by step solution using Newmark integration method (for each incremental load) (Bathe 1982).**

A. Initial Conditions:

1. Form stiffness matrix $\overline{K}$, mass matrix M and damping matrix C_l.
2. Initialize ^0u, $^0\dot{u}$ and $^0\ddot{u}$.
3. Select time step size Δt, parameters α and δ , and calculate integration constants:

$$\delta \geq 0.50; \; \alpha \geq 0.25(0.5+\delta)^2$$

$$a_0 = \frac{1}{\alpha \Delta t^2}; \; a_1 = \frac{\delta}{\alpha \Delta t}; \; a_2 = \frac{1}{\alpha \Delta t}; \; a_3 = \frac{1}{2\alpha} - 1;$$

$$a_4 = \frac{\delta}{\alpha} - 1; \; a_5 = \frac{\Delta t}{2}\left(\frac{\delta}{\alpha} - 2\right); \; a_6 = \Delta t(1-\delta); \; a_7 = \delta \Delta t$$

4. Form effective stiffness matrix $\hat{K}$: $\hat{K} = \overline{K} + a_0 M + a_1 C_l$
5. Triangularize $\hat{K}$: $\hat{K} = LDL^T$.

B. For each time step:

1. Calculate effective loads at time $t + \Delta t$:

$$^{t+\Delta t}\hat{R} = {}^{t+\Delta t}\overline{R} + M(a_0{}^t u + a_2{}^t\dot{u} + a_3{}^t\ddot{u}) + C_l(a_1{}^t u + a_4{}^t\dot{u} + a_5{}^t\ddot{u})$$

2. Solve for displacements at time $t + \Delta t$:

$$LDL^T \; {}^{t+\Delta t}u = {}^{t+\Delta t}\hat{R}$$

3. Calculate accelerations and velocities at time $t + \Delta t$:

$$^{t+\Delta t}\ddot{u} = a_0({}^{t+\Delta t}u - {}^t u) - a_2{}^t\dot{u} - a_3{}^t\ddot{u}$$

$$^{t+\Delta t}\dot{u} = {}^t\dot{u} + a_6{}^t\ddot{u} + a_7{}^{t+\Delta t}\ddot{u}$$

Acceleration

$\ddot{u}$

$^{t+\Delta t}\ddot{u}$

$\alpha = \dfrac{1}{6}$(Linear)

$\alpha = \dfrac{1}{4}$(Cons tan t)

$\alpha = \dfrac{1}{8}$(Stepped)

$^{t}\ddot{u}$

t

$t+\Delta t$

Time (t)
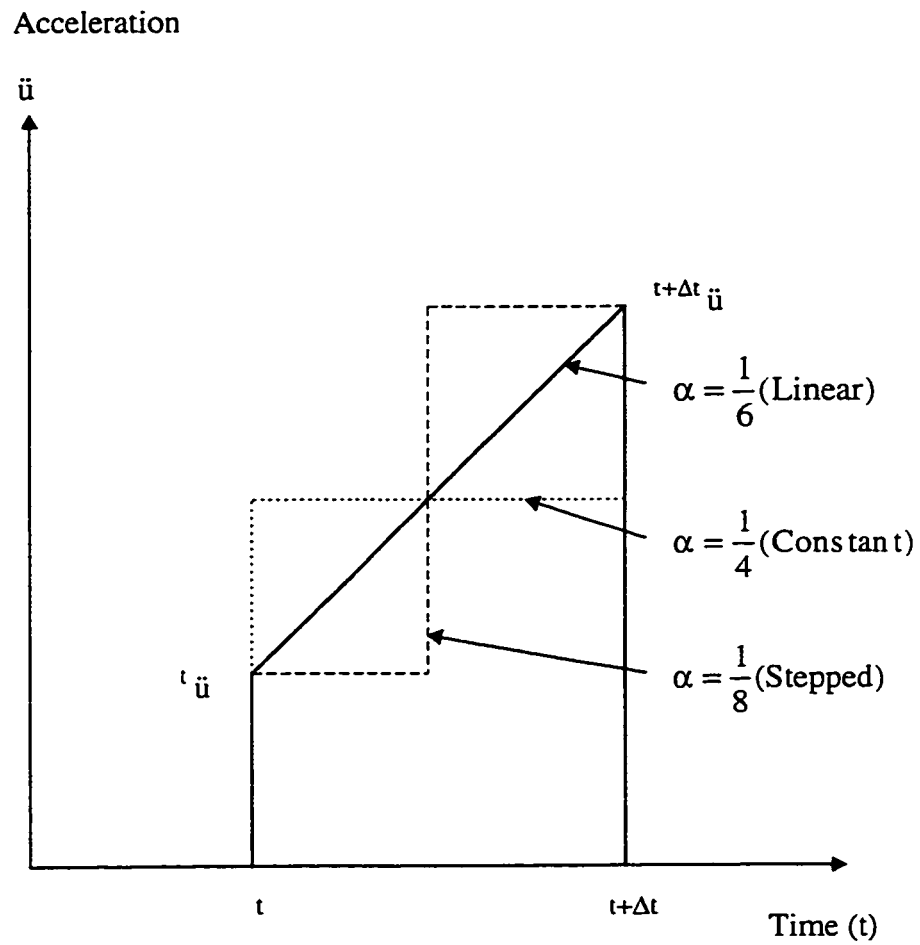
Figure 3.5   Newmark time integration scheme for various types of acceleration (after Bathe 1982).

is used iteratively inside each load step until a specified tolerance in the unbalanced load vector is achieved.

3.3.3 Geometrical nonlinearity

The geometrical nonlinearity solution method adopted in the present problem uses the updated Lagrangian technique; however, only a first order approximation, in which mesh nodal coordinates are updated and the stiffness matrix is recalculated for every new incremental step, is implemented in the computer code. The solution of the geometrical nonlinearity was developed for equation 3.26, $\left({}_t^t\mathbf{K}_L + {}_t^t\mathbf{K}_{NL}\right)\mathbf{u} = {}^{t+\Delta t}\mathbf{R} - {}_t^t\mathbf{F} - \mathbf{M}^{t+\Delta t}\ddot{\mathbf{u}}$, obtained from the dynamic solution. Incremental load steps are used with constant time steps Δt in the dynamic solution. According to Britto and Gunn (1987), updating of nodal point coordinates is equivalent to a first order approximation of an updated Lagrangian formulation. Cook (1981) states that in the updated Lagrangian (Eulerian) formulation, coordinates are updated to produce a new reference state. In the finite element context the conventional stiffness matrix $\mathbf{K}_L$ is extended by higher order terms ($\mathbf{K}_{NL}$). Strains in the local system are usually small enough that higher order terms can be omitted, thus the omission of $\mathbf{K}_{NL}$ in this formulation.

3.3.4 Constitutive relationship

The constitutive tensor $\mathbf{C}$ defines the stress-strain relations used in the finite element calculations. It is required for calculation of element stiffness matrices and stress vectors.

A hypoelastic material is considered here, in which the constitutive tensor relates incremental stresses to incremental strains. A modification to the original hyperbolic relationship is also made so that C is also related to rates of strain.

The constitutive model considered and modified here, was presented by Shen and Kushwaha (1993). Shen and Kushwaha (1993) began with the constitutive relationship derived by Duncan and Chang (1970) (see section 2.41), in which the tangent modulus of elasticity is represented by:

$$E_s = \left[1 - \frac{R_f(\sigma_1 - \sigma_3)}{(\sigma_1 - \sigma_3)_f}\right]^2 Kp_a\left(\frac{\sigma_3}{p_a}\right)^n = \left[1 - \frac{R_f(1 - \sin\phi)(\sigma_1 - \sigma_3)}{2c\cos\phi + 2\sigma_3\sin\phi}\right]^2 Kp_a\left(\frac{\sigma_3}{p_a}\right)^n$$

(3.36)

They then represented the rate effect using a relationship used by Qun and Shen (1988) for wet soils: $B_s = \ln(\dot{\varepsilon}/\dot{\varepsilon}_0)$. It is noted that logarithmic relationships are typically used for saturated soils (Gudehus 1977; Gudehus et al. 1977; Yong and Japp 1968).

Glancey et al. (1996) used a linear shear strength versus speed relationship for the semi-empirical analysis developed for the work on standard reference tools. The equation $\tau_s = \tau_0 + \tau_1 S$ was used by Glancey et al. (1996) to describe an elasto-plastic soil failure. Here, τ_s is the soil shear strength (kPa), τ_0 is a soil parameter related to the static component of shear strength (kPa), τ_1 is a soil parameter related to the dynamic component of shear strength (kPa·s/m) and S is the operating speed (m/s). Preliminary results of draft versus tool speed obtained for this thesis in the soil bin also suggest a linear relationship between soil shear strength and speed.

In this thesis, the strain rate effect is represented in a similar way to Glancey (1996), by a linear viscous relationship $AN(\dot{\varepsilon} - \dot{\varepsilon}_0)$, incorporated in the constitutive relationship as:

$$(\sigma_1 - \sigma_3)_f = (\sigma_1 - \sigma_3)_{f0} + AN(\dot{\varepsilon} - \dot{\varepsilon}_0) \quad \text{for } \dot{\varepsilon} > \dot{\varepsilon}_0$$
$$(\sigma_1 - \sigma_3)_f = (\sigma_1 - \sigma_3)_{f0} \quad \text{for } \dot{\varepsilon} \le \dot{\varepsilon}_0 \qquad (3.37)$$

where:

$AN \quad = \text{constant} \, (\, kPa \cdot s \,),$

$$\dot{\varepsilon} = \frac{\partial \varepsilon}{\partial t} = \sqrt{\dot{\varepsilon}_1^2 + \dot{\varepsilon}_2^2 + \dot{\varepsilon}_3^2} \qquad (3.38)$$

$\qquad = \text{resultant strain rate } (s^{-1}),$

$\dot{\varepsilon}_0 \quad = \text{resultant reference strain rate in the axial direction, obtained}$

$\qquad \text{from conventional quasi-static triaxial tests } (s^{-1}).$

The strain rate relationship defined by equation 3.37 ($(\sigma_1 - \sigma_3)_f = 2\tau_s$) will have a growing or contracting effect on the (quasi-static) Mohr-Coulomb failure surface and on the hyperbolic relationship as well. It is similar to linear viscous effects (see Figure 3.6). Even in viscoplasticity for soils, it is more usual to associate surfaces of yielding or failure (e.g., Baladi and Rohani 1984) with a simple relation among surfaces of different strain rates; for instance, a linear viscous model.

Substituting equation 3.37 into equation 3.36 and combining the result with the Mohr-Coulomb failure criterion, the following equation is obtained:

τ

Dyntool

viscoplastic
(clay type)

ideally plastic

linearly viscous

ε̇
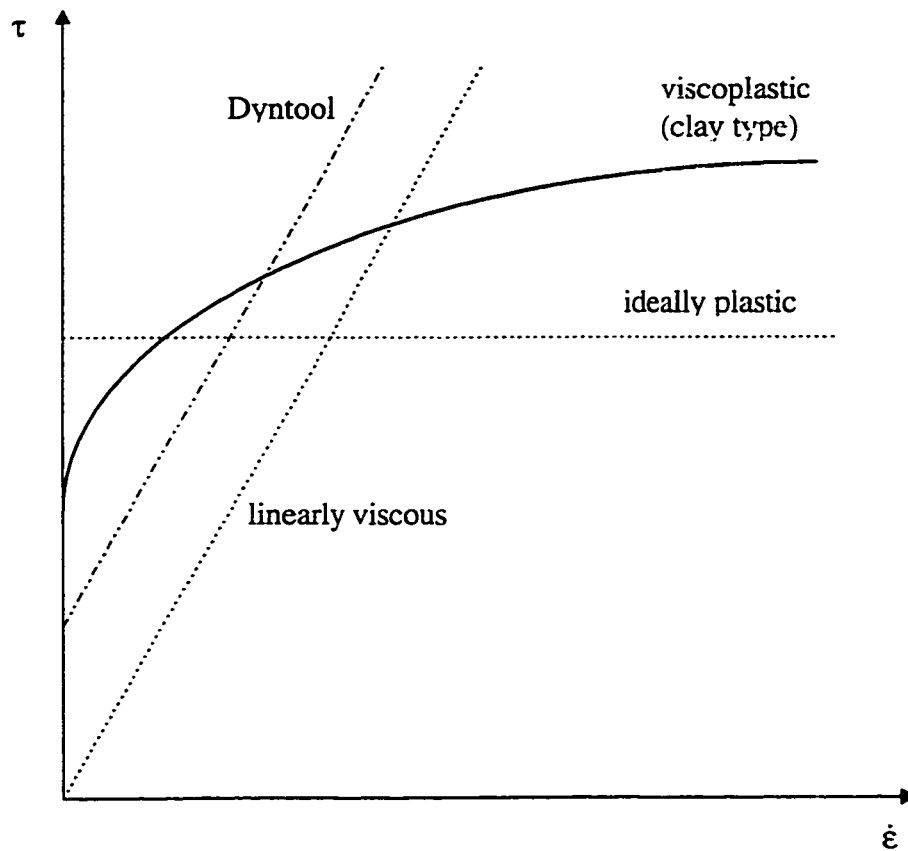
Figure 3.6   **Simplified stress-strain rate behaviour of a visco-plastic material**

(after Gudehus 1977). Also shown in the stress-strain rate behaviour

expressed by equation 3.37.

$$E_s = \left[1 - \frac{R_f(\sigma_1 - \sigma_3)}{\dfrac{2c\cos\phi + 2\sigma_3\sin\phi}{(1-\sin\phi)} + AN(\dot{\varepsilon} - \dot{\varepsilon}_0)} \right]^2 Kp_a \left(\frac{\sigma_3}{p_a} \right)^n \quad \text{for } \dot{\varepsilon} > \dot{\varepsilon}_0$$

$$E_s = \left[1 - \frac{R_f(1-\sin\phi)(\sigma_1 - \sigma_3)}{2c\cos\phi + 2\sigma_3\sin\phi} \right]^2 Kp_a \left(\frac{\sigma_3}{p_a} \right)^n \quad \text{for } \dot{\varepsilon} \leq \dot{\varepsilon}_0$$

$$(3.39)$$

For the case $\dot{\varepsilon} \leq \dot{\varepsilon}_0$, the relationship assumes the original Duncan and Chang (1970) formulation. The constitutive matrix used in the incremental relationship $\sigma_{ij} = C\varepsilon_{ij}$ can be written as:

$$C = \frac{E_s}{(1+v)(1-2v)} \begin{bmatrix} (1-v) & v & v & 0 & 0 & 0 \\ v & (1-v) & v & 0 & 0 & 0 \\ v & v & (1-v) & 0 & 0 & 0 \\ 0 & 0 & 0 & \left(\dfrac{1-2v}{2}\right) & 0 & 0 \\ 0 & 0 & 0 & 0 & \left(\dfrac{1-2v}{2}\right) & 0 \\ 0 & 0 & 0 & 0 & 0 & \left(\dfrac{1-2v}{2}\right) \end{bmatrix}$$

$$(3.40)$$

So far, the formulation was developed for soil compression. Failed elements, either in shear or in tension, have their tangential modulus reduced by a factor $(1/1000)$ to approximate small soil stiffness at failure. Duncan and Chang (1970) adopted a small residual modulus for soil elements after failure. Failure in tension is assumed when the major principal stress is greater than the soil cohesion. Failure by shear is assumed when

instantaneous deviatoric stresses, $(\sigma_1 - \sigma_3)$, reach the instantaneous deviatoric stresses at failure, $(\sigma_1 - \sigma_3)_f = 2\tau_s$.

A variable Poisson's ratio in the form presented by Chi et al. (1993a), is assumed for the quasi-static case and this equation is assumed unchanged in the dynamic case:

$$v = a_1 + b_1 \frac{(\sigma_1 - \sigma_3)}{(\sigma_1 - \sigma_3)_f} \qquad (3.41)$$

Constants a_1 and b_1 must be adjusted by curve fitting of the stress-strain data obtained from quasi-static triaxial tests. The same path is assumed for either loading or unloading.

Unfortunately, hypoelastic models based on variable Poisson's ratio v and elastic modulus E may present instabilities when failure occurs (Chen 1985). This observation was verified by preliminary analysis of data in this study. For the narrow tools tested, a small displacement (even less than 1 mm) sometimes caused instabilities in the program and analysis could not continue. This was because upon failure the elastic modulus was reduced to almost zero (one thousandth of initial value) leading to numerical oscillations. This behaviour was intensified with the presence of the lumped mass matrix and the dynamic system of equations.

Thus, upon failure, another constitutive form for the equations must be investigated (Desai and Siriwardane 1984, Britto and Gunn 1987). In an alternative formulation, the bulk and shear modulus of elasticity are considered separately (Desai and Siriwardane 1984). Upon failure, only the bulk modulus, K, is reduced close to zero and the shear modulus, G, remains unchanged. Thus, the failed soil can still maintain its

capacity to sustain shear stresses, but not hydrostatic stresses. The moduli G and K are

defined as follows:

$$G = \frac{E}{2(1+v)} \tag{3.42}$$

$$K' = \frac{E}{3(1-2v)} \tag{3.43}$$

and the elastic relationship is :

$$\sigma_{ij} = \left(K' - \frac{2G}{3}\right)I'_1\delta_{ij} + 2G\varepsilon_{ij} \tag{3.44}$$

where:

$$I'_1 = \varepsilon_{ii},$$

the first invariant of the strain tensor.

The constitutive matrix then becomes:

$$C = \begin{bmatrix} K' + \dfrac{4G}{3} & K' - \dfrac{4G}{3} & K' - \dfrac{4G}{3} & 0 & 0 & 0 \\ & K' + \dfrac{4G}{3} & K' - \dfrac{4G}{3} & 0 & 0 & 0 \\ & & K' + \dfrac{4G}{3} & 0 & 0 & 0 \\ & & & 2G & 0 & 0 \\ & \text{sym} & & & 2G & 0 \\ & & & & & 2G \end{bmatrix} \tag{3.45}$$

3.4 Computational Algorithms

3.4.1 Description

The finite element solution of the narrow cutting tool problem was implemented in

a FORTRAN computer code modified from the code referenced in Shen and Kushwaha

(1995b). The basic governing equations used in the modified code, were described previously (equations 3.39, 3.40 and 3.41). The original computer code (named Fep23) utilized subroutines based on the program code of Zienckiewicz (1977), and the program Fep2 from the University of Beijing (Agricultural Engineering Dept.), version 2, written by Li Mingui (in Chinese). The dynamic solution, using mainly the modified Newmark method, was based on the procedure given by Bathe (1982), already mentioned previously. The original computer code (Fep23) was modified to assume the present form. The modified code is named Dyntool and listed in Appendix B.

The modifications of the original code leading to the new Dyntool code were as follows:

1) An Euclidian Vector Norm convergence criterion was introduced in the code. The criterion was used to determine the number of iterations to solve soil element nonlinearities according to a predetermined tolerance. The modified Newton-Raphson method was already used in the original code to solve material non-linearities.

2) Rate-dependent variable AN was incorporated in the program according to equation 3.39. The soil element modulus of elasticity E_s now depends on a linear relationship of stress rates differences, $AN(\dot{\epsilon} - \dot{\epsilon}_0)$.

3) The code was first altered to solve the inertial problem named Dyntool. The code, considering inertial terms, is used to solve the soil modeled with stiffness and mass effects (equation 3.26).

4) Poisson's ratio relationship was modified to incorporate the variable form, (equation 3.41) into the Dyntool code. Therefore, the Dyntool code simulated a material with

variable Poisson's ratio and variable elastic modulus. The Poisson's ratio was set to a value near 0.5 ($v=0.499$) when soil reached failure, indicating no further soil volume change (Chi et. al 1993b).

5) The soil tangent modulus of failed elements was divided by a constant parameter at every load iteration and kept at a residual value after the modulus reached a small value (<0.5 kPa) as indicated by Duncan and Chang (1970). Thus, soil strength upon failure increases slightly with strains, avoiding the small stiffness matrix values which cause numerical instabilities.

6) Initial displacements, velocities and accelerations were initialized outside of the incremental load step loops and feedback of dynamic effects were then incorporated according to flow charts in Figures 3.7 and 3.8. An equivalent load vector was incorporated according to equations given in Table 3.1, where the viscous term was omitted for Dyntool in the inertial solution, and the inertial term was omitted for Dyntool-2 in the viscous solution. The mass matrix was already lumped and calculated only once before incremental loop steps start.

7) The Dyntool code was broken into small subroutines to be more efficiently processed by the FORTRAN software running on Pentium machines. Double precision for main variables was implemented.

8) The preprocessor was adapted to accommodate new input parameters into Dyntool code. Data files were created to allow processed data to be exported to the ANSYS commercial code for plotting. The procedure was used to take advantage of ANSYS
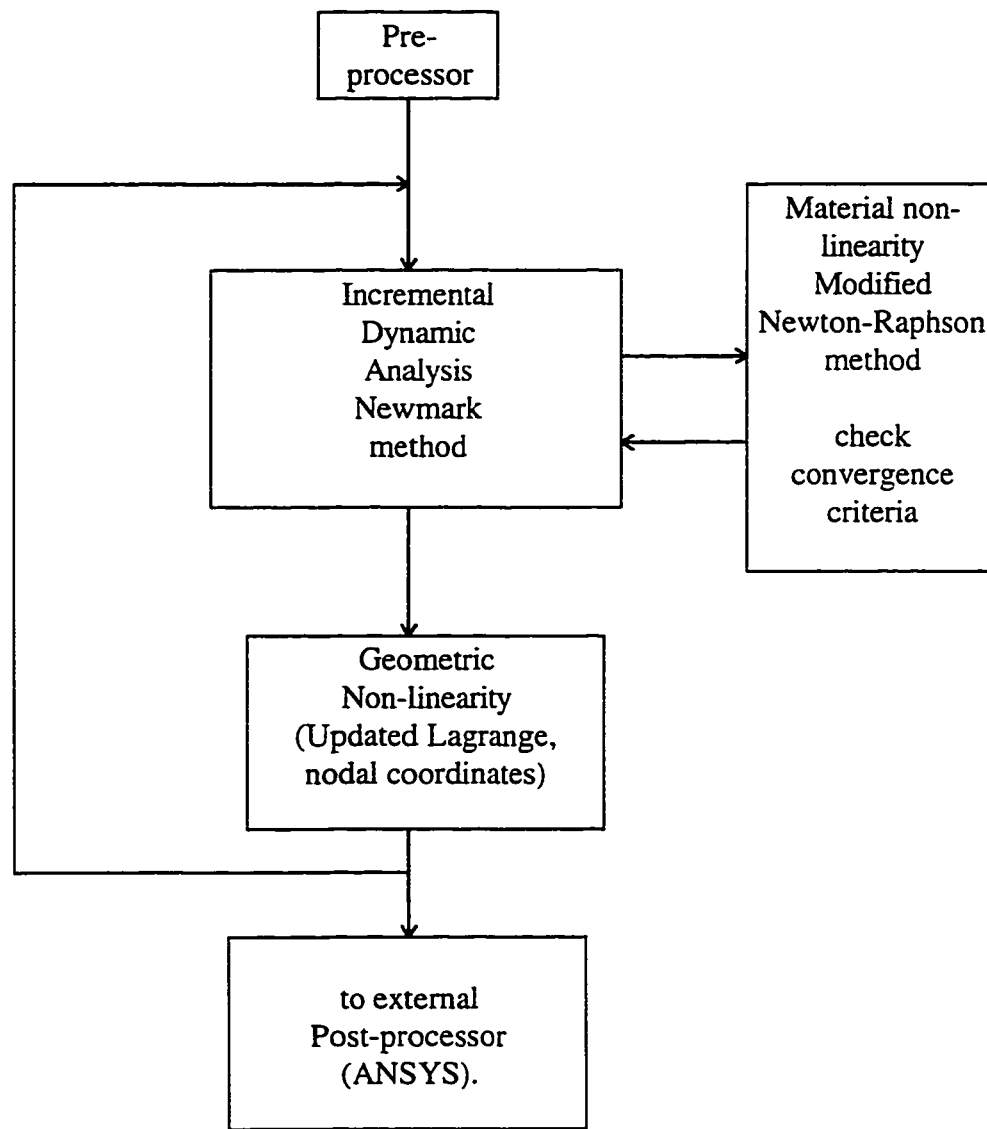
Figure 3.7   General flow chart of the main program structure.

Start

Read input data

GENERATES
- Mesh
- Load vector forces/ prescribed displacements

Determine profile of global array (K) (Zienkiewicz 1977)

Determine value of known displacements (impose tool displacements B.C.)

Determine incremental time step
Δt = incremental tool displacement/tool velocity

Calculate Newmark coefficients (Table 3.1)

Form lumped mass matrix (equation 3.27)

INITIALIZE
- Displacements
- Tool nodal reactions, velocities and accelerations

Incremental load steps loop

- Initialize stiffness array
- Form global stiffness array
- Assemble global equivalent stiffness array
- LDL^T of stiffness matrix
- Form external load vector
- Modify prescribed displacements
- Solve for displacements (forward elimination and back substitution)

(Zienkiewicz 1977) & (Table 3.1)

Modified Newton-Raphson iteration loop,

- Form effective load vector (includ. veloc. and accel.)
- Solve for displacement increments in the iteration

Check for Euclidean Norm convergence criteria for displacement (10^{-2}), (equation 3.47)

Calculate new displacements, velocities and accelerations (Newmark)

UPDATE
- Nodal coordinates (Updated Lagrangian)
- Stress, strain ($\sigma_{ij} = C\varepsilon_{ij}$, equation 3.16)
- Element tangential modulus (averaged)
- Write data to file

END

Figure 3.8   Detailed flow chart of the main program structure.

114

graphics capabilities (plotting, screen views in 3D, mesh numbering) to facilitate interpretation of the results. However, ANSYS solver modules were not used.

General and more detailed flow charts of the main program structure 'Dyntool' are presented in Figures 3.7 and 3.8, respectively. The program tree is presented in Appendix C. Input sample data are included in Appendix D. The algorithm was written to simulate a soil, initially at rest, cut by a tool running at constant speed. Total tool displacement is divided into increments. Each increment, divided by speed, determines the time increment used in the Newmark constant acceleration method. Displacements, velocities and acceleration vectors are initialized in the preprocessing block, so that the first solution is static. Subsequent solutions are dynamic, because, besides displacements, velocities and acceleration vectors are fed back to form the load vector in the next incremental load step, and so on until the total load is attained.

The number of incremental load steps multiplied by prescribed tool incremental displacements (passive loading) gives the total final displacement of the tool. The main program structure is described as follows:

The preprocessing phase opens input data files, generates the soil mesh, boundary conditions, applies external loads and forms the lumped mass matrix. A profile of the stiffness matrix is stored with pointer vectors which is used for solving the equilibrium equations for displacements in the other phases.

Material nonlinearities are solved using the already described modified Newton-Raphson method (section 3.3.1). One tangential stiffness matrix is calculated for each updated mesh in the incremental step. However, the same matrix is kept unchanged for the

modified Newton-Raphson (material nonlinearity) iterations. The Euclidian Vector mode convergence criterion is used to stop iterations at a prescribed tolerance (i.e., 1%) in displacement increments to solve material nonlinearities. Stresses are calculated at the end of incremental iterations, so that the new material tangent matrix can be updated. Also, nodal coordinates and load vectors are updated, so that, a new tangent stiffness matrix can be recalculated for the next incremental load step (see section 3.3, Figure 3.8 and Table 3.1). The code presents a "spaghetti structure", updating it to a modern programming structure code is still in progress and is not fully implemented in this dissertation.

3.4.2 Pre/post processors

Preprocessing is quite limited as only nodal linear generations are available for meshing. The same applies for element and boundary condition generations. No graphical user interface is available. Graphical analysis is more a necessity than just convenience, particularly when the number of nodes and elements are large. In fact, it is more the rule than the exception for three-dimensional analysis using solid elements.

Results output by the program are stored in matrix form. The use of an external post processor is required. A commercially available finite element program, ANSYS 5.1, with graphics capabilities was used to pre- and post-process undeformed and deformed soil structures at each incremental step.

3.4.3 Convergence criterion

The convergence criterion used for the modified Newton-Raphson method was the Euclidean vector norm. Incremental displacements were adopted as variables of the convergence criterion, instead of unbalanced load vectors, for programming convenience. This criterion is presented by Siriwardane (1980), Bathe (1982) and Shen and Kushwaha (1995b), and is also used in other commercial programs. The assumed specified tolerance was 10^{-2}. The Euclidean vector norm is defined as:

$$\|V\|_2 = \left(\sum_{i=1}^{n} |v_i|^2 \right)^{\frac{1}{2}}$$

(3.46)

Where $\|V\|_2$ is a norm of vector V of order n. In this case n will represent the number of degrees of freedom.

The convergence criterion is defined for incremental iterated displacements in relation to incremental displacements as:

$$conv.\,criter. = \frac{\|\Delta(\Delta u)\|_2}{\|\Delta u\|_2}$$

(3.47)

where:

Δu = nodal incremental displacements (inside incremental iteration but outside modified Newton-Raphson loop),

$\Delta(\Delta u)$ = nodal increment of the incremental displacement vector (inside modified Newton-Raphson loop).

3.4.4 Equation solver

The utilized solver for the equilibrium equation uses the LDL^T triangularization method for the stiffness matrix. It is well described by Zienckiewickz (1977). The complete solution is obtained by back substitution, after the matrix is triangularized.

The adopted scheme has the advantage that it minimizes memory space, since only the essential part of the stiffness array is stored (i.e., zeros are not stored) by the use of pointers. The solution implemented in the adopted code is applied only for symmetric matrices. Another advantage is that the LDL^T solution matches the Newmark scheme proposed by Bathe (1982). Therefore, solution of equilibrium equations is fast and memory allocation is optimized. The program has been written such that memory is only limited by the computer capacity (in this case for Pentium processor PC's).

Summary

This chapter has shown the developed soil constitutive model for soil-tool interactions based on one of the simplest theories available to include inertial and strain rate effects in a soil constitutive relationship. A model with a dynamic AN parameter including strain rate effects, and with inertial effects was proposed. As it will be seen in chapter 5, the model was modified after numerical problems occurred in the simulations. The modified model including viscous terms independent of the stiffness matrix proved more satisfactory, nevertheless, the model still needs modification.

CHAPTER 4

EXPERIMENTAL APPARATUS AND PROCEDURES

4.1   Soil Bin Monorail System

To verify the theoretical analysis, a monorail system was designed and built to drive high-speed tools in the soil bin facility of the Department of Agricultural and Bioresource Engineering, University of Saskatchewan (Figure 4.1). The monorail system is capable of driving soil tools at a maximum steady state speed of 10 m/s under load. Maximum draft is 1.5 kN at 10 m/s.

The main frame of the monorail consists of a 9 m long I-beam which guides a sliding tool carriage. Small ball bearings mounted on the carriage provide the sliding action on the beam. The beam is supported by transverse arm beams which pivot about points to the side of the soil bin. A hydraulic piston may lower the system parallel to the soil surface for the working position, or can be used to raise the system to allow preparation of the soil for tests. This combination maintains the flexibility to control water content, soil leveling and compaction level, as well as operating the monorail system.

A hydraulic drive system is used to accelerate and stop the carriage over a very short periods of time. A variable displacement piston pump (model 23, Sundstrand, La Salle, IL) operated by a 30 kW electric motor (Reliance, Columbus, OH) powered the drive system (size 661, Reeves, Cleveland, OH). The oil is maintained in a closed loop at high flow. A solenoid valve (O26 48360 H, Hagglunds Denison Company, Delaware, OH)

Figure 4.1 High speed monorail system built in the soil bin facility in the Department of Agricultural and Bioresource Engineering, University of Saskatchewan.

piloted by the control box shifts the oil flow to the main circuit to operate the hydraulic motor. The motor drives a roller chain which operates the tool carriage. The hydraulic circuit is given in Appendix E.

In the initial design, the sudden discharge of oil to the system produced transient oscillations. This effect was corrected by installing an adjustable bypass damping valve in the motor line (Figure 4.2). Various adjustments to the variable bypass valve make it possible to control the ripple effect on the carriage speed. Velocity smoothing was controlled to desirable levels by experimentation.

The stopping action is obtained by the solenoid valve. The oil supply is cut off when a magnet installed in the carriage is detected by a limit switch wired to the electronic box.

The instrumentation is capable of measuring and storing force data and corresponding tool velocities (Figure 4.3). One stationary (PC 80386) and another on board computer TDS2020 (Triangle Digital Services, London, England) were used to collect data. The control box emits a triggering pulse to both computers and activates the solenoid valve simultaneously to initiate data acquisition.

The tool holder is equipped with six load cells (one SSM-2000 and five SSM-1000, Interface, Scottsdale, AZ) (Figure 4.4). This arrangement makes possible measurement of forces in three directions (see Kepner et al. (1972) for details). The signals from the load cells are conditioned by on-board signal conditioners and scanned by the A/D input of a 16 bit on-board computer (TDS2020). Data are collected at 9.5 milliseconds intervals. A static calibration of the measured tool forces was performed with
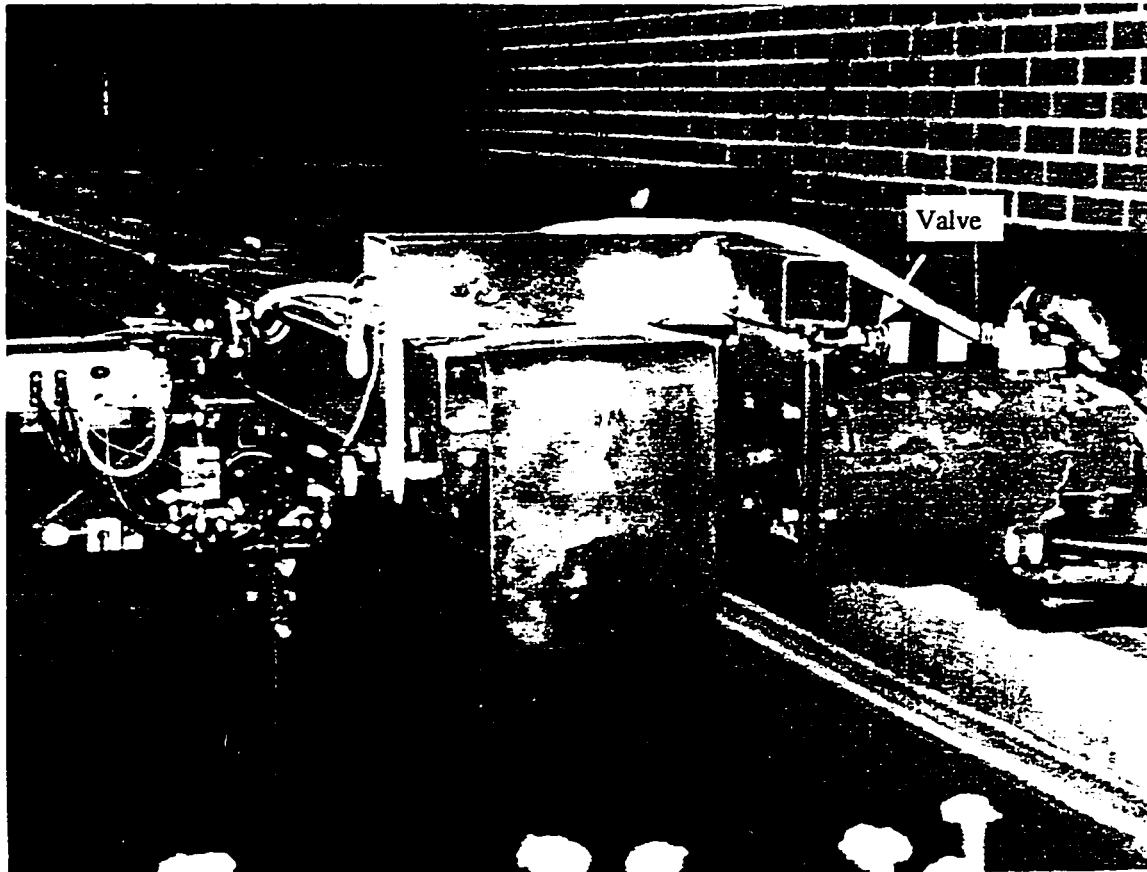
Valve

Figure 4.2 Adjustable bypass damping valve in the motor line removes transient

oscillations produced by a sudden discharge of oil in the system.
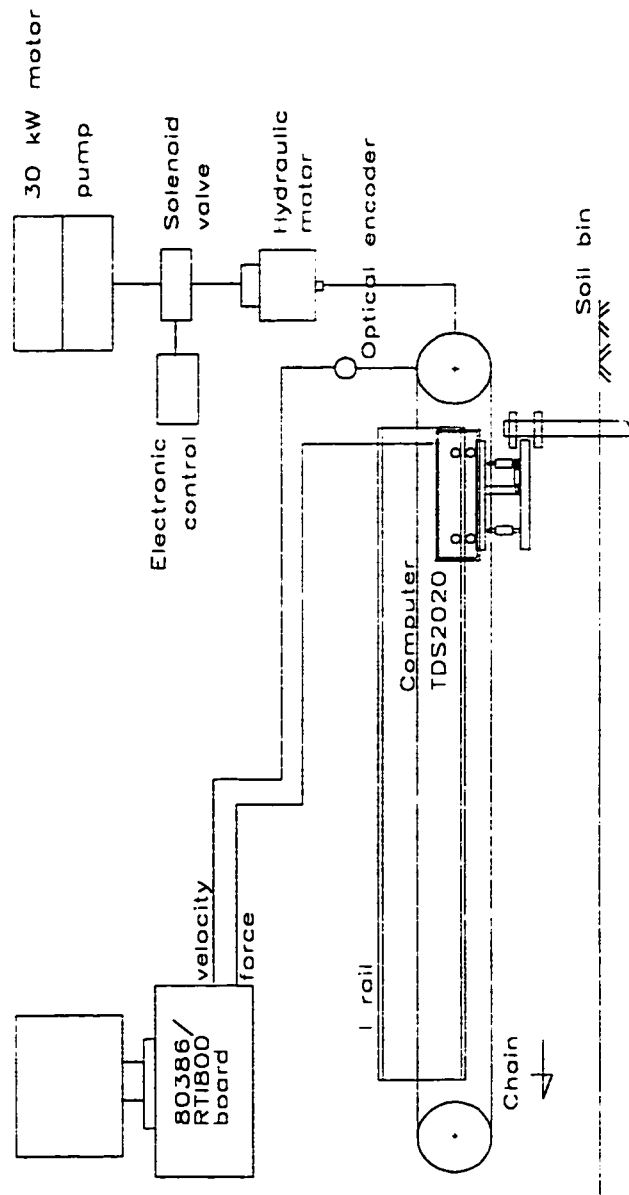
Figure 4.3   Instrumentation for measuring and storing force and tool velocity data.

123
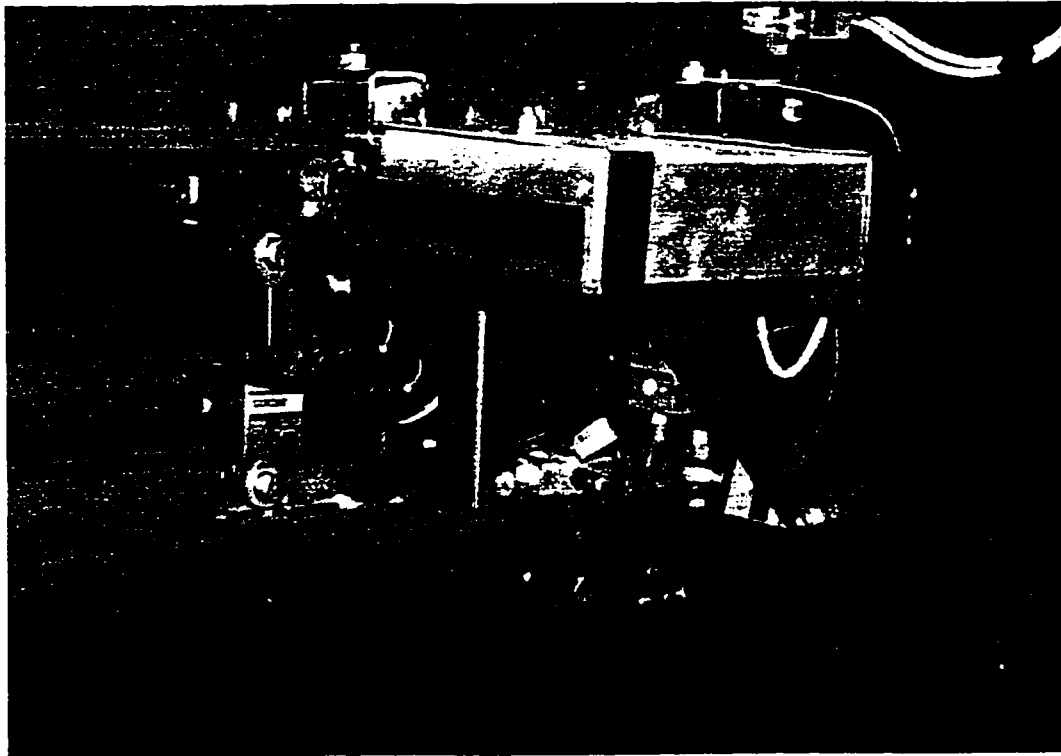
Figure 4.4   Tool holder equipped with six load cells for force measurement in three orthogonal directions.

a load cell (SSM-5000, Interface, Scottsdale, AZ) pulling the tool tip in the longitudinal, transverse and vertical directions, and simultaneously recording the system reaction forces measured in all directions. Typical measurement errors in the longitudinal direction were 0.9%. Cross-sensitivity among load cells produced, for the transversal direction 0.9% and for the vertical direction 1.9% the value of the tool pulling force.

The speed is measured by an optical encoder (IY-1728-0906, Servo Systems Co., Montville, NJ) connected to the shaft of the chain sprocket. The digital signal is processed by an interface board (RTI-800, Analog Devices, Norwood, MA) installed in the 80386 computer. Speed data were collected at 5.7 milliseconds intervals.

4.2 Experimental Procedure - Model Verification

4.2.1 Dynamic soil bin test procedure

Table 4.1 presents properties of the soil, a silty clay-loam, used in the soil bin tests. The soil was carefully prepared using the soil processing unit (Figures 4.5 and 4.6). The soil was first rototilled and gradually brought to the desired water content by spraying water. Once the desired water content had been reached a small amount of water was applied at each rototiller operation to compensate for evaporative losses. The soil was then leveled and packed. A sheep-foot packer was used to pack subsoil followed by a smooth roller to pack the surface soil.

Different compaction levels were obtained by varying the number of compacting roller passes. A low compaction level was obtained with two passes of the sheep-foot roller and four passes of the flat roller. A hard compaction level was obtained with ten
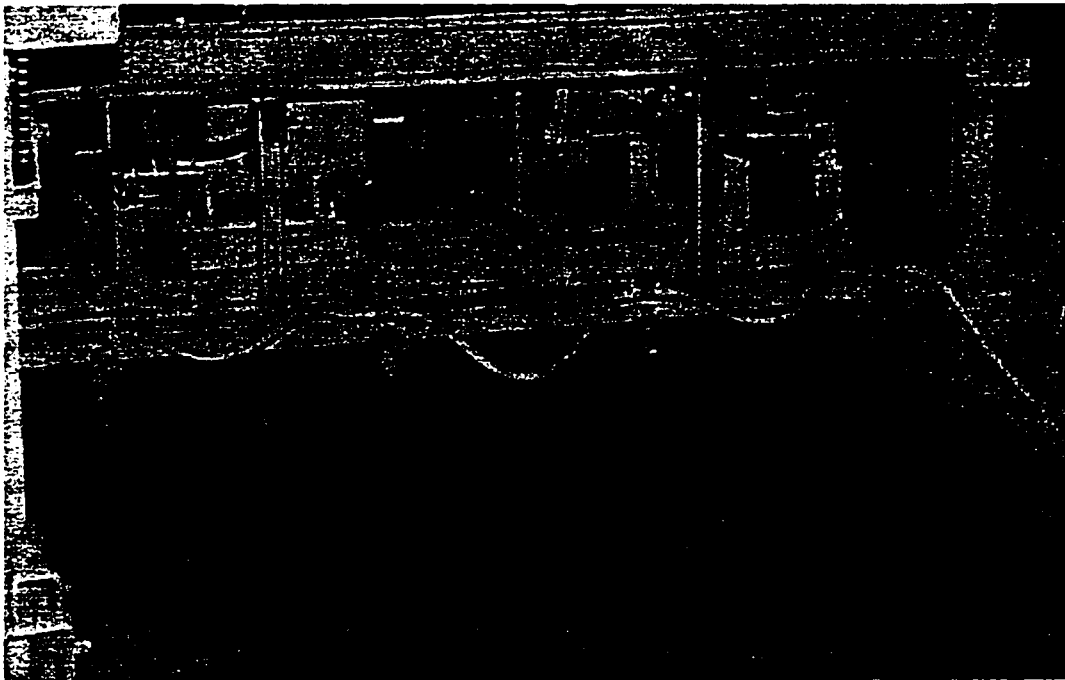
Figure 4.5 Soil being prepared by the soil processing unit.
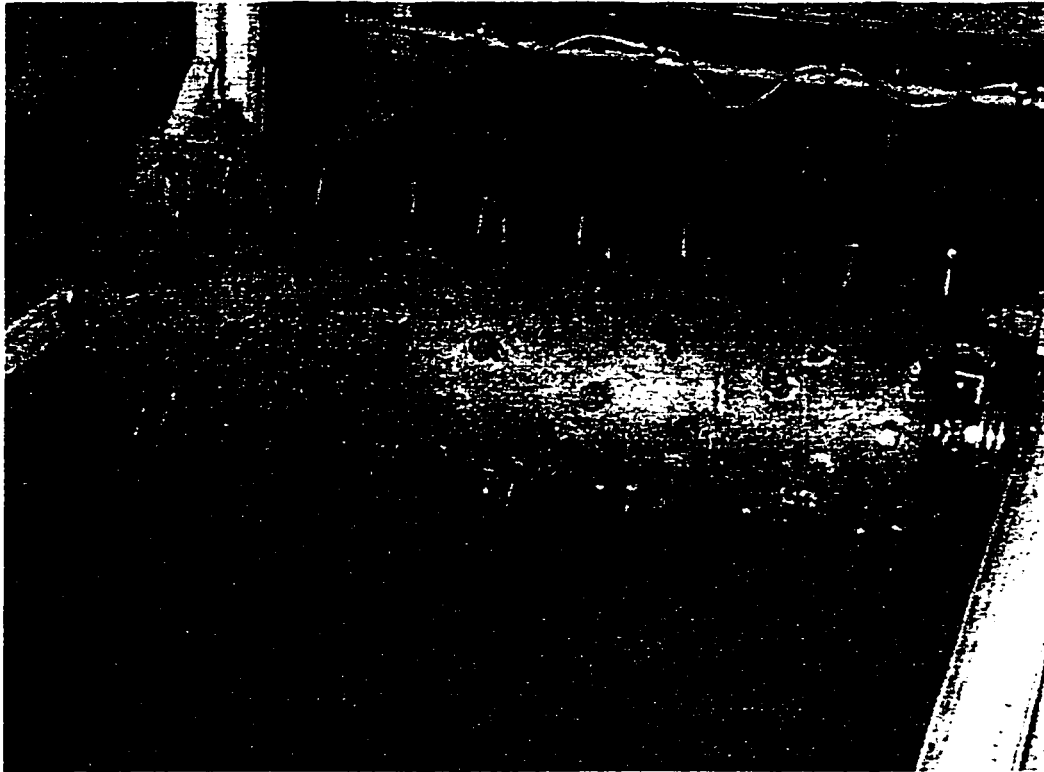
Figure 4.6   Soil being leveled and packed by the sheep-foot packer.

Table 4.1   Soil properties.

Sand (%)	Silt (%)	Clay (%)	Water Content (% db)	Plastic Limit (%)	Liquid Limit (%)
47.5	24.2	28.3	12.3 (0.7)	18.8	32.9

Standard deviation in parentheses.

passes of the sheep-foot roller and four passes of the flat roller. The hard compaction level more closely simulates field conditions during tillage operations.

After each run, three core samples, 50 mm diameter by 50 mm high, were collected for water content analysis and bulk density measurements. Additionally, cone index measurements were taken at six depths, replicated seven times along the length of the soil bin. A standard cone penetrometer S 313.2 (ASAE 1990) and a 50 mm diameter by 50 mm high core sampler were used to determine soil strength and density properties. The cone penetrometer rod was marked every 25 mm. Soil core samples were collected for weighing and determination of wet bulk density at 0-50 and 50-100 mm depths. The samples were collected from regions in the soil bin where the tool would have attained steady state speeds. Soil samples were oven dried for 24 hours at $105°$ C for water content and dry bulk density determination. Figure 4.7 shows all tool shapes employed in the basic design and in the extended design tests.

The initial set of trials involved testing a flat, triangular and elliptical tool shapes at three speeds (2.8, 5.6 and 8.4 m/s), two depths of operation (50 and 100 mm), and two compaction levels ('soft' and 'hard') (Table 4.2). The elliptical tool was further tested at extended operating speeds (Table 4.3). An average water content of 12.3% was

Flat   Triangular   Elliptical 4:1

(mm)
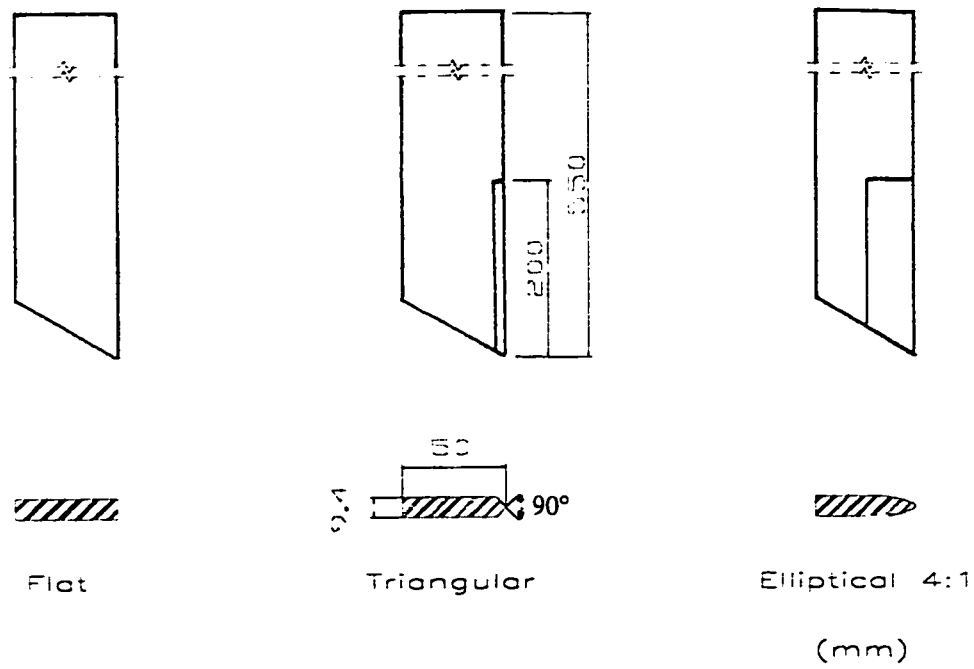
Figure 4.7   **Tool shapes used in the soil bin experiments.**

Table 4.2   **Experimental design adopted for the initial tests.**

Tool type	Width (mm)	Depth (mm)	Water content (%)	Bulk density soft (Mg/m^3)	hard	Tested speeds (m/s)
1 Flat	9.4	50	12.3	1.15 (0.04)	1.21 (0.03)	2.8 5.6 8.4
2 Flat	9.4	100	12.3	1.22 (0.05)	1.33 (0.04)	2.8 5.6 8.4
3 Triangular	9.4	50	12.3	1.15 (0.04)	1.21 (0.03)	2.8 5.6 8.4
4 Triangular	9.4	100	12.3	1.22 (0.05)	1.33 (0.04)	2.8 5.6 8.4
5 Elliptical	9.4	50	12.3	1.15 (0.04)	1.21 (0.03)	2.8 5.6 8.4
6 Elliptical	9.4	100	12.3	1.22 (0.05)	1.33 (0.04)	2.8 5.6 8.4

Three replications for each trial.
Standard deviations in brackets.

Table 4.3   **Experimental design adopted for the extended tests (hard compaction level).**

Tool type	Width (mm)	Depth (mm)	Water content (%)	Bulk density (Mg/m^3)	Speed range (m/s)
Elliptical	9.4	100	12.3	1.32	0.5 - 10.0
Elliptical	9.4	100	17.0	1.45	0.5 - 8.4
Elliptical	4.7	100	17.0	1.45	0.5 - 10.0

Three replications for each trial.

maintained for all runs. Each data point consisted of three replications. The soil was roto-tilled once for each test run.

Extended trials included refinement for the elliptical tool working in the speed range of 0.5 up to 10.0 m/s at 12.3% water content. The water content was then increased to 17.0%. Two elliptical tools were tested: the same 9.4 mm wide elliptical tool and another one with half the width. The tools were tested over speed ranges from 0.5 up to 8.5 m/s and 0.5 to 10 m/s, respectively.

After the soil had been carefully prepared and leveled the system was lowered from the storage position and the tool carriage was moved to the start position with the tool tip just above the soil surface. The tool was then lowered to the desired working depth. The on-board computer (TDS2020) was set to run on its own battery supply and the stationery computer was set on waiting mode. A triggering pulse generated by the electronic box simultaneously started the stationary computer, the on-board computer and the hydraulic drive. The carriage accelerated, reached the nominal steady state speed, and finally the break action was activated. The on-board computer was then connected to the stationary computer to download the measured tool forces and speeds to the PC-computer hard disc.

After each run was performed, the I-beam frame was lifted and the resulting soil profile was recorded with a plastic profilometer. The profilometer consisted of sliding plastic pins, approximately 2 mm wide, regularly distributed along a 300 mm long pin holder bar. There was no space between pins. The pins were displaced over the disturbed soil to closely follow the soil profile. The profile was then traced on paper with a pen.

Photo and images using a video camera were recorded for posterior analysis of soil disturbance.

The soil was then prepared again for the next test run as described above. Using the above system, it was possible to collect one replication of draft versus operating speed per soil preparation. Three replications of the same point measurement could usually be completed per day.

4.2.2 Quasi-static triaxial/shear box test procedures

Triaxial tests were conducted to measure soil response at slow (quasi-static) loading rates. The resulting soil stress-strain curves were needed to calculate quasi-static parameters used in the described analytical soil model (chapter 3).

The triaxial cell (10 kN, ELE International Ltd., Hemel Hempstead, Hertfordshire, England) used is a conventional design (Chi 1989) (Figure 4.8). Drained triaxial tests were performed to represent shallow top soil cut by the soil tools (depth of 50 and 100 mm). The equipment allows axial soil specimen compression at constant confining pressures produced by the cell water pressure. In the drained test a coarse porous stone is used at the base of the cylindrical soil specimen. The stone allows air and water to escape from the soil specimen during soil compression.

The same soil with characteristics from the soil bin trials, in terms of water content and bulk density, were used to reproduce the remolded soil in the triaxial and shear box tests. The soil test procedure included first sieving air dried soil through a #10 US Standard sieve with 2 mm round openings.
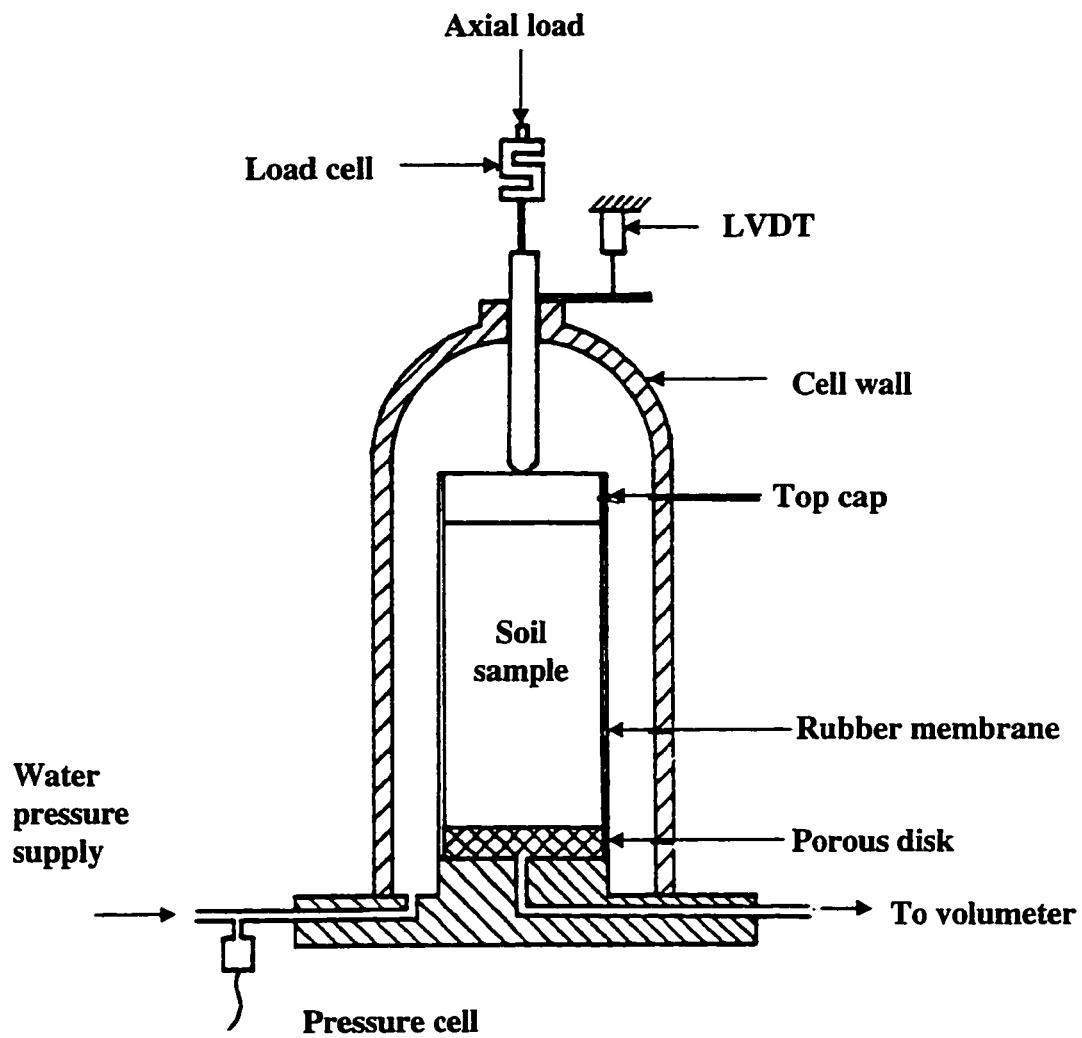
Figure 4.8 Conventional triaxial apparatus used for drained soil tests (Chi 1989).

Cylindrical soil specimens, 52 mm in diameter and 106 mm in length, were carefully produced by statically compacting soil in layers using a split compaction mold. Triaxial tests were conducted under confining pressures of 0, 30, 60 and 90 kPa. After isotropic consolidation, the samples were loaded to failure at a rate of 3 mm/min, corresponding to a reference strain rate of 0.03 min^{-1}.

A volumeter similar to that described by Dunlap and Weber (1971) and Chi (1989) was used to measure specimen volume change (Figure 4.9). The volume change in the soil sample during loading was calculated from (Chi 1989):

$$\Delta V' = \frac{\Delta p V_0'}{p_a + \Delta p} \tag{4.1}$$

where:

$\Delta V'$ = volume change in soil sample during loading,

V_0' = total air volume in sample, line and test chamber before loading,

p_a = atmospheric pressure,

Δp = pressure change in the volumeter chamber during loading,

A pressure transducer (model DP103-26, Valydine Northridge, CA) with range of 3.5 kPa ($\pm$ 1%) was used to monitor the pressure change Δp. A 50 ml syringe was used to calibrate the volumeter.

The axial force applied to the specimen was measured by a 2.4 kN load cell (model SSM-500, Interface, Scottsdale, AZ). Displacement was measured using an LVDT (7DCDT1000, Hewlett Packard Co., Andover, MA). Axial load, confining pressure, axial displacement and pressure change were recorded by a Campbell 21X Micrologger
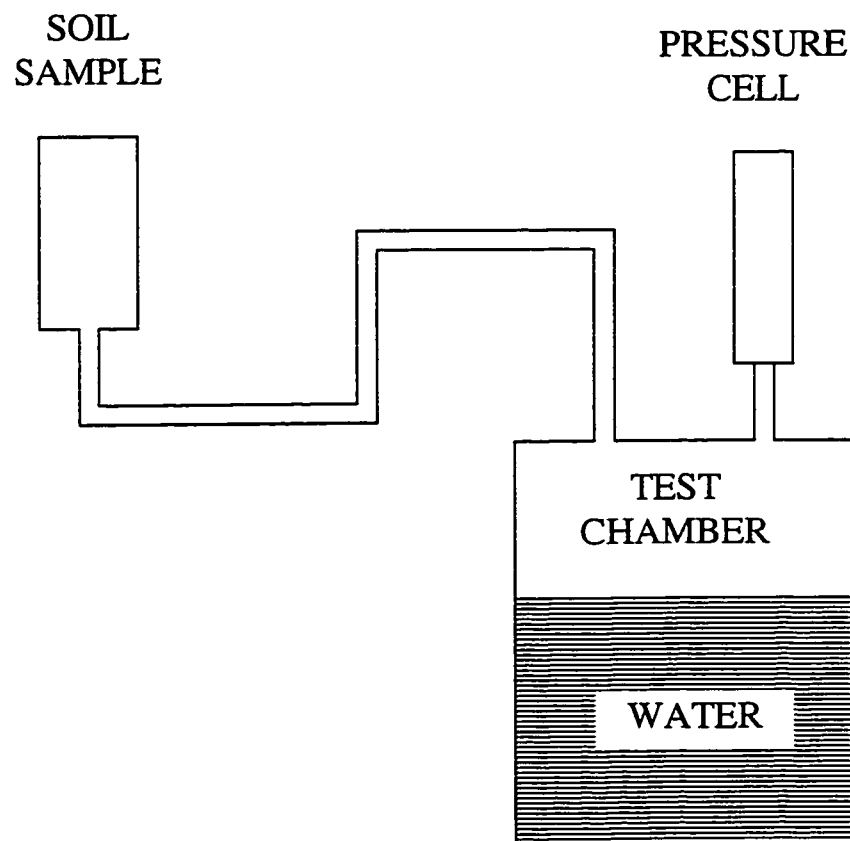
Figure 4.9   **Schematic diagram of volumeter (Chi 1989).**

(Campbell Scientific Inc., Logan, Utah). These data were later processed to give stresses, strains and volume changes and to calculate Poisson's ratio. The test was assumed to occur at constant temperature. The room was temperature controlled (estimated variation within ±1°C for a 30 minute period) and the complete test was usually less than 30 minutes.

Soil parameters obtained from triaxial tests are given in Table 4.4. Parameters (R_f, n, k, c, ϕ, v) were calculated using the procedures of Duncan and Chang (1970) and Chi (1989).

A modified direct shear box apparatus was used to evaluate quasi-static soil-tool interface parameters (Figure 4.10). A polished steel block, the same tool material used in the soil bin tests, served as the base of the shear box.

The shear stress-displacement relationships were derived for DH and WH in the soil direct shear box tests. The parameters were obtained following the work of Clough and Duncan (1971) and results are presented in Table 4.5. Confined pressures were averaged values: 30, 60, 90 and 150 kPa. Experimental confining pressures varied between ±1 kPa approximately.

Different normal pressures (30, 60, 90 and 150 kPa) were obtained by hanging dead weights on the machine. Shearing speed was set to 0.02 mm/s. A 4.5 kN load cell (model SSM-1000, Interface, Scottsdale, AZ) was used to measure axial loads and a Campbell 21X Micrologger (Campbell Scientific Inc., Logan, Utah) recorded forces and time. The loading speed was assumed constant for the shear box apparatus.

Table 4.4   Soil parameters obtained from triaxial tests.

	R_f	k	n	c	ϕ	$v^{\bullet}$	$a_I^{\clubsuit}$	$b_I^{\clubsuit}$
	-	(kPa)	-	(kPa)	(deg.)	-	-	-
DH^{+}	0.70	24.54	0.000	6.7	39.3	0.38	0.4287	0.0658
WH^{++}	0.73	15.82	-0.156	11.7	36.8	0.34	-	-
DL^{+++}	0.73	19.04	-0.045	6.1	37.1	0.33	-	-

$\bullet$ Poisson's ratio averaged over four tests.
$\clubsuit$ Variable Poisson's parameters a_I and b_I according to Chi et al. (1993a), equation 3.41.
$+$ DH - hard soil condition, 50-100 mm depth, water content 12.3%, bulk density
        1.33 Mg/m^3.
$++$ WH - hard soil condition, 50-100 mm depth, water content 17.0%, bulk density
        1.45 Mg/m^3.
$+++$ DL - soft soil condition, 0-50 mm depth, water content 12.3%, bulk density
        1.15 Mg/m^3.

Table 4.5   Parameters obtained from shear box tests.

	R_f	k	n	C_a	δ'
	-	(kPa/mm)	-	(kPa)	(degrees)
DH^{+}	0.88	92.31	0.356	0.6	23.8
WH^{++}	0.87	87.27	0.535	8.3	24.0

$+$ DH - hard soil condition, 50-100 mm depth, water content
        12.3%, bulk density 1.33 Mg/m^3.
$++$ WH - hard soil condition, 50-100 mm depth, water content
        17.0%, bulk density 1.45 Mg/m^3.

Normal load

12 mm

Porous stone

Shear load

Soil sample

Failure plane

2 mm

Steel block
100 x 100 mm

100 mm
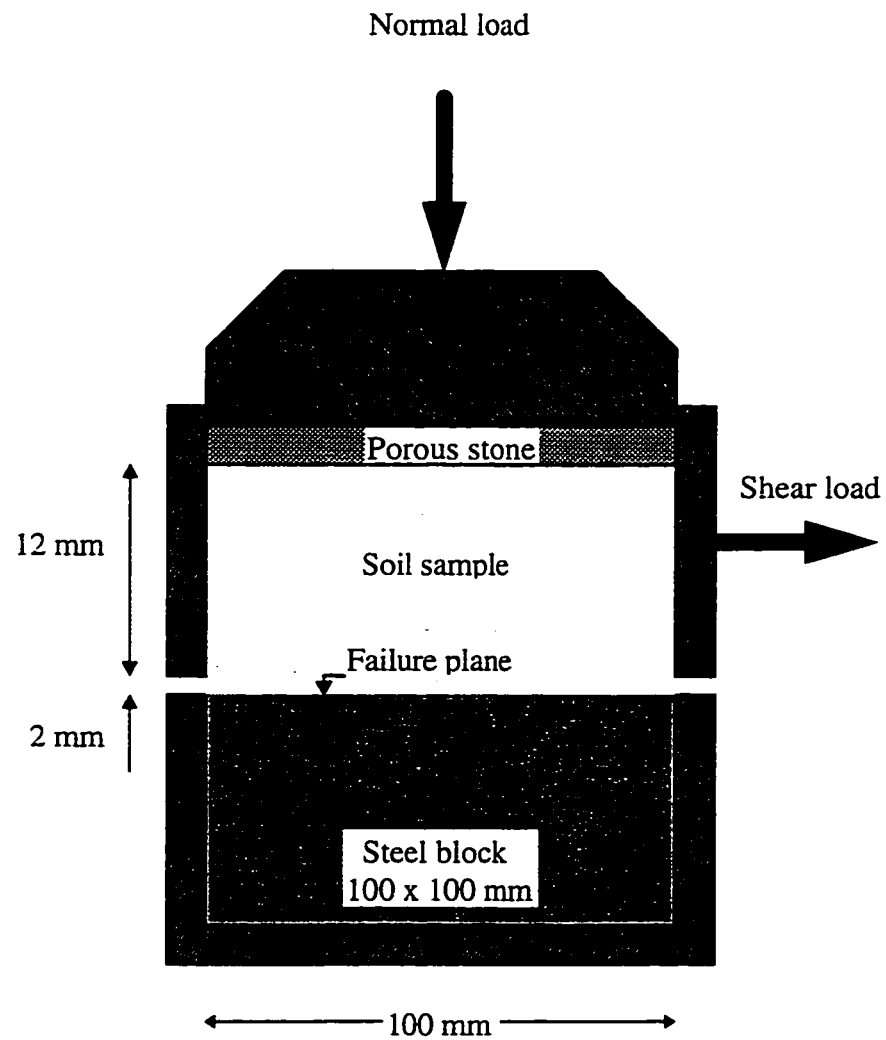
Figure 4.10   Modified direct shear box apparatus used to evaluate quasi-static soil

tool interface parameters (after Chi 1989).

Large strains occurred for soil cutting and also for triaxial tests. Axial true stresses and strains were calculated as described by Chi (1989).

Typical experimental data from a triaxial test are shown in Figure 4.11. Deviatoric stress and Poisson's ratio are presented for a confining pressure of 90 kPa and loading rate of 0.05 mm/s.

$$\sigma_a = \frac{P}{A_0(1 + 2\varepsilon_r)} \tag{4.2}$$

$$\varepsilon_a = -\ln\left(\frac{l}{l_0}\right) \qquad l < l_0 \quad \therefore \quad \varepsilon_a > 0 \tag{4.3}$$

$$\Delta\varepsilon_r = \frac{1}{2}\left(\frac{\Delta V'}{V_0'} - \Delta\varepsilon_a\right) \tag{4.4}$$

where, for compressive values taken as positive;

σ_a = true axial stress (kPa),

ε_a = true axial strain, (assumed large),

P   = axial load (kN),

A_0 = initial specimen cross section area (m^2),

ε_r = radial strain,

l_0 = initial length of specimen (m),

l   = length of specimen during loading (m),

$\dfrac{\Delta V'}{V_0'}$ = volumetric strain $\Delta\varepsilon_v = \Delta\varepsilon_a + 2\Delta\varepsilon_r$, (assumed small),

$\Delta V'$ = volume change (m^3),

V_0' = initial volume (m^3).
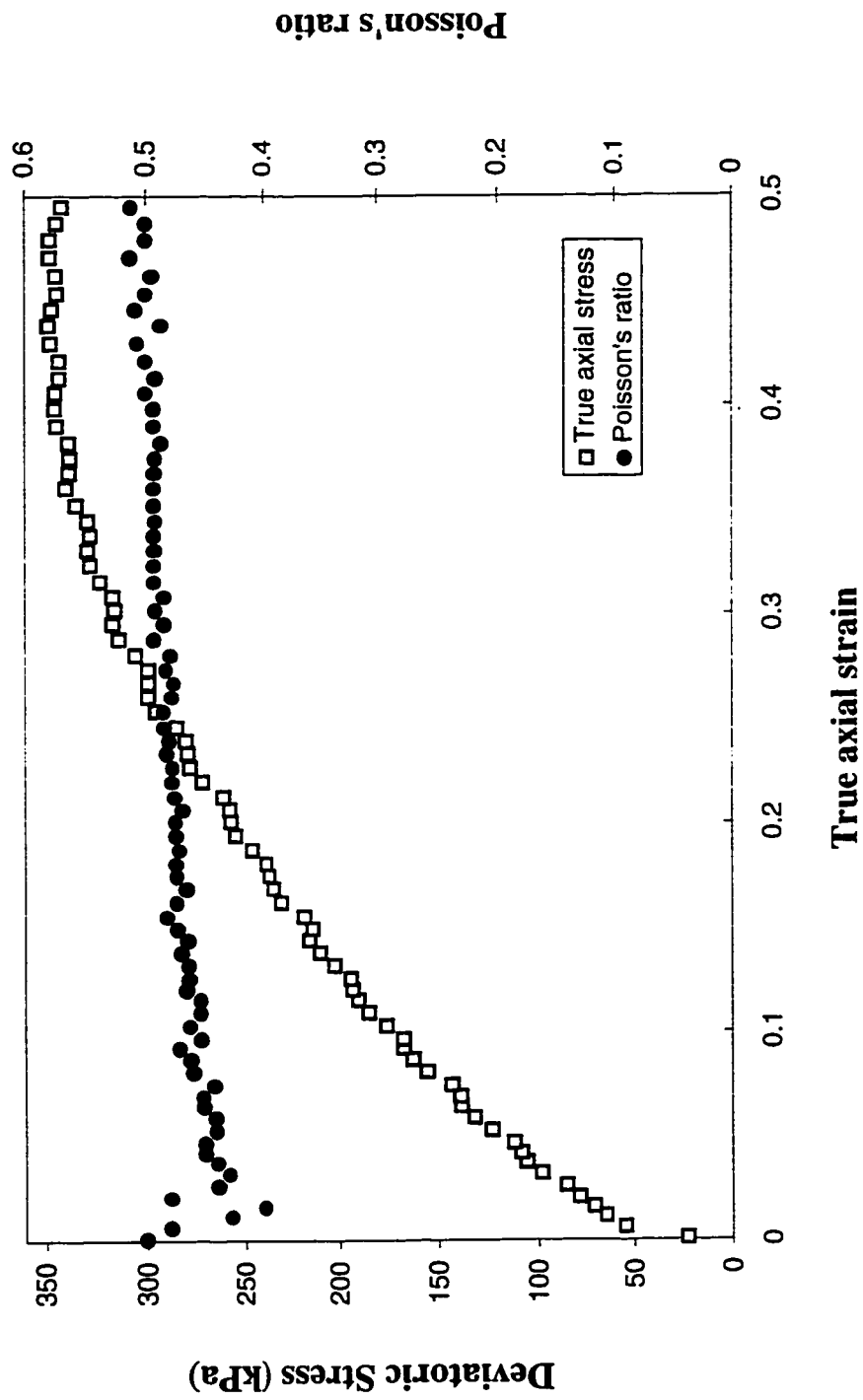
Figure 4.11 Typical deviatoric stress and Poisson's ratio vs. axial strain for a triaxial test with 90 kPa confining pressure and 0.05 mm/s loading speed.

Poisson's ratio was calculated as $v = -\Delta\varepsilon_r / \Delta\varepsilon_a$, which was used in this study. Alternatively, it can also be calculated as $v = 0.5\,(1 - \Delta\varepsilon_v / \Delta\varepsilon_a)$, where Δ stands for incremental values and $\Delta\varepsilon_a$ the incremental strain value in the axial direction of a conventional cylindrical triaxial test; however, not used in this study.

4.3 Reference Tool Dynamic Parameter estimation

A reference tool method was developed to verify the validity of the numerical code Dyntool, and to estimate the dynamic parameter AN. As shown in the next chapter, the Dyntool model did not adequately represent the dynamic soil cutting problem due to numerical instabilities and lack of sensitivity in the draft values as tool shapes changed. Then, a new soil constitutive relationship, where the viscous parameters represented by C_l were independent of the stiffness matrix, was implemented in a code, named the Dyntool-2. The Dyntool-2 proved to be more successful than the Dyntool code. The same reference tool procedure to obtain dynamic parameter AN for the Dyntool code was used with the Dyntool-2 code to determine the dynamic viscous parameter C_l . Only the procedure considering AN with the Dyntool code is presented here, however, using C_l with the Dyntool-2 code may be similarly considered.

A flat reference tool was initially run in the soil at a constant depth. Draft versus speed data were recorded and used along with the Dyntool code to estimate AN. Further computations using the code with a triangular tool shape mesh were used to predict tool draft at corresponding speeds of the tool running at the same operating depth.

The parameters needed for numerical model simulation consist of static parameters obtained using quasi-static triaxial tests and an additional dynamic parameter AN (equation 3.39). To obtain the dynamic parameter AN, the linear relationship obtained for the experimental draft-velocity curves is used. All quasi-static parameters are assumed unchanged for the dynamic case; however, the dynamic parameter will produce an expanding dynamic failure surface. The expanding surface is dependent on soil strain rates.

Data of draft versus speed obtained from the flat reference tool run in the high speed monorail test are used as a reference curve. A numerical simulation using the program Dyntool with different dynamic parameters AN is run to obtain a response surface, i.e., a region of different predicted numerical drafts versus speed. Discrete tool speeds are associated with a particular AN value when the experimental value of tool draft corresponds to the predicted draft of the response surface. The same procedure is repeated for various tool speeds to estimate values of AN in the desired speed range. Therefore, discrete dynamic parameters are estimated for a range of discrete tool speeds. The estimated dynamic parameters related to tool speed can then be used to predict soil tool response (draft x speed) corresponding to the discrete tool speeds for a triangular tool or other tool geometries for the same soil conditions and constant working depth.

To verify the validity of the numerical program code Dyntool considering the inertial equation, a two-part procedure was necessary, namely, i) quasi-static, and ii) dynamic verification, because an appropriate dynamic solution for a sample case was not found in the literature.

Simulations using the Dyntool program were compared with the analysis of a circular footing on clay presented by Duncan and Chang (1970) to check the validation of the quasi-static numerical code. Data of draft versus speed were obtained for a flat reference tool running at the depth of 100 mm in a hard compacted soil with 12.3% water content. A flat reference tool is used together with the numerical code, Dyntool, to obtain the dynamic parameter AN. The dynamic parameter was then used to calculate the response of the triangular or other different tool shapes working at same tool depth at the calculated discrete tool speeds.

CHAPTER 5

RESULTS AND DISCUSSION

This chapter presents the results and discussion of the experimental data from the monorail system, dynamic response and power analysis, soil disturbance and pulverization, and evaluation of the soil constitutive model for tool draft.

5.1   Experimental Results

5.1.1 Dynamic response of monorail system

Tool forces and operating speeds measured with the monorail system indicate the dynamics of the monorail system performs adequately. At steady state speed, the tool carriage mass (~ 10 kg including tool) did not introduce any inertial components to the force measurements. This was confirmed by running the tool and carriage at various speeds under no soil load, i.e., while the tool was not cutting any soil, which had been previously removed from the tool path. A typical no load run of a flat tool operating at 5.6 m/s is shown in Figure 5.1. Data points were averaged at every ten points (running average) in order to interpret data. A loaded run with the tool cutting the soil at 100 mm depth is shown in Figure 5.2. The tool reached steady state speed for the load and for the no load cases during at least 0.3 s. Tool reactions were stable during this time interval and indicated an approximate null value on the no load run (average -12 N).
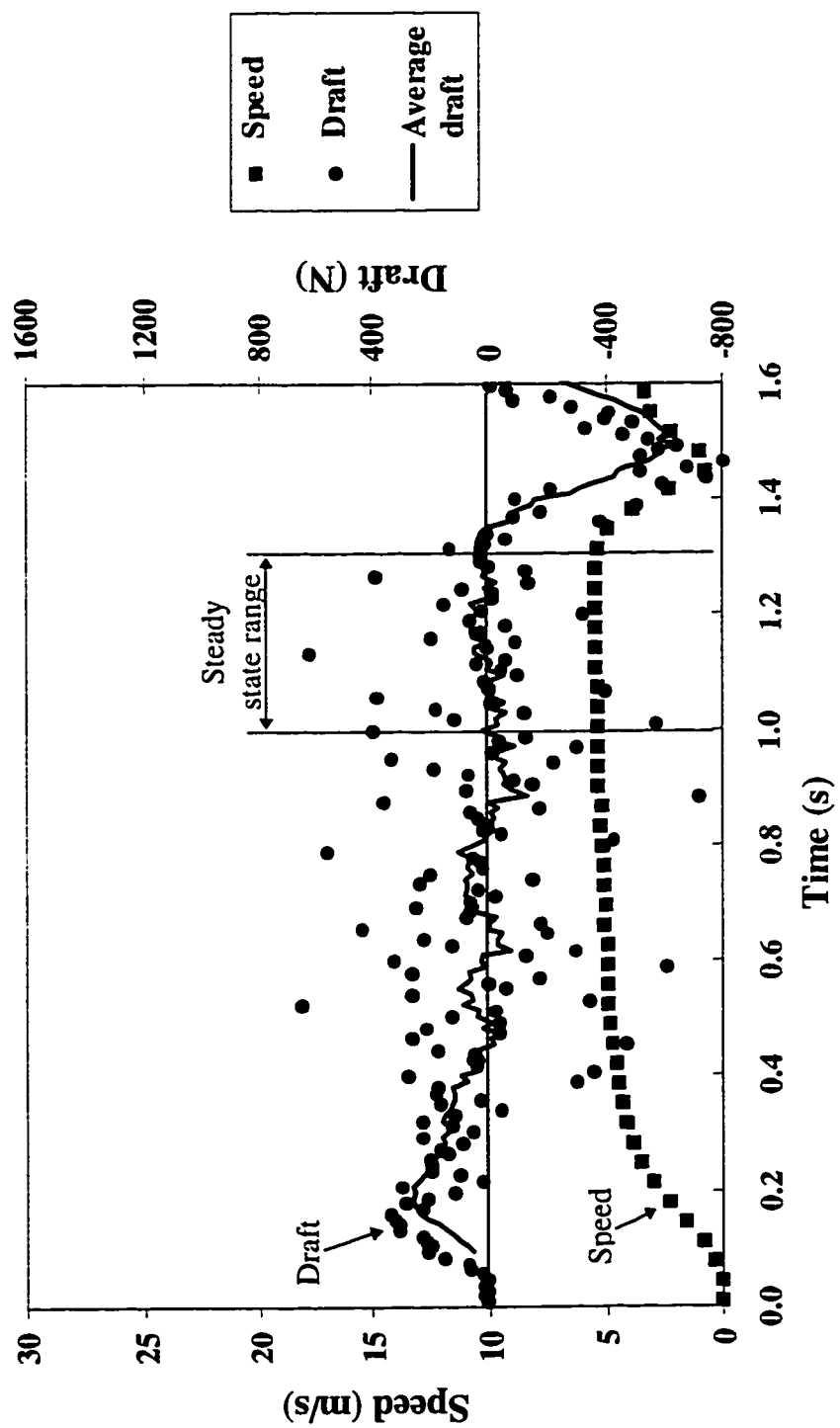
Figure 5.1 Draft versus speed results for the flat tool running at a steady state speed of 5.6 m/s with the tool not engaged into the soil.
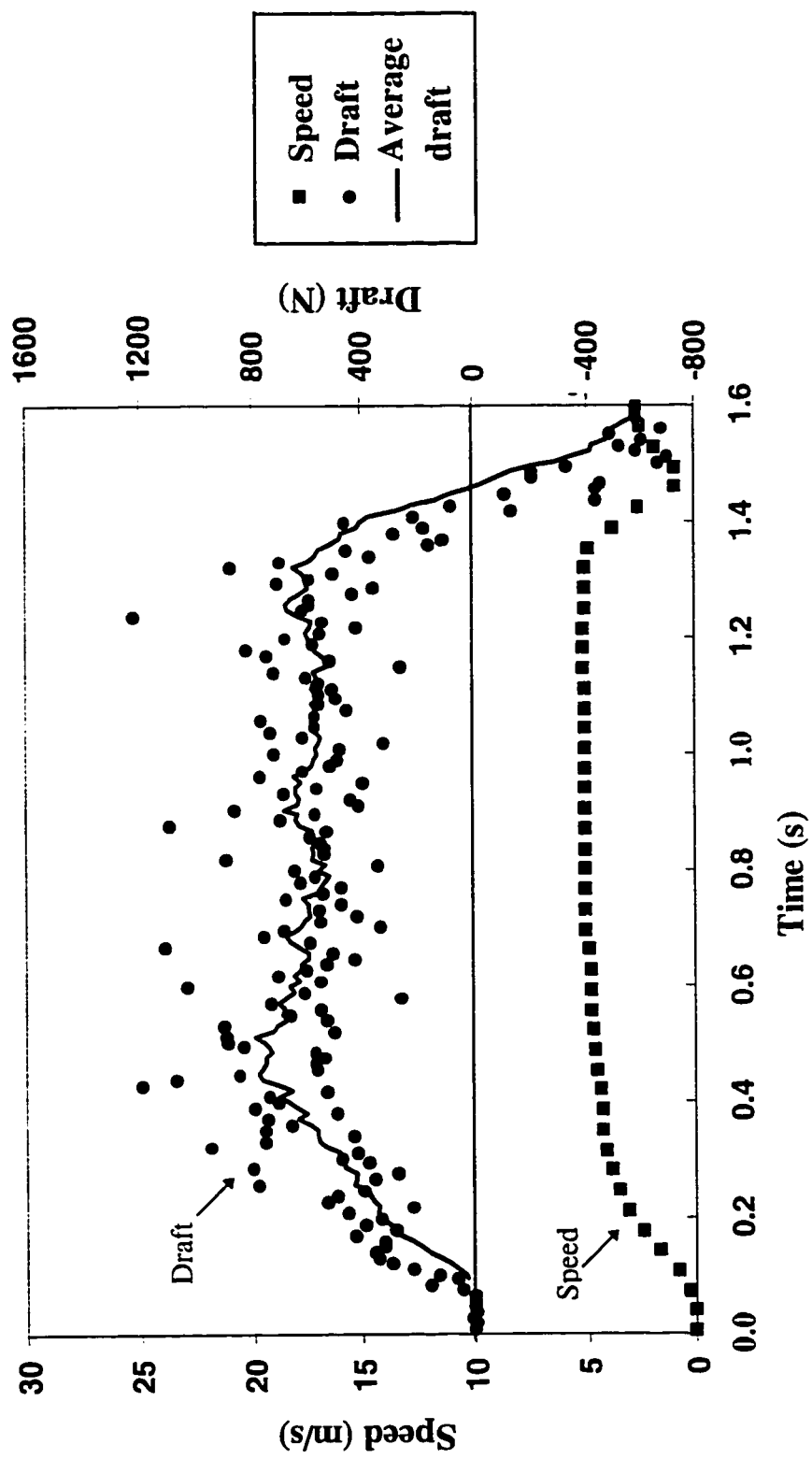
Figure 5.2   Draft versus speed results for the flat tool running at a steady state speed of 5.6 m/s with the tool engaged

into the soil at a depth of 100 mm.

146

Data points in Figures 5.1 and 5.2 indicate that the variability in the draft reduced when soil load was introduced into the system, probably due to strong damping effects produced by the soil mass. Results from a power spectral density analysis reinforce this statement. The objective of doing the power spectral density analysis was to detect the periodic fluctuation of the tool draft. The analysis was performed for the data of the basic experimental design. The constant component of draft (the average) was subtracted from the data points to analyze only oscillating components. Figures 5.3 and 5.4 show the power spectral density analysis of draft force F_x performed for the data of Figures 5.1 and 5.2, respectively. Integration of the areas underneath the curves indicated that the total power spectral density with no load (9.8×10^5 N^2) was almost twice the level when soil load was present (5.0×10^5 N^2). When the tool was moving without engaging the soil, load shocks on the bearings and the I-rail caused a wide frequency band to be generated from zero up to approximately 50 Hz (Figure 5.3). Although aliasing does not affect the DC component of the draft signal, and power spectral density values were damped, it could still be present in the signal. A complete frequency analysis of the draft signal is suggested. Based on the findings of this section on dynamic response of the monorail system, the monorail system is capable of adequately measuring tool draft versus speed data.

5.1.2 Effect of soil condition and tool shape on draft

Figure 5.5 shows average cone index profiles for the hard and soft-packed soil in the soil bin for an average soil water content of 12.3%. Table 5.1, representing soft and
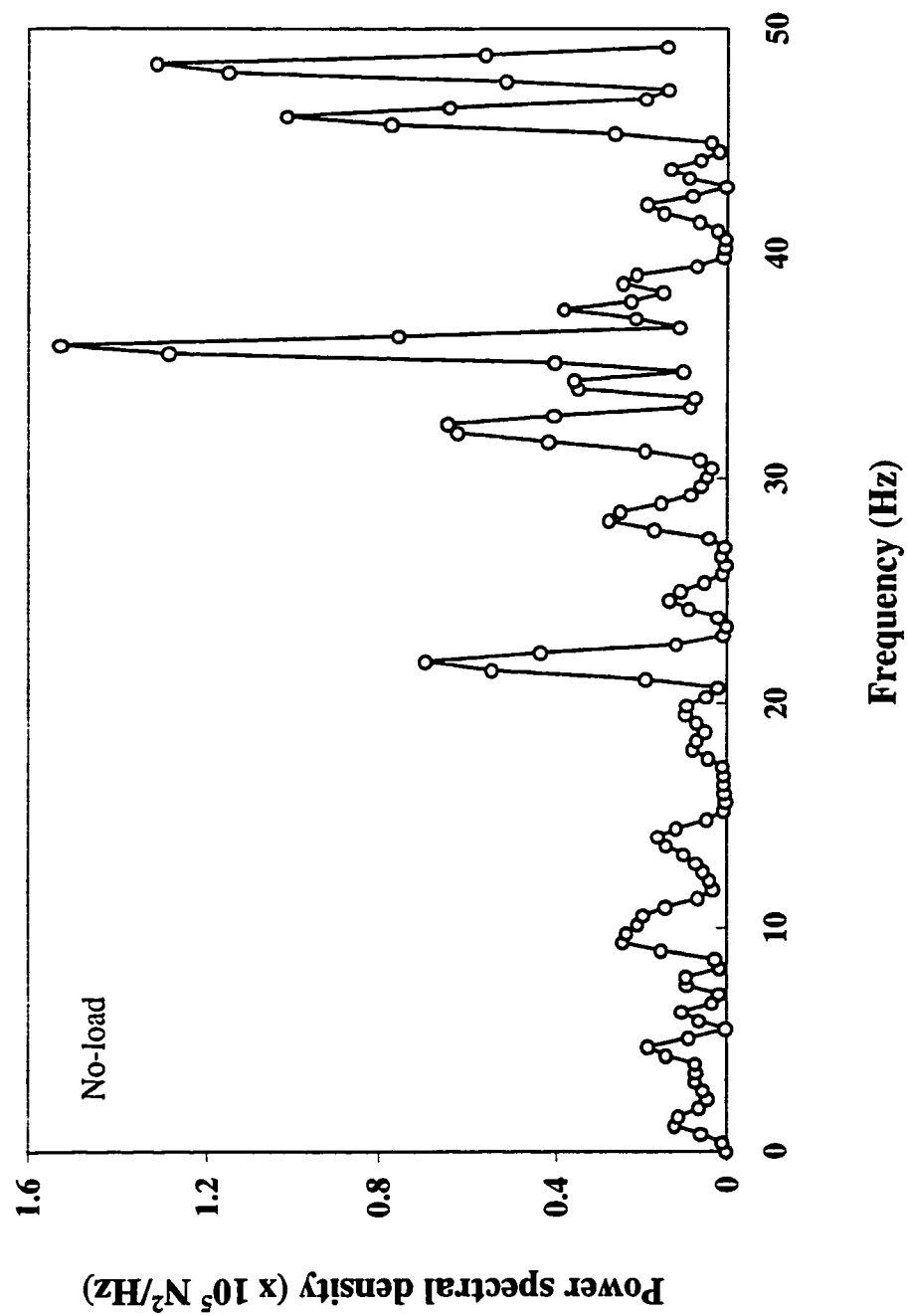
Figure 5.3   Power spectral density analysis resulted for the flat tool running at a steady state speed of 5.6 m/s with the tool not engaged into the soil.
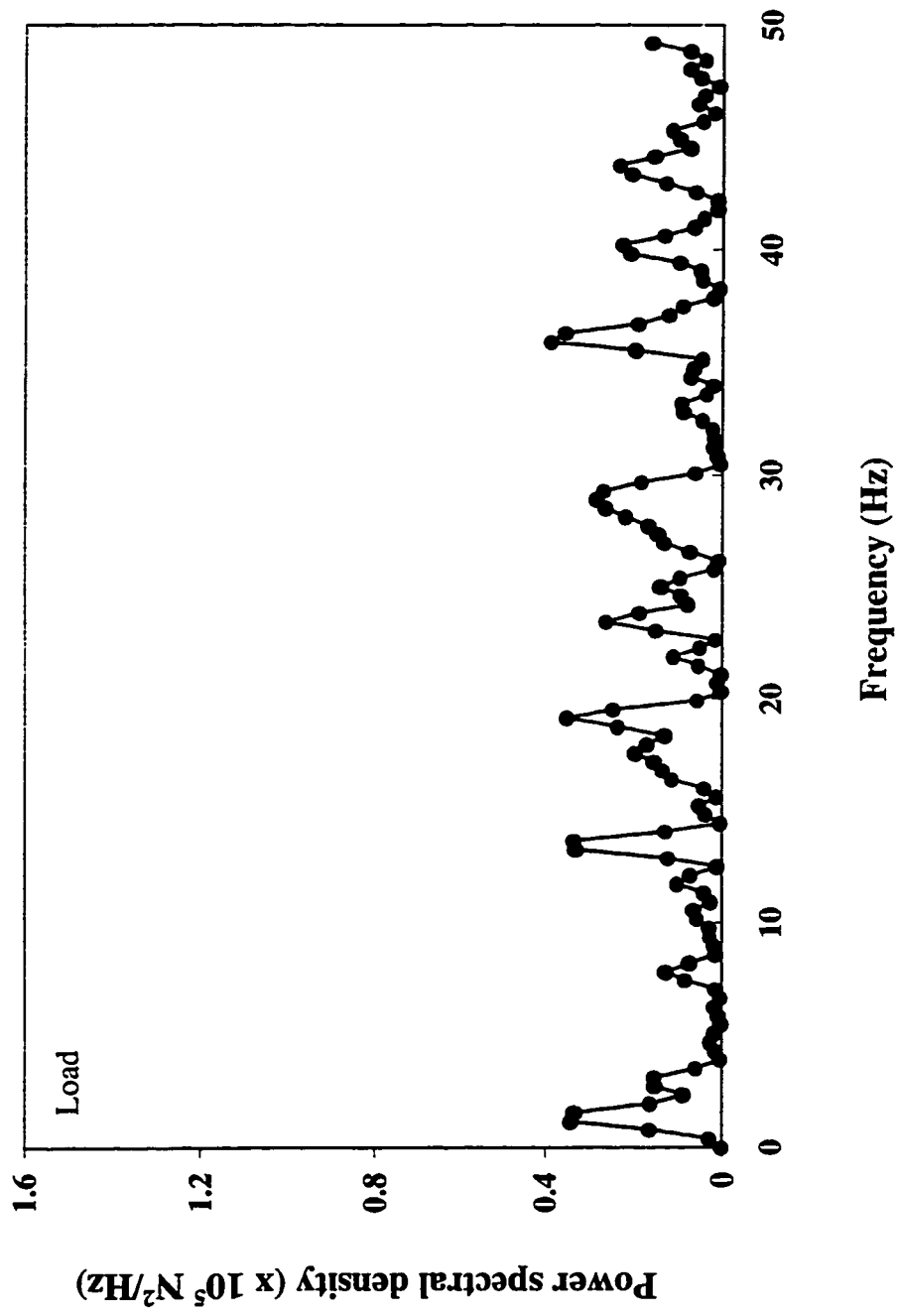
Figure 5.4   Power spectral density analysis resulted for the flat tool running at a steady state speed of 5.6 m/s with the tool engaged into the soil at a depth of 100 mm.
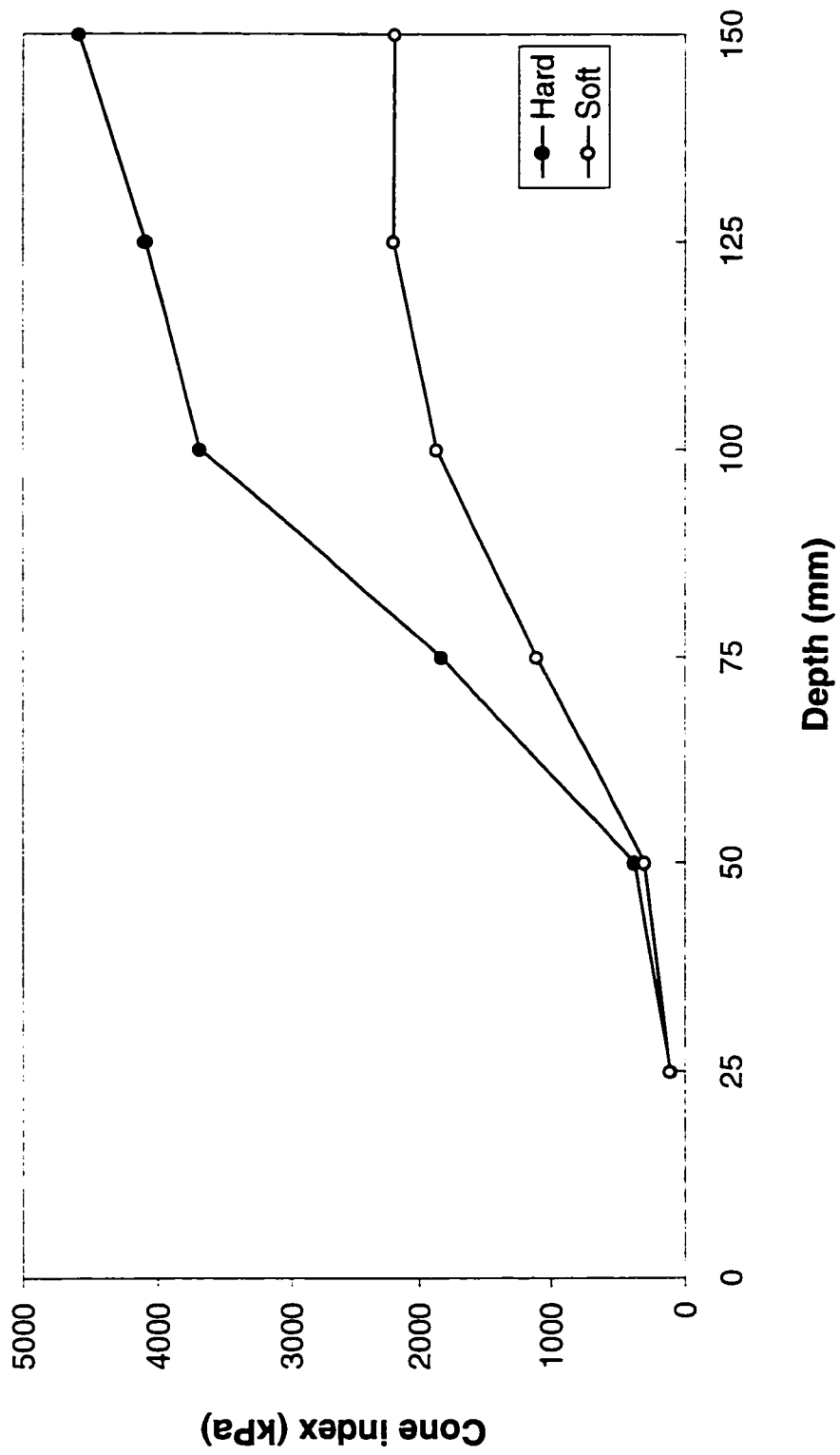
Figure 5.5 Average cone index profiles for the hard and soft soil compaction levels in the soil bin for average water content of 12.3%.

Table 5.1 Cone index versus depth for soft and hard soil compaction and respective bulk densities. The soft soil condition had a water content of 12.6% ± 0.86%. The hard soil condition had a water content of 11.9% ± 0.43%.

Depth (mm)	Cone index (kPa)		Bulk density (Mg/m^3)	
	Soft	Hard	Soft	Hard
25	113 (0.37)	110 (0.77)		
50	304 (0.54)	380 (0.65)	1.15 (0.03)	1.21 (0.02)
75	1103 (0.44)	1830 (0.44)		
100	1868 (0.25)	3685 (0.26)	1.22 (0.04)	1.33 (0.03)
125	2193 (0.22)	4083 (0.30)		
150	2186 (0.29)	4577 (0.36)		

(Coefficient of variation in decimal in parenthesis)

hard compaction conditions, summarizes average cone index for depths from 25 to 150 mm, soil bulk densities and soil water content.

Low values of standard deviations for soil water contents were detected across the length of the soil bin; however, cone index readings presented relatively high values of coefficient of variation. The soil preparation method might have been partially responsible for the relatively high variation of soil penetration strength. The use of a hand-held penetrometer could have contributed to the variations also. It was observed that the sheep pack roller produced spots with concentrated higher compaction levels at approximately

150 mm intervals. Although the packing action of the sheep-foot roller was intended to pack the subsoil only, the soil surface was also affected.

Draft results for various tool shapes from the initial set of trials (see Table 4.2) are presented in Figures 5.6 and 5.7.

A linear draft versus speed behaviour was then assumed for the data and linear regression was performed for the whole data split according to tool type, depth of operation, and soil packing level. High values of R^2 were obtained. Intercept and slope values are also shown for each trial (Table 5.2).

When soil strength conditions were harder, tool shape had a more pronounced effect on the average slope value calculated at the two operating depths with each soil compaction level and tool type (Table 5.2). For the soft packed soil with tool operating depth of 50 mm different tool types did not produce substantial changes on draft-speed requirements (curves 1, 3 and 5, Figure 5.6). The small changes in intercept and slope values obtained for this treatment support this result. However, an increase in speed still produced increase in draft. For the remaining conditions, elliptical tools presented the lowest, and flat tools the highest draft requirements.

Average slope values obtained from the two operating depths under the same soil conditions decreased as tool shape became more streamlined. This trend in the slopes is also clearly seen from curves 2, 4 and 6 in Figure 5.7. The streamlining effect suggests that tools were been dragged through, rather than 'cutting', the soil. Increase in the operating depth substantially increased the draft demand for the three tool shapes and two soil conditions studied.
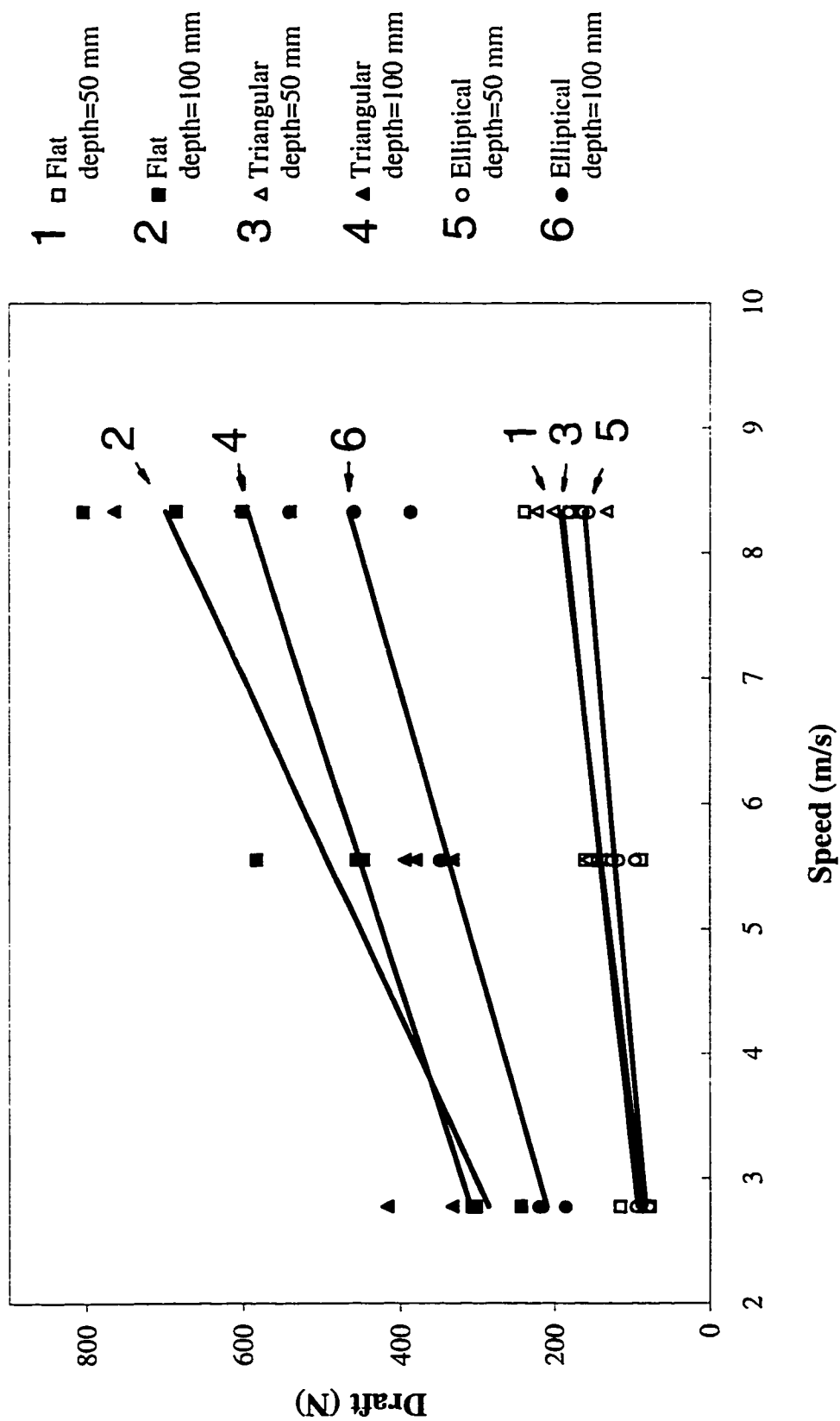
Figure 5.6 Tool draft in soft compacted soil condition obtained in the basic design test series.

Legend:

1 □ Flat depth=50 mm

2 ■ Flat depth=100 mm

3 △ Triangular depth=50 mm

4 ▲ Triangular depth=100 mm

5 ○ Elliptical depth=50 mm

6 ● Elliptical depth=100 mm

X-axis: Speed (m/s)

Y-axis: Draft (N)

153
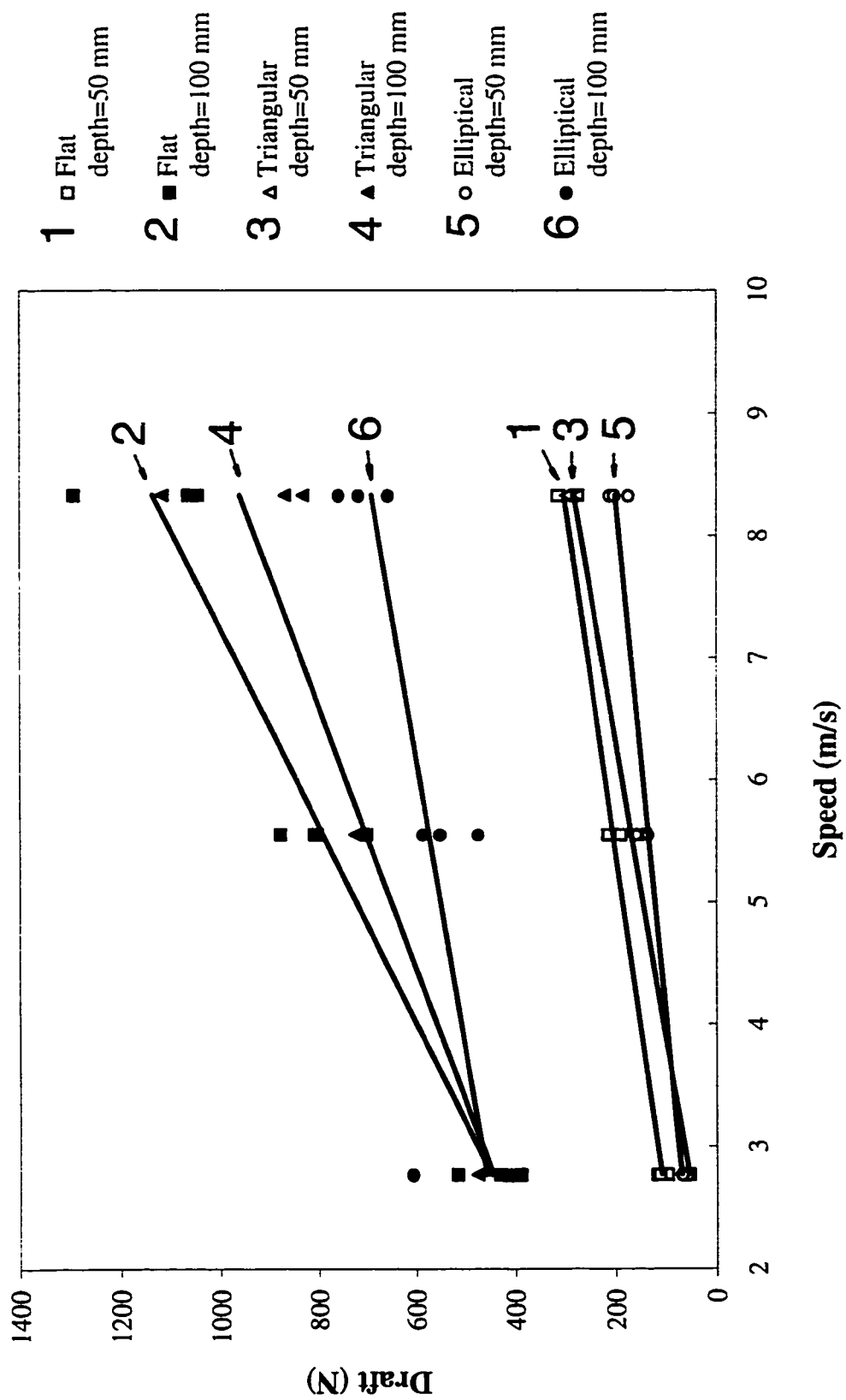
Figure 5.7 Tool draft in the hard compacted soil condition obtained in the basic design test series.

Table 5.2 Summary of linear regression analysis of the entire data split according to tool shape, depth of operation, and soil packing level.

	Depth (mm)	Intercept (N)	Slope (N·s/m)	R^2
Soft soil				
1 Flat	50	31	19	0.712
2 Flat	100	80	74	0.879
3 Triangular	50	41	18	0.741
4 Triangular	100	167	51	0.646
5 Elliptical	50	41	14	0.863
6 Elliptical	100	82	46	0.883
Hard soil				
1 Flat	50	13	35	0.975
2 Flat	100	102	124	0.919
3 Triangular	50	-58	41	0.981
4 Triangular	100	186	93	0.860
5 Elliptical	50	4	24	0.936
6 Elliptical	100	341	42	0.654

Coefficient of determination, R^2.

Data obtained from the basic test design were primarily intended to verify the mathematical model. Use of this data to perform a statistical analysis would require a split plot analysis. Intercepts and slopes calculated with the basic design draft-speed data (Table 5.2) could be used to develop the split plot analysis. However, the data did not present sufficient degrees of freedom for the error terms in the analysis to be small enough to give meaningful results. Therefore, a factorial statistical analysis is reported in the following. This analysis is not quite proper because of nesting effects involved among variables of classes; instead, replicates would be better interpreted as subsamples.

A statistical 3x2x2x3 factorial analysis of data for the 12.3% soil water content was developed using the statistical package SAS^R (SAS 1985). Appendix F shows input data and a sample SAS program. An analysis on the residual errors indicated that these error terms presented a reasonably normal distribution curve, with only a very slight indication of skewness. Residuals were tightly concentrated around a zero mean value.

The analysis of variance was performed using the SAS GLM procedure. All data (108 data points) were considered by combining soft-packed and hard-packed soil results. The following treatments (variables of classes) were considered: tool shape (T), tool depth of operation (D), speed (S) and soil bulk density B(D) along with the interactions: TxD, TxB(D), TxS, DxS, TxDxS, B(D)xS and TxB(D)xS (Table 5.3).

A coefficient of determination, R^2, of 0.968 and a coefficient of variation of 16.8% were obtained for this analysis.

156

Table 5.3   Statistical analysis of soil condition, tool depth, speed and tool shape along with interactions for the basic test design (12.3% water content).

Factor	df	Pr>F	Significance
T	2	0.0001	**
D	1	0.0001	**
TxD	2	0.0001	**
B(D)	2	0.0001	**
TxB(D)	4	0.3421	—
S	2	0.0001	**
TxS	4	0.0001	**
DxS	2	0.0001	**
TxDxS	4	0.0073	**
B(D)xS	4	0.0004	**
TxB(D)xS	8	0.0098	**

** significant at 1% level of confidence, — not significant,
T = tool shape,
D = tool depth of operation,
TxD = tool shape versus tool depth interaction,
B(D) = soil bulk density,
TxB(D) = tool shape versus soil bulk density interaction,
S = speed,
TxS = tool shape versus speed interaction,
DxS = tool depth versus speed interaction,
TxDxS = tool shape versus tool depth versus speed interaction,
B(D)xS = soil bulk density versus speed interaction,
TxB(D)xS = tool shape versus soil bulk density versus speed interaction.

Elliptical tool shapes

Results were based on the experimental design adopted in Table 4.3 in which only elliptical tool shapes were used. Figure 5.8 shows draft results of all runs for these tests. Three cases were measured: a) tool width of 9.4 mm, soil water content of 17.0% and soil bulk density of 1.45 Mg/m^3, b) tool width of 4.7 mm, soil water content of 17.0% and soil wet bulk density of 1.45 Mg/m^3 and c) tool width of 9.4 mm, soil water content of 12.3% and bulk density of 1.33 Mg/m^3.

All three conditions produced high linear correlation coefficients. All cases show draft increases with speed. The slopes of the curves indicate the effect of speed on draft. Slope was reduced when tool width was reduced by half in the same soil structures (Figure 5.8(ii)). This effect can be explained by a reduction of mobilized soil volume when tool width is reduced. Consequently, less soil is exposed to viscous effects, producing less draft in relation to increases in speed. From the cases studied up to here, draft increased linearly with speed with high correlation.

Soil packed to different bulk densities at different water contents form different structures. Thus, two different soil water contents and two different soil bulk densities indicate the effects of two different soil structures, i.e., one soil structure has a bulk density of 1.45 Mg/m^3 with 17.0% water content and the other 1.33 Mg/m^3 with 12.3% water content. The regression intercept increased when soil water content and bulk density increased simultaneously. However, the draft versus speed slope increased slightly.

(ii) Effect of tool width
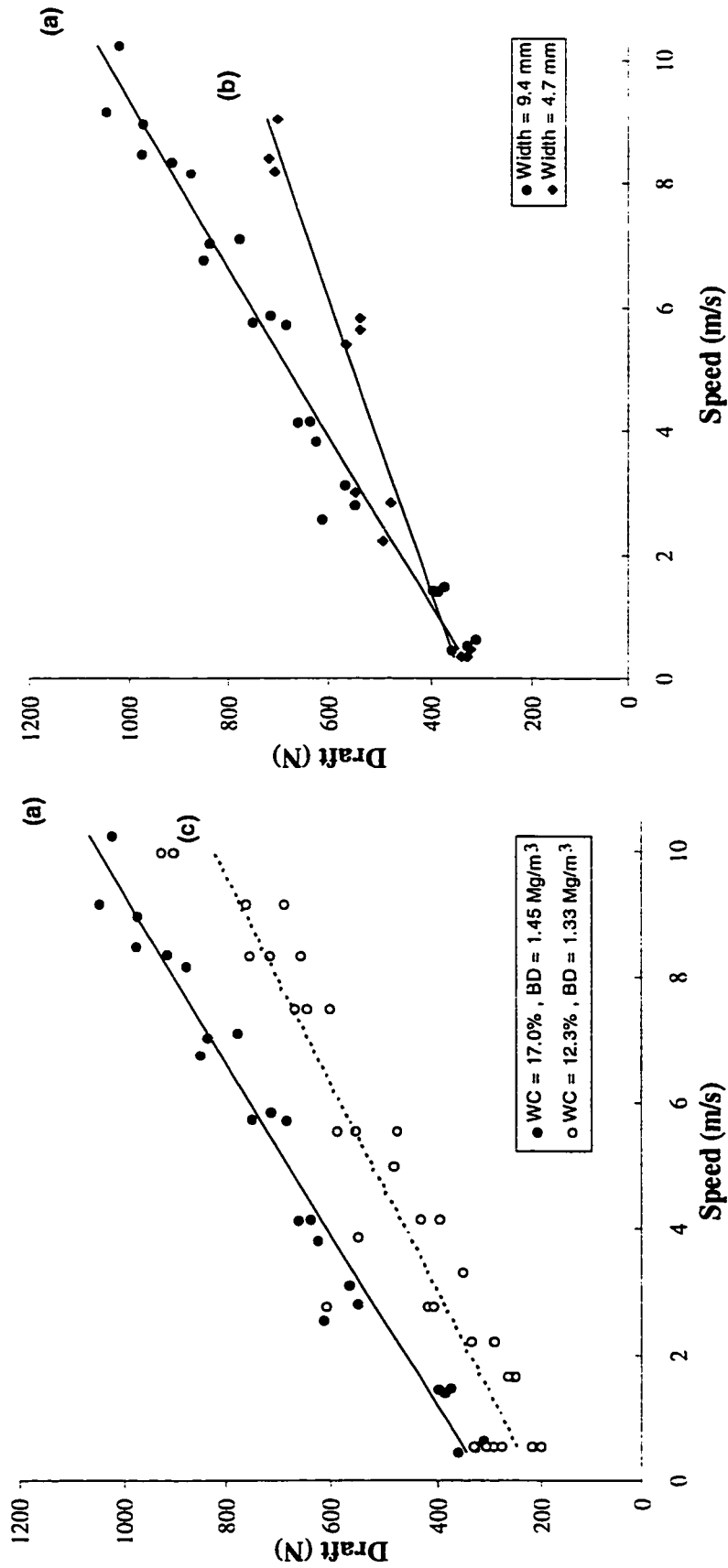
(i) Effect of soil structure

Figure 5.8   Draft results of all runs of the extended design test series with elliptical tools operating at 100 mm depth. Solid

lines (a, b) with closed symbols represent dense/wet soil structure (17.0% water content, 1.45 Mg/m^3 bulk density);

dashed line (c) with open symbols represents loose/dry soil structure (12.3% water content, 1.33 Mg/m^3 bulk density).

159

The most remarkable change was a translation of the regression line, i.e., an increased intercept (mostly due to bulk density increase).

A great number of data points per curve were available for each soil structure and tool shape. Three orthogonal forces on the tools were measured. Results of the narrow elliptical tool Figure 5.8, (case b) are shown in Figure 5.9. Both figures showed draft forces, F_x, were much higher in magnitude when compared with vertical forces, F_z. Vertical forces, F_z, were less than 15% of the magnitude of longitudinal forces, F_x. Therefore, this study was concerned only with draft forces, F_x. Further studies are required if vertical forces are to be included in the analysis. Transverse forces, F_y, should produce zero magnitude resultant force values due to tool symmetry. Experimental data confirm values of transversal forces close to zero. Transverse forces were thus not considered in subsequent analyses.

5.1.3 Power analysis

An analysis of power per operating depth, P_w, (Darmora and Pandey 1985) was conducted since the parameters need to determine P_w were readily available (see equation 2.1). Soil properties vary over the operating depth, since the soil becomes stiffer and more dense at higher depths. Power measurements have to be interpreted as an average of the total depth. It is still a good measurement, however, because of the above it reflects only the particular soil condition for which it is evaluated.
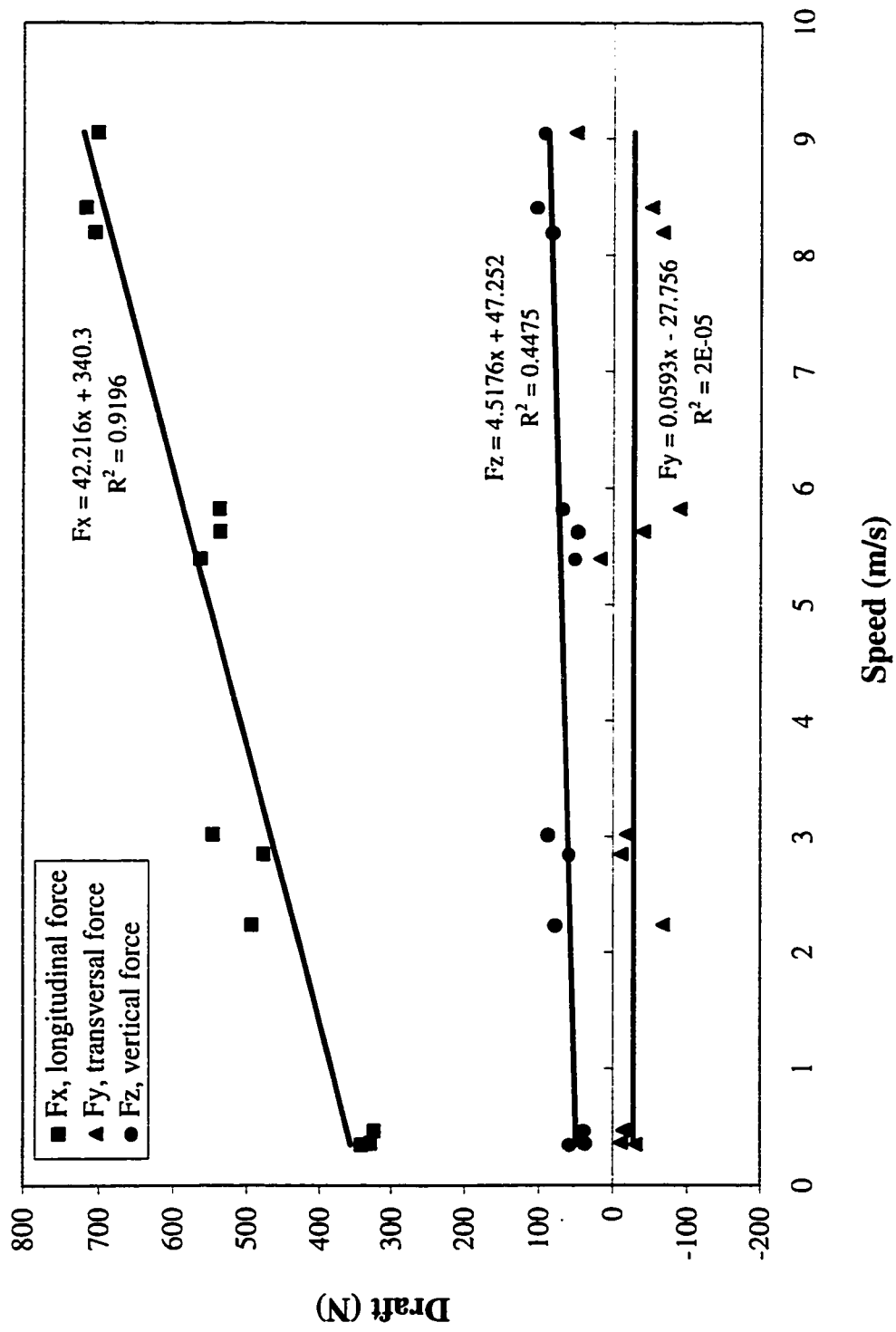
Figure 5.9   Draft results of the narrow elliptical tool, 4.7 mm wide for 17.0 % soil water content (case b).

161

Figures 5.10 to 5.12 present calculated values of P_w. Figures 5.10 and 5.11 were obtained from the basic test design data, while Figure 5.12 is for the extended test data. Figure 5.10 shows power per operating depth P_w for the soft packed soil at 12.3% water content. Figure 5.11 shows P_w values for the hard packed soil at the same soil water content. Values of P_w from Figure 5.12 were calculated from the extended test design data with elliptical tools.

Multiple regression analysis based on a polynomial relationship was performed for the extended test data. Sufficient degrees of freedom were available for this analysis. Table 5.4 shows results of the best fit regression coefficients. A similar analysis was not performed for the basic test design because there were insufficient degrees of freedom.

Figures 5.10 to 5.12 show that power per operating depth increased with speed of operation for all cases. A trend was identified for power values when comparing the lowest and the highest operating speeds, 2.8 m/s and 8.4 m/s, respectively. At the lowest speed, power P_w presented a narrow span range for all tool shapes. At the highest speed, the power P_w presented a wide span range. While at low speed of operation, change in shape does not produce much change in P_w , at high speeds, different tool shapes produce substantial changes in P_w . On soft packed soil (Figure 5.10) a six fold increase in P_w was observed for a threefold increase in speed at a 50 mm depth (curves 1, 3, 5). For the depth of 100 mm (curves 2, 4, 6), increase in P_w was about seven fold for the same speed range (2.8 to 8.4 m/s). The value of P_w is much more influenced by depth of operation and tool shape at high speeds of operation. At low speeds these two factors are less remarkable. Depth of operation was a major factor increasing expenditure of power. These results
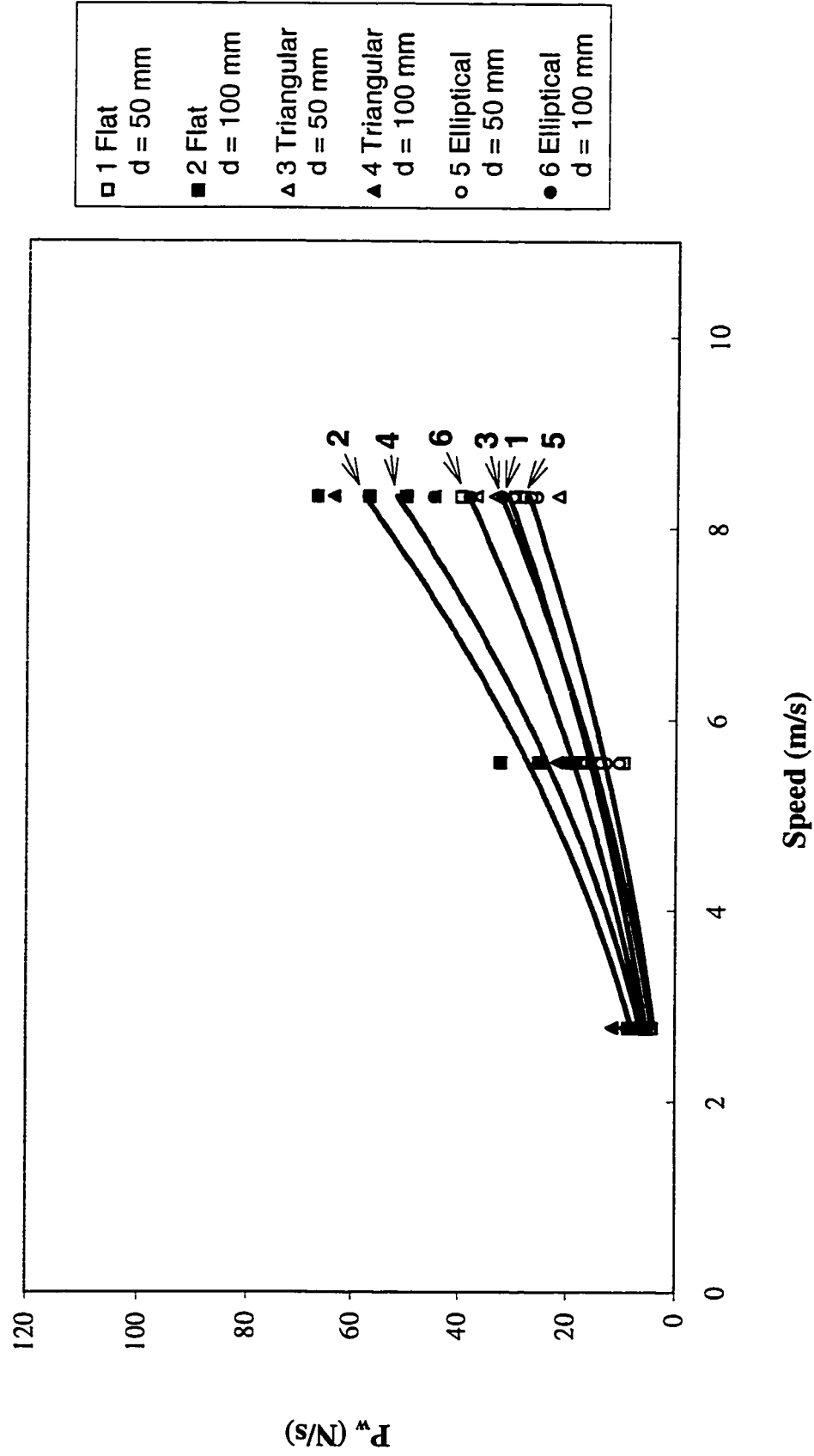
Figure 5.10 Power per operating depth, P_w, for tool operating in the soft packed soil condition at 12.3% water content.

Legend:
- □ 1 Flat d = 50 mm
- ■ 2 Flat d = 100 mm
- △ 3 Triangular d = 50 mm
- ▲ 4 Triangular d = 100 mm
- ○ 5 Elliptical d = 50 mm
- ● 6 Elliptical d = 100 mm

Axis: P_w (N/s) vs Speed (m/s)
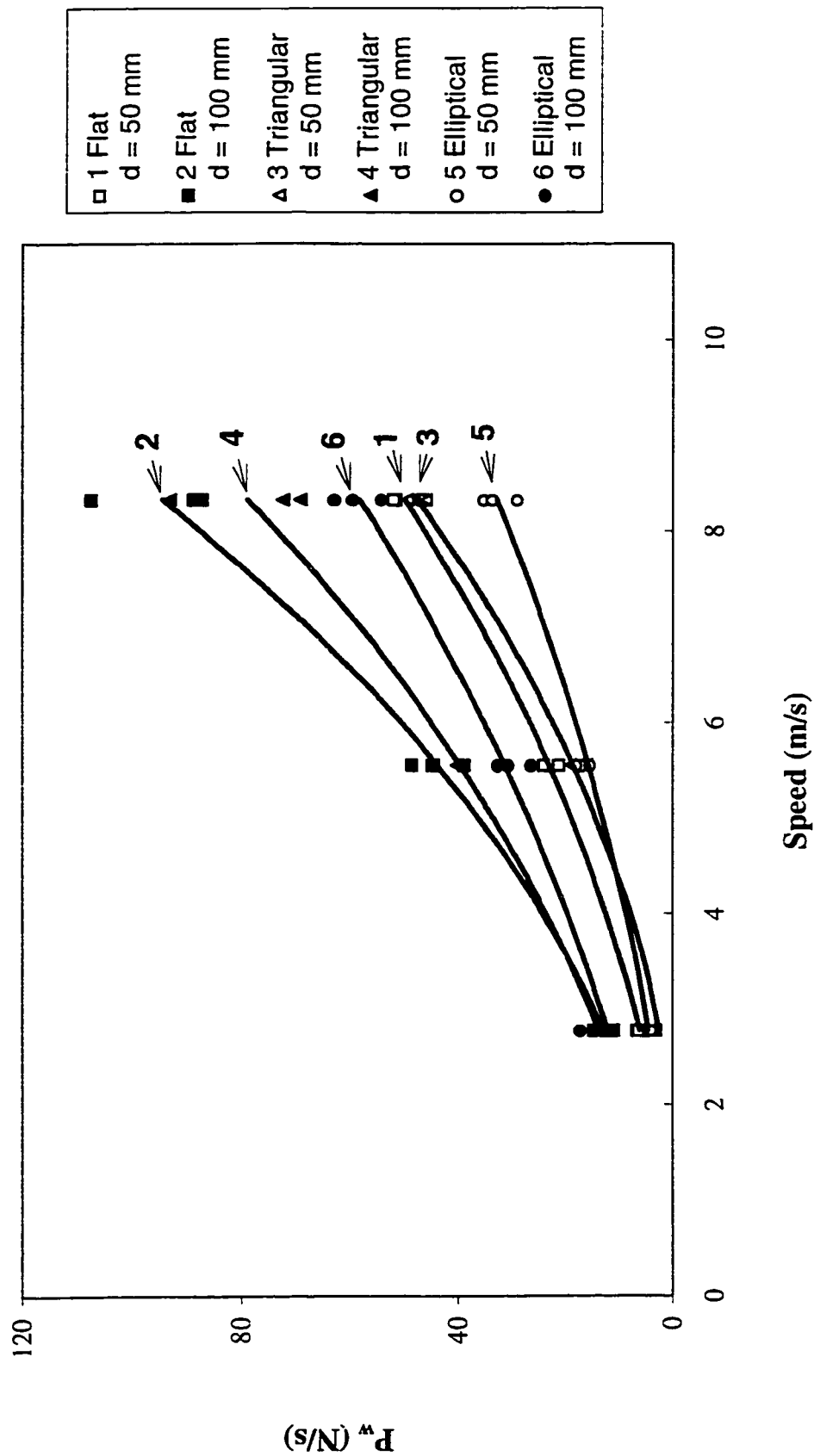
Figure 5.11 Power per operating depth, P_w, for tool operating in the hard packed soil condition at 12.3% water content.
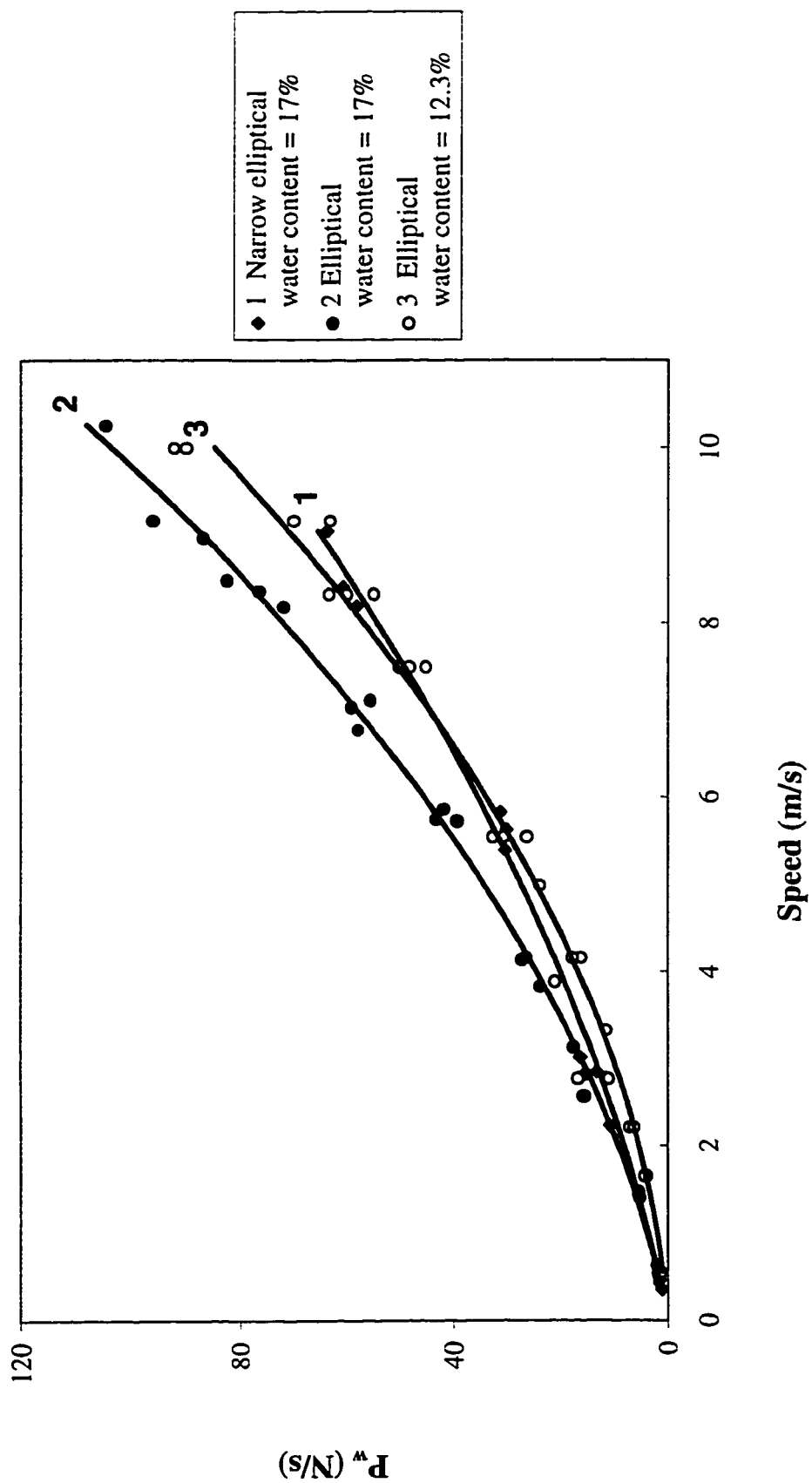
Figure 5.12 P_w values for elliptical tools operating in the hard packed soil condition.

165

Table 5.4 **Multiple regression analysis for the extended tests data with elliptical tools, showing results of the polynomial law regression.**

Width (mm)	Water content (%)	Bulk Density (Mg/m^3)	A*	B*	R^2
4.7	17.0	1.45	4.4225	3.3785	0.9948
9.4	17.0	1.45	0.7025	3.3563	0.9950
9.4	12.3	1.33	0.7116	1.3824	0.9866

* $Y = AX^2 + BX$, where $Y = P_w$ (power per depth, W/m), $X = S$ (speed, m/s).

were expected, since at higher operating depths more soil volume is considered and soil strength increased as indicated by increasing cone index values (Table 5.1).

Results from the hard packed soil condition (Figure 5.11) showed similar trends compared with soft packed soil. However, P_w increased ten fold for the operating depth of 50 mm (curves 1, 3, 5). For the depth of 100 mm (curves 2, 4, 6), a five to seven-fold increase occurred depending upon tool shape.

Regression curves presented in Figure 5.12 for the elliptical tools show consistent behaviour. A four to fivefold increase in P_w was observed for the 2.8-8.4 m/s speed range, at the operating depth of 100 mm (curves 1 and 3).

The change in soil structure from a combination of loose/dry (12.3% water content, 1.33 Mg/m^3 bulk density) to wet/dense (17.0%, 1.45 Mg/m^3) produced an increase of 50% in P_w for the speed of 2.8 m/s. For the speed of 8.4 m/s, P_w increased by 30%. Soil structure represented an important factor in soil draft.

From previous cases, the most favorable condition in terms of lowest draft requirement was running an elliptical tool, at a shallow depth of 50 mm on a soft packed soil. For this tool, a three-fold increase in operating speed (2.8 to 8.4 m/s) produced a six fold increase in P_w.

There is potential for tool draft optimization. Changes in rake angle and tool geometry to make the tool more aggressive, can reduce power requirements. It is interesting to note that P_w increases with speed supports the findings of strong damping effects that were obtained from the power spectral density analysis.

5.1.4 Soil disturbance and pulverization

Analysis of soil disturbance in relation to tool type and operating speed was performed. Figures 5.13 to 5.16 show results of cross-sectional soil profiles measured with the profilometer. These data were available only in analog form. A statistical analysis of profile parameters such as that done by Tessier et al. (1989) would require conversion of data to digital form for numerical computation. A statistical analysis would also require a larger number of profilometer replicates, since disturbed cross section patterns collected along the tool path produced great variability. Analysis here was limited to visual interpretation of Figures 5.13 to 5.16.

Two tool shapes (flat and elliptical), two depths of operation (50 and 100) mm, and two speeds 2.8 and 8.4 m/s were considered as presented in the figures. Each trial was replicated three times. Each graph line shown is one replication of the profilometer measurements. Due to the limited profilometer width (300 mm), right and left sides of the
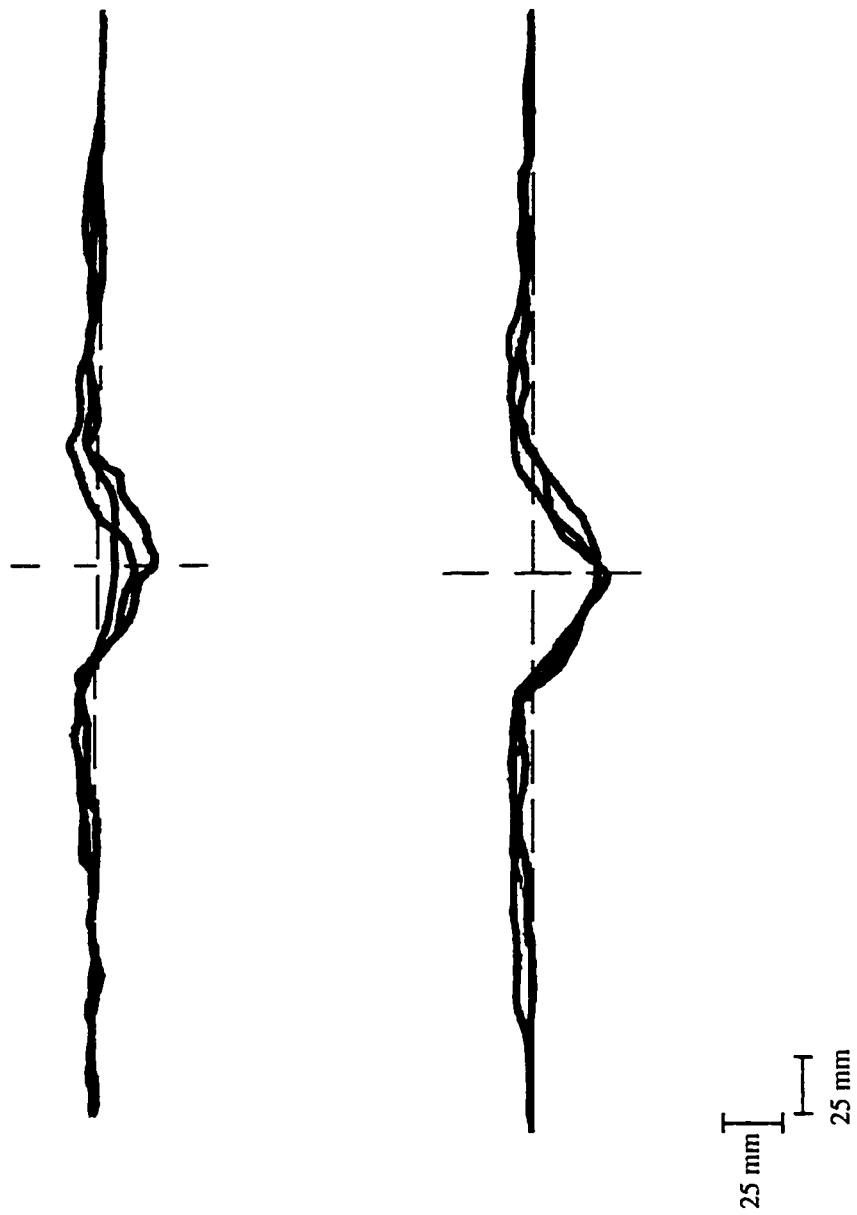
Figure 5.13 Cross-section of soil profiles measured with profilometer for soil disturbed by a flat tool operating at speeds of 2.8 m/s (bottom) and 8.4 m/s (top) at a depth of 50 mm.
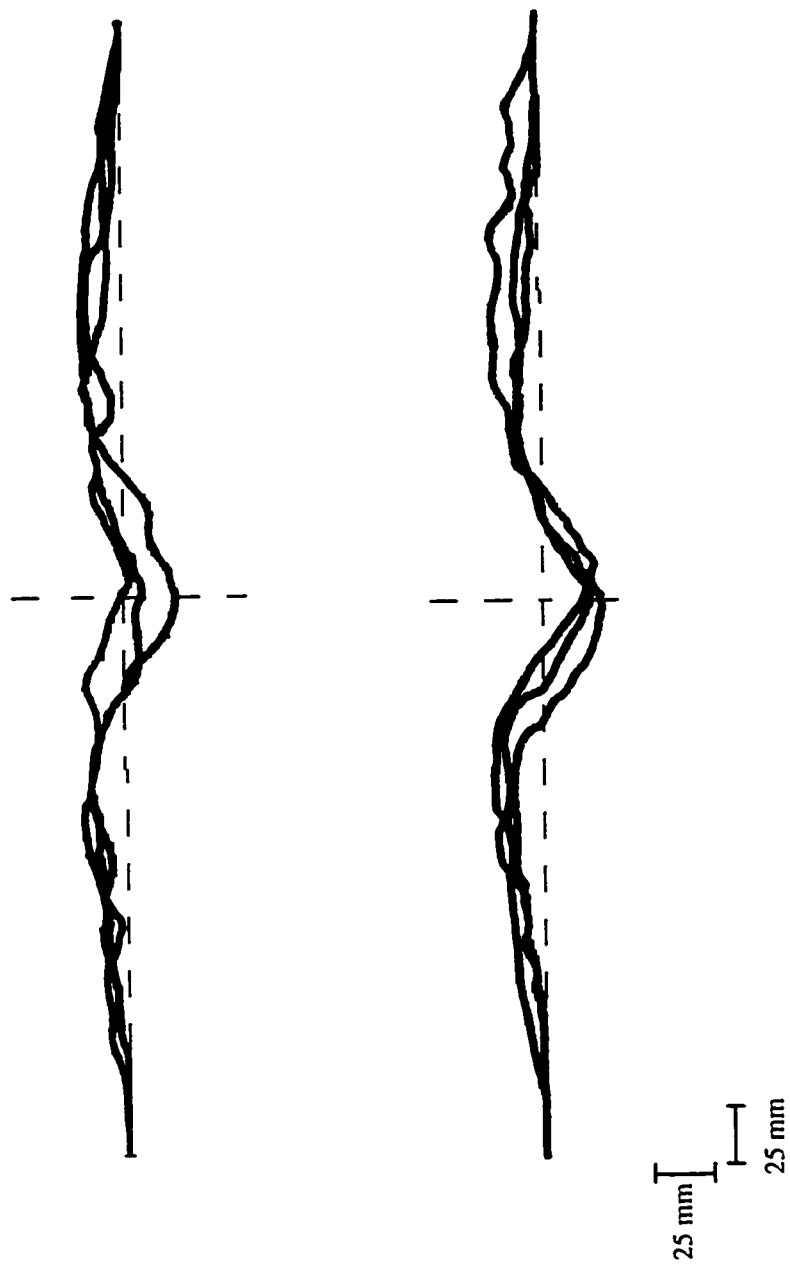
Figure 5.14 Cross-section of soil profiles measured with profilometer for soil disturbed by a flat tool operating at speeds of 2.8 m/s (bottom) and 8.4 m/s (top) at a depth of 100 mm.

25 mm

25 mm
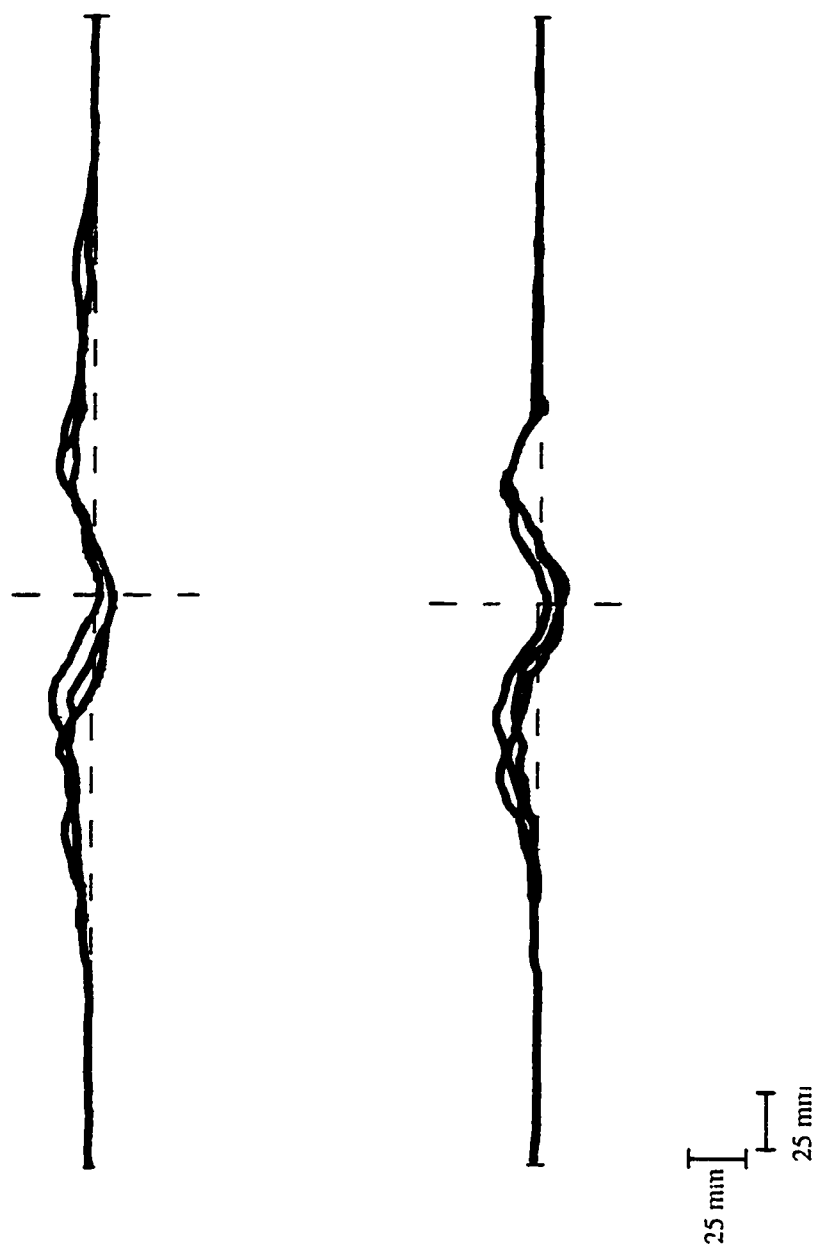
Figure 5.15 Cross-section of soil profiles measured with profilometer for soil disturbed by an elliptical tool operating at speeds of 2.8 m/s (bottom) and 8.4 m/s (top) at a depth of 50 mm.

25 mm

25 mm
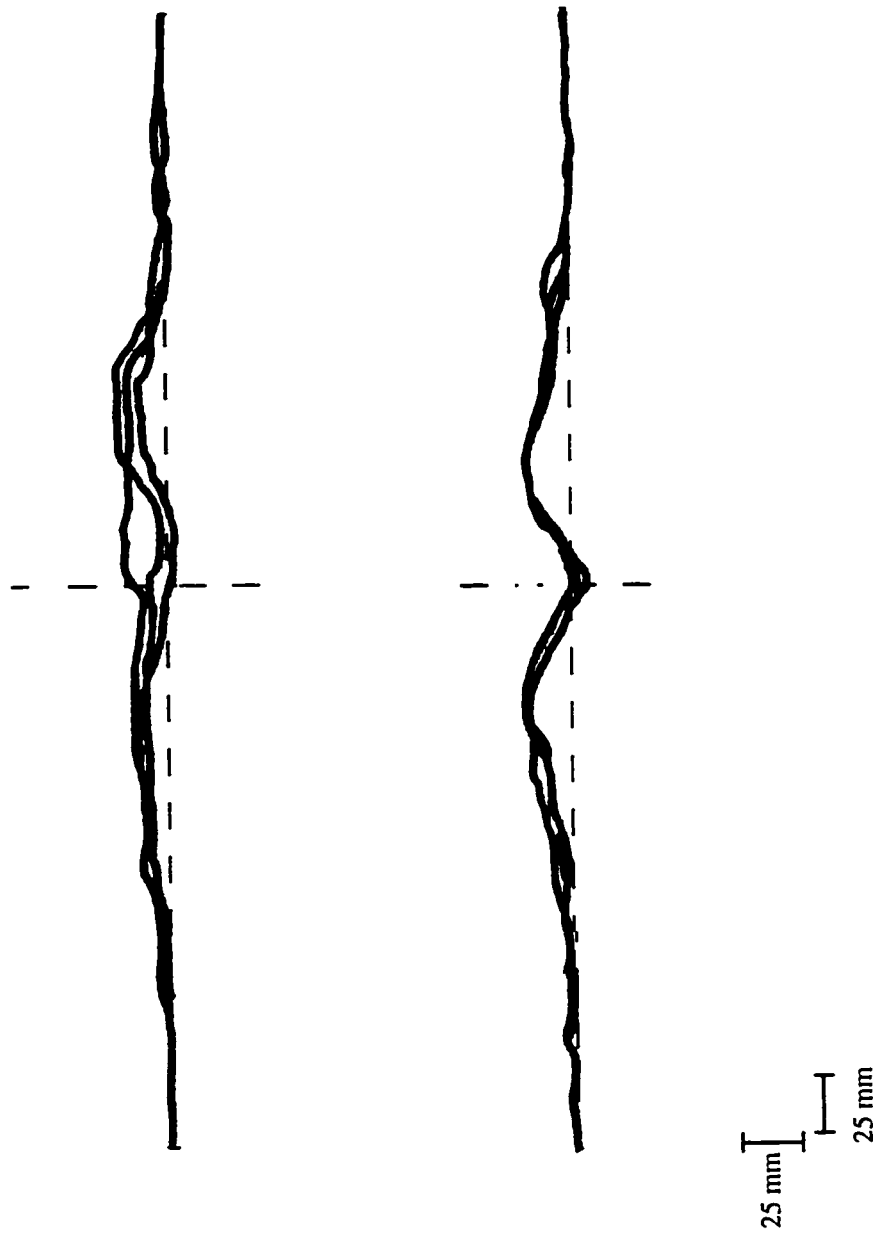
Figure 5.16 Cross-section of soil profiles measured with profilometer for soil disturbed by an elliptical tool operating at speeds of 2.8 m/s (bottom) and 8.4 m/s (top) at a depth of 100 mm.

25 mm

25 mm

centre line were measured separately. Lower curves on each figure were produced by tools operating at 2.8 m/s. Upper curves corresponded to tools operating at 8.4 m/s. Figures 5.13 and 5.14 correspond to flat tools, and figures 5.15 and 5.16 to elliptical ones. The disturbed soil does not necessarily indicate the tool depth, because during the cutting process soil was thrown so that some soil particles fell back and refilled the furrow.

Visual comparison between results from tools working at the 50 mm depth (Figures 5.13 & 5.15) versus the same tool types working at the 100 mm depth (Figures 5.14 & 5.16) indicated larger soil disturbance for the 100 mm depths.

Soil particles were thrown sideways due to tool action. Flat tools spread more soil sideways than elliptical tools in all cases shown. Stream-lined tools produced a narrower soil spread pattern; for instance, compare Figure 5.13 (bottom) and Figure 5.15 (bottom).

The greater soil disturbance produced by an increase in operating speed can be visualized in each figure by comparing results from 2.8 and 8.4 m/s speeds. For all cases, from the lowest to highest speed, the furrow level was filled to an upper level and raised mostly with more pulverized soil. Figure 5.17 shows soil disturbance and pulverization produced by the passage of flat tools with a depth of 100 mm and speeds of 2.8, 5.6 and 8.4 m/s for a soil water content of 12.3%. Figure 5.17 supports soil disturbance trends obtained in the traces shown in Figures 5.13 to 5.16.

It would have been desirable to measure the cross sectional area of soil particles after the loose thrown soil had been removed from the surface. Some difficulties arose, however, such as being able to remove soil without disturbing the remaining soil, and

5.6 m/s

2.8 m/s
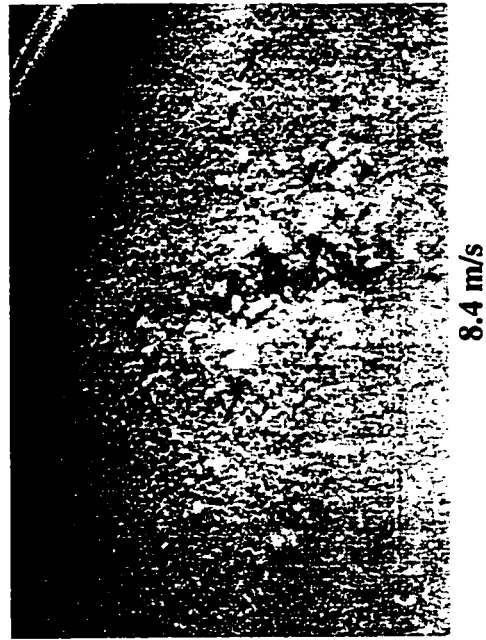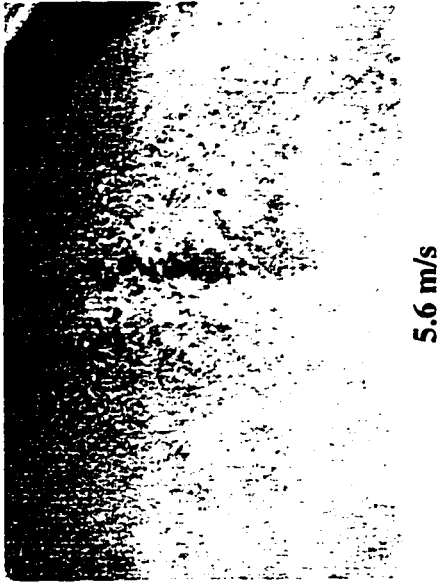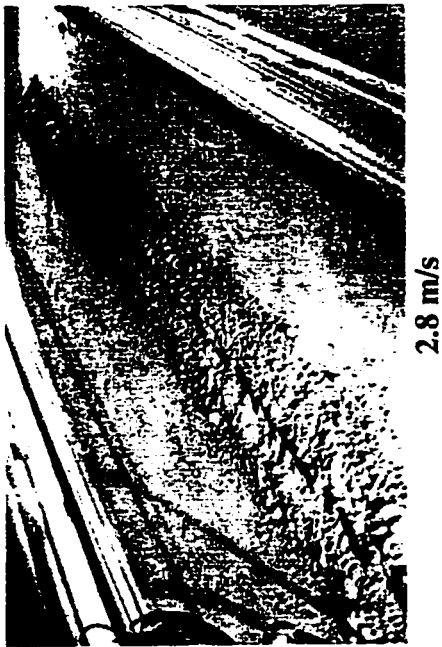
8.4 m/s

Figure 5.17   Soil disturbance and pulverization produced by flat tools running at 100 mm operating depth at speeds of 2.8, 5.6 and 8.4 m/s and an average soil water content of 12.3%.

identifying the boundary between loose and undisturbed soil. It also becomes more difficult to obtain cross-sectional areas due to changes in the reference soil level or datum.

It is helpful to define the soil structures to be used as follows: DL dry/loose (water content 12.3%, bulk density 1.15 Mg/m^3); DH dry/dense (water content 12.3%, bulk density 1.33 Mg/m^3); and, WH wet/dense (water content 17.0%, bulk density 1.45 Mg/m^3).

A narrower soil spread pattern was observed for WH compared to DL tests. In these tests, tool draft was higher. The increase in draft and decrease in soil spread indicated that an extra resistance to tool movement was provided by the different soil structures. Damping forces became more evident. The relatively short distance that soil was thrown away from the tool path suggests low influence of inertial forces for the investigated conditions (Personal communication, W. J. Chancellor, Professor Emeritus, University of California, Davis 1996).

Soil pulverization was a reflection of the power required to cut soil. In general, increasing tool speed increased soil pulverization; however, the resulting furrows did not appear to change considerably. Quantification of the cross-sectional area with disturbed soil removed would be desirable in future work. The R_i index presented in the literature would also be of value (equation 2.2). To do this a large number of profilometer replicates would be required. Recording and analyzing these data would require great computational capabilities. It would thus be more appropriate to use an automated process of data collection and processing.

5.2 Evaluation of Soil Constitutive Model for Tool Draft

Three steps were accomplished in this part of the study: (1) An available finite element code (Dyntool) was modified to implement the procedure described by Duncan and Chang (1970). To test the code, a static analysis of a circular footing on clay, reported by Duncan and Chang (1970) was implemented using soil parameters given in their paper. (2) Results from the triaxial tests on the DH soil structure were used to simulate quasi-static triaxial tests to calibrate the model with experimental parameters. A variety of dynamic simulations were implemented to determine appropriate time steps and mesh refinements. (3) Performance of narrow tools, of flat and triangular shapes, were simulated under both static and dynamic conditions. Flat tools were used as reference tools to determine the dynamic soil parameters which, along with the static parameters obtained from triaxial tests, were used to predict draft forces for the triangular tools.

5.2.1 Quasi-static sample case verification

Finite element analysis of the settlement of a circular footing on a pure clay soil was reported by Duncan and Chang (1970). Parameters used in the numerical modeling and results of average footing pressure versus displacements obtained by Duncan and Chang (1970) are given in Table 5.5 and results of the simulation will be presented along with simulations from this thesis for comparison (model I).

The numerical code used in this thesis (Dyntool) employs three-dimensional eight-node brick elements. The original analysis by Duncan and Chang (1970) was developed for a two-dimensional axisymmetric problem. Figure 5.18 shows the mesh used by Duncan

175
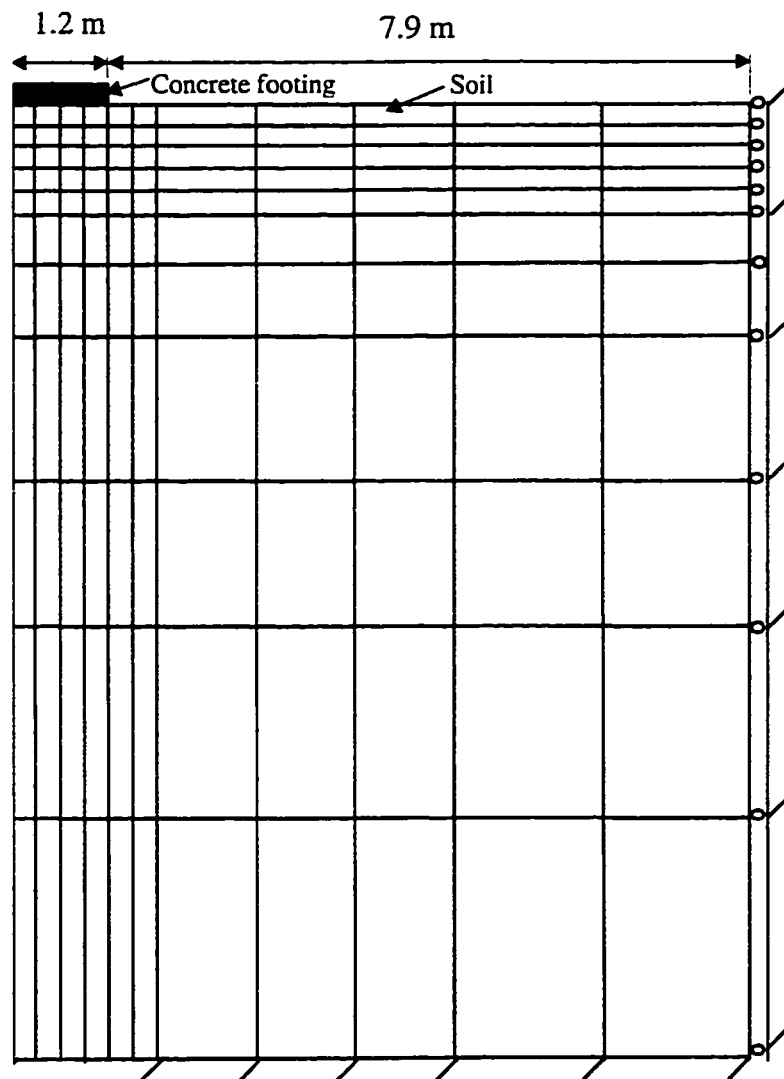
Figure 5.18 Mesh for analysis of two-dimensional settlement of circular footing on a pure clay soil used by Duncan and Chang (1970).

Table 5.5   **Parameters used in finite element analysis of a circular footing on clay by Duncan and Chang (1970).**

k	n	R_f	c (kPa)	ϕ	Unit weight (kN/m³)	ν
50	0	0.9	53	0	17.3	0.48

and Chang (1970). They used four node isoparametric and axisymmetric elements. They presented their simulation results in a graphical form. The settlement curve predicted by Duncan and Chang will be compared against simulated three-dimensional settlement curves obtained using Dyntool.

Figure 5.19 shows a top view of the mesh and restraints used in the Dyntool analysis. The three-dimensional mesh shown makes use of symmetry. The one quarter section of the circular footing is considered equivalent to the original two-dimensional Duncan and Chang's problem. Average pressure was obtained by dividing footing reaction by the area of the quarter footing. Load was imposed in small displacement steps along the longitudinal direction.

Soil elements in compression and tension were modeled using the hyperbolic model (equation 2.25) until element failure. Elements in tension were assigned a confining pressure equal to zero. When element failure occurred, its modulus of elasticity was divided by an arbitrary factor (500) and a residual modulus of elasticity value of 1.0 kPa was assumed. The value of the tangent elastic matrix (equations 3.21, 3.40 for $E_s=E_t$, 3.17 and 2.25) that is calculated based on the tangent modulus of elasticity and Poisson's ratio, was updated for new load iterations by dividing the current values of the tangent modulus
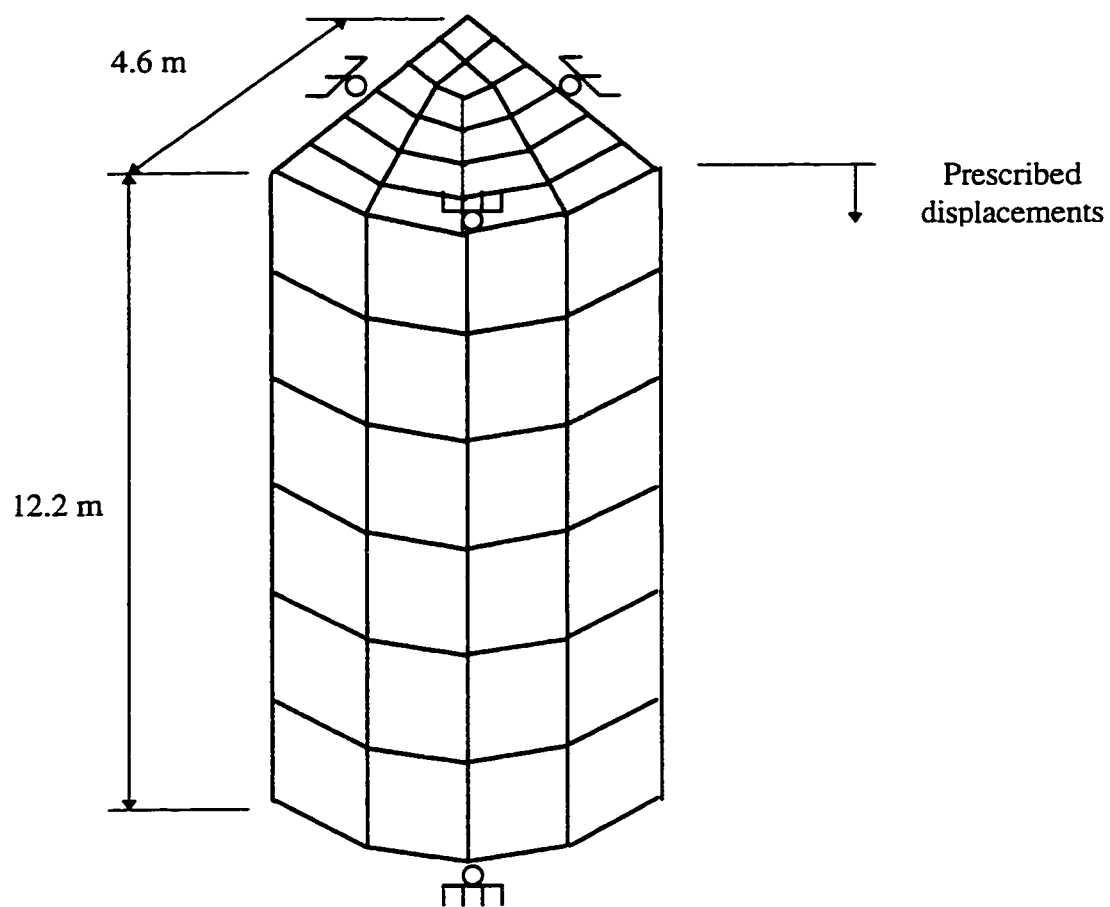
Figure 5.19 Three-dimensional mesh and restraints used with Dyntool simulations of two-dimensional circular footing.

of elasticity (which compose the tangent elastic matrix, not the initial modulus) until a residual value in the order of 1 kPa was reached. As reported by Duncan and Chang (1970), the residual value of tangent moudulus of elasticity of the failed element affects the shape of the final portion of the footing settlement curve to some degree (i.e., the 'reference curve' shown in Figure 5.20). When soil elements failed in tension a value equal to soil cohesion was adopted for the soil shear strength. After failure, Poisson's ratio was assumed constant and close to a value of 0.5 (i.e., incompressible). The value used was 0.499. Prior to failure, Poisson's ratio was assumed a constant equal to 0.48. This procedure is the same as that implemented by Duncan and Chang (1970). Soil weight was implemented in the form of concentrated nodal forces. A tolerance of 1% was used in the Euclidean norm convergence criterion of the modified Newton-Raphson procedure (equations 3.46 and 3.47).

The original loading increments applied to the footing by Duncan and Chang (1970) were quite large (i.e., 26.75 kPa), probably due to computing limitations of that time. In this thesis, load steps were adopted, as close as possible, to represent equivalent loading increments used in the paper. Twenty five prescribed displacements of 50 mm were adopted in this thesis. Figure 5.20 shows results of the Dyntool simulations as well as the original Duncan and Chang (1970) solution. There was no significant improvement in the Dyntool settlement calculation for refinements beyond 0.005 m, i.e., calculations with smaller displacement increment sizes.

The tangent elastic matrix had to be divided by an 'arbitrary' factor after soil failure. Figure 5.21 shows the effect of choice of this dividing parameter on predictions.
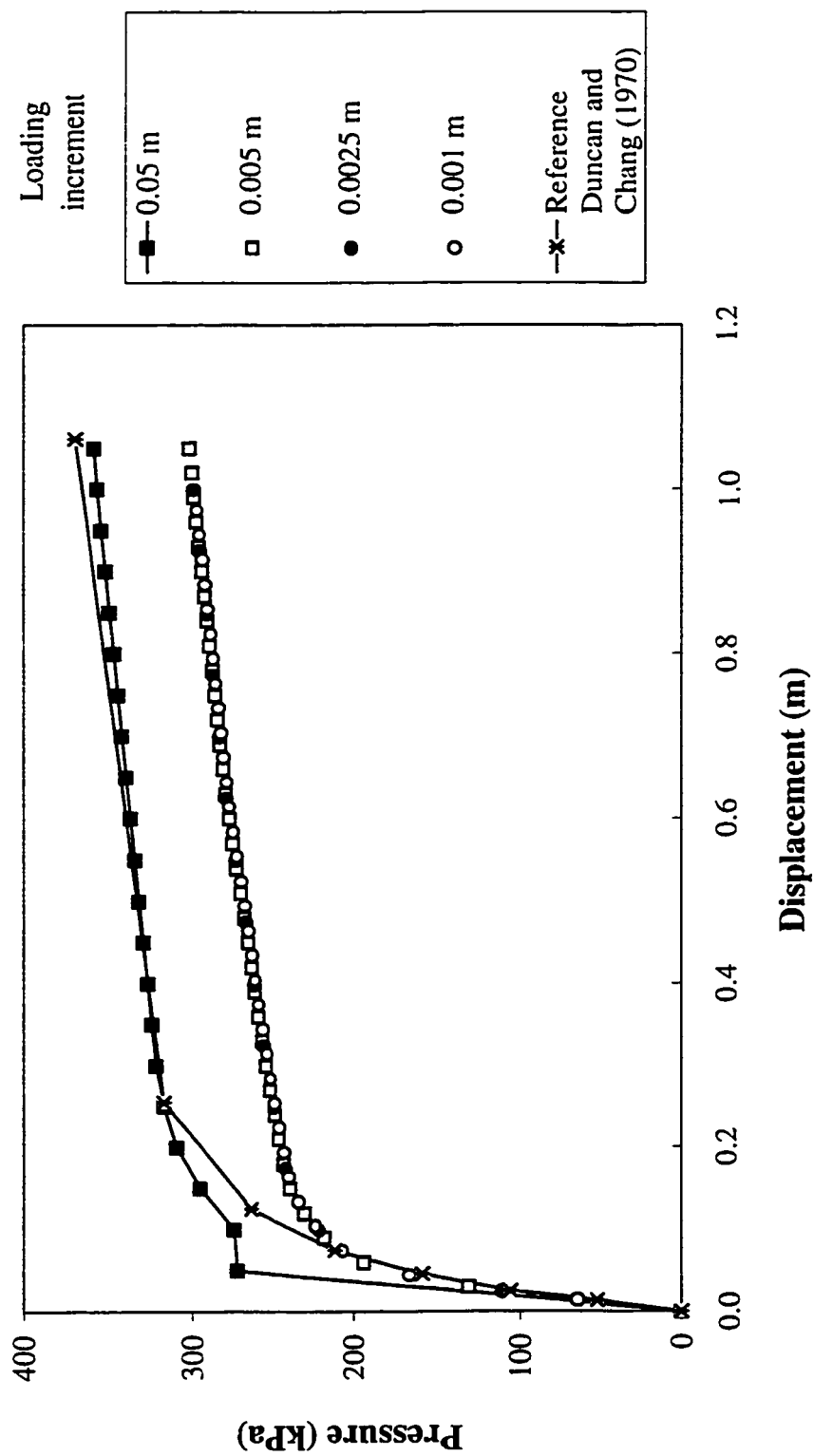
Figure 5.20 Pressure vs. displacement beneath circular footing predicted by Dyntool. Different loading steps showed no significant improvement in settlement calculation with refinements smaller than 0.005 m when compared with the results of the circular footing reported by Duncan and Chang (1970).
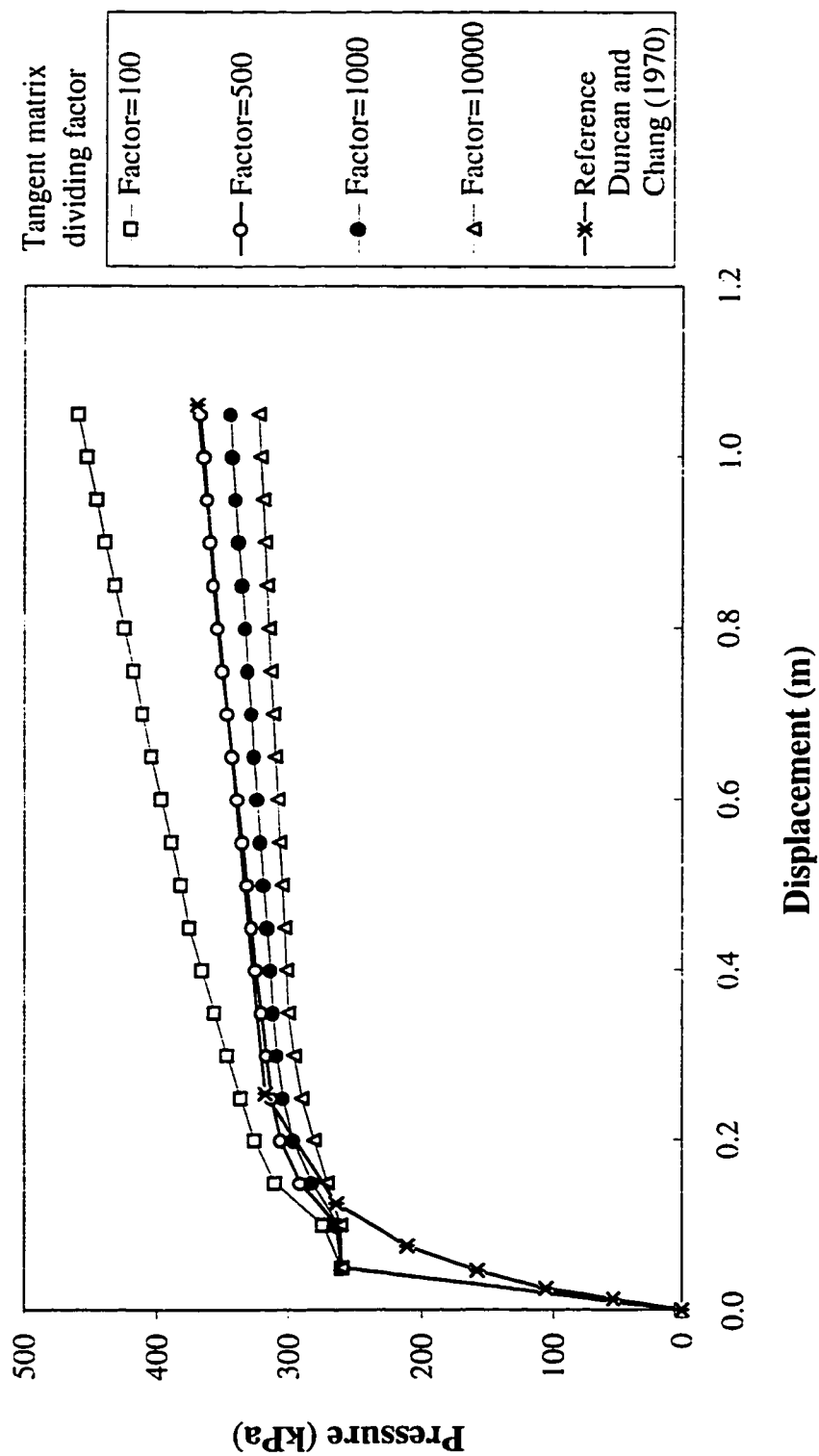
Figure 5.21 Effect of the factor dividing the tangent elastic matrix after soil failure on Dyntool pressure displacement predictions for circular footing. All simulations were run with a constant loading step of 0.05 m.

The figure clearly shows that the model was sensitive to the choice of factor since large loading steps also produced significant differences in the results (Figure 5.20). The model was calibrated with known data (i.e., 'reference' in Figures 5.20 and 5.21), which is the footing settlement solution curve reported by Duncan and Chang (1970). Having done this, the Dyntool code was shown to adequately solve the Duncan and Chang (1970) model equations.

As can be seen, determination of some model constants are arbitrary, i.e., there is no well defined criterion for its determination. 'Calibration' of the static model was achieved here by determining model parameters that reproduced, as near as possible, Duncan and Chang's solution for footing average settlement pressure versus displacements. Despite all these difficulties, a reasonable correlation of the settlement predictions by using Dyntool with the reported Duncan and Chang (1970) solution was obtained.

5.2.2 Triaxial tests

Parameters obtained from DH triaxial tests were used in numerical simulations using Dyntool and predictions were compared with the DH experimental data. Although good stress-strain predictions are generally expected between experimental and analytical data for quasi-static monotonic loading, the model as implemented had great difficulty reproducing the soil test behaviour, particularly after failure, unless first calibrated with known cases.

The previous section described calibration of the static model. Before verification of the dynamic model, it was first necessary to 'calibrate' the quasi-static form of the model. In this first step, measurements of reaction forces versus top cap displacements for quasi-static triaxial tests were compared with numerical simulations. Soil properties and results from DH samples were used. In the second stage (model II), numerical simulations representing triaxial tests were performed to investigate incorporation of dynamic components in the model. Details of these steps were as follows:

I) A variable Poisson's ratio was used in the simulation (Chi et al. 1993b). Parameters a_1 and b_1 (equation 3.41) were available for DH samples (Table 4.5). The mesh and concentrated loads simulating confining pressure are shown in Figure 5.22. The magnitudes of the applied forces were determined by dividing the desired confining pressure by the sample surface area and then applying equivalent forces at the element nodes. The total force representing the confining pressure was applied in the first time step, and after that set to zero. In the subsequent time steps the only loading applied were prescribed displacements of the specimen top cap. In this way, second and subsequent simulations started from a state of stress referring to the desired confining pressure applied in the first step. Applying the total confining pressure in the first step was preferred over applying it in small increments since test specimens were first consolidated and then sheared by increasing the axial load under controlled displacement conditions. In this incremental analysis the total load is not reapplied in subsequent steps, because this would represent increased confining pressure for these steps. The confining pressure was applied

Prescribed
displacements

→ Forces

△ Restraints
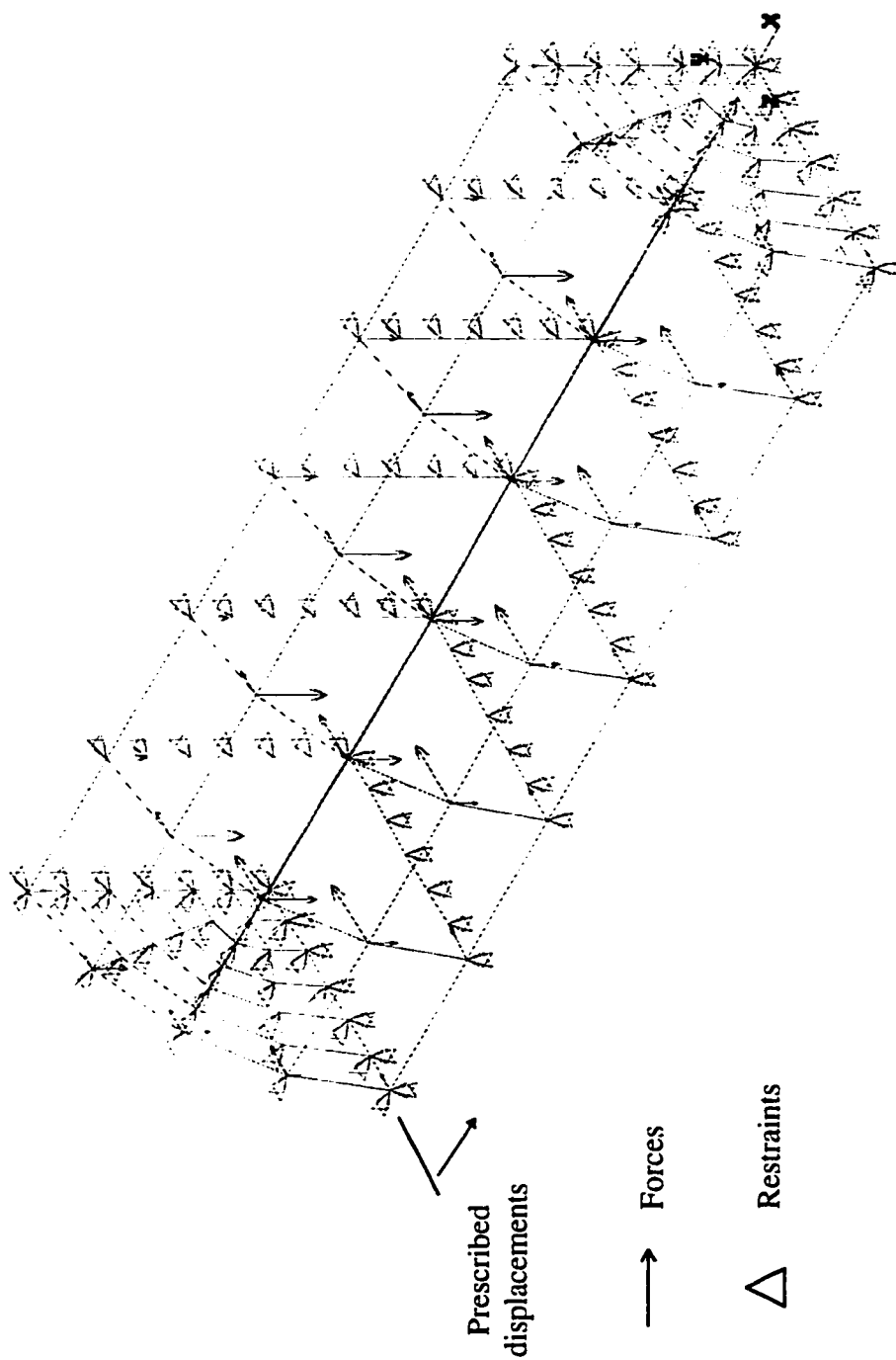
Figure 5.22 Mesh and applied concentrated loads simulating confining pressure for quasi-static triaxial tests using Dyntool.

to the quarter specimen in the form of concentrated loads radially applied to the external surface of the soil specimen.

Numerical simulations and experimental data are presented for unconfined specimens and for constant confining pressures of 30, 60 and 90 kPa in Figure 5.23. The application of the total deformation was divided into displacement increments of 0.2 mm for unconfined conditions and for a confining pressure of 30 kPa, 0.4 mm for 60 kPa and 0.55 mm for 90 kPa confining pressure. Experimental confining pressures varied between ±1 kPa approximately.

Very good agreement between analytical and experimental data was obtained for a confining pressure of 60 kPa over all displacements, which were large. The displacement of 40 mm corresponds to an axial true strain of 47%. For all confining pressures there was good agreement between analytical and experimental data for relatively small true strains, (~ 10%). However, for the 90 kPa confining pressure, predictions significantly underestimated experimental data for displacements beyond 10 mm (9.9% strain). Prediction trends diverged as displacements became larger. For smaller confining pressures (i.e., 0 and 30 kPa) predictions overestimated axial forces consistently for higher strains.

The numerical predictions were quite sensitive to the choice of value for the failure ratio R_f. Some of the above discrepancies can be explained by the choice of R_f value. The value of R_f had been calculated as an average of all R_f obtained from all confining pressure cases, despite the variation among the values. Very good predictions were obtained for the confining pressure of 60 kPa which had a measured R_f value approximately equal to the
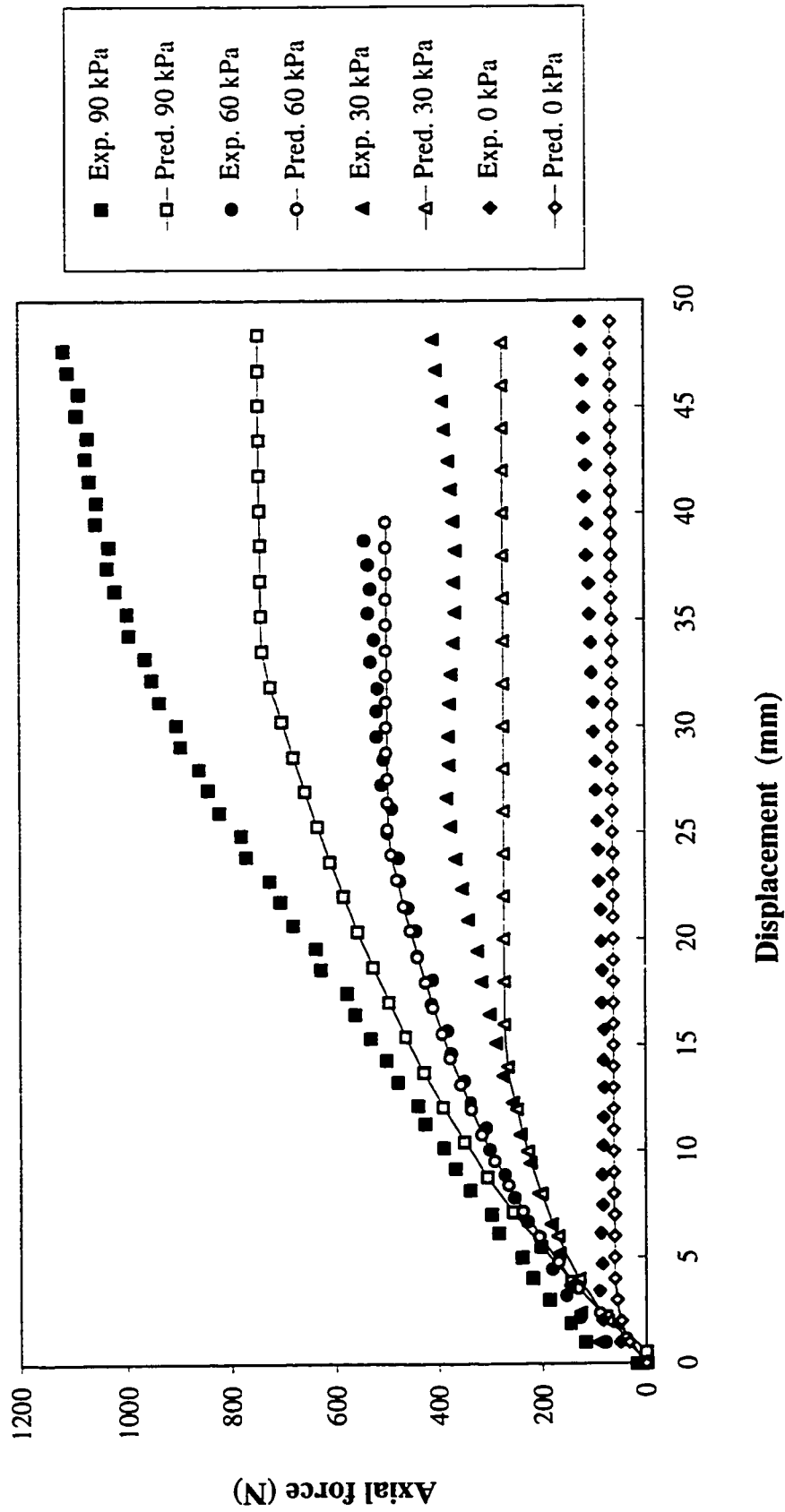
Figure 5.23   Numerical simulations (variable Poisson's ratio model) and experimental data for triaxial specimens under various confining pressures and a loading rate of 0.05 mm/s.

average 0.7. Discrepancies occurred as correct values of R_f diverged from the average value. However, further refinements on R_f were not considered a major concern at this point since the model was approximately reproducing the soil behaviour. End cap effects, due to friction of the specimen ends against the top cap and the porous disk sitting on the pedestal, may also contribute to these discrepancies. The specimen ends are modeled frictionless, however, friction always occur in the measurements.

The adopted hyperbolic model (equations 3.21, 3.17, 3.40 for $E_s=E_t$ and 2.25), using a variable Poisson's ratio (equation 3.41), was thus deemed to justify proceeding with the investigation of dynamic numerical simulation. At this stage, the finite element code, Dyntool, was deemed to satisfactorily solve the theoretical equations for quasi-static conditions.

II) In the next step strain rate effects were added to the static model according to equation 3.39, which makes use of the dynamic parameter AN. Viscous effects were incorporated in the stiffness matrix (equation 3.26). At this stage inertial terms were still neglected, i.e., masses of soil particles were set equal to zero (i.e., $\rho = 0$, equation 3.27, since **M=0**) (Model II).

A top cap speed of 8.4 m/s was simulated for a triaxial test subjected to a confining pressure of 60 kPa. The effect of different values of strain rate coefficients, AN, were investigated. Figure 5.24 shows predicted specimen force reactions vs. displacements curves with AN values varying from zero up to 1000. Dynamic reaction forces when AN was equal to 1000, increased up to five times in relation to the static case (i.e., AN=0). The influence of AN on 'viscous' strength decreased with higher AN values. For instance,
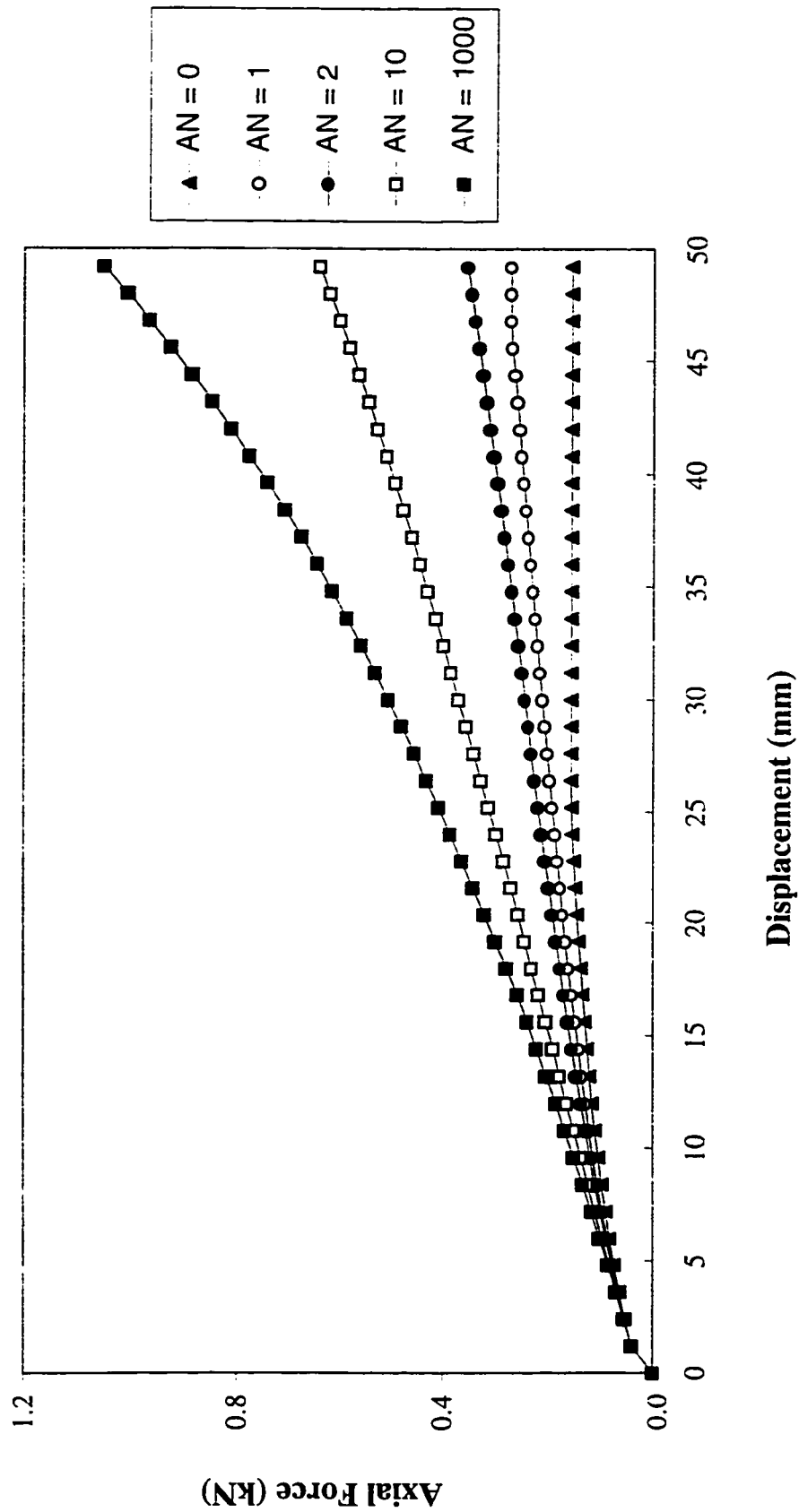
Figure 5.24 Simulation of triaxial specimen load-deformation for a top cap speed of 8.4 m/s and a confining pressure of

60 kPa. Various strain rate coefficients, AN, were investigated with values ranging from zero to 1000.

an AN value of AN=10 approximately tripled the predicted force (Figure 5.24) as compared to AN=0. These simulations were performed to verify if the model could be sensitive to different dynamic terms AN and also to see what happens to the specimen as a result of this simulation. The data in the literature is not for same conditions in these triaxial tests; however the simulations can be compared with respect to order of magnitude. Soil strength versus speed data published in the literature (see Figures 2.4 to 2.7) show increases on tool drafts in the order of 1.5 to 4 times the quasi-static value, which indicates that the order of magnitude of the predicted top cap reactions is adequate for the ranges of AN used in these simulations. Figure 5.25 shows a cross-sectional area of the deformed soil specimen when a 8.4 m/s speed was imposed at the top cap with ends totally restrained. As can be seen, the cross-section bulged non-symmetrically indicating non-homogeneous deformation. Fast triaxial test simulation was not compared in this study to experimental data because of experimental difficulties, such as loading the short specimen with constant fast speed and maintaining the confining pressure constant during the test.

Figure 5.26 demonstrates the sensitivity of soil reactions to different loading speeds from static to 8.4 m/s. A value of AN=2 was used in these simulations since it gave an intermediate curve between minimum and maximum simulations in Figure 5.24. Change in speed was seen to be able to mobilize strain rate (viscous) effects from the soil. and increased top cap reactions were generated from increased top cap speeds.

Incorporation of inertial effects (equation 3.26) in the model II, (i.e., equations 3.21, 3.17, 3.40, 3.39, 3.41, 3.26 and 3.27; which will be referred to from henceforth as model III) produced reactions shown in Figures 5.27 and 5.28. Loading speeds were
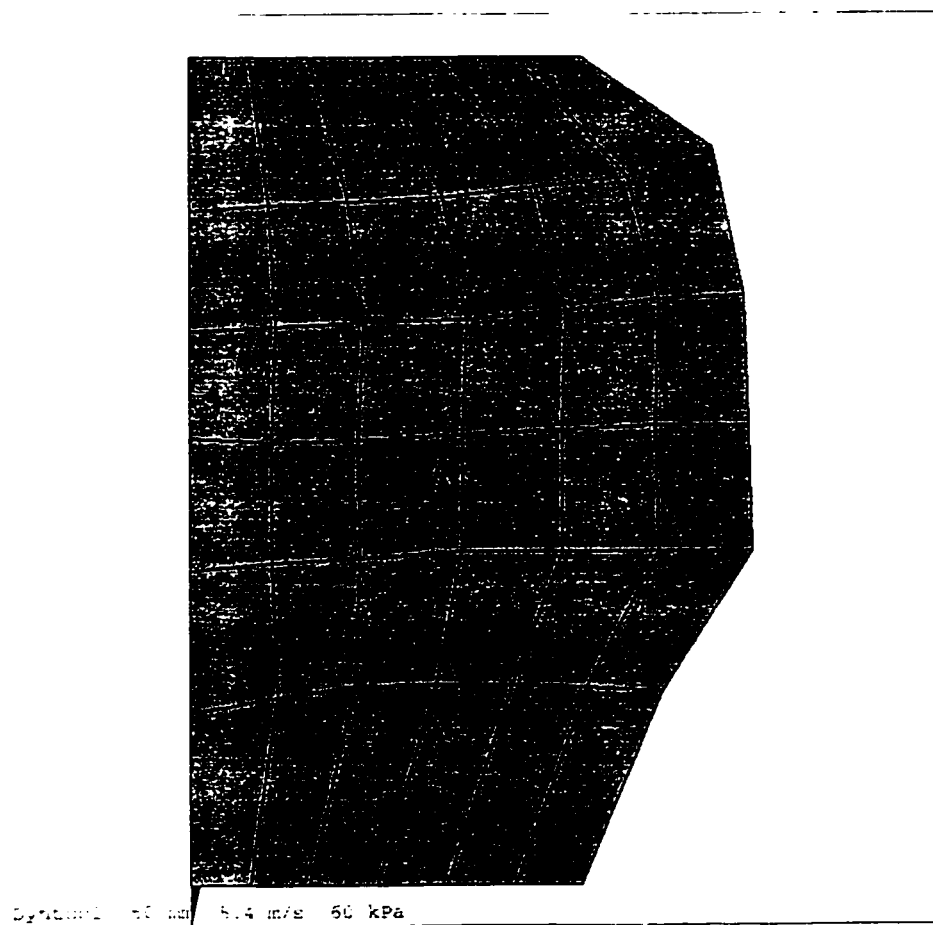
Figure 5.25   Finite element predicted cross-sectional area of a deformed triaxial

soil specimen when a 8.4 m/s loading rate was imposed at the top cap.
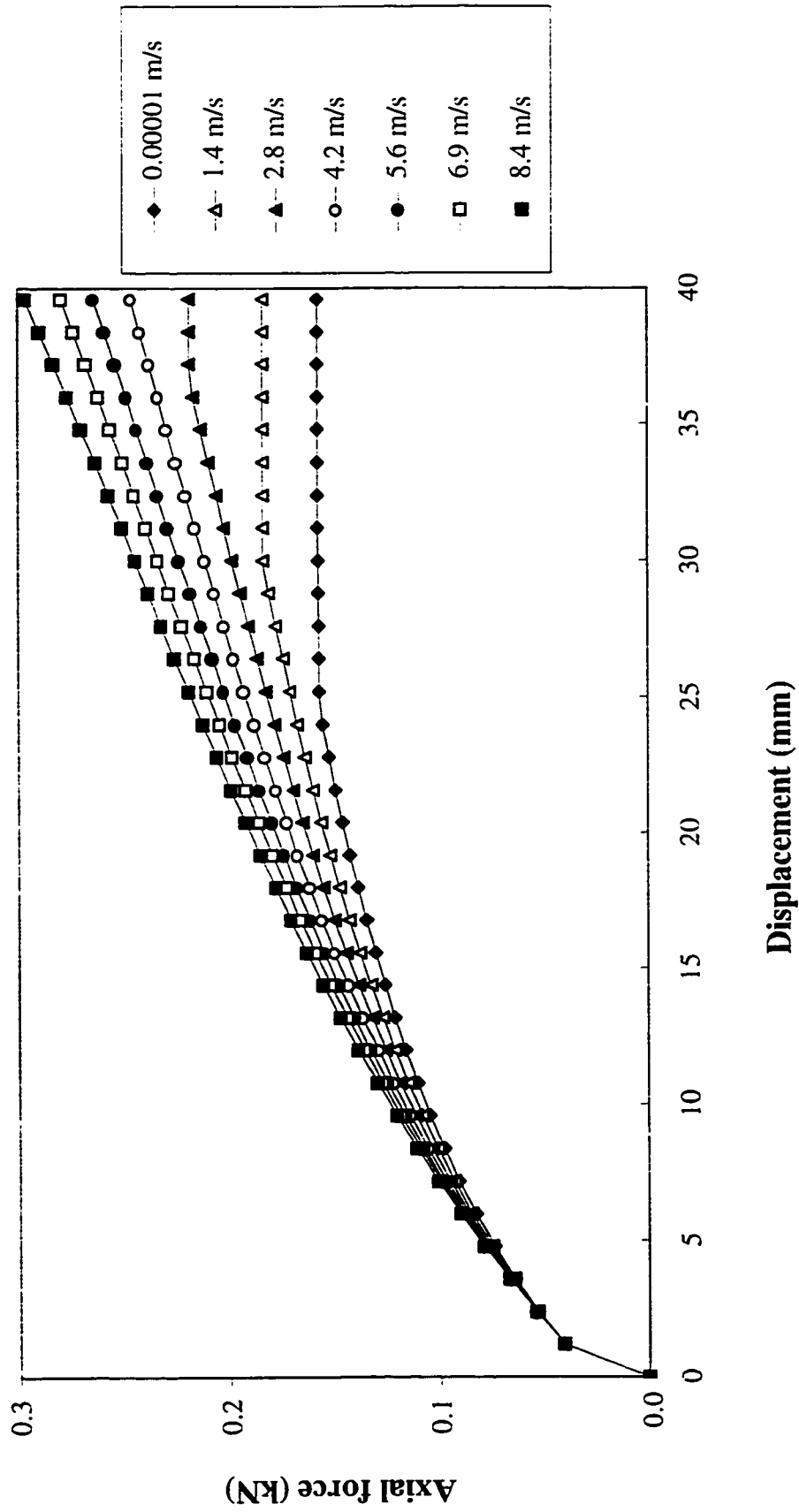
Figure 5.26   Effect of loading speed on predicted force-deformation characteristics of triaxial specimens.

191
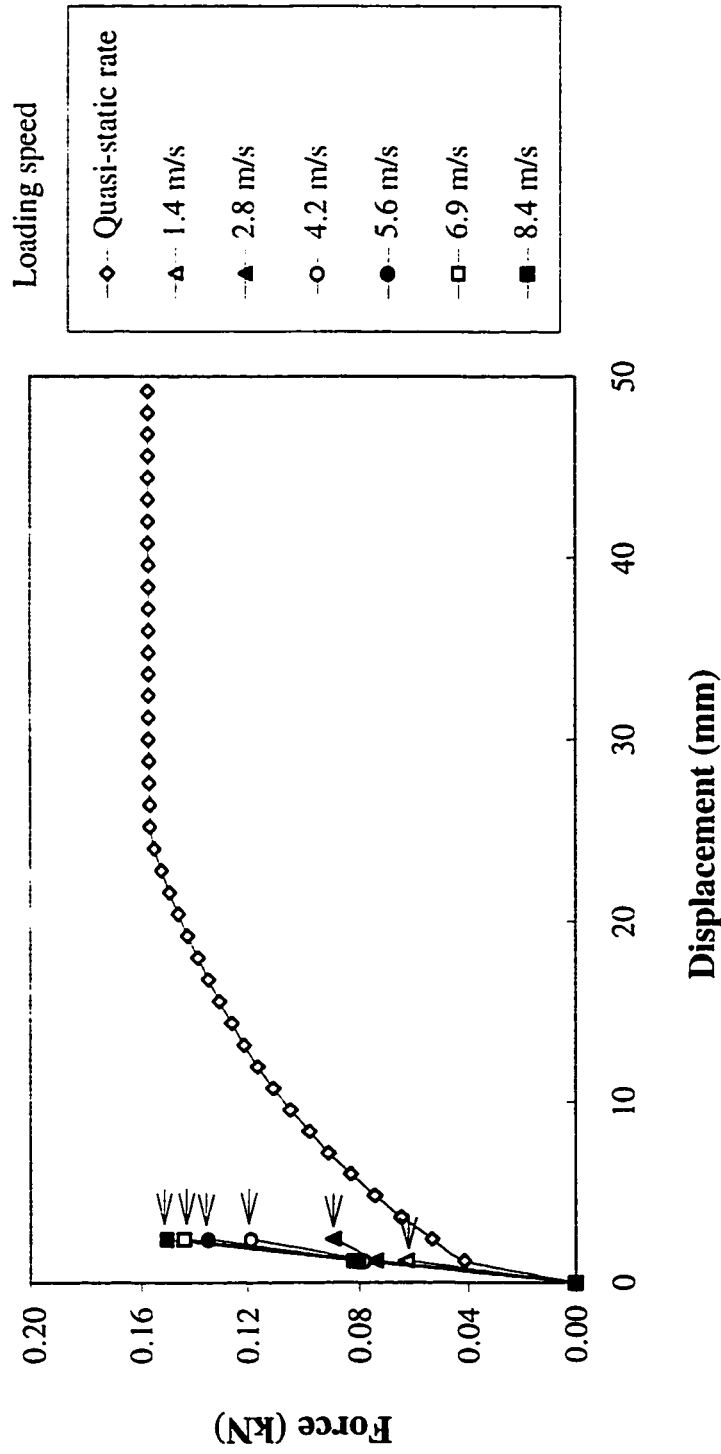
Figure 5.27 Predicted force-deformation behaviour of triaxial specimens using nonlinear elastic model with variable Young's modulus and Poisson's ratio and inertial components. Incorporation of inertial effects created numerical instabilities. Arrows show points at which program had to be terminated because of numerical problems.
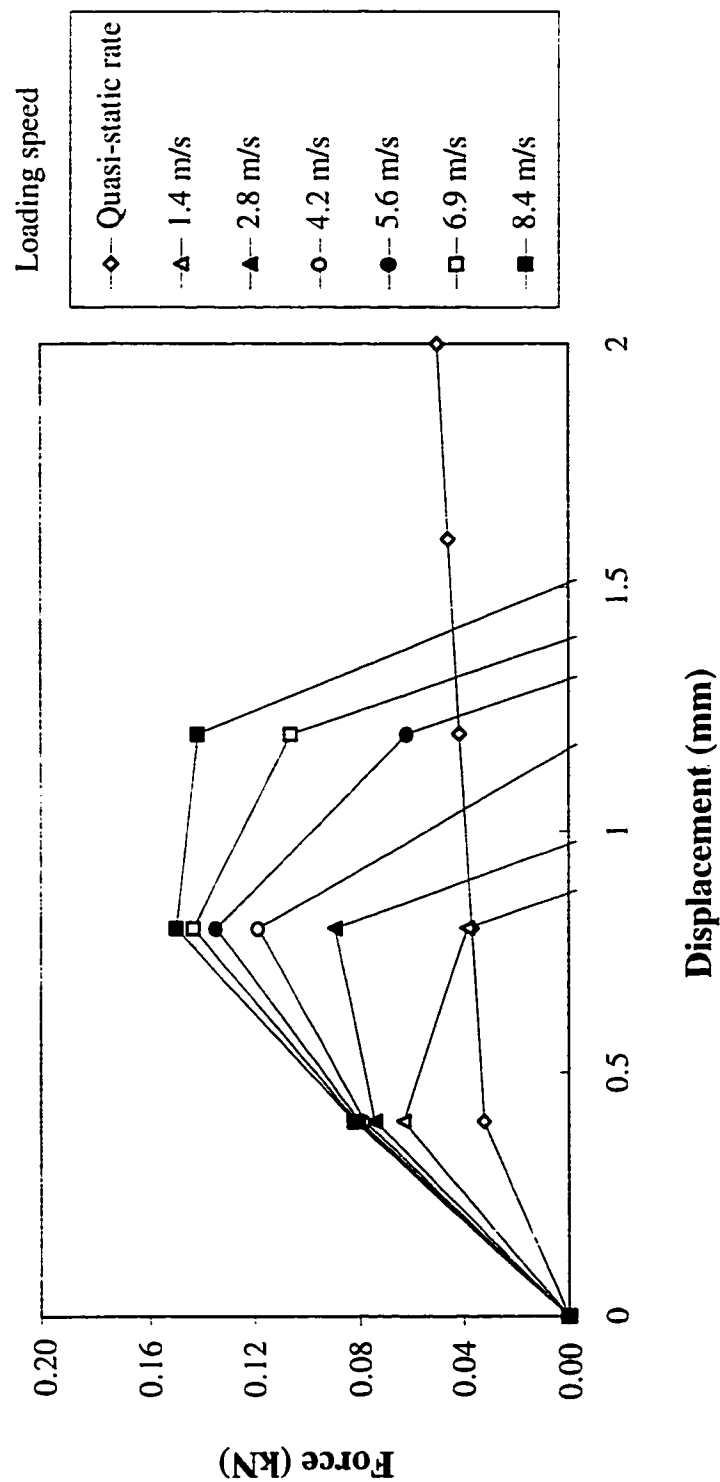
Figure 5.28 Predicted force-deformation behaviour of triaxial specimens using nonlinear elastic model with variable Young's modulus and Poisson's ratio and inertial components showing numerical instabilities occured when inertial effects were incorporated (detailed view of Figure 5.27).

varied from quasi-static (10^{-5} m/s) up to 8.4 m/s. Both figures show stable response reactions for quasi-static conditions. Predictions of large static displacements were achievable, agreeing with experimental tests, and that which is expected from tillage operations. However, incorporation of inertial effects created numerical instabilities. Oscillations ending in numerical over- or under-flow values occurred for all dynamic cases (speeds 0.5-8.4 m/s) and the program had to be interrupted. Total dynamic top cap displacements did not even reach 1 mm (less than 1% strain) before problems began. Thus, the model does not show adequate behaviour when soil elements approach failure under dynamic conditions.

It seems the dynamic case only aggravates problems which may already occur in static cases. Even for static cases, when the displacements are very large (> 50 mm) many elements fail and numerical instabilities also occur, leading to numerical over-flow of estimated reactions. According to Chen and Baladi (1985), for the hypoelastic model when the determinant of the material response function equals to zero, i.e., $\det\left|C_{ijkl}(\sigma_{mn})\right| = 0$, material instability or failure occurs. When tangential modulus of elasticity and Poisson's ratio, E_t and ν, are used, the behaviour near failure cannot be adequately described. Therefore, it results from their statements that the determination of the stiffness matrix generates numerical instabilities ($\det \mathbf{K} \rightarrow 0$).

5.2.3 Flat and triangular tool simulations

Despite all the problems above associated with model III, analysis was still extended to confirm these findings using the real cutting tool problem. For these simulations experimental tool data were also available for comparison, providing further justification for need to change the model formulation.

Coarse meshes of 171 nodes and 92 elements (Figure 5.29) were used to simulate the flat and the triangular tools. The triangular faced tool mesh was obtained by relocating node coordinates of the original flat mesh corresponding to the soil-tool interface. A more refined mesh consisting of 1399 nodes and 1040 elements (Figure 5.30) was also used for the flat tool simulations.

Incorporation of dynamic inertial effects (model III) in the flat and triangular coarse meshes produced numerical instabilities as shown in Figures 5.31 and 5.32; just as had occurred with the dynamic triaxial simulations. Total tool displacements were small, i.e., less than 1 mm, when instabilities started to occur.

The refined mesh shown in Figure 5.30 was processed for AN values of 2, 10^3 and 10^6, with soil mass neglected. Loading consisted of 100 steps of 0.1 mm prescribed displacements. Simulations were not capable of producing significant tool reactions when the smallest to the largest value of AN were adopted (10^{-20} to 10^{20}). Failed elements did not respond adequately to viscous effects because division of the tangent elastic modulus of the soil by a constant value also divided viscous effects, which had been moved to the stiffness matrix. For the case of narrow tools, failure was initiated early, even under very small displacements (0.3 mm).

0.20 m

0.50 m

0.15 m
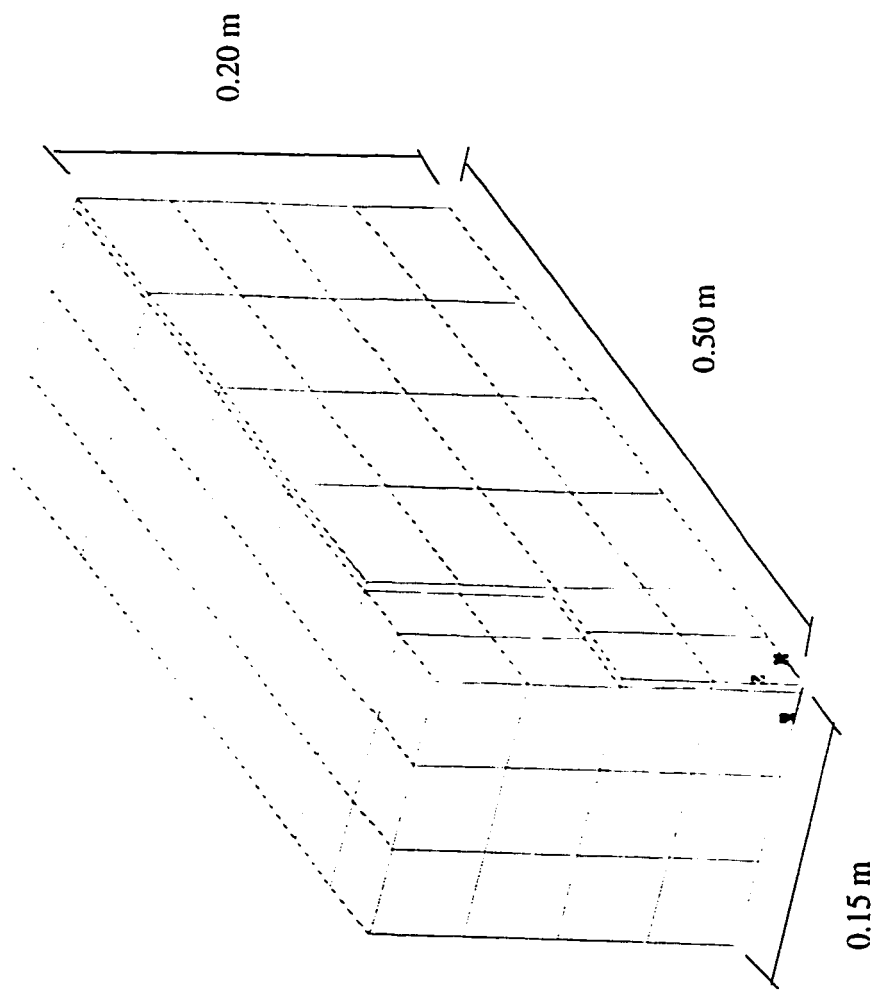
Figure 5.29   Coarse mesh of 171 nodes and 92 elements used to simulate the flat tool.
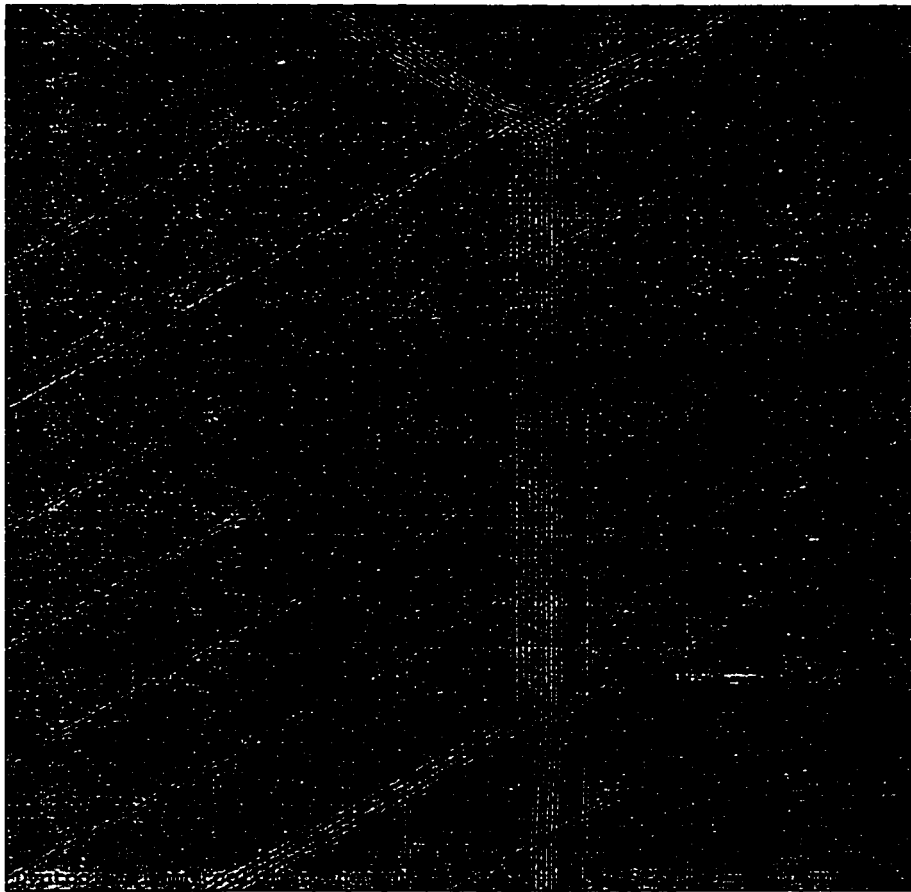
Figure 5.30 Refined (deformed) mesh consisting of 1399 nodes and 1040 elements used to simulate the flat tool.
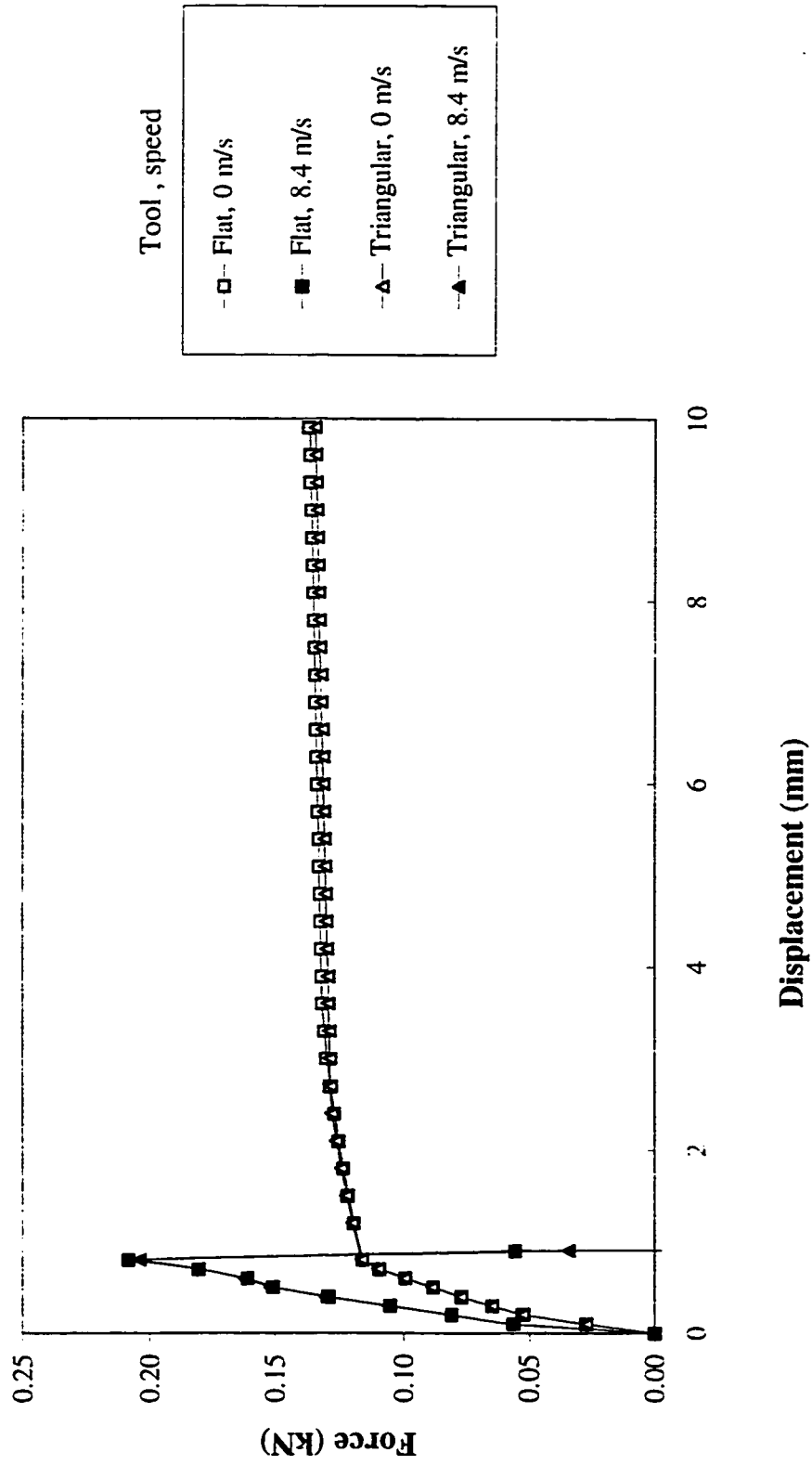
Figure 5.31 Difference in draft for static and dynamic loading imposed on the coarse flat and triangular tool meshes.
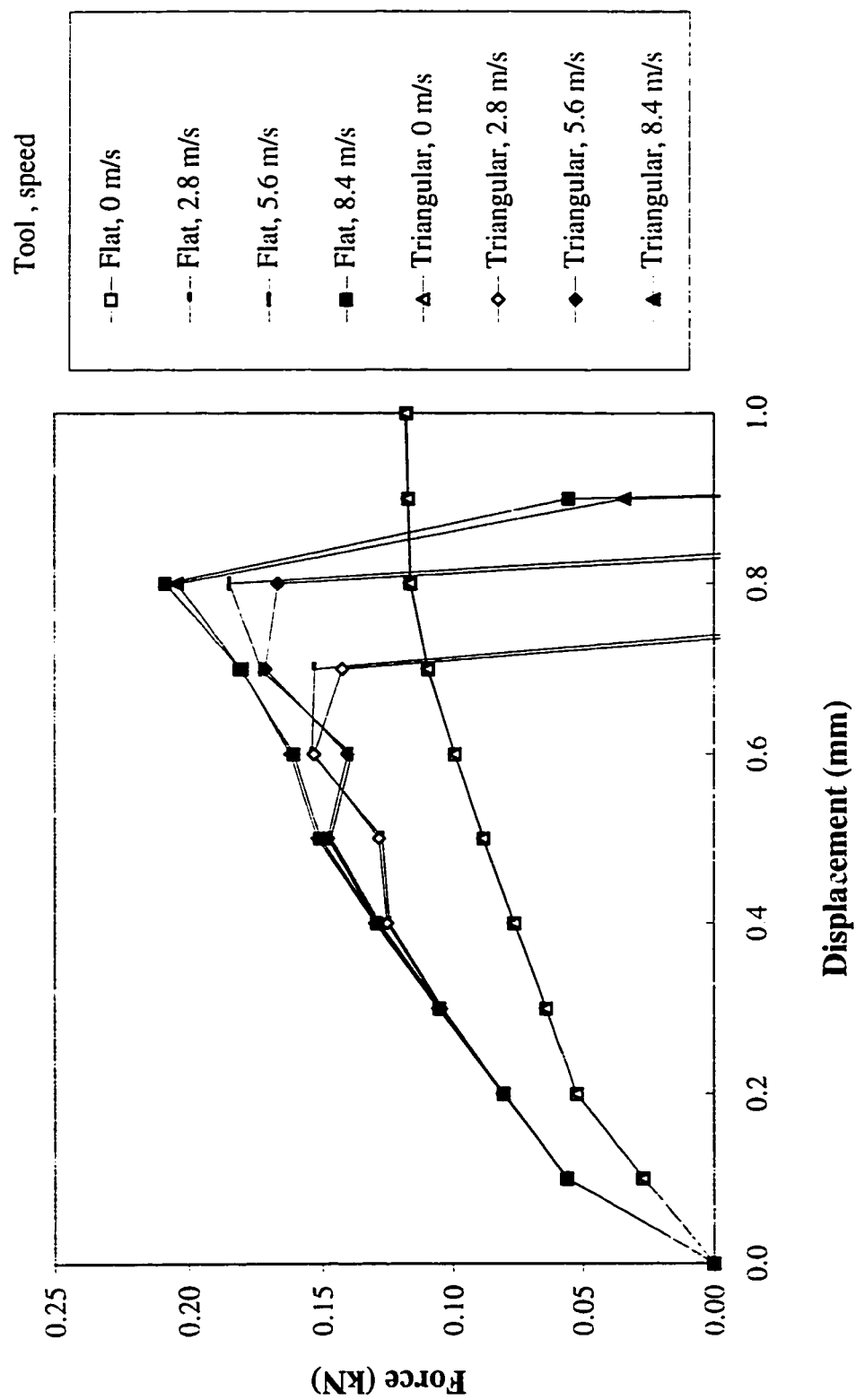
Figure 5.32 Incorporation of dynamic inertial effects in prediction of tool performance with flat and triangular coarse meshes produced numerical instabilities.

5.2.4 Model modification for narrow tool simulation

In summary, the numerical simulations of triaxial tests and of narrow tools showed that, in its present form, the model with viscous effects (incorporated in the stiffness matrix) and with inertial effects, i.e., model III, cannot satisfactorily simulate dynamic soil loading, which is the primary aim of this research. The model might be considered sufficient for a limited number of applications using simple static stress loading paths. Soil behaviour was simulated adequately only during the early stages of loading, before failure had been initiated. Incorporation of inertial effects generated numerical instabilities in all considered cases. Removing inertial terms and dealing with damping, or viscous, terms incorporated in the stiffness matrix (model II) delayed onset of numerical instabilities but was not capable of predicting the significant differences in the reaction forces of the flat versus the triangular edged narrow tools.

It follows that if the mass of soil can be neglected, then numerical oscillations might be avoided. Under such conditions, the magnitudes of the stiffness matrix coefficients should have high enough values to avoid numerical oscillations. However, inclusion of the dynamic soil parameter, AN in the stiffness matrix (equations 3.21, 3.39 and 3.40), was not capable of producing considerable changes in the predicted tool draft. This does not agree with the experimental data obtained for the narrow tools tested over a range of speeds in the soil bin.

It was noted during soil bin tests that the disturbed soil was thrown only short distances from the tool path. This observation suggests that inertial effects are negligible relative to viscous effects, which in contrast, would be substantial.

The constitutive finite element formulation was modified to incorporate lumped damping effects while keeping the stiffness matrix free of damping or strain rate effects, and neglecting inertial effects, that is:

$$\mathbf{C}_l \dot{\mathbf{u}} + \overline{\mathbf{K}} \mathbf{u} = \overline{\mathbf{R}} \tag{5.1}$$

where the $\overline{\mathbf{R}}$ is the external load vector, where the inertial forces are neglected (equation 3.32), $\mathbf{u}$ are displacements and $\overline{\mathbf{K}}$ the stiffness matrix (F/L). This will be referred as model IV. In this formulation the damping coefficient $\mathbf{C}_l$ is in the lumped matrix form (F·T/L), (Desai and Abel 1972),

$$\mathbf{C}_l = \int_V \mu \, \mathbf{\Psi}^T \mathbf{\Psi} \, dV \tag{5.2}$$

μ = material damping (F·T/L),

$\mathbf{\Psi}$ = matrix of functions $\mathbf{\Psi}_i$ which have unit value over the region tributary to

         node i and zero elsewhere,

V = element local domain (L^3).

In the lumped formulation procedure damping terms are placed at nodal points, in directions of the assumed displacement degrees of freedom (Desai and Abel 1972). The lumped damping matrix can be obtained by dividing the total element damping equally among the element nodes. No interaction is assumed between nodal damping. Thus, there is no interaction among damping components in the lumped damping matrix. The result is a purely diagonal damping matrix.

The $\overline{\mathbf{K}}$, the stiffness matrix, is given by equations 3.21, 3.39 with AN=0 (Duncan and Chang 1970), 3.40 and 3.41. That is:

The tangent modulus of elasticity,

$$E_s = \left[1 - \frac{R_f(\sigma_1 - \sigma_3)}{\dfrac{2c\cos\phi + 2\sigma_3\sin\phi}{(1-\sin\phi)}} \right]^2 K p_a \left(\frac{\sigma_3}{p_a} \right)^n \tag{5.3}$$

the constitutive matrix,

$$C = \frac{E_s}{(1+v)(1-2v)} \begin{bmatrix} (1-v) & v & v & 0 & 0 & 0 \\ v & (1-v) & v & 0 & 0 & 0 \\ v & v & (1-v) & 0 & 0 & 0 \\ 0 & 0 & 0 & \left(\dfrac{1-2v}{2}\right) & 0 & 0 \\ 0 & 0 & 0 & 0 & \left(\dfrac{1-2v}{2}\right) & 0 \\ 0 & 0 & 0 & 0 & 0 & \left(\dfrac{1-2v}{2}\right) \end{bmatrix} \tag{5.4}$$

the linear stiffness term for each element,

$$\mathbf{K}_L = \iiint\limits_{V_{lu}} \mathbf{B}^T \mathbf{C} \mathbf{B} \det \mathbf{J} \, dr \, ds \, dt \tag{5.5}$$

and a variable Poisson's ratio,

$$v = a_1 + b_1 \frac{(\sigma_1 - \sigma_3)}{(\sigma_1 - \sigma_3)_f}. \tag{5.6}$$

Stiffness was calculated according to the verified Dyntool code with AN equal to zero, i.e., static condition (equation 3.39). The Dyntool code was modified to incorporate the new numerical solution. In the Dyntool-2 code, stiffness still obeyed the hyperbolic formulation with variable Poisson's ratio but inertial terms were removed. Damping and

strain rate values, previously neglected in the Newmark formulation (Bathe 1982), were now reincorporated in the Dyntool-2 code (Appendix B). The integration scheme gives an approximate solution of equation 5.1 similar to that presented in Table 3.1; however, the equation presented in item 4 of part A is replaced by:

$$\hat{\mathbf{K}} = \overline{\mathbf{K}} + a_1 \mathbf{C}_1 \tag{5.7}$$

and the equation presented in the item 1 of part B is replaced by:

$$^{t+\Delta t}\hat{\mathbf{R}} = {}^{t+\Delta t}\overline{\mathbf{R}} + \mathbf{C}_1(a_1\,{}^t\mathbf{u} + a_4\,{}^t\dot{\mathbf{u}} + a_5\,{}^t\ddot{\mathbf{u}}) \tag{5.8}$$

The general procedure of adopting a damping term as explained above was based on the one dimensional findings of Kocker and Summers (1988) in which a viscoelastic model was found to best represent soil (Chancellor 1994). This was expected to reduce numerical instability problems.

5.2.5 Predictions using a reference tool

Up to this stage of the model development, it had not been possible to use a flat tool as a reference tool to determine viscous parameters (AN with Dyntool), which would then be used in the model to predict the behaviour of another tool shape. A preliminary investigation with this goal is presented in this section. However, due to problems with Dyntool, C_1 viscous parameters with the Dyntool-2 code are used instead.

The Dyntool-2 finite element code was run using the coarse flat and triangular meshes referred to in the previous section (Figures 5.29 & 5.33). The flat tool was used as a reference tool to obtain C_1 parameters for different speeds of operation by comparing

0.20 m

0.50 m

0.15 m
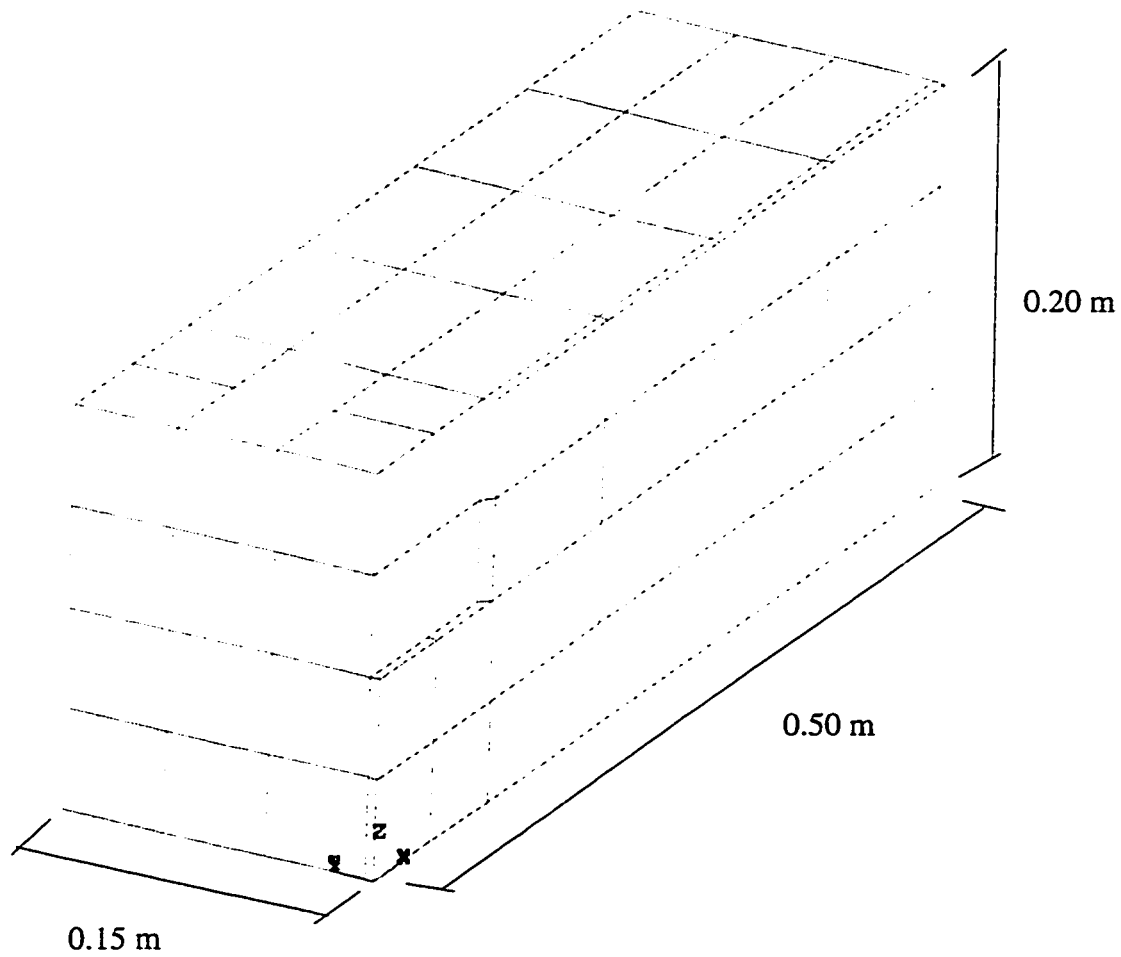
Figure 5.33 **Discretization of the coarse triangular tool mesh used with the code Dyntool-2 in which lumped viscous effects are formulated externally from the stiffness matrix.**

simulations with experimental results. The value of C_l obtained in this way, and speed were then used in the computer code to predict triangular tool drafts.

First, draft forces were predicted using an initial set of damping coefficient, C_l, and based on the error of predictions compared with experimental values, another value of damping was selected for subsequent computations. Typically, around four to five iterations were performed before convergence to a solution was reached. Five speeds between 2.8 and 8.4 m/s were simulated for a flat tool operating at a depth of 100 mm. The calculated maximum draft force of each speed was compared with the draft data obtained from experimental measurements with the flat tool. Figure 5.34 shows the calculated drafts for the reference tools. Peak values of draft from the force versus displacement curves were used to determine damping coefficients. Displacements beyond attainment of the peak value started to produce numerical oscillations and the numerical analysis had to be interrupted. The peak value represents the maximum strength the soil mobilizes at which point failure starts to occur more intensively. Interpolations and extrapolations of C_l were performed until the error between experimental and predicted drafts was within 1.0 N.

A strong trend of increasing in the damping coefficient C_l occurred with increase in tool speed (Figure 5.35). Plotted on a logarithmic C_l scale, an approximately linear increase in the lumped damping coefficient C_l for the lower speed range from 2.8 up to 5.6 m/s occurred. At a higher speed range from 5.6 up to 8.4 m/s another approximately linear relationship of logarithm of damping C_l with speed can be assumed. At approximately 5.6 m/s a sharp change occurred in the damping trend. Damping increased with speed at the
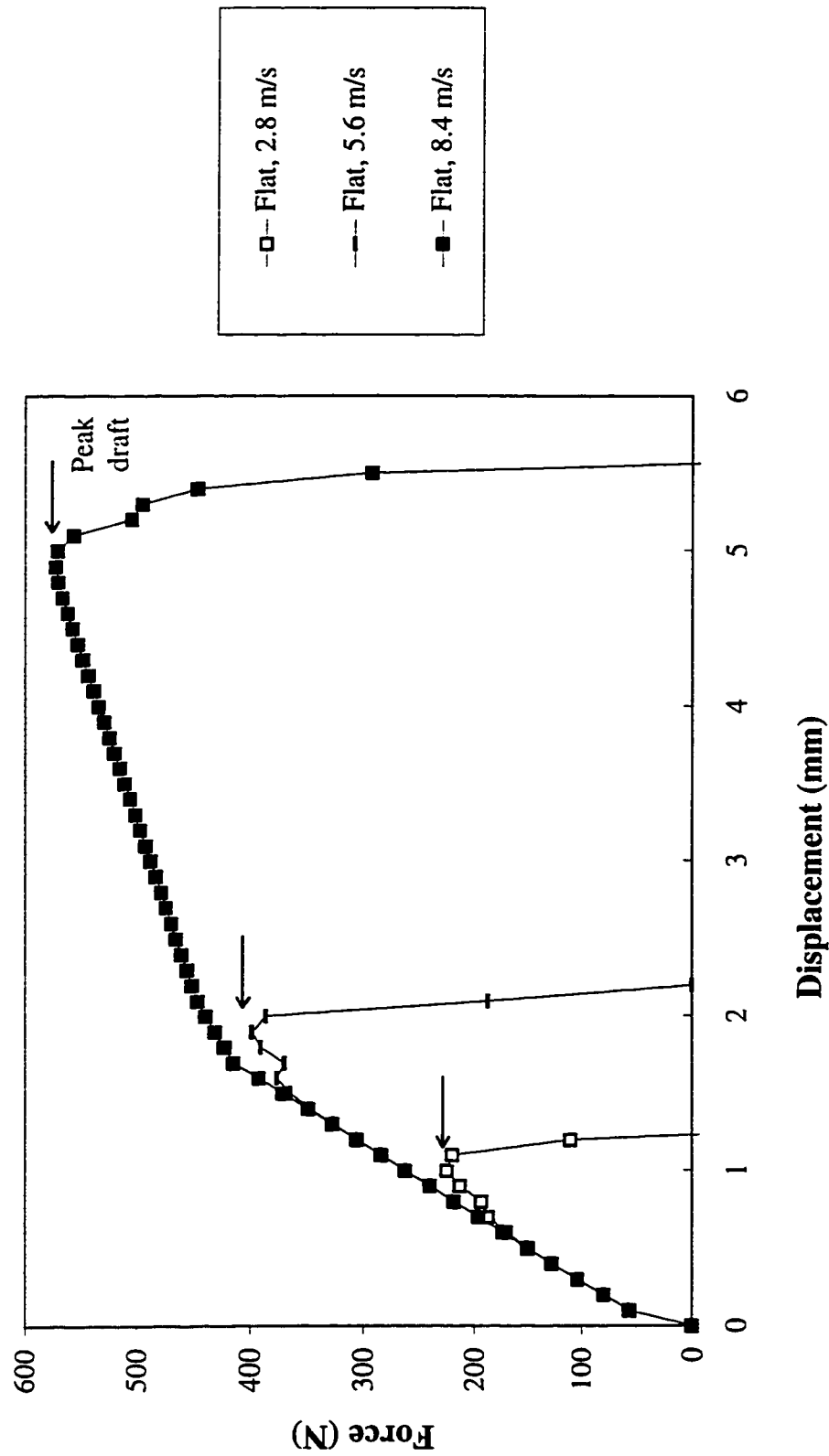
Figure 5.34 Predicted flat tool draft versus displacements used to determine the set of dynamic soil parameters C_i. Arrows show peak draft.
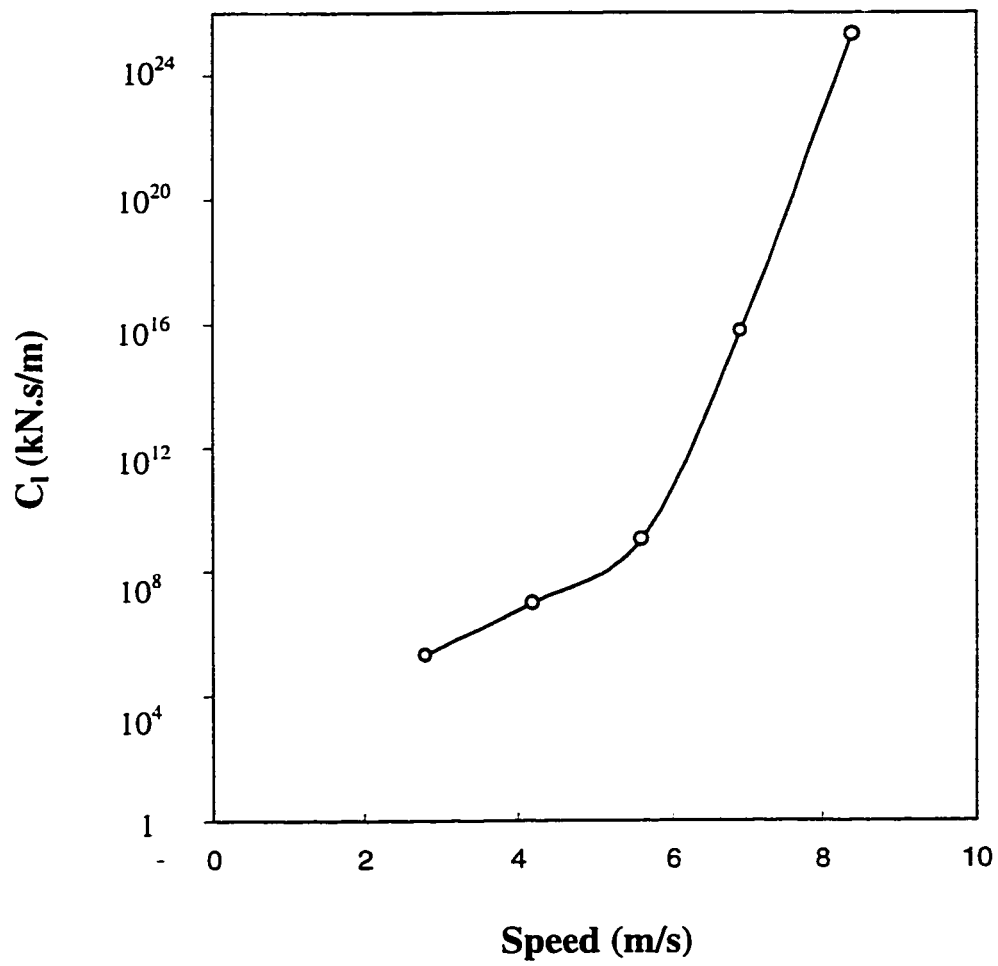
Figure 5.35 Damping coefficients C_l determined using reference tool method increased rapidly with tool speed.

approximate rate of 4×10^8 kN s^2/m^2 for the lower speed range up to 5.6 m/s speed. The slope of the line for the higher speed range was 7×10^{24} kN s^2/m^2. Although, a rapidly increasing damping versus speed relationship was obtained, at least the model (model IV) was sensitive enough for the predicted drafts to correlate with experimental measurements (Figure 5.36). Further study in which damping and inertial terms are separated would be required to better evaluate the effect of inertial components in the model.

Once the values of damping coefficients C_l were obtained for various speeds, the finite element code was used to estimate drafts for the triangular tool at the same speeds. The triangular mesh (Figure 5.33) was used to compute draft forces for each tool speed. Figure 5.37 shows predicted and experimental triangular forces versus displacements at three operating speeds. The model correctly predicted lower drafts for the triangular tools than the flat tools. In view of the coarse mesh used, results are reasonable. Only two brick elements had been used to represent tool shape. The utilized coarse mesh could have introduced a stiffer than expected response for the soil elements. A finer mesh was not used for this case. Predictions of the triangular tool draft overestimated experimental measurements by less than 1% at the speed of 2.8 m/s and by 25% at 8.4 m/s. Mesh refinement and re-sizing of loading steps should improve predictions, although this was not done for this study. Even though improved soil models could possibly better predict soil behaviour after failure, at least the present damping modification was capable of providing predictions based on a reference tool and finite element analysis. This presented a significant improvement over analyses reported in earlier sections.
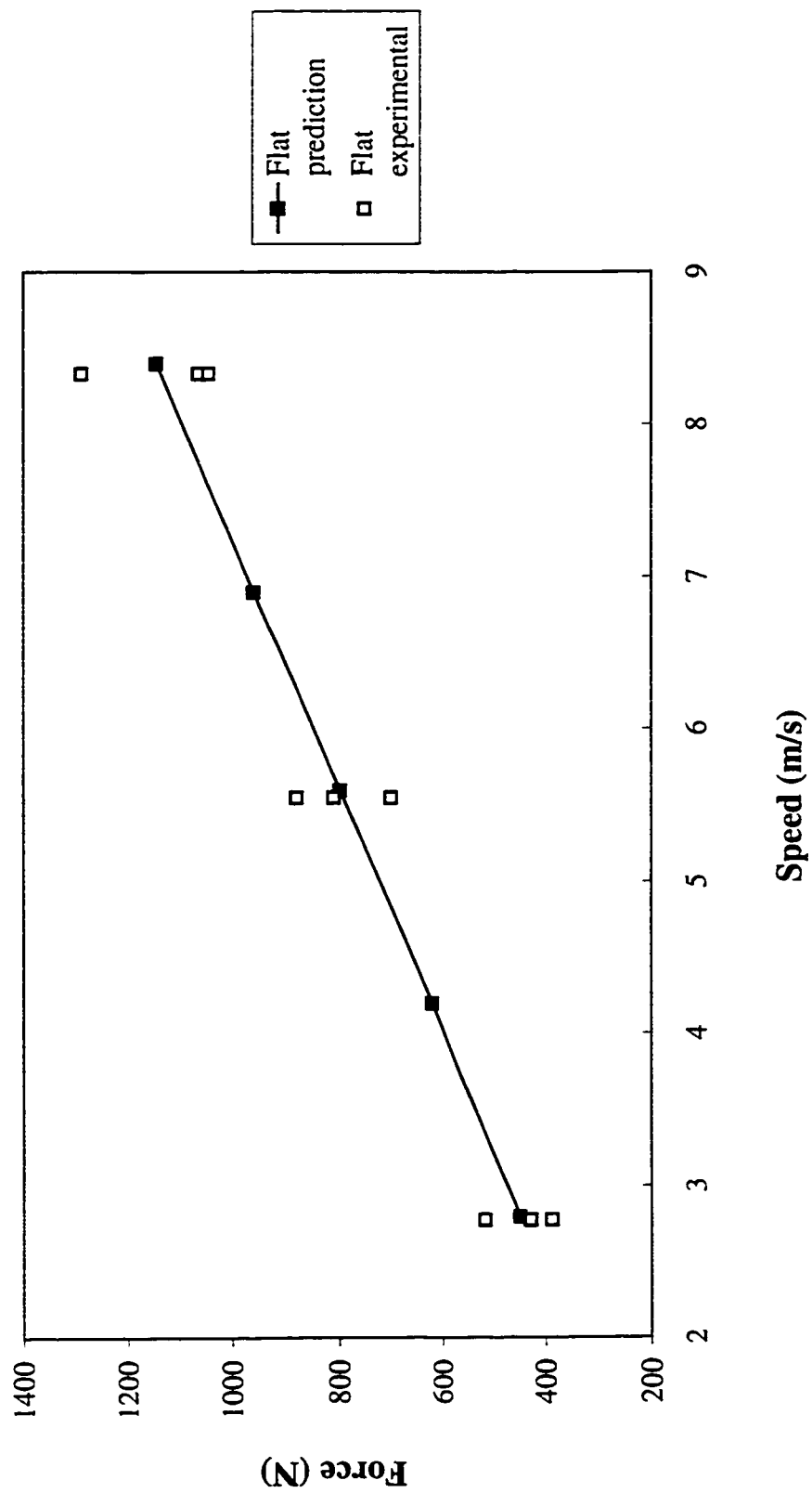
Figure 5.36 Flat tool draft prediction determined by using C_I coefficients compared with experimental points.
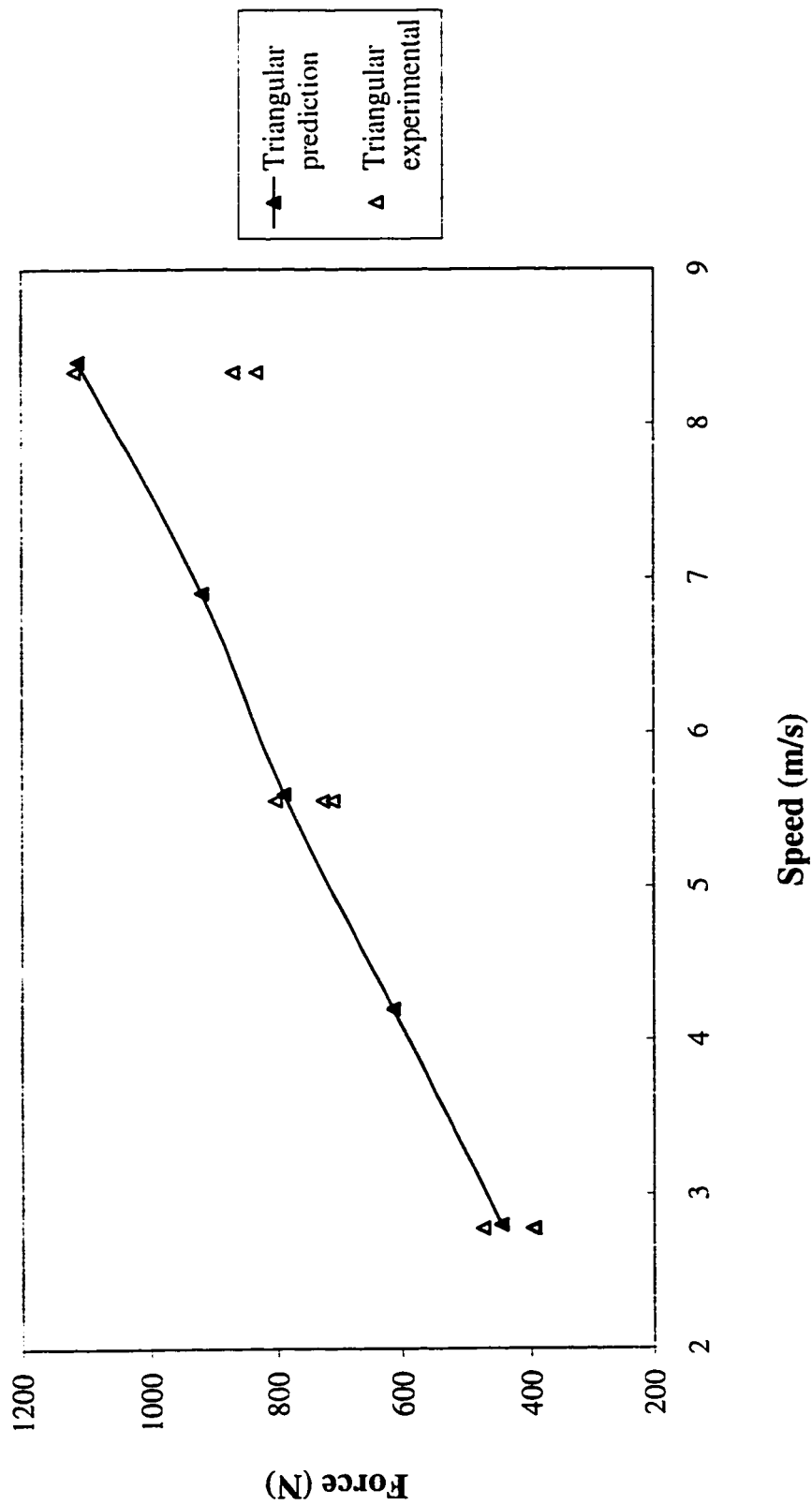
Figure 5.37 Triangular tool draft predictions compared with experimental draft measured by using the triangular tool.

Correct trends were obtained, but triangular tool average draft was overpredicted using the adopted stiff coarse mesh.

The reference tool procedure described here successfully combined a finite element prediction with a standard reference tool in an inverse method to determine the dynamic soil damped lumping coefficient C_l. In theory, it should be possible to use it to 'calibrate' all soil parameters (including static ones) to the soil conditions, although at this stage this was not done. Further work would be required to accomplish this.

5.3 Summary of Results and Discussion

Results presented in this chapter included: a) experimental soil-tool data and statistical analyses; b) determination of soil parameters; and, c) numerical simulations using a finite element code Dyntool, and its modifications.

5.3.1 Experimental results

All tools showed linear increases of draft with operating speed. Tool draft requirements were lowest for the soft packed soil with the elliptical tool working at a shallow depth (50 mm). Depth of operation and speed had substantial effects on the tool draft. The shape of the tools was important. The more streamlined elliptical tool shape resulted in reduced draft. Elliptical, triangular and flat tool shapes presented the lowest to the highest draft requirements, in that order. This streamlining effect suggests that viscous drag forces, rather than soil cutting forces, predominate. Power per operating depth also increased with tool speed, represented by a polynomial law for the case of the elliptical tools (the only cases which presented enough degrees of freedom for this analysis). Soil disturbance and pulverization increased with increased tool speeds.

5.3.2 Simulations

Soil was modeled as a hypoelastic material with strain rates incorporated in the tangential modulus of elasticity and inertial soil mass in the equilibrium equation. The Dyntool code was first verified using a quasi-static example available in the literature (Duncan and Chang 1970). When simulation of dynamic cases were performed, numerical instabilities occurred when soil elements approached failure. Using the flat and triangular tool meshes, instabilities appeared for small displacements, usually smaller than 1 mm. Several steps were tried to solve the problem. The removal of the inertial term ($\mathbf{M}\ddot{\mathbf{u}}$) from the model reduced numerical oscillations. Triaxial simulations showed that the model was sensitive to the strain rate parameter incorporated in the stiffness matrix, AN, but this was not the case when a narrow tool was simulated. Modifications to this model involved removing strain rate effects from the stiffness matrix and introducing a damping matrix C_l in the equilibrium equation. This reduced numerical instabilities, so that larger tool displacements could be simulated. Nevertheless, displacements were still limited to less than 10 mm, thus not completely solving the problem.

A reference tool procedure was used to estimate dynamic damping coefficients C_l. The estimated damping coefficients increased rapidly with increases in tool speed, particularly for speeds from 5.6 to 8.4 m/s. The modified model (Dyntool-2) was still not completely satisfactory in modeling the soil cutting problem (mainly due to numerical instabilities), particularly when soil approached failure. However, reasonable results were obtained. Predictions using triangular tools showed correct trends and errors were on the order of 1% for the speed of 2.8 m/s, and 25% error at 8.4 m/s. The use of the reference

tool shows promise, since all dynamic and static model soil parameters can in theory be obtained by doing in-situ tests with a simple tool shape, eliminating the need for laborious laboratory tests (e.g. triaxial tests) with remolded soil specimens.

For the range of speeds tested a 'blunt' (i.e., elliptical) tool presented lower draft demand than a sharp (i.e, triangular) tool. These experimental results suggested that tool drag predominated over soil cutting. This finding was further supported by the modelling exercise, in which viscous terms were much more important rather than inertial terms (which in fact could be neglected). Excessive manipulation and remoulding of the soil in the soil bin, without allowing enough time for soil cementation bonds to re-form, may be the main reason for this behaviour. Field testing in cemented soils would be required to investigate both drag and cutting forces behaviour.

CHAPTER 6

<u>SUMMARY AND CONCLUSIONS</u>

The effect of operation speed on the behaviour of narrow tillage tools has been studied only to a very limited extent up to the present time. Theoretical aspects include determination of static and dynamic soil properties. In this study, static soil parameters were determined from conventional triaxial tests, while a new technique for the determination of a dynamic soil damping parameter was proposed and a preliminary verification carried out. The concept was developed based on developments of standard reference tools previously adopted by other researchers. The technique relies on measurements of a standard reference tool draft which is used as an inverse method to determine a dynamic soil parameter and a finite element method implemented in the Dyntool code to solve model equations. The technique needs further development and hopefully can aid in the design of new narrow tillage tools. The most successful soil model verified here was a simple viscoelastic one. A three-dimensional model was used due to the nature of narrow tillage tool behaviour.

As a part of this research, a unique soil bin high speed tool testing device was developed. An electrical motor of 30 kW was adequate to drive the carriage system having an approximately 10 kg mass, along a 9 m long rail. The successful testing of tillage tools in an ordinary, short (9 m), soil bin facility at speeds up to 10 m/s is an important development. Another important aspect of high speed operation of tillage tools, i.e. the

power demand, was analyzed. Power per operating depth increased with speed for all studied cases.

The following conclusions are drawn from this study:

Objective 1. To accomplish objective 1, a unique 9-m long monorail equipment and instrumentation were developed to drive and to measure draft forces and speed of narrow tools working in a soil bin. The system worked satisfactorily for the range of tested speeds of 0.5 to 10 m/s. Tool steady-state speeds were attained and maintained for approximately 1-3 m. The amount of scatter of draft data points, supported by a power spectral density analysis of draft data, showed that the system worked with reduced draft fluctuations when a tool moved while engaged in the soil. Roughness meters, i.e. a profilometer, was used to assess soil tillage disturbance.

Rectangular, triangular and elliptical shaped narrow tools were evaluated using the developed system. Power spectral density analysis of draft data indicated substantial soil damping effects. Power per operating depth, P_w , increased with tool speed; draft forces also increased with speed. High speeds of operation represented more remarkable differences in P_w than low ones when comparing different tool shapes. Depth of operation was a major factor increasing expenditure of power per depth of operation. The elliptical tool shape showed better P_w performance.

Photographic and video camera analysis indicated increasing soil crumbling with increasing tool speed. Three replications on soil disturbance measurements by using profilometers were not sufficient for statistical considerations. Difficulties arose in trying

to measure the cross-sectional area of the disturbed soil around the tool path. Quantification of these parameters could not be addressed in the present work.

Soil preparation was reflected in the draft results. Maximum measured average tool draft (rectangular tool, width of 9.4 mm, operating depth 100 mm) was 1.2 kN at 8.4 m/s. Soil properties, however, where found to be highly sensitive to the soil preparation method. Measured soil cone index values showed large coefficients of variance (22-77%, at 12.3% average water content).

Tool shape, depth of operation and speed had substantial influence on draft. Data of soft pack soil for the depth of 50 mm did not show substantial change in draft for the investigated tool shapes. It was the only condition that did not present a significant influence of tool shape on draft.

When soil structure had greater bulk densities shape effects were much more evident. Comparisons among tool shapes indicated elliptical, triangular and rectangular tool shapes, had lower to higher draft requirements in increasing order. All cases showed linear draft vs. speed relationships and high values of R^2.

Soil was thrown only a relatively small distance away from the tool path, indicating low influence of inertial forces but high viscous effects on tool draft.

Objective 2. A viscoelastic based constitutive model was developed. Models did not satisfactorily handle soil behaviour close to soil failure. As a result, difficulties were encountered in implementing the model in a finite element formulation; specifically numerical instabilities were prevalent in dynamic cases.

A fundamental problem was revealed during the literature review. It seems that hypoelastic models with variable Young's modulus and Poisson's ratio cannot adequately predict soil behaviour close to failure. In situations when the determinant of the stiffness matrix is equal to zero, (det $|C| = 0$), material instability or failure occurs. In this thesis, while this was already a problem when running quasi-static large deformations, it became even more aggravated when attempting to simulate dynamic cases, particularly for narrow tools since failure is initiated immediately on very small tool displacements (<1 mm).

Some values of soil parameters in the Duncan and Chang (1970) model are arbitrary so that calibration is required. Inclusion of a variable Poisson's ratio into quasi-static triaxial modeling provided good predictions when compared with experimental measurements. However, dynamic simulations incorporating inertial effects and viscous effects directly in the stiffness matrix $\overline{K}$, where $M\ddot{u} + \overline{K}u = \overline{R}$, produced numerical oscillations when the soil approached failure. When failure was reached, low values of the stiffness matrix introduced strong oscillations, particularly with the inertial dynamic model.

Neglecting inertial effects $M\ddot{u}$ from the analysis, while still considering viscous effects by incorporating them in the stiffness matrix, and with a residual value set to the stiffness matrix for soil elements at failure (see Duncan and Chang 1970) solved problems with numerical oscillations. However, the resulting model gave poor predictions when

strain rate effects where introduced; the model did not produce increased draft response when tool speed was increased.

When damping effects were considered separately and removed from the stiffness matrix to produce a system equation of the form $C_1 \dot{u} + \overline{K} u = \overline{R}$, better predictions were obtained. The use of high damping values, C_l, in the numerical analysis reduced, but did not eliminate, oscillation effects. The equivalent stiffness matrix $\overline{K}$ resulted in higher numerical values of stiffness so that oscillations simply occurred at slightly larger tool displacements (1 to 5 mm).

Objective 3. An innovative procedure was proposed to determine dynamic soil damping properties by using the reference tool concept combined with finite element analysis and static soil properties determined using conventional methods. Damping rate coefficients representing dynamic soil properties were obtained from rectangular reference tool runs and then used in the finite element model to estimate draft forces for triangular tools. Even though the soil finite element mesh used was coarse and the soil model was only satisfactory prior to soil failure, the model was capable of predicting distinguishing features of flat versus triangular tool performance. Correct trends were produced, but values of draft versus speed were overpredicted by 1% to 25%, with the higher differences obtained at higher speeds. Thus, the preliminary trials show that the method proposed has promise, but a more complete, broader investigation is required.

In conclusion, there is still a need to develop appropriate soil constitutive models to improve simulation analysis. Correct modeling of soil failure is particularly important for the tillage tool cutting problem.

CHAPTER 7

RECOMMENDATIONS AND SUGGESTIONS

FOR FUTURE RESEARCH

The following are suggestions arising from the work presented in this thesis.

1) Empirically test and improve different tool shapes in terms of draft and soil disturbance in the soil bin by means of the developed high speed equipment. Soil openers might be tested and compared.

2) Develop adequate automated instrumentation to measure disturbed soil cross-sectional profiles and cutting areas. Automation will facilitate obtaining enough replications for statistically sound analysis. Equipment with greater data storage capacity is needed.

3) Design and develop adequate depth controller devices in order to make practical field applications viable for high speeds. Also, potential applications in 'controlled traffic' monorail systems shows promise and should be investigated.

4) Perform fundamental studies of soil cutting over high speed dynamic range (W. J. Chancellor, Professor Emeritus, UC Davis, Personal communication, 1996). This might include soil cutting with a wire cutting materials with various viscosities and even water beds. The purpose is to isolate fundamental soil effects.

5) Investigate the use of viscoplastic models of soil behaviour which would handle soil failure in a more adequate form. Optimizing for a minimum number of dynamic parameters while considering static parameters constant might greatly facilitate dynamic analysis.

6) Proceed with a complete study based on the reference tool concept described in this thesis. In theory there is no need to rely on determination of static parameters from static triaxial tests since all static and dynamic parameters can be obtained from response surfaces and inverse techniques. Changes in load steps, more mesh refinement and a more suitable constitutive model might be required (see Rubinstein et al. 1994).

7) The use of full advantage of pre- and post-processors from commercial finite element programs is strongly recommended. This will be particularly needed for meshes with a large number of degrees of freedom, which is very common in three dimensional analysis.

8) Higher orders of approximation for updated Lagrangian schemes are also recommended to avoid errors for large load steps. In this thesis updated nodal coordinates were used. The implementation of full Newton Raphson method is also recommended.

REFERENCES

Antmam, S. S. 1995. Nonlinear problems of elasticity. In *Nonlinear Plasticity*, Eds. John

    F., J. E. Marsden and L. Sirovich, pp. 603-604. Berlin: Springer-Verlag.

Araya, K. and R. Gao. 1995. A non-linear three dimensional finite element analysis of

    subsoiler cutting with pressurized air injection. *Journal of Agricultural*

    Engineering Research 61:115-128.

Aref, K. E. , W. J. Chancellor and D. R. Nielsen. 1975. Dynamic shear strength properties

    of unsaturated soils. *Transactions of the ASAE* 18(5):818-823.

ASAE Data D497. 1993. Agricultural machinery management data. ASAE Standards, 40th

    Ed., St. Joseph, MI: ASAE.

ASAE Standards S313.2. 1990. Soil penetrometer. ASAE Standard S313.2, 37th Ed.

    1990. St. Joseph, MI: ASAE.

Azyamova, E. N. 1963. Studies of dynamics of deformation of soil. *Trudy*

    (TSNIIMESKH) Minsk 1:131-139. (Translated by W. R. Gill, National Tillage

    Machinery Laboratory, USDA-ARS, Auburn, AL).

Bailey, A. C., C. E. Johnson and R. L. Schafer. 1984. Hydrostatic compaction of

    agricultural soils. *Transactions of the ASAE* 27(4):925-955.

Baladi, G.Y. and Rohani, B. 1984. Development of an elastic-viscoplastic constitutive

    relationship for earth materials. In *Mechanics of Engineering Materials*, Eds.

    Desai, C. S. and R. H. Gallagher, pp. 23-46. New York, NY: John Wiley &

    Sons.

Bathe, H. J. 1982. *Finite Element Procedures in Engineering Analysis*. Englewood Cliffs, NJ: Prentice-Hall.

Bathe, K. J., E. Ram and E. L. Wilson. 1975. Finite element formulation for large deformation dynamic analysis. *International Journal for Numerical Methods in Geomechanics* 9:353-386.

Britto, A. M. and M. J. Gunn. 1987. *Critical State Soil Mechanics via Finite Elements*. New York, NY: John Wiley & Sons.

Byrne, P. M. 1987. Geomechanics. In *Finite Element Handbook*, Eds. Kardestuncer, H. and D. G. Norrie, Chapter 3. New York, NY: McGraw-Hill.

Chancellor, W. J. 1994. Soil physical properties. In *Advances in Soil Dynamics*, Ed. P.D. Hansen. ASAE Monograph Number 12, pp. 21-254. St. Joseph, MI:ASAE.

Chancellor, W. J. and S. K. Upadhyaya. 1994. Effects of stability mechanisms during triaxial tests of cylindrical soil samples on stress ratio vs. strain ratio relations. In *Proceedings of the 2nd International Conference in Soil Dynamics*, Silsoe, Bedford, pp. 1-17.

Chen, W. 1984. Constitutive modelling in soil mechanics In *Mechanics of Engineering Materials*, Eds. Desai, C. S. and R. H. Gallagher, pp. 91-120. New York, NY: John Wiley & Sons.

Chen, W. F. and G. Y. Baladi. 1985. *Soil Plasticity, Theory and Implementation*. New York, NY: Elsevier Science Publishers.

Chen, W. and A. F. Saleb. 1982. *Constitutive Equations for Engineering Materials*. Vol.1. New York, NY: John Wiley & Sons.

Chi, L. 1989. Three dimensional nonlinear finite element modeling of soil failure with tillage tools. Ph.D. dissertation, University of Saskatchewan, Saskatoon, Sakatchewan.

Chi, L. and R. L. Kushwaha. 1990. A non-linear 3-D finite element analysis of soil failure with tillage tools. *Journal of Terramechanics* 27(4):343-366.

Chi, L. , S. Tessier and C. Laguë. 1993a. Finite element predictions of soil compaction induced by various running gears. *Transactions of the ASAE* 36(3):629-636.

Chi, L. , S. Tessier and C. Laguë. 1993b. Finite element modeling of soil compaction by liquid manure spreaders. *Transactions of the ASAE* 36(3):637-644.

Chi, L. , S. Tessier, E. McKyes and C. Laguë. 1993c. Modeling mechanical behavior of agricultural soils. *Transactions of the ASAE* 36(6):1563-1570.

Clough, G. W. and J. M. Duncan. 1971. Finite element analysis of retaining wall behaviour. *Journal of Soil Mechanics and Foundation Division ASCE* 97(SM12):1657-1673.

Coleman, B. D. and W. Noll, 1961. Foundations of linear viscoelasticity. In *Continuum Mechanics III. Foundations of Elasticity Theory*, Ed. Truesdell, C. A. Vol. 3, pp.297-307. 1965. New York, NY: Gordon and Breach Science Publishers.

Cook, R. D. 1981. *Concepts and Applications of Finite Element Analysis*, 2nd ed. New York, NY: John Wiley & Sons.

Darmora, D. P. and K. P. Pandey. 1995. Evaluation of performance of furrow openers of combined seed and fertilizer drills. *Soil & Tillage Research* 34: 127-139.

Das, B. M. 1993. *Principles of Soil Dynamics*. Boston, MA: Pws-Kent Publishing.

Davis, R. O. and Mullenger, G. 1978. A rate-type constitutive model for soil with a critical state. *International Journal for Numerical and Analytical Methods in Geomechanics* 2:255-282.

Desai, C. S. and J. F. Abel. 1972. *Introduction to the Finite Element Method. A Numerical Method for Engineering Analysis.* New York, NY: Van Nostrand Reinhold Co.

Desai, C. S. and H. V. Phan. 1980. Three-dimensional finite element analysis including material and geometric nonlinearities. In *Computational Methods in Geomechanics,* Ed. J. T. Oden. pp.205-224. Amsterdan The Netherlands: North-Holland Publishing Co.

Desai, C. S., H. V. Phan and J. V. Perumpral. 1982. Mechanics of three-dimensional soil-structure interaction. *Engineering Mechanics Division ASCE* 108(EM5):731-747.

Desai, C. S., H. V. Phan and S. Sture. 1981. Procedure, selection and application of plasticity models for a soil. *International Journal for Numerical Methods in Geomechanics* 5:295-311.

Desai, C. S. and H. J. Siriwardane. 1984. *Constitutive Laws for Engineering Materials.* Englewood Cliffs, NJ: Prentice-Hall.

Desai, C. S. and D. Zhang. 1987. Viscoplastic model for geologic materials with generalized flow rule. *International Journal of Numerical Methods and Analysis Methods in Geomechanics.* 11:603-620.

Desbiolles, J. M. A. , R. J. Godwin, J. Kilgour and B. S. Blackmore. 1994b. Cone penetrometer and tillage force prediction. In *Proceedings of the 2nd International Conference on Soil Dynamics*, Silsoe, Bedford; pp. 25-26.

Desbiolles, J. M. A. , V. Kirisci, R. J. Godwin, J. Kilgour and B. S. Blackmore. Soil strength and tillage force prediction. 1994a. In *Proceedings of the 2nd International Conference on Soil Dynamics*, Silsoe, Bedford; pp. 22-24.

Dhatt, G. and G. Touzot. 1984. *The Finite Element Method Displayed*. New York, NY: John Wiley & Sons.

Drucker, D. C., R. E. Gibson and D. J. Hankwe. 1955. Soil mechanics and work-hardening theory of plasticity. In *Proceedings of the American Society of Civil Engineers* Vol. 81, Paper 798, pp.1-14.

Duncan, J. M. and C. Y. Chang. 1970. Nonlinear analysis of stress and strain in soils. *Journal of Soil Mechanics and Foundation Division ASCE* 96(SM5):1629-1653.

Dunlap, W. H. and J. A. Weber. 1971. Compaction of an unsaturated soil under a general state of stress. *Transactions of the ASAE* 14(4):601-611.

Eringen, A. C. 1962. *Nonlinear Theory of Continuous Media*. New York, NY: McGraw-Hill.

Fung, Y. C. 1977. *A First Course in Continuum Mechanics*. 2nd ed. Englewood Clifs, NJ: Prentice-Hall.

Gee-Clough, D., J. Wang and W. Kanok-Nukulchai. 1994. Deformation and failure in wet clay soil: Part 3. Finite element analysis of cutting of wet clay by tines. *Journal of Agricultural Engineering Research* 58:121-131.

Gill, W. R. and G. E. Vanden Berg. 1968. *Soil Dynamics in Tillage and Traction*. Handbook No. 316. Washington DC. USDA Deptment of Agriculture.

Glancey, J. L. and S. K. Upadhyaya. 1990. A testing procedure for agricultural implements. ASAE Paper No. 90-1542, St. Joseph, MI:ASAE.

Glancey J. L., S. K. Upadhyaya, W. J. Chancellor and J. W. Rumsey. 1996. Prediction of agricultural implement draft using an instrumented analog tillage tool. *Soil & Tillage Research* 37: 47-65.

Godwin and Spoor. 1977. Soil failure with narrow tines. *Journal of Agricultural Engineering Research* 22(4):213-228.

Godwin, R. J. , G. Spoor and M. S. Soomro. 1984. The effect of tine arrangement on soil forces and disturbance. *Journal of Agricultural Engineering Research* 30:47-56.

Grisso, R. D. and J. V. Perumpral. 1985. Review of models for predicting performance of narrow tillage tools. *Transactions of the ASAE* 28(4):1062-1067.

Grisso, R. D. , M. Yasin and M. F. Kocker. 1994. Tillage implement forces operating in silty clay loam. ASAE Paper No. 94-1532, St. Joseph, MI:ASAE.

Gudehus, G. 1977. Some interactions of finite element methods and geomechanics: A survey. In *Finite Elements in Geomechanics*, Ed. G. Gudehus, pp. 1-31. New York, NY: John Wiley & Sons.

Gudehus, G., M. Goldscheider and H. Winter. 1977. Mechanical properties of sand and clay and numerical integration methods: some sources of errors and bounds of accuracy. In *Finite Elements in Geomechanics*, Ed. G. Gudehus, pp.121-150. New York, NY: John Wiley & Sons.

Harrigan, T. M. and C. A. Rotz. 1994. Draft of major tillage and seeding equipment. ASAE Paper No. 94-1533, St. Joseph, MI:ASAE.

Hassan, A. El-Domiaty and W. J. Chancellor. 1970. Stress-strain characteristics of a saturated clay soil at various rates of strain. *Transactions of the ASAE* 13(5):685-689.

Haupt, P. 1993. On the mathematical modelling of material behaviour in continuum mechanics. *Acta Mechanica* 100:129-154.

Hendrick, J. G. and W. R. Gill. 1973. Soil reaction to high speed cutting. *Transactions of the ASAE* 16(3):401-403.

Hettiarachi, D. R. P. 1987. A critical state soil mechanics model for agricultural soils. *Soil Use & Management* 3(3):94-105.

Hettiarachi D. R. P. and J. R. O'Callaghan. 1980. Mechanical behaviour of agricultural soils. *Journal of Agricultural Engineering Research* 25:239-259.

Hettiaratchi D. R. P. and A. R. Reece. 1967. Symmetrical three-dimensional soil failure. *Journal of Terramechanics* 4(3):45-67.

Johnson, W. E. 1977. Conservation tillage in western Canada. In *Conservation Tillage Problems and Potentials*. Ankeny, IO: Soil Conservation Society of America.

Kardestuncer, H. and D. H. Norrie. 1987. *Finite Element Handbook*. New York, NY: McGraw-Hill.

Katsygin, V. V. 1961. Investigation of the infuence of increasing operating speeds of

machines on crumbling of soil and the expenditure of energy. *Voprosy*

Zemledel'cheskoi Mekhaniki, Vol.7 (Part2) Section 2:49-59. (Translated by

W. R. Gill, National Tillage Machinery Laboratory, USDA-ARS, Auburn, AL).

Katsygin, V. V. 1964. Relation of draft of agricultural machines to operation speed.

Voprosy Sel'skohozyaistvennoi Mekhaniki, Section 2, 96-119, Vol. XII.

(Translated by W.R.Gill, National Tillage Machinery Laboratory, USDA-ARS,

Auburn, AL).

Kawamura. W. 1985. Soil dynamics and its application to tillage machineries. In

Proceedings of the International Conference on Soil Dynamics, Auburn. Alabama,

Vol. 2: 179-191. Auburn, AL, USA : ICSD Conference.

Kepner, R. A., R. Bainer and E. L. Barger. 1972. *Principles of farm machinery.*

Westport, CT: The Avi Publishing Co.

Kirby, J. M. 1989. Measurements of the yield surfaces and critical state of some

agricultural soils. *Journal of Soil Science* 40:167-182.

Kocker, M. F. and J. D. Summers. 1988. Wave propagation theory for evaluating dynamic

soil stress-strain models. *Transactions of the ASAE* 31(3):683-691, 694.

Kondner, R. L. 1963. Hyperbolic stress-strain response: Cohesive soils. *Journal of Soil*

Mechanics and Foundations Division ASCE 89(SM):115-143.

Koolen, A. J. and H. Kuipers. 1983. *Agricultural Soil Mechanics*. Berlin: Springer-

Verlag.

Kushwaha, R. L. and R. K. Foster. 1993. Field evaluation of grain drill furrow openers under conservation and conventional tillage systems. *Canadian Agricultural Engineering* 35(4):253-260.

Kushwaha, R. L. and J. Shen. 1995. Finite element analysis of the dynamic interaction between soil and tillage tool. *Transactions of the ASAE* 37(5):1315-1319.

Lee, E. H. 1962. Viscoelasticity. In *Handbook of Engineering Mechanics*, Ed. Flügge, W. Ch.53, pp.1-22. New York, NY: McGraw-Hill.

Linke, C. and R. L. Kushwaha. 1992. High speed evaluation of draft with a vertical blade. ASAE Paper No. 92-1019, St. Joseph, MI:ASAE.

Liu, Y. and Z. Hou. 1985. Three dimensional nonlinear finite element analysis of soil cutting by narrow blades. In *Proceedings of the International Conference on Soil Dynamics*, 2:322-337. Auburn, AL, USA : ICSD Conference.

Lubliner, J. 1990 . *Plasticity Theory*. New York, NY: MacMillan.

Luth, H. J. and R. D. Wismer. 1971. Performance of plane soil cutting blades in sand. . *Transactions of the ASAE* 14(2):255-259, 262.

Malvern, L. E. 1969. *Introduction to the Mechanics of a Continuous Medium*. Englewood Cliffs, NJ: Prentice-Hall.

McKyes, E. 1985. *Soil Cutting and Tillage*. Amsterdan, The Netherlands: Elsevier.

McKyes, E. and O. S. Ali. 1977. The cutting of soil by a narrow blade. *Journal of Terramechanics* 14(2):43-58.

McKyes, E. and F. L. Desir. 1984. Prediction and field measurements of tillage tool draft forces and efficiency in cohesive soils. *Soil & Tillage Research* 4:459-470.

Mojlaj, E. J., D. Wulfsohn and B. A. Adams.1992. Analysis of soil cutting using critical

state soil mechanics. ASAE Paper No. 92-1501. St. Joseph, MI:ASAE.

Newmark, N. M. 1959. A method of computation for structural dynamics. *Journal of the*

Engineering Mechanics Division ASCE 85(EM3):67-94.

Niyamapa, T. K. and V. M. Salokhe. 1992. Soil failure under undrained quasi static and

high speed triaxial compression test. *Journal of Terramechanics* 29(2):195-205.

Oida, A. 1984. Analysis of rheological deformation of soil by means of finite element

method. *Journal of Terramechanics* 21(3):237-251.

Olson, D. J. and J. A. Weber. 1965. Effect of speed on soil failure patterns in front of

model tillage tools. SAE Paper No. 65-0691. Warrandale, PA:SAE.

Panwar, J. S. and J. C. Siemens. 1972. Shear strength and energy of soil failure related to

density and moisture. *Transactions of the ASAE* 15(3):423-427.

Payne, P. C. J. 1956. The relationship between the mechanical properties of soil and the

performance of simple cultivation implements. *Journal of Agricultural*

Engineering Research 1:23-50.

Perumpral, J. V., R. D. Grisso and C. S. Desai. 1983. A soil-tool model based on limit

equilibrium analysis. *Transactions of the ASAE* 26(4):991-995.

Perzina, P. 1966. Fundamental problems in viscoplasticity. *Advances in Applied*

Mechanics 9:243-377.

Qun, Y. and Shen, J. 1988. Research on the rheological properties of wet soils Part I)

Flow characteristics. In *Proceedings of the 2nd Asia-Pacific Conference of the*

ISTVS, Bangkok, Thailand, pp.23-34.

Rao, S. S. 1982. *The Finite Element Method in Engineering*. Oxford, UK: Pergamon Press.

Roscoe, K. H., A. N. Schofield and C. P. Wroth. 1958. On the yielding of soils. *Geotechnique* 8(1):22-53.

Rowe, R. J. and K. K. Barnes. 1961. Influence of speed on elements of draft of a tillage tool. *Transactions of the ASAE* 4:55-57.

Rubinstein, D. , S. K. Upadhyaya and M. Sime. 1994. Determination of *in-situ* engineering properties of soil using response surface methodology. *Journal of Terramechanics* 31(2):67-92.

SAS. 1985. *Users Guide: Statistics*, Cary, NC: SAS Institute Inc.

Saskatchewan Prairie Care. 1991. Practical soil & water management choices. Bulletin No. 11, 24 pp. Winnepeg, MB: Ducks Unlimited Canada.

Schofield, A. and P. Wroth. 1968. *Critical State Soil Mechanics*. New York, NY: McGraw-Hill.

Scott, J. and I. Yule. 1993. Development of a high speed plough. *The Agricultural Engineer* 48(4):118-119.

Shen, J. and R. L. Kushwaha. 1993. Three-dimensional non-linear and dynamic finite element analysis of tillage. ASAE Paper No. 93-3580. St. Joseph, MI:ASAE.

Shen, J. and R. L. Kushwaha. 1995a. Stress-strain rate relation of agricultural soils. *Canadian Agricultural Engineering* 37(1):19-28.

Shen, J. and R. L. Kushwaha 1995b. Investigation of an algorithm for non-linear and

    dynamic problems in soil-machine systems. *Computers and Electronics in*

    Agriculture 13:51-66.

Shibusawa, S. 1992. Fractals in clods formed with rotary tillage. *Journal of*

    Terramechanics 29(1):107-115.

Siemens, J. C. , J. A. Weber and T. H. Thornburn. 1965. Mechanics of soil as influenced

    by model tillage tools. *Transactions of the ASAE* 8(1):1-7.

Siriwardane, H. J. 1980. Nonlinear soil-structure interaction analysis of one-, two-, and

    three-dimensional problems using finite-element method. Ph.D. thesis.

    Virginia Polytechnic Institute and State University, Blacksburg, VA.

Sitkei, G. 1985. Basic regularities of soil clod breakup at the seedbed preparation. In

    Proceedings of the International Conference on Soil Dynamics, 2:364-376.

    Auburn, AL, USA : ICSD Conference.

Stafford, J. V. 1979. The performance of a rigid tine in relation to soil properties and

    speed. *Journal of Agricultural Engineering Research* 24:41-56.

Stafford, J. V. 1984. Force prediction models for brittle and flow failure of soil by

    draught tillage tools. *Journal of Agricultural Engineering Research* 29:51-60.

Stafford, J. V. and B. Ambler. 1990. Sensing spatial variability of seedbed structure.

    ASAE Paper No. 90-1624. St. Joseph, MI:ASAE.

Swick, W. C. and J. V. Perumpral. 1988. A model for predicting soil-tool interaction.

    Journal of Terramechanics 25(1):43-56.

Terzaghi, K. 1943. *Theoretical Soil Mechanics*. New York, NY: John Wiley & Sons.

Tessier, S., R. I. Papendick, K. E. Saxton and G. M. Hyde. 1989. Roughness meter to
  measure seed row geometry and soil disturbance. *Transactions of the ASAE*
  32(6):1871-1873.

Truesdell, C. A. 1955. Hypoelasticity. *Journal of Rational Mechanics and Analysis*.
  4:83-133.

Truesdell, C. A. and Noll, W. 1965. The non-linear field theories of mechanics. In
  Encyclopedia of Physics, Vol. 3/3. Berlin: Springer-Verlag.

Truesdell, C. A. and R. A. Toupin. 1960. The classical field theories. *In Encyclopedia of
  Physics*, Ed. S. Flügge, Vol. 3/1. Berlin: Springer-Verlag.

University of Saskatchewan. 1987. Guide to farm practice in Saskatchewan. Division
  of Extension and Community Relations. University of Saskatchewan, Saskatoon,
  SK, Canada. pp. 50-52.

Upadhyaya, S. K. 1984. Prediction of tillage implement draft. ASAE Paper No. 84-1518.
  St. Joseph, MI: ASAE.

Upadhyaya, S. K. 1994. Soil constitutive modeling - linear and nonlinear elasticity: A
  tutorial presentation. ASAE Paper No. 94-1071. St. Joseph, MI: ASAE.

Upadhyaya, S. K. , D. Rubinstein and M. Sime. 1993. An inverse solution technique to
  determine engineering properties of materials. ASAE Paper No. 93-1084. St.
  Joseph, MI: ASAE.

Vetrov, Y. A. and V. P. Stanevski. 1969. The investigation of the factors of the speed of
  cutting soils. *Mining Construction and Highway Machines* 8:21-26. (Translated by
  W.R.Gill, National Tillage Machinery Laboratory, USDA-ARS, Auburn, AL).

Wang, J. and D. Gee-Clough. 1993. Deformation and failure in wet clay: Part 1, stress-strain relationships. *Journal of Agricultural Engineering Research* 54:37-55.

Wheeler, P. N. and R. J. Godwin. 1994. Soil dynamics of single and multiple tines at speeds up to 20 KPH. In *Proceedings of the 2nd International Conference in Soil Dynamics*, Silsoe, Bedford; pp. 108-109.

Wheeler, P. N. and R. J. Godwin. 1996. Soil dynamics of single and multiple tines at speeds up to 20 km/h. *Journal of Agricultural Engineering Research* 63:243-250.

Wismer, R. D. and H. J. Luth. 1972. Rate effects in soil cutting. *Journal of Terramechanics* 8(3):11-21.

Wroth, C. P. and G. T. Houlsby. 1980. A critical state model for predicting the behavior of clays. In *Proceedings of the Workshop on Limit Equilibrium, Plasticity and Generalized Stress-Strain in Geotechnical Engineering*, pp. 592-627, New York, NY: ASCE.

Wulfsohn, D. 1994. Critical state soil mechanics. ASAE Paper No. 94-1073. St. Joseph, MI: ASAE.

Xie, X. and D. Zhang. 1985. An approach to 3-D nonlinear FE simulative method for investigation of soil-tool dynamic system. In *Proceedings of the International Conference on Soil Dynamics*, Auburn, Alabama, 2:412-427.

Yong, R. N. and A. W. Hanna. 1977. Finite element analysis of plane soil cutting. *Journal of Terramechanics* 14(3):103-125.

Yong, R. N. and R. D. Japp. 1968. Stress-strain behavior of clays in dynamic

compression. In *Vibration effects of earth-quackes on soils and foundations*,

ASTM STP 450, pp. 233-246. Philadelphia, PA:ASTM.

Zeng, D. and Y. Yao. 1992. A dynamic model for soil cutting by blade and tine. *Journal

of Terramechanics* 29(3):317-327.

Zienkiewicz, O. C. 1977. *The Finite Element Method*, 3rd ed. Maidenhead, England:

McGraw-Hill.

Zuo, Y. , D. C. Erbach and S. J. Marley. 1995. Soil structure evaluation by use of fiber-

optic sensor. ASAE Paper No. 95-1317. St. Joseph, MI: ASAE.

APPENDICES

Appendix A: Review of tensors and tensor notation.

Appendix B: Program codes Dyntool and Dyntool-2.

Appendix C: Dyntool program tree.

Appendix D: Flat tool input sample data.

Appendix E: Monorail hydraulic circuit.

Appendix F: SAS input sample data and sample program.

Appendix G: Steady state draft vs. speed data shown on Figure 5.1.

Appendix A

Tensors and tensor notation

Definition

Consider (in a Cartesian coordinate system) a set of axis (x_i), with the corresponding set of unit vectors (e_i) (also known as the basis of the coordinate system), and another set (x_i^*) with the basis (e_i^*). The β_{ij} is the cosine of the angle between the x_i^*-axis and the x_j-axis, i.e., $e_i^* \cdot e_j = \beta_{ij}$.

A tensor of rank or order n is a quantity **T** represented in a basis (e_i) by a component array $\{T_{i_1i_2...i_n}\}(i_1i_2...i_n = 1, 2, 3)$ and in another basis (e_i^*) by the component array $\{T_{i_1i_2...i_n}^*\}(i_1i_2...i_n = 1, 2, 3)$ where,

$$T_{i_1i_2...i_n}^* = \beta_{i_1k_1}\beta_{i_2k_2}\cdots\beta_{i_nk_n}T_{k_1k_2...k_n} \tag{A.1}$$

Example of tensor quantities are stress, strain and moment of inertia.

Notation

Indicial and tensor notation provide an economic manner to write complicated and long mathematical expressions. Three coordinates of a point, denoted by x, y, z or x_1, x_2, x_3, can be compactly expressed as:

$$x_i, i = 1, 2, 3 \tag{A.2}$$

In the case of a second order notation,

$$x_{ij}, i, j = 1, 2, 3 \tag{A.3}$$

represents,

$$
\begin{aligned}
i &= 1, j = 1, 2, 3 \\
i &= 2, j = 1, 2, 3 \quad \Rightarrow \\
i &= 3, j = 1, 2, 3
\end{aligned}
\quad
\begin{pmatrix}
x_{11} & x_{12} & x_{13} \\
x_{21} & x_{22} & x_{23} \\
x_{31} & x_{32} & x_{33}
\end{pmatrix}
\tag{A.4}
$$

and, in general, the number of terms N in an indicial notation of nth order can be expressed as: $N = 3^n$.

$$\tag{A.5}$$

The 'summation convention' is defined as follows: the symbol $\displaystyle\sum_i$ may be omitted (i.e., it is implied) if the summation (dummy) index (say i) appears exactly twice in each term of sum. Example:

$$
a_i b_i = a_1 b_1 + a_2 b_2 + a_3 b_3. \tag{A.6}
$$

If a subscript occurs precisely once in one term of an expression it is called a 'free index'; if a subscript occurs precisely twice in one term of an expression it is called a 'dummy index'; it is a mistake if the subscript occurs more than twice.

The Kronecker delta is defined as,

$$
\delta_{ij} = \begin{cases} 1 & \text{if } i = j \\ 0 & \text{if } i \neq j \end{cases} = \delta_{ji} \tag{A.7}
$$

A comma is used to indicate differentiation; thus for example, the partial derivative form of $\partial u_i / \partial x_i$ can be simplified to the form $u_{i,i}$. The first subscript refers to the component of **u**, and the comma indicates partial derivative with respect to the second subscript correspondent to the relevant coordinate axis.

Details on this subject are available in Desai and Siriwardane (1984), Lubliner (1990), and Chen and Saleeb (1982).

Appendix B

Dyntool program code

```
C.....INCREMENTAL ANALYSIS VERSION 1.0 FOR VAX 3100 with iteration
C.....and with constant time step (Bathe algorithm)
      PROGRAM FEP2
C.....FEM SOFTWARE FOR MACHINE-SOIL SYSTEM
C.....VERSION 1.0
C.....WRITTEN BY JIE  SHEN.
C.....DEC.19, 1993
C.....FORTRAN COLUMN MAJOR
      IMPLICIT REAL*8 (A-H,O-Z)
      LOGICAL EXFIL
      REAL T0,DT,SECNDS
      CHARACTER*9 FI,FO
      CHARACTER NAMINP(9),NAMOUT(9),HEAD*50,HEAD1*50
      COMMON/HEAD/HEAD1
      EQUIVALENCE (FI,NAMINP(1)),(FO,NAMOUT(1))
      DATA FI,FO/'    .DAT','    .OUT'/
      DATA HEAD/' FEM SOFTWARE FOR MACHINE-SOIL SYSTEM 1.0  '/
      HEAD1=HEAD
      WRITE(*,1000)
      WRITE(*,*) ' INPUT FILE NAME (5 LETTERS ONLY) :'
      READ (*,'(5A1)') (NAMINP(I),I=1,5)
      DO I=1,5
        NAMOUT(I)=NAMINP(I)
      END DO
      INQUIRE(FILE=FO,EXIST=EXFIL)
      IF(EXFIL)THEN
        OPEN(6,FILE=FO,STATUS='OLD')
      ELSE
        OPEN(6,FILE=FO,STATUS='NEW')
      END IF
      OPEN(5,FILE=FI,STATUS='OLD')
C*****************************
      inquire(file='output.fil',exist=exfil)
      if(exfil) then
            open(7,file='output.fil',status='old')
            close(7,status='delete')
      endif
      open(7,file='output.fil',status='new')
C.........................
      inquire(file='disp.fil',exist=exfil)
      if(exfil) then
```

```fortran
            open(81,file='disp.fil',status='old')
            close(81,status='delete')
      endif
      open(81,file='disp.fil',status='new')
C.........................
      inquire(file='VELO.fil',exist=exfil)
      if(exfil) then
            open(84,file='VELO.fil',status='old')
            close(84,status='delete')
      endif
      open(84,file='VELO.fil',status='new')
C.........................
      inquire(file='ACCE.fil',exist=exfil)
      if(exfil) then
            open(85,file='ACCE.fil',status='old')
            close(85,status='delete')
      endif
      open(85,file='ACCE.fil',status='new')
C.........................
      inquire(file='fail.fil',exist=exfil)
      if(exfil) then
            open(82,file='fail.fil',status='old')
            close(82,status='delete')
      endif
      open(82,file='fail.fil',status='new')
C.........................
      inquire(file='gaus.fil',exist=exfil)
      if(exfil) then
            open(83,file='gaus.fil',status='old')
            close(83,status='delete')
      endif
      open(83,file='gaus.fil',status='new')
C.........................
      inquire(file='PLOTDISP.fil',exist=exfil)
      if(exfil) then
            open(86,file='PLOTDISP.fil',status='old')
            close(86,status='delete')
      endif
      open(86,file='PLOTDISP.fil',status='new')

C.........................
      inquire(file='LREAC.FIL',exist=exfil)
      if(exfil) then
            open(89,file='LREAC.FIL',status='old')
            close(89,status='delete')
```

```
      endif
      open(89,file='LREAC.FIL',status='new')

      WRITE(89,*) 'LREAC.FIL - NDF, TOOL LOCAL REAC: X,Y,Z'

C.........................
c     MAXM=30000 ------> 33000
c     MAXR=50000 ------> 85000
c     MAXA=500000 ------> 910000
      WRITE(6,1000)HEAD
      T0=SECNDS(0.0)
      CALL PCONTR(FO)
      DT=SECNDS(T0)
      WRITE(*,600)DT
600   FORMAT(' ',' Lapsed time = ',F10.1,' sec.')
1000  FORMAT(/A50/)
      END


C.....Modified  Uriel A. Rosa   feb 08/96
C..............................................................
      SUBROUTINE ADDSTF(LD,JP,S,NST)
      IMPLICIT REAL*8 (A-H,O-Z)
C.....STIFFNESS MATRIX ASSEMBLAGE
      PARAMETER (MAXA=910000)
      CHARACTER Y
      COMMON/PRINT/Y
      COMMON/A/A(MAXA)
      COMMON/CDATA/NDF,NDM,NEN,NEJ,NE,NEQ
      COMMON/ELDATA/LM,N,MA,MCT,IEL,NEL
      DIMENSION LD(*),JP(*),S(NST,NST)
      IF(Y.EQ.'Y'.OR.Y.EQ.'y') WRITE(*,2000) N,S
2000  FORMAT(' ELEMENT NUMBER ',I4,' ELEMENT STIFFNESS'/(6E12.5))
      DO 200 J=1,NST
      K=LD(J)
      IF(K.LE.0) GO TO 200
      L=JP(K)-K
      DO 100 I=1,NST
      M=LD(I)
      IF(M.GT.K.OR.M.LE.0) GO TO 100
         M=L+M
         A(M)=A(M)+S(J,I)
100   CONTINUE
200   CONTINUE
      RETURN
      END
```

242

```fortran
C.............................................
      SUBROUTINE BASBLY(B,P,LD,NS)
      IMPLICIT REAL*8 (A-H,O-Z)
      DIMENSION B(*),P(*),LD(*)
C.....ASSEMBLE THE LOAD VECTOR
      DO 100 I=1,NS
      II=LD(I)
      IF(II.GT.0) B(II)=B(II)+P(I)
100   CONTINUE
      RETURN
      END


C.............................................
      SUBROUTINE BOUN(ID)
      IMPLICIT REAL*8 (A-H,O-Z)
      COMMON /CDATA/NDF,NDM,NEN,NJ,NE,NEQ
      COMMON /FLAG_BLO/ GE_FLAG,DY_FLAG,DB_FLAG,MA_FLAG,UL_FLAG,
     * ST_FLAG,SC_FLAG
      LOGICAL GE_FLAG,DY_FLAG,DB_FLAG,MA_FLAG,UL_FLAG,
     * ST_FLAG,SC_FLAG
      DIMENSION ID(NDF,*),IDL(6)
      CHARACTER*6 BC
      DATA BC/' B.C. '/
C.....RESTRAINT CONDITIONS INPUT
4     IF(DB_FLAG) WRITE(6,2000) (I,BC,I=1,NDF)
      IF(SC_FLAG) WRITE(*,2000) (I,BC,I=1,NDF)
      DO 10 I=1,NJ
      DO 10 J=1,NDF
10    ID(J,I)=0
      N=0
      NG=0
402   L=N
      LG=NG
      READ(5,*) N,NG,(IDL(I),I=1,NDF)
50    IF(N.LE.0 .OR. N.GT.NJ) GO TO 60
      DO 51 I=1,NDF
      ID(I,N) =IDL(I)
51    IF(L.NE.0 .AND. IDL(I).EQ.0 .AND. ID(I,L).LT.0) ID(I,N)=-1
      LG=ISIGN(LG,N-L)
52    L=L+LG
      IF((N-L)*LG .LE.0) GO TO 402
      DO 53 I=1,NDF
      LMLG = L-LG
53    IF(ID(I,LMLG).LT.0) ID(I,L) =-1
```

243

```fortran
      GO TO 52
60    DO 58 N=1,NJ
      DO 56 I=1,NDF
      IF(ID(I,N).NE.0) GO TO 57
56    CONTINUE
      GO TO 58
57    IF(DB_FLAG) WRITE(6,2005) N,(ID(I,N),I=1,NDF)
      IF(SC_FLAG) WRITE(*,2005) N,(ID(I,N),I=1,NDF)
58    CONTINUE
      RETURN
C.....FORMATS
2000  FORMAT(/5X,'NODAL BOUNDARY CONDITIONS'//2X,'NODE',7(I4,A6)/1x)
2005  FORMAT(I6,7(I7,3X))
      END


C..........................................................
C.....UPDATE ALL NODE COORDINATE AFTER EACH LOAD INCREMENTAL
STEP
      SUBROUTINE CUPDATE(X,UR,ID,F,IX,NEN1)
      IMPLICIT REAL*8 (A-H,O-Z)
      LOGICAL IT_FLAG
      COMMON/CDATA/NDF,NDM,NEN,NJ,NE,NEQ
      COMMON/ITFACE/NINT,THITA,H
      COMMON/PROCESS/NPROP,NITEM,IT_FLAG
      DIMENSION X(NDM,*),UR(*),ID(NDF,*),F(NDF,*),IX(NEN1,*)
      DO 110 N=1,NJ
      DO 110 I=1,NDM
      K=ID(I,N)
      IF(K.LT.0) X(I,N)=X(I,N)+F(I,N)
      IF(K.GT.0) X(I,N)=X(I,N)+UR(K)
110   CONTINUE
c     CS=COS(THITA)
c     SN=SIN(THITA)
c     DO 120 N=1,NE
c     MA=IX(NEN1,N)
c     IF(MA.EQ.NINT) THEN
c       I1=IX(1,N)
c       I2=IX(2,N)
c       X(1,I2)=X(1,I1)-H*CS
c       X(2,I2)=X(2,I1)-H*SN
c     ENDIF
c120   CONTINUE
      RETURN
      END
```

```fortran
* DEFINITI.FI                                                    i
      LOGICAL TRUE,FALSE
      INTEGER OK,EOF
      PARAMETER (TRUE=.TRUE.,FALSE=.FALSE.,OK=0,EOF=-1)

C..............................................................
      SUBROUTINE ELDAT(IX,NEN1)
      IMPLICIT REAL*8 (A-H,O-Z)
      COMMON /CDATA/NDF,NDM,NEN,NJ,NE,NEQ
      COMMON /FLAG_BLO/ GE_FLAG,DY_FLAG,DB_FLAG,MA_FLAG,UL_FLAG,
     * ST_FLAG,SC_FLAG
      DIMENSION IX(NEN1,*),IDL(9)
      LOGICAL ERR,GE_FLAG,DY_FLAG,DB_FLAG,MA_FLAG,UL_FLAG,
     * ST_FLAG,SC_FLAG
C.....ELEMENT DATA INPUT
2     L=0
      L1=1
      I=1
      DO 206 I=1,NE,50
      IF(DB_FLAG) WRITE(6,2001) (K,K=1,NEN)
      IF(SC_FLAG) WRITE(*,2001) (K,K=1,NEN)
      J=MIN0(NE,I+49)
      DO 206 N=I,J
      IF(L-N) 200,202,203
200   READ (5,*,ERR=15) L,LX,LK,(IDL(K),K=1,NEN)
      IF(L.EQ.0 .AND. L1.EQ.0) GO TO 15
      L1=LX
      IF(L.LT.0) GO TO 15
      IF(L.EQ. 0) L= NE+1
      IF(LX.EQ.0) LX=1
      IF(L-N) 201,202,203
201   IF(DB_FLAG) WRITE(6,3001) L,N
      IF(SC_FLAG) WRITE(*,3001) L,N
      ERR = .TRUE.
      GO TO 206
202   NX=LX
      DO 207 K=1,NEN
      IF(IDL(K).GT.NJ.OR.IDL(K).LT.0) GO TO 208
207   IX(K,L) =IDL(K)
      IX(NEN1,L) =LK
      GO TO 205
203   CONTINUE
      IX(NEN1,N) = IX(NEN1,N-1)
      DO 204 K=1,NEN
      IX(K,N) = IX(K,N-1) +NX
```

```
      IF(IX(K,N-1).EQ.0) IX(K,N)=0
      IF(IX(K,N).GT.NJ .OR. IX(K,N).LT.0) G O TO 208
204   CONTINUE
205   IF(DB_FLAG) WRITE(6,2002) N,IX(NEN1,N),(IX(K,N),K=1,NEN)
      IF(SC_FLAG) WRITE(*,2002) N,IX(NEN1,N),(IX(K,N),K=1,NEN)
      GO TO 206
208   IF(DB_FLAG) WRITE(6,3002) N
      IF(SC_FLAG) WRITE(*,3002) N
      ERR=.TRUE.
206   CONTINUE
2001  FORMAT(//5X,'ELEMENTS CONNECTION'//1X,'ELEM MATE',
     1    10(I2,' NODE')/(10X,10(I2,' NODE')))
2002  FORMAT(2I5,10I7/(10X,10I7))
3001  FORMAT(5X,'**FATAL ERROR** ELEMENT',I5,' APPEARS AFTER
ELEMENT'
     1 ,I5)
3002  FORMAT(5X,'**FATAL ERROR** ELEMENT',I5,' HAS ILLEGAL NODES')
15    RETURN
      END


C....................................................
      SUBROUTINE ELEMLIB(D,UL,URL,X,XLO,IX,S,P,VL,I,J,K,ISW)
      IMPLICIT REAL*8 (A-H,O-Z)
C.....ELEMENT LIBRARY
      REAL*8 P(K),S(K,K),UL(1),URL(1)
      DIMENSION IX(1),D(1),X(1),XLO(1),VL(ndf,*)
      COMMON/CDATA/NDF,NDM,NEN,NJ,NE,NEQ
      COMMON /ELDATA/ LM,N,MA,MCT,IEL,NEL
      IF(IEL.LE.0.OR.IEL.GT.30) GO TO 400
c     IF(IEL.EQ.11) GO TO 11
c     IF(IEL.EQ.16) GO TO 16
c     IF(IEL.EQ.17) GO TO 17
c     IF(IEL.EQ.18) GO TO 18
      IF(IEL.EQ.26) GO TO 26
c     IF(IEL.EQ.27) GO TO 27
c     IF(IEL.EQ.28) GO TO 28
C     IF(IEL.EQ.29) GO TO 29
C     IF(IEL.EQ.30) GO TO 30
C     IF(IEL.EQ.31) GO TO 31
C     IF(IEL.EQ.32) GO TO 32
c11   CALL ELMT11(D,U,X,IX,S,P,I,J,K,ISW)
c     GO TO 100
c16   CALL ELMT16(D,UL,URL,X,XLO,IX,S,P,VL,I,J,K,ISW)
c     GO TO 100
c17   CALL ELMT17(D,U,X,IX,S,P,VL,I,J,K,ISW)
```

```
c    GO TO 100
c18   CALL ELMT18(D,U,X,IX,S,P,VL,I,J,K,ISW)
c    GO TO 100
c21   CALL ELMT21(D,U,X,IX,S,P,VL,I,J,K,ISW)
c    GO TO 100
26   CALL ELMT26(D,UL,URL,X,XLO,IX,S,P,VL,I,J,K,ISW)
     GO TO 100
c27   CALL ELMT27(D,U,X,IX,S,P,VL,I,J,K,ISW)
c    GO TO 100
c28   CALL ELMT28(D,U,X,IX,S,P,VL,I,J,K,ISW)
c    GO TO 100
C29   CALL ELMT29(D,U,X,IX,S,P,VL,I,J,K,ISW)
C    GO TO 100
C30   CALL ELMT30(D,U,X,IX,S,P,VL,I,J,K,ISW)
C    GO TO 100
C31   CALL ELMT31(D,U,X,IX,S,P,VL,I,J,K,ISW)
C    GO TO 100
C32   CALL ELMT32(D,U,X,IX,S,P,VL,I,J,K,ISW)
C    GO TO 100
100  RETURN
400  WRITE(*,4000) IEL
     STOP
4000 FORMAT(5X,' **FATAL ERROR**  ELEMENT CLASS NUMBER',I5,'
INPUT')
     END


c.....Uriel A.Rosa .... June 4,96
c.....Uriel A.Rosa .... June 2,96
c.....Modified   Uriel A. Rosa   Feb 10/96 ; May-18-96 (Poisson) UAR
c
     SUBROUTINE ELMT26(D,UL,URL,XL,XLO,IX,S,P,VL,NDF,NDM,NST,ISW)
     IMPLICIT REAL*8 (A-H,O-Z)
     CHARACTER  HEAD*50,WD*11,WDD*10,FILENAME(12),fi*12
C.....THREE-DIMENSIONAL, ISOTROPIC, NON-LINEAR, STRAIN RATE-
DEPENDENT
C.....ELASTICITY ELEMENT WITH 8 NODES. THE TANGENT MODULUS Es IS
EXPRESSED
C.....ON THE BASIS OF DUNCAN-CHANG MODEL (1970).
C.....DESIGNED BY JIE SHEN
C.....NOV. 14, 1993
     REAL*8 D(*),XL(NDM,*),XLO(NDM,*)
     COMMON /ELDATA/ LM,N,MA,MCT,IEL,NEL
     COMMON /HEAD/HEAD
     COMMON /CDATA/ N1,N2,NEN,NJ,NE,NEQ
     COMMON /DYNAMICS/ SPEED,DT,THITA,BATA,GAMA
```

```
      COMMON /FLAG_BLO/
GE_FLAG,DY_FLAG,DB_FLAG,MA_FLAG,UL_FLAG,
   *  ST_FLAG,SC_FLAG
      DIMENSION UL(NDF,*),URL(NDF,*),IX(*),S(NST,NST),P(NST),
   * VL(NDF,*),SHP(4,8),SHPO(4,8),XG(8),YG(8),ZG(8),WG(8),SIG(9)
   * ,EPS(6)
C    Grefe(I4) UAR
      DIMENSION GREFE(3)

      DIMENSION DEPS(6),DEPSR(3),DSIG(6),WDD(2),V(20),G(4),GG(3)
   * ,SIGN(3)
      LOGICAL
FLAG,GE_FLAG,DY_FLAG,DB_FLAG,MA_FLAG,UL_FLAG,ST_FLAG,
   * SC_FLAG
      EQUIVALENCE (FI,FILENAME(1))
      DATA WD/'3-D PROBLEM'/
      DATA WDD/'SHEAR FAILURE','TENSILE FAILURE'/
      data fi /'middata .fil'/
C
C.... GO TO CORRECT ARRAY PROCESSOR
      GO TO(1,2,3,4,5,4,4), ISW
C.... INPUT MATERIAL PROPERTIES
1     NMA=ma+48
      filename(8)=char(NMA)
      INQUIRE(FILE=fi,EXIST=FLAG)
      IF(FLAG) THEN
          OPEN(NMA,FILE=fi,status='old')
          CLOSE(NMA,STATUS='DELETE')
      END IF
      OPEN(NMA,FILE=fi,ACCESS='DIRECT',status='new',RECL=160,
   * FORM='UNFORMATTED')
c.....D(1)=Ks(-);D(2)=ns(-);D(3)=Xun(-);D(4)=Rho(kN/m^3);D(5)=L(-)
c.....D(6)=K(-);D(7)=Cohn(kPa);D(8)=Fai(Degree);D(9)=Rsf(-);D(10)=Bs(-)
c.....D(11)=dEpsn(0)(1/s);D(12)=St(-);D(13)=Sc(-);D(14)=Ms(-)
      READ(5,*) D(1),D(2),D(3),D(4),D(5),D(6),D(7),D(8),D(9),D(10)
   * ,D(11),D(12),D(13),D(14)
      Es=D(1)*100.
      XUN=D(3)
      L=int(D(5))
      K=int(D(6))
      IF(L.EQ.0) L=2
      IF(K.EQ.0) K=1
      L = MIN0(4,L)
      D(5) = L
      K = MIN0(4,MAX0(1,K))
```

```fortran
      D(6) = K
      G(1)=Es*(1.-XUN)/(1.+XUN)/(1.-2.*XUN)
      G(2)=XUN*G(1)/(1.0E0-XUN)
      G(3)=Es/2.0E0/(1.0E0+XUN)
C.....SET INITIAL STRESSES AND STRAINS TO ZERO AND ELASTIC MATRIC G
      DO 12 I1=1,20
12    V(I1)=0.0
      DO 14 I=1,3
      NN1=15+I
      V(NN1)=G(I)
14    CONTINUE
      MMM=NE*8
      DO 16 I2=1,MMM
16    WRITE (NMA,REC=I2) (V(I),I=1,20)
      LINT=0
      WRITE(*,2000) D(1),D(2),D(3),D(4),L,K,D(7),D(8),D(9),D(10)
     *  ,D(11),D(12),D(13),D(14)
      WRITE(6,2000) D(1),D(2),D(3),D(4),L,K,D(7),D(8),D(9),D(10)
     *  ,D(11),D(12),D(13),D(14)
      WRITE(7,2000) D(1),D(2),D(3),D(4),L,K,D(7),D(8),D(9),D(10)
     *  ,D(11),D(12),D(13),D(14)
      WRITE(*,2050) (G(I),I=1,3)
      WRITE(6,2050) (G(I),I=1,3)
      WRITE(7,2050) (G(I),I=1,3)
      WRITE(6,2001) HEAD
         RETURN
C..... WTITE INFORMATION ON SCREEN
2     RETURN
c.........................................................
3     NMA=MA+48
      L = int(D(5))
      L=2
C    IF(L*L*L.NE.LINT) CALL PGAUSS3(L,LINT,XG,YG,ZG,WG)
      CALL PGAUSS3(L,LINT,XG,YG,ZG,WG)
      DO 36 L9 = 1,LINT
      NNN=(N-1)*8+L9
      READ(NMA,REC=NNN) (V(I),I=1,20)
      DO 32 I=1,3
32    G(I)=V(I+15)
      CALL SHP3 (XG(L9),YG(L9),ZG(L9),XL,SHP,XSJ,NDM,NEL,IX,.FALSE.)
C..........................................................
      XXSJ = XSJ*WG(L9)
C..........................................................
C.....CALCULATE THE ELEMENT STIFFNESS MAREIX S
      GG(1)=G(1)*XXSJ
```

```
      GG(2)=G(2)*XXSJ
      GG(3)=G(3)*XXSJ
      NSL=NEL*NDF
      DO 34 J=1,NEL
      J1=(J-1)*NDF
      DO 34 K=J,NEL
      K1=(K-1)*NDF
      S(J1+1,K1+1)=S(J1+1,K1+1)+SHP(1,J)*SHP(1,K)*GG(1)+SHP(2,J)*
     1 SHP(2,K)*GG(3)+SHP(3,J)*SHP(3,K)*GG(3)
      S(J1+1,K1+2)=S(J1+1,K1+2)+SHP(1,J)*SHP(2,K)*GG(2)+SHP(2,J)*
     1 SHP(1,K)*GG(3)
      S(J1+1,K1+3)=S(J1+1,K1+3)+SHP(1,J)*SHP(3,K)*GG(2)+SHP(3,J)*
     1 SHP(1,K)*GG(3)
      S(J1+2,K1+1)=S(J1+2,K1+1)+SHP(2,J)*SHP(1,K)*GG(2)+SHP(1,J)*
     1 SHP(2,K)*GG(3)
      S(J1+2,K1+2)=S(J1+2,K1+2)+SHP(2,J)*SHP(2,K)*GG(1)+SHP(1,J)*
     1 SHP(1,K)*GG(3)+SHP(3,J)*SHP(3,K)*GG(3)
      S(J1+2,K1+3)=S(J1+2,K1+3)+SHP(2,J)*SHP(3,K)*GG(2)+SHP(3,J)*
     1 SHP(2,K)*GG(3)
      S(J1+3,K1+1)=S(J1+3,K1+1)+SHP(3,J)*SHP(1,K)*GG(2)+SHP(1,J)*
     1 SHP(3,K)*GG(3)
      S(J1+3,K1+2)=S(J1+3,K1+2)+SHP(3,J)*SHP(2,K)*GG(2)+SHP(2,J)*
     1 SHP(3,K)*GG(3)
      S(J1+3,K1+3)=S(J1+3,K1+3)+SHP(3,J)*SHP(3,K)*GG(1)+SHP(2,J)*
     1 SHP(2,K)*GG(3)+SHP(1,J)*SHP(1,K)*GG(3)
C....FORM LOWER PART BY SYMMETRY
      S(K1+1,J1+1)=S(J1+1,K1+1)
      S(K1+2,J1+1)=S(J1+1,K1+2)
      S(K1+3,J1+1)=S(J1+1,K1+3)
      S(K1+1,J1+2)=S(J1+2,K1+1)
      S(K1+2,J1+2)=S(J1+2,K1+2)
      S(K1+3,J1+2)=S(J1+2,K1+3)
      S(K1+1,J1+3)=S(J1+3,K1+1)
      S(K1+2,J1+3)=S(J1+3,K1+2)
      S(K1+3,J1+3)=S(J1+3,K1+3)
34    CONTINUE
36    CONTINUE
      RETURN
C..................................................................
C.....MODIFY TANGENT MODULUS,OUTPUT RESULTS AND CALCULATE
FORCE RESIDUE
C... SET STRESS HISTORY
4     NMA=MA+48
      L=int(D(5))
      Ess=D(1)*100.
```

```
      XUN=D(3)
      FAI=D(8)*3.1415926/180.0
      Rsf=D(9)
      C=D(7)
C     IF(L*L*L.NE.LINT) CALL PGAUSS3(L,LINT,XG,YG,ZG,WG)
      L=2
      CALL PGAUSS3(L,LINT,XG,YG,ZG,WG)
      DO 430 L9 = 1,LINT
      NNN=(N-1)*8+L9
      READ(NMA,REC=NNN) (V(I),I=1,20)
      do 402 I=1,3
402   G(I)=V(I+15)
      DO 404 I=1,6
404   EPS(I)=V(I)
      DO 406 I=1,9
      SIG(I)=V(I+6)
406   CONTINUE
C.... COMPUTE ELEMENT STRESSES, STRAINS, AND FORCES
C.....COMPUTE ELEMENT SHAPE FUNCTIONS
      CALL SHP3 (XG(L9),YG(L9),ZG(L9),XL,SHP,XSJ,NDM,NEL,IX,.FALSE.)
C.................................................
C.... COMPUTE STRAINS AND COORDINATES
      DO 408 I = 1,6
408   DEPS(I) = 0.0
      XX = 0.0
      YY = 0.0
      ZZ = 0.0
      VX = 0.0
      VY = 0.0
      VZ = 0.0
      DO 410 JK = 1,NEL
      XX = XX + SHP(4,JK)*XL(1,JK)
      YY = YY + SHP(4,JK)*XL(2,JK)
      ZZ= ZZ + SHP(4,JK)*XL(3,JK)
      VX = VX + SHP(4,JK)*VL(1,JK)
      VY = VY + SHP(4,JK)*VL(2,JK)
      VZ = VZ + SHP(4,JK)*VL(3,JK)
C.....COMPUTE INCREMENTAL STRAINS
      DEPS(1) = DEPS(1) + SHP(1,JK)*URL(1,JK)
      DEPS(2)=DEPS(2)+SHP(2,JK)*URL(2,JK)
      DEPS(3) = DEPS(3) + SHP(3,JK)*URL(3,JK)
      DEPS(4)=DEPS(4)+SHP(2,JK)*URL(1,JK)+SHP(1,JK)*URL(2,JK)
      DEPS(5)=DEPS(5)+SHP(3,JK)*URL(2,JK)+SHP(2,JK)*URL(3,JK)
410   DEPS(6)=DEPS(6)+SHP(3,JK)*URL(1,JK)+SHP(1,JK)*URL(3,JK)
      DO 411 I=1,3
```

```fortran
411   DEPSR(I)=DEPS(I)/DT
      SRXYZ=SQRT(DEPSR(1)**2.+DEPSR(2)**2.+DEPSR(3)**2.)
      VXYZ=SQRT(VX*VX+VY*VY+VZ*VZ)
C.... COMPUTE STRESS
      DSIG(1) =G(1)*DEPS(1)+G(2)*DEPS(2)+G(2)*DEPS(3)
      DSIG(2) =G(2)*DEPS(1)+G(1)*DEPS(2)+G(2)*DEPS(3)
      DSIG(3) =G(2)*DEPS(1)+G(2)*DEPS(2)+G(1)*DEPS(3)
      DSIG(4)=G(3)*DEPS(4)
      DSIG(5)=G(3)*DEPS(5)
      DSIG(6)=G(3)*DEPS(6)
C.....COMPUTE TOTAL STRESSES AND STRAINS
      DO 412 II=1,6
412   SIG(II)=SIG(II)+DSIG(II)
      DO 413 I=1,6
413   EPS(I)=EPS(I)+DEPS(I)
      IF(ISW.EQ.6.OR.ISW.EQ.7) GO TO 426
      CALL PSTRES3(SIG,SIG(7),SIG(8),SIG(9))
C.......................................................
C.....SAVE PRESENT STRESS DATA
      DO 414 I=1,6
      V(I)=EPS(I)
414   CONTINUE
      DO 416 I=1,9
416   V(I+6)=SIG(I)

c        WRITE(6,2060) L9,N
c         WRITE(6,*) 'SIGMA7=',SIG(7),'SIGMA8',SIG(8),'SIGMA9',SIG(9)
c         WRITE(89,3333) 'SIGMA7,8,9=',SIG(7),SIG(8),SIG(9)


C...........................................................
C.....CHECK THE STATE OF  STRESS OF EACH UNIT
c*****************************************
C....ISIG(7)I<ISIG(9)I WHEN BOTH SIG(7) AND SIG(9) ARE LE 0.
C....THEREFORE, SIGMA 3 SHOULD BE -SIG(7)
C
C....INITIALIZATION

C......tt --> strain rate difference
      TT=SRXYZ-D(11)
c    IF(D(14).GT.0.001) THEN
c        IF(TT.GT.1.0.AND.DY_FLAG) Ess=Ess*TT**D(14)
c    END IF
      IF(D(2).LT.1E-6.OR.SIG(7).GT.0.0) THEN
          XX=1.0
      ELSE
```

```
      IF(D(2).GT.0.001) THEN
          XX=(-SIG(7)/100.)**D(2)
        ELSE
         XX=1.0
        END IF
      END IF
C     IF(DB_FLAG) WRITE(6,*) 'TT=',TT**D(16),'XX=',XX
C.....TREATMENT OF FAILED ELEMENTS
      IF(V(19).GE.0.5.OR.V(20).GE.0.5) THEN


c -------------------------------------------------------------------
c     May 18/96 UAR  If tension or shear failure -> then Poisson ratio is
c       set to xun=0.49 or 0.499 according to Duncan&Chang (1976-thesis)
c       for a occurance of no volume change at failure; (Jose H.F.Pereira).
c -------------------------------------------------------------------
      Xun=0.499
      Es=Ess*XX/D(12)

C     UAR
c     WRITE(*,*) "L9 N",L9,N
c     WRITE(*,*) "Es",Es
C     UAR

          GO TO 420
      END IF
C.....TENSILE FAILURE CRITERION ( WHEN SIG(7)>0 )
      IF(SIG(7).GT.0.) THEN
          TC=C*D(13)
          IF(SIG(7).GE.TC) THEN
           IF(ST_FLAG) THEN
            Es=Ess/D(12)
            V(20)=1.0
           ELSE
            Es=Ess
           END IF
            GO TO 420
           ELSE
            SIGMAF=2.0*C*COS(FAI)/(1.0-SIN(FAI))
            GO TO 419
           END IF
      END IF
C.....SHEAR FAILURE CRITERION ( WHEN SIG(7)<0 )
      SIGMAF=(2.0*C*COS(FAI)-2.0*SIG(7)*SIN(FAI))/
     * (1.0-SIN(FAI))
      IF(DB_FLAG) WRITE(6,*) ' OLD SIGMAF=',SIGMAF
```

```
c.....criteria tt>0 ---> incorporate strain rate effects in sigmaf
418  IF(TT.GT.0.0.AND.DY_FLAG) SIGMAF=SIGMAF+d(10)*TT
     IF(DB_FLAG) WRITE(6,*) ' NEW SIGMAF=',SIGMAF
C
C.....SHEAR FAILURE (sigma1-sigma3)>sigmaf
419  QQ13=(SIG(7)-SIG(9))-SIGMAF
     IF(QQ13.GT.1.0E-6) THEN
c     WRITE(6,2010) N,WDD(1)
C     WRITE(*,2010) N,WDD(1)
        Es=Ess*XX/D(12)
        V(19)=1.0
        GOTO 420
     END IF
C.....NO SHEAR FAILURE
     DNG=D(9)*(SIG(7)-SIG(9))/SIGMAF
     IF (DNG.GE.0.99) DNG=0.99
     Es=Ess*XX*(1.-DNG)*(1.-DNG)


c......UAR
c......Chi's triaxial parameters to correct Poisson's ratio
c......for UAR triaxial test soil DH00-90.
     CHIA=0.4287
     CHIB=0.0658


     RSP=(SIG(7)-SIG(9))/SIGMAF
c......RSP (Poisson's strength ratio) <=1.0 => Poisson=CHIA+CHIB*RSP
c.................................... > 1.0 => Poisson=0.499
     XUN=CHIA+CHIB*RSP


     IF (RSP.GT.1.0) THEN
      WRITE(*,*) 'RSP>1.0'
      XUN=0.499
     END IF


c     WRITE(*,*) 'Poisson=',XUN
c......UAR


C.....FORM ELASTIC MATRIC DD
420  G(1)=Es*(1.-XUN)/(1.+XUN)/(1.-2.*XUN)
     G(2)=XUN*Es/(1.+XUN)/(1.-2.*XUN)
     G(3)=Es/(2.0*(1.0+XUN))


c     WRITE(89,*) 'Es',Es
```

```fortran
c.....................    IF(DB_FLAG) THEN
C..........Failured elements...............
C       WRITE(6,*) 'G(1)=',G(1),'G(2)=',G(2),'G(3)=',G(3)
C       IF(V(19).GT.0.5) WRITE(7,*) L9,' OF ',N,' IS SHEAR FAILED'
c       IF(V(19).GT.0.5) WRITE(*,*) L9,' OF ',N,' IS SHEAR FAILED'

C       IF(V(20).GT.0.5) WRITE(7,*) L9,' OF ',N,' IS TENSILE FAILED'
c       IF(V(20).GT.0.5) WRITE(*,*) L9,' OF ',N,' IS TENSILE FAILED'
c.....................    ENDIF


    IF(MA_FLAG) THEN
      DO 422 I4=1,3
422    V(I4+15)=G(I4)
    END IF
C.....................................................
    WRITE(NMA,REC=NNN) (V(I),I=1,20)
C.............................................................
C.... OUTPUT STRESSES AND STRAINS
    IF(MCT.GT.0) GO TO 424
c    WRITE(6,2001) HEAD
    MCT = 50
424  MCT=MCT-2
C.....ONLY OUTPUT INFORMATION AT GAUSSAN POINT 1
c    IF(L9.EQ.1) THEN
c    WRITE(6,2002) L9,N,MA,(SIG(II),II=1,5),XX,YY,EPS,SIG(6)
c    ENDIF
    GOTO 430
C.............................................................
426  XXSJ = XSJ*WG(L9)
    J1 = 1
    DO 428 J9 = 1,NEL
    IF(ISW.EQ.7.OR.ISW.EQ.6) THEN
      P(J1)=P(J1)-(SHP(1,J9)*DSIG(1)+SHP(2,J9)*DSIG(4)+
   *  SHP(3,J9)*DSIG(6))*XXSJ
      P(J1+1)=P(J1+1)-(SHP(2,J9)*DSIG(2)+SHP(1,J9)*DSIG(4)+
   *  SHP(3,J9)*DSIG(5))*XXSJ
      P(J1+2)=P(J1+2)-(SHP(3,J9)*DSIG(3)+SHP(2,J9)*DSIG(5)+
   *  SHP(1,J9)*DSIG(6))*XXSJ
        GOTO 428
    END IF
      P(J1)=P(J1)-(SHP(1,J9)*SIG(1)+SHP(2,J9)*SIG(4)+
   *  SHP(3,J9)*SIG(6))*XXSJ
      P(J1+1)=P(J1+1)-(SHP(2,J9)*SIG(2)+SHP(1,J9)*SIG(4)+
   *  SHP(3,J9)*SIG(5))*XXSJ
```

```fortran
      P(J1+2)=P(J1+2)-(SHP(3,J9)*SIG(3)+SHP(2,J9)*SIG(5)+
     *  SHP(1,J9)*SIG(6))*XXSJ
428   J1 = J1 + NDF
430   CONTINUE
C.....AVERAGE TANGENTIAL MODULUS IN EACH ELEMENT
      IF(ISW.EQ.4.AND.MA_FLAG) THEN
          DO 432 I=1,3
      SIGN(I)=0.0
432     G(I)=0.0
      DO 436 L9 = 1,LINT
      NNN=(N-1)*8+L9
      READ(NMA,REC=NNN) (V(I),I=1,20)
          DO 434 I=1,3
          IF(V(19).GT.0.5.OR.V(20).GT.0.5) SIGN(I)=1.0
434     G(I)=G(I)+V(I+15)/8.0
436     CONTINUE
          DO 440 L9=1,LINT
      NNN=(N-1)*8+L9
          READ(NMA,REC=NNN) (V(I),I=1,20)

c     UAR
c     minimum value for residual elastic modulus=0.50 kPa
      GREFE(16)=1.0*(1.-XUN)/(1.+XUN)/(1.-2.*XUN)
      GREFE(17)=1.0*XUN/(1.+XUN)/(1.-2.*XUN)
      GREFE(18)=1.0/(2.0*(1.0+XUN))
c     UAR
c     gdivi = value to divide Et after failure
      GDIVI=1000.0
c     UAR

          DO 438 I4=1,3
          IF(SIGN(I4).GE.0.5) THEN
c         V(I4+15)=1.E-6
c     UAR  G()/1000 means "Es"/1000
      V(I4+15)=V(I4+15)/GDIVI
c         minimum value for residual elastic modulus=0.50 kPa
      IF(V(I4+15).LT.GREFE(I4+15)) THEN
          V(I4+15)=GREFE(I4+15)
      END IF
c     UAR
c     Write(*,*) 'G(i)=',V(16),V(17),V(18)
          GOTO 438
      END IF
      V(I4+15)=G(I4)
438   CONTINUE
```

```
        WRITE(NMA,REC=NNN) (V(I),I=1,20)
440     CONTINUE
    END IF
C............
    RETURN
C.....ISOPARAMETRIC ELEMENT MASS MATRIX FOR PLANE PROBLEMS
C    P=DIAGONAL (LUMPED) MASS ARRAY (IN VECTOR)
C.....COMPUTE MATRIX AT EACH INTEGRATION POINT
5    L=int(D(5))
    L=2
C    IF(L*L*L.NE.LINT) CALL PGAUSS3(L,LINT,XG,YG,ZG,WG)
    CALL PGAUSS3(L,LINT,XG,YG,ZG,WG)
    DO 504 L9 = 1,LINT
    CALL SHP3 (XG(L9),YG(L9),ZG(L9),XL,SHP,XSJ,NDM,NEL,IX,.FALSE.)
    DMASS=D(4)*XSJ*WG(L9)
    DO 502 I=1,NEL
        P(3*I-2)=P(3*I-2)+DMASS*SHP(4,I)
        P(3*I-1)=P(3*I-2)
        P(3*I)=P(3*I-2)
502 CONTINUE
504 CONTINUE
    RETURN
C.......................................................
C.... FORMATS FOR INPUT-OUTPUT
2000 FORMAT(/5X,43H 3-D, ISOTROPIC, NON-LINEAR, RATE-DEPENDENT /
    * 5X,49HELASTICITY ELEMENT WITH EIGHT NODES(DUNCAN-CHANG) //
    1 10X,3HKs=,E15.5,3H(-)/
    2 10X,3Hns=,E15.5,3H(-)/
    3 10X,4HXUN=,E15.5,3H(-)/
    4 10X,4HRho=,E15.5,8H(kN/m^3)/
    5 10X,2HL=,I4/
    6 10X,2HK=,I4/
    7 10X,2HC=,E15.5,5H(kPa)/
    8 10X,4HFai=,E15.5,8H(Degree)/
    9 10X,4HRsf=,E15.5,3H(-)/
    * 10X,3HBs=,E15.5,3H(-)/
    1 10X,8HdEps(0)=,E15.5,5H(1/s)/
    2 10X,3HSt=,E15.5,3H(-)/
    3 10X,3HSc=,E15.5,3H(-) /
    4 10X,3HMs=,E15.5,3H(-) /)
2001 FORMAT(/A50/5X,16HELEMENT STRESSES/2X,15HGAUSS POINT----,
    * //1X,18H  ELEMENT MATERIAL,
    1  3X,9H11-STRESS,3X,9H12-STRESS,3X9H22-STRESS,4X,
    2  8H1-STRESS,4X,8H2-STRESS/2X,7H1-COORD,2X,7H2-COORD,3X,
    3  9H11-STRAIN,3X,9H12-STRAIN,3X,9H22-STRAIN,12X,5HANGLE)
```

```
2002  FORMAT(2x,I3,/2I9,5E12.3/2F9.3,3E12.3,F18.2/1X)
C     FORMAT(/5X,18HELEMENT NO. & MATE,3X,9H11-STRESS,11H  12-
STRESS,
C     * 12H---22-STRESS,4X,8H1-STRESS,4X,8H2-STRESS/5X,10H-----STATE,
C     & 2X,11HOF THE UNIT,/5X,2I9,5E12.3,5X,A10)
2010  FORMAT(/2X,12HELEMENT NO.=,I7,2X,10H----STATE=,A30)
2020  FORMAT(/5X,8(6F9.4)/)
2040  FORMAT(2x,18HRATIO OF BRAKING= ,F12.9,4H ET=,F7.3/)
2050  FORMAT(/5X,28HINITIAL ELASTIC MATRIC VALUE/,'G(1)=',F18.7,
    1  'G(2)=',F18.7,'G(3)=',F18.7)
2060  FORMAT(/5X,15HGAUSS POINT----,I2,12H NO. OF ELEM,2X,I3)
3333  format(a14,3f12.4)
      END


      SUBROUTINE SHP3 (SS,TT,YY,X,SHP,XSJ,NDM,NEL,IX,FLG)
      IMPLICIT REAL*8 (A-H,O-Z)
      REAL*8 X
      LOGICAL FLG
      DIMENSION SHP(4,*),X(NDM,*),QS(8),QT(8),QY(8),XS(3,3)
    1  ,SX(3,3),IX(*)
      DATA QS/0.5E0,-0.5E0,-0.5E0,0.5E0,0.5E0,-0.5E0,-0.5E0,
    1  0.5E0/,QT/-0.5E0,-0.5E0,-0.5E0,-0.5E0,0.5E0,0.5E0,
    1  0.5E0,0.5E0/,QY/-0.5E0,-0.5E0,0.5E0,0.5E0,-0.5E0,-0.5E0,
    1  0.5E0,0.5E0/
C.... FORM 8-NODE ISOPARAMETER ELEMENT SHAPE FUNCTIONS
      DO 100 I = 1,8
      PS=0.5E0+QS(I)*SS
      PT=0.5e0+QT(I)*TT
      PY=0.5e0+QY(I)*YY
      SHP(1,I) = QS(I)*PT*PY
      SHP(2,I) = PS*QT(I)*PY
      SHP(3,I) = PS*PT*QY(I)
100   SHP(4,I)= PS*PT*PY
C     do 101 i=1,8
C101   write(*,*) 'shp(1,i)',shp(1,i),'shp(4,i)',shp(4,i)
C.... CONSTRUCT JACOBIAN AND ITS INVERSE
      DO 130 I = 1,NDM
      DO 130 J = 1,3
      XS(I,J) = 0.0
      DO 130 K = 1,NEL
130   XS(I,J) = XS(I,J) + X(J,K)*SHP(I,K)
C     write(*,*) 'xs(1,1)',xs(1,1),'xs(2,2)',xs(2,2),'xs(3,3)',xs(3,3)
C...FORM JACOBIAN DETERMINANT
      XSJ=XS(1,1)*XS(2,2)*XS(3,3)+XS(2,1)*XS(3,2)*XS(1,3)
    1  +XS(3,1)*XS(1,2)*XS(2,3)-XS(1,3)*XS(2,2)*XS(3,1)
```

```
    1 -XS(2,1)*XS(1,2)*XS(3,3)-XS(1,1)*XS(3,2)*XS(2,3)
C   write(*,*) 'xsj=',xsj
    IF(FLG) RETURN
    SX(1,1)=(XS(2,2)*XS(3,3)-XS(2,3)*XS(3,2))/XSJ
    SX(1,2)=(XS(1,3)*XS(3,2)-XS(3,3)*XS(1,2))/XSJ
    SX(1,3)=(XS(2,3)*XS(1,2)-XS(1,3)*XS(2,2))/XSJ
    SX(2,1)=(XS(3,1)*XS(2,3)-XS(3,3)*XS(2,1))/XSJ
    SX(2,2)=(XS(1,1)*XS(3,3)-XS(1,3)*XS(3,1))/XSJ
    SX(2,3)=(XS(2,1)*XS(1,3)-XS(1,1)*XS(2,3))/XSJ
    SX(3,1)=(XS(2,1)*XS(3,2)-XS(2,2)*XS(3,1))/XSJ
    SX(3,2)=(XS(3,1)*XS(1,2)-XS(1,1)*XS(3,2))/XSJ
    SX(3,3)=(XS(1,1)*XS(2,2)-XS(2,1)*XS(1,2))/XSJ
C.... FORM GLOBAL DERIVATIVES
    DO 140 I = 1,NEL
    TP=SHP(1,I)*SX(1,1)+SHP(2,I)*SX(1,2)+SX(1,3)*SHP(3,I)
    TQ=SHP(1,I)*SX(2,1)+SHP(2,I)*SX(2,2)+SX(2,3)*SHP(3,I)
    SHP(3,I)=SHP(1,I)*SX(3,1)+SHP(2,I)*SX(3,2)+SX(3,3)*SHP(3,I)
    SHP(2,I)=TQ
140 SHP(1,I)=TP
    K=IX(1)
    RETURN
    END



    SUBROUTINE PGAUSS3(L,LINT,X,Y,Z,W)
C.... GAUSS POINTS AND WEIGHTS FOR TWO DIMENSIONS
C
    IMPLICIT REAL*8 (A-H,O-Z)
    COMMON /ELDATA/ LM,N,MA,MCT,IEL,NEL
    DIMENSION QX(8),QY(8),QZ(8),X(*),Y(*),Z(*),W(*)
    DATA QX/1.,-1.,-1.,1.,1.,-1.,-1.,1./,
    1 QY/-1.,-1.,-1.,-1.,1.,1.,1.,1./
    DATA QZ/-1.,-1.,1.,1.,-1.,-1.,1.,1./
    LINT = L*L*L
C.... 2X2X2 INTEGRATION
    G=1.0E0/SQRT(3.0E0)
    DO 21 I=1,8
    X(I)=G*QX(I)
    Y(I)=G*QY(I)
    Z(I)=G*QZ(I)
21  W(I)=1.0E0
    RETURN
    END

    SUBROUTINE PSTRES3(SIG,P1,P2,P3)
```

```
C.... COMPUTE PRINCIPAL STRESSES (3 DIMENSIONS)
C
      IMPLICIT REAL*8 (A-H,O-Z)
      DIMENSION SIG(6),A(4),RT1(2),RT2(2),RT3(2)
C.... STRESSES MUST BE STORED IN ARRAY SIG(6) IN THE ORDER
C    TAU-XX,TAU-YY,TAU-ZZ,TAU-XY,TAU-YZ,TAU-XZ
        AI1=SIG(1)+SIG(2)+SIG(3)
        AI2=SIG(1)*SIG(2)+SIG(2)*SIG(3)+SIG(1)*SIG(3)-SIG(4)*SIG(4)
   1 -SIG(5)*SIG(5)-SIG(6)*SIG(6)
        AI3=SIG(1)*SIG(2)*SIG(3)+2.*SIG(4)*SIG(5)
   1 *SIG(6)-SIG(1)*SIG(5)*SIG(5)-SIG(2)
   1 *SIG(6)*SIG(6)-SIG(3)*SIG(4)*SIG(4)
        A(1)=1.
        A(2)=-AI1
        A(3)=AI2
        A(4)=-AI3
      TOL=0.001
      CALL CUBIC(A,RT1,RT2,RT3,TOL,NOROOT)
      P1=RT1(1)
      P2=RT2(1)
      P3=RT3(1)
      IF(P1.LT.P2) THEN
      P=P1
      P1=P2
      P2=P
      END IF
      IF(P1.LT.P3) THEN
      P=P1
      PP=P2
      P1=P3
      P2=P
      P3=PP
      END IF
      IF(P2.LT.P3) THEN
      P=P2
      P2=P3
      P3=P
      END IF
      RETURN
      END


      SUBROUTINE CUBIC(A,RT1,RT2,RT3,TOL,NOROOT)
C
C   THIS SUBROUTINE FINDS THE ROOTS (REAL OR REAL AND
C   COMPLEX) TO ANY CUBIC EQUATION.
```

```fortran
C
      IMPLICIT REAL*8 (A-H,O-Z)
      DIMENSION A(4),C(4),RT1(2),RT2(2),RT3(2), B(2)
      ZERO = TOL/10.
      IF(ABS(A(1) ) - ZERO) 7,7,12
7     CALL QUADRT(A(2), RT1,RT2,TOL,NOROOT)
      RETURN
12    NOROOT = 3
      IT = 0
      DO 1 I = 2,4
1     A(I) = A(I)/A(1)
      A(1) = 1.0
      IF(ABS(A(2)).LE.ZERO) GO TO 2
      NDA = 3
      B(1) = 1.0
      B(2) = -(A(2)*.333333)
      CALL LINCNG(A,NDA,B,C)
      IT = 1
      GO TO 4
2     DO 3 I = 1,4
3     C(I) = A(I)
4     X = (C(4)*C(4))*.25 + (C(3)**3) *.037037
      IF(X.LT.0.0) GO TO 9
      X = SQRT(X)
      Y = -(C(4)*.5)
      I = 1
      RT1(I) = Y + X
5     N = 0
      IF(RT1(I).LT.0.0) N = 1
      IF(ABS(RT1(I)).LE.ZERO) GO TO 6
      RT1(I) = EXP((ALOG(ABS(RT1(I))))*.333333)
      IF(N.EQ.1) RT1(I) = -RT1(I)
6     IF(I.EQ.2) GO TO 8
      I = 2
      RT1(I) = Y - X
      GO TO 5
8     RT2(2) = ((RT1(1) - RT1(2))*.5)*1.732051
      RT1(1) = RT1(1) + RT1(2)
      RT1(2) = 0.0
      RT2(1) = - RT1(1) * .5
      RT3(1) = RT2(1)
      RT3(2) = -RT2(2)
      GO TO 11
9     ZZ = ABS(C(3))
      X = -(C(4)*.5)/SQRT((ZZ**3)*.037037)
```

```
      ANG= ACOS(X)
      Y = 2.0*(SQRT(ZZ*.333333))
      ANG = ANG*.333333
      RT1(1) = Y*COS(ANG)
      RT2(1) = Y*COS(ANG + 2.09440)
      RT3(1) = Y * COS(ANG + 4.18879)
      RT1(2) = 0.0
      RT2(2) = 0.0
      RT3(2) = 0.0
   11 IF(IT.EQ.0) RETURN
      RT1(1) = RT1(1) + B(2)
      RT2(1) = RT2(1) + B(2)
      RT3(1) = RT3(1) + B(2)
      RETURN
      END
      SUBROUTINE QUADRT(A,ROOT1,ROOT2,TOL,NOROOT)
C
C   THIS SUBROUTINE SOLVES ANY QUADRATIC EQUATION OF THE FORM
C   A(1)X**2 + A(2)X + A(3) FOR REAL OR IMAGINARY ROOTS.
C
      IMPLICIT REAL*8 (A-H,O-Z)
      DIMENSION A(3), ROOT1(2), ROOT2(2)
      ZERO = TOL/10.
      IF(ABS(A(1)) - ZERO) 2,2,1
    2 IF(ABS(A(2)) - ZERO) 3,3,4
    3 NOROOT = 0
      RETURN
    1 NOROOT = 2
      X = A(2)*A(2) - 4.0 *A(1) * A(3)
      Y = A(1) + A(1)
      Z = SQRT(ABS(X))/Y
      W = -A(2)/Y
      IF(X.LT.0.0) GO TO 7
      ROOT1(1) = W + Z
      ROOT1(2) = 0.0
      ROOT2(1) = W - Z
      ROOT2(2) = 0.0
      RETURN
    7 ROOT1(1) = W
      ROOT1(2) = Z
      ROOT2(1) = W
      ROOT2(2) = -Z
      RETURN
    4 NOROOT = 1
      ROOT1(1) = -A(3)/A(2)
```

```fortran
      ROOT1(2) = 0.
      RETURN
      END

      SUBROUTINE LINCNG(A,NDA,B,C)
C
C     SUBROUTINE TO MAKE A LINEAR CHANGE OF VARIABLES
C     IN A GIVEN POLYNOMIAL.
C
      IMPLICIT REAL*8 (A-H,O-Z)
      DIMENSION A(1), B(2), C(1)
      B1PWR = 1.0
      NZ = NDA + 1
      DO 4 I = 1,NZ
    4 C(I) = A(I)
    6 DO 8 I = 2,NZ
    8 C(I) = C(I) + C(I-1)*B(2)
      C(NZ) = C(NZ)*B1PWR
      NZ = NZ - 1
      B1PWR = B1PWR*B(1)
      IF (NZ.GT.1) GO TO 6
      C(1) = C(1) * B1PWR
      RETURN
      END


C.....................................................
      SUBROUTINE EQLOAD(I,NP,W,A,XL,F)
      IMPLICIT REAL*8 (A-H,O-Z)
      DIMENSION F(6)
      IF(I.GT.4) GO TO 10
      IF(I.LE.3) WL=W/XL
      S=(1.-2.*NP)
      GO TO (1,2,3,4) I
    1 F(4)=WL*A
      F(1)=W-F(4)
      RETURN
    2 B=XL-A
      F(2+NP)=WL*B*B*(2.*A+XL)/XL/XL
      WAB=WL*A*B
      F(3-NP)=S*WAB*B/XL
      F(5+NP)=W-F(2+NP)
      F(6-NP)=-S*WAB*A/XL
      RETURN
    3 B=XL-A
      F(5+NP)=6.*WL*A*B/XL/XL
```

```
      F(2+NP)=-F(5+NP)
      F(3-NP)=S*WL*B*(B-2.*A)/XL
      F(6-NP)=S*WL*A*(A-2.*B)/XL
      RETURN
4     W1=W*XL/20.
      W2=A*XL/20.
      F(2+NP)=7.*W1+3.*W2
      F(3-NP)=S*(3.*W1+2.*W2)*XL/3.
      F(5+NP)=3.*W1+7.*W2
      F(6-NP)=-S*(2.*W1+3.*W2)*XL/3.
      RETURN
10    WRITE(6,2000) I
2000  FORMAT(' ** ERROR ** EQUIVALENT LOAD TYPE',I6,' HAS BEEN
      INPUT')
      RETURN
      END


C......................................................
      SUBROUTINE FORBACK(A,B,JP,N)
      IMPLICIT REAL*8 (A-H,O-Z)
      DIMENSION A(*),B(*),JP(*)
C.....FORWARD REDUCTION
      IJ=2
      DO 200 I=2,N
      MI=I-JP(I)+JP(I-1)+1
      DO 100 J=MI,I-1
      B(I)=B(I)-A(IJ)*B(J)
      IJ=IJ+1
100   CONTINUE
      IJ=IJ+1
200   CONTINUE
C.....REFORM THE RIGHT HAND SIDE
      DO 300 I=1,N
      JPI=JP(I)
      B(I)=B(I)*A(JPI)
300   CONTINUE
C.....BACK SUBSTITUTION
      IJ=IJ-1
      DO 500 I=N,2,-1
      MI=I-JP(I)+JP(I-1)+1
      DO 400 J=I-1,MI,-1
      IJ=IJ-1
400   B(J)=B(J)-A(IJ)*B(I)
      IJ=IJ-1
500   CONTINUE
```

```fortran
      RETURN
      END

C..... Modified Uriel A. Rosa    Feb 01/96
C...................................
C.....GENERATE DATA FILE TO DETERMINE THE COORDINATES OF GAUSS
POINTS
C...................................
      SUBROUTINE GAUSS(XC,XL,IX,NEN1)
      IMPLICIT REAL*8 (A-H,O-Z)
      DIMENSION XC(NDM,*),IX(NEN1,*),XL(NDM,*)
      DIMENSION SHP(4,9)
      DIMENSION SG(16),TG(16),WG(16),CGAUSS(3,8)
      COMMON/CDATA/NDF,NDM,NEN,NJ,NE,NEQ
      LINT=0
      DO 300 N=1,NE
      DO 108 I=1,NEN
      II=IX(I,N)
      IF(II.NE.0) GO TO 105
      GO TO 108
105   IID=II*NDF-NDF
      NEL=I
      DO 106 J1=1,NDM
106   XL(J1,I)=XC(J1,II)
108   CONTINUE
C....................
      L=2
      IF(NDM.EQ.2) THEN
        IF(L*L.NE.LINT) CALL PGAUSS(L,LINT,SG,TG,WG)
      ENDIF
      IF(NDM.EQ.3) THEN
c       IF(L*L*L.NE.LINT) CALL PGAUSS3(L,LINT,XG,YG,ZG,WG)
      ENDIF
      DO 200 L=1,LINT
      IF(NDM.EQ.2) THEN
        CALL SHAPE(SG(L),TG(L),XL,SHP,XSJ,NDM,NEL,IX,.FALSE.)
      ENDIF
      IF(NDM.EQ.3) THEN
c       CALL SHP3(XG(L),YG(L),ZG(L),XL,SHP,XSJ,NDM,NEL,IX,.FALSE.)
      ENDIF
      DO 120 I=1,NDM
120   CGAUSS(I,L)=0.0
      DO 130 I=1,NDM
      DO 130 J=1,NEL
130   CGAUSS(I,L)=CGAUSS(I,L)+SHP(NDM+1,J)*XL(I,J)
```

```
200   CONTINUE
      WRITE(83,1000) ((CGAUSS(I,J),I=1,NDM),J=1,LINT)
300   CONTINUE
      RETURN
1000  FORMAT(3E15.7)
      END


C.......................................
      SUBROUTINE GENVEC(NDM,X,CD,FC,NJ,ERR)
C.....GENERATE REAL DATA ARRAYS BY LINEAR INTERPOLATION
      IMPLICIT REAL*8 (A-H,O-Z)
      COMMON /FLAG_BLO/ GE_FLAG,DY_FLAG,DB_FLAG,MA_FLAG,UL_FLAG,
     * ST_FLAG,SC_FLAG
      CHARACTER CD*18,FC*6
      LOGICAL ERR,GE_FLAG,DY_FLAG,DB_FLAG,MA_FLAG,UL_FLAG,
     * ST_FLAG,SC_FLAG
      REAL*8 X(NDM,*),XL(6)
      ERR=.FALSE.
      N=0
      NG=0
102   L=N
      LG=NG
      READ (5,*,ERR=999) N,NG,(XL(I),I=1,NDM)
101   IF (N.LE.0.OR.N.GT.NJ) GO TO 109
      DO 103 I=1,NDM
103   X(I,N) = XL(I)
      IF (LG) 104,102,104
104   LG=ISIGN(LG,N-L)
      LI= (IABS(N-L+LG)-1)/IABS(LG)
      DO 105 I=1,NDM
105   XL(I)=(X(I,N)-X(I,L))/LI
106   L = L+LG
      IF((N-L)*LG.LE.0) GO TO 102
      IF(L.LE.0.OR.L.GT.NJ) GO TO 108
      DO 107 I=1,NDM
      LMLG=L-LG
107   X(I,L)=X(I,LMLG)+XL(I)
      GO TO 106
108   IF(DB_FLAG) WRITE(6,3000) L,CD
      IF(SC_FLAG) WRITE(*,3000) L,CD
      ERR=.TRUE.
      GO TO 102
109   CONTINUE
      DO 110 I=1,NJ,50
      IF(DB_FLAG) WRITE(6,2000) CD,(K,FC,K=1,NDM)
```

```fortran
      IF(SC_FLAG) WRITE(*,2000) CD,(K,FC,K=1,NDM)
      N=MIN0(NJ,I+49)
      DO 110 J=I,N
      IF(SC_FLAG) WRITE(*,2009)J,(X(L,J),L=1,NDM)
110   IF(DB_FLAG) WRITE(6,2009)J,(X(L,J),L=1,NDM)
      RETURN
999   ERR=.TRUE.
      RETURN
2000  FORMAT(/5X,A18/2X,5HNODE ,6(I6,A6))
2008  FORMAT(I10,32H HAS NOT BEEN INPUT OR GENERATED)
2009  FORMAT(I6,6F12.4)
3000  FORMAT(5X,' **FATAL ERROR** ATTEMPT TO GENERATE NODE',I5,
     1       ' IN', A18)
      END


C.......................................................
      SUBROUTINE LDLT(A,JP,N)
C.....LDLT TRIANGULAR DECOMPOSITION
      IMPLICIT REAL*8 (A-H,O-Z)
      DIMENSION A(*),JP(*)
      NK=JP(N)
      A(1)=1.0/A(1)
      IJ=1
      II=2
      ID1=JP(1)
      DO 500 I=2,N
      ID2=JP(I)
      MI=I-ID2+ID1+1
      MJ=1
      DO 300 J=MI,I-1
      IJ=IJ+1
      IF(J.EQ.1) GO TO  100
      MJ=J-JP(J)+JP(J-1)+1
100   AIJ=A(IJ)
      MIJ=MAX0(MI,MJ)
      IK=JP(I)-I+MIJ
      JK=JP(J)-J+MIJ
      DO 200 K=MIJ,J-1
      AIJ=AIJ-A(IK)*A(JK)
      IK=IK+1
      JK=JK+1
200   CONTINUE
      A(IJ)=AIJ
300   CONTINUE
      II=IJ+1
```

```fortran
      AII=A(II)
      IJ=JP(I-1)+1
      DO 400 J=MI,I-1
      JJ=JP(J)
      AIJ=A(IJ)
      A(IJ)=A(IJ)*A(JJ)
      AII=AII-AIJ*A(IJ)
      IJ=IJ+1
400   CONTINUE
      A(II)=1.0/AII
      ID1=ID2
500   CONTINUE
      RETURN
      END


C..........................................
      SUBROUTINE MODIFY(U,LD,S,DUL,NS)
      IMPLICIT REAL*8 (A-H,O-Z)
      REAL*8 U,DUL,S
      DIMENSION U(1),LD(1),S(NS,1),DUL(1)
      COMMON/DYNAMICS/SPEED,DT,THITA,BATA.GAMA
      DO 110 I=1,NS
      K=LD(I)
      IF(K.LE.0) GO TO 110
      DO 100 J=1,NS
100   U(K)=U(K)-S(I,J)*DUL(J)
110   CONTINUE
      RETURN
      END


C..........................................
      SUBROUTINE MZERO(M,N)
      IMPLICIT REAL*8 (A-H,O-Z)
      DIMENSION M(N)
      DO 100 I=1,N
100   M(I)=0.0
      RETURN
      END


c.....(Dynat7) UAR May-30-96
c    (Dynat6) UAR May-24-96
C.....Modified...Uriel A. Rosa  Feb 10/96
C.........................................
      SUBROUTINE PCONTR(FO)
      IMPLICIT REAL*8 (A-H,O-Z)
```

268

```fortran
      REAL*8 TOLRUUR,TOLRUR,TOLC
      PARAMETER (MAXM=33000,MAXR=85000,MAXA=910000)
C.....IN SUBROUTINE ADDSTF, THERE IS ANOTHER PARAMETER
STATEMENT TO
C.....DEFINE MAXA WHICH ALSO NEED BE CHAGED, IF CHANGE HAPPENS
TO THE ABOVE
C.....MAXA. NOTE MAXM FOR INTEGER ARRAY, MAXR FOR REAL ARRAY,
AND MAXA FOR
C.....TOTAL STIFFNESS ARRAY
      CHARACTER FO*9,CFLAG*5,CH_FLAG*7
      LOGICAL ERR,ASEM,GE_FLAG,DY_FLAG,DB_FLAG,MA_FLAG,UL_FLAG,
     * ST_FLAG,IT_FLAG,SC_FLAG
      COMMON/M/M(MAXM)
      COMMON/R/R(MAXR)
      COMMON/A/A(MAXA)
      COMMON/CDATA/NDF,NDM,NEN,NJ,NE,NEQ
      COMMON/MDATA/NUMMAT
      CHARACTER FD*25,FORC*6,P
      COMMON/PRINT/P
      COMMON/ASEM/ASEM
C.....NPROP DENOTES NUMBER OF TOTAL INCREMENT STEPS
C.....NITEM DENOTES NUMBER OF TOTAL ITERATION STEPS DURING EACH
LOADING STEP
      COMMON/PROCESS/NPROP,NITEM,IT_FLAG
      COMMON/DYNAMICS/SPEED,DT,THITA,BATA,GAMA
C    GE_FLAG FOR IDENTIFING LINEAR OR NON-LINEAR GEOMETRIC
ANALYSIS
C    DY_FLAG FOR IDENTIFING STATIC OR DYNAMIC ANALYSIS
C    DB_FLAG FOR IDENTIFING OUTPUT STATUS FOR DEBUG OR NOT
C    MA_FLAG FOR IDENTIFING VARIABLE OR CONSTAT STIFFNESS
C    UL_FLAG FOR IDENTIFING UPDATED OR TOTAL LAGRANGINA METHOD
C    ST_FLAG FOR CONSIDERING TENSILE FAILURE INFLUENCE ON SHEAR
STRENGTH
C    SC_FLAG FOR SHOWING THE INFORMATION ON SCREEN
      COMMON /FLAG_BLO/ GE_FLAG,DY_FLAG,DB_FLAG,MA_FLAG,UL_FLAG,
     * ST_FLAG,SC_FLAG
      DATA FORC/' FORC '/FD/' NODAL FORCE/DISPL'/
C.....READ IN CONTROL DATA

      I=0
2     READ(5,'(A5)') CFLAG
      IF(CFLAG.EQ.'MSFEM'.OR.CFLAG.EQ.'msfem') I=1
      IF(I.EQ.0) GO TO 2
      READ(5,*)   NJ,NE,NUMMAT,NDF,NDM,NEN
      WRITE(*,2000) NJ,NE,NUMMAT,NDF,NDM,NEN
```

```
      WRITE(6,2000) NJ,NE,NUMMAT,NDF,NDM,NEN
      NEN1=NEN+1
      NNEQ=NJ*NDF
      NST=NDF*NEN
      NSW=NE*NEN
C.....INTEGER ARRAY POINTERS
      NIX=1
      NID=NIX+NEN1*NE
      NLD=NID+NNEQ
      NJP=NLD+NST
      NTEN=NJP+NNEQ
      NSHE=NTEN+NSW
      NENDI=NSHE+NSW
C.....REAL ARRAY POINTERS
      NXC=1
      NUXC=NXC+NJ*NDM
      NXCO=NUXC+NJ*NDM
      ND=NXCO+NJ*NDM
C.....LIMITTED TO 19 PARAMETERS FOR EACH KIND OF MATERIAL.
C.....THE 20TH IS THE ELEMENT TYPE NUMBER.
      NXL=ND+20*NUMMAT
      NXLO=NXL+NEN*NDM
      NUL=NXLO+NEN*NDM
      NURL=NUL+2*NST
      NS=NURL+NST*2
      NP=NS+NST*NST
      NF=NP+NST
      NPF=NF+NNEQ
      NTF=NPF+NNEQ
      NTPF=NTF+NNEQ
      NU=NTPF+NNEQ
      NFR=NU+NNEQ
      NUR=NFR+NNEQ
      NUUR=NUR+NNEQ
      NSM=NUUR+NNEQ
      NU1=NSM+NNEQ
      NV1=NU1+NNEQ
      NW1=NV1+NNEQ
      NU2=NW1+NNEQ
      NV2=NU2+NNEQ
      NW2=NV2+NNEQ
      NWW=NW2+NNEQ
      NUI=NWW+NNEQ
      NVL=NUI+NNEQ
      NENDR=NVL+NST
```

270

```
C
C    NWW -- INCREMENTAL ACCELERATION;
C
C
     CALL SETMEM(NENDI,MAXM,ERR)
     IF(ERR) THEN
     WRITE(*,3000)
     WRITE(6,3000)
     STOP
     END IF
     CALL SETMEM(NENDR,MAXR,ERR)
     IF(ERR) THEN
     WRITE(*,3001)
     WRITE(6,3001)
     STOP
     END IF
     CALL MZERO(M(1),NENDI)
     CALL PZERO(R(1),NENDR)
C.....MESH GENERATION
     CALL PMESH(R(NXC),R(NXLO),M(NIX),M(NID),R(ND),R(NUL),R(NURL)
     * ,R(NS),R(NP),NEN1,NST)
     CALL GENVEC(NDF,R(NF),FD,FORC,NJ,ERR)
     IF(ERR) GO TO 20

c    UAR
c    DO 800 I1=1,NDM*NJ
c800  WRITE(88,*) R(NID+I1-1)


C      WRITE(88,1088) (J,(XC(I,J),I=1,NDM),J=1,NJ)
C      1088  FORMAT ((('  N,',I5,3(',',E15.7))))
c    UAR

     DO 3 I1=1,NDM*NJ
3     R(NXCO+I1-1)=R(NXC+I1-1)
C.....DEFINE THE PROFIL FOR GLOBAL STIFFNESS MATRIX STORAGE
     CALL PROFIL(M(NJP),M(NID),M(NIX),NEN1,NK)
     CALL SETMEM(NK,MAXA,ERR)
     IF(ERR) THEN
     WRITE(*,3500)
     STOP
     ENDIF
c    WRITE(*,*)' DO YOU WANT TO OUTPUT ELEMENT STIFFNESS (Y/N)?'
c    READ (*,'(A)') P
     P='N'
```

```
C.....DETERMINE NON-ZERO DISPLACEMENT BOUNDARY CONDITION
MAGNITUDE
      CALL VALBOUN(R(NF),M(NID),RDB)
C.....DETERMINE COORDINATES OF GAUSS POINTS
c     CALL GAUSS(R(NXC),R(NXL),M(NIX),NEN1)
C.....INITIAL PARAMETERS(SPEED(M/S))
      NPROP=1
      WRITE(*,*)'INPUT SPEED(M/S):2.5, 5.0, 10.0 OR 15.0:'
      READ(5,*) SPEED,NSTEP,NITEM,N_W
      write(7,*) 'speed(m/s)=',speed
      write(*,*) 'speed(m/s)=',speed
      write(81,*) speed
      WRITE(84,*) SPEED
      WRITE(85,*) SPEED
      WRITE(82,*) SPEED
      WRITE(86,*) SPEED
      WRITE(*,*)'INPUT TOTAL STEPS:/'
C     READ(*,*) NSTEP
      write(7,*) 'TOTAL STEPS=',NSTEP
      write(*,*) 'TOTAL STEPS=',NSTEP
      write(81,*) nstep
      WRITE(84,*) NSTEP
      WRITE(85,*) NSTEP
      WRITE(82,*) NSTEP
      WRITE(86,*) NSTEP
      write(7,*) 'ITERATION STEPS=',NITEM
      write(*,*) 'ITERATION STEPS=',NITEM
      write(*,*) 'interval(m)=',RDB
      write(7,*) 'interval(m)=',RDB
      IF(RDB.LE.1.E-6) RDB=1

c     UAR
      IF(RDB.LE.1.E-6) write(*,*) 'Warning: RDB=1'
      IF(RDB.LE.1.E-6) write(7,*) 'Warning: RDB=1'
c     UAR

      DT=RDB/SPEED
      IF(N_W.EQ.0) THEN
          write(*,*) 'NEWMARK METHOD'
          write(7,*) 'NEWMARK METHOD'
      ELSE
          write(*,*) 'WILSON METHOD'
          write(7,*) 'WILSON METHOD'
      ENDIF
      READ(5,'(A7)') CH_FLAG
```

```fortran
IF(CH_FLAG.EQ.'DY_FLAG'.OR.CH_FLAG.EQ.'dy_flag') THEN
    DY_FLAG=.TRUE.
    write(*,*) 'DYNAMIC SOLVING SCHEME'
    write(7,*) 'DYNAMIC SOLVING SCHEME'
ELSE
    DY_FLAG=.FALSE.
    write(*,*) 'STATIC SOLVING SCHEME'
    write(7,*) 'STATIC SOLVING SCHEME'
ENDIF
READ(5,'(A7)') CH_FLAG
IF(CH_FLAG.EQ.'GE_FLAG'.OR.CH_FLAG.EQ.'ge_flag') THEN
    GE_FLAG=.TRUE.
    write(*,*) 'NON-LINEAR GEOMETRIC SOLVING SCHEME'
    write(7,*) 'NON-LINEAR GEOMETRIC SOLVING SCHEME'
ELSE
    GE_FLAG=.FALSE.
    write(*,*) 'LINEAR GEOMETRIC SOLVING SCHEME'
    write(7,*) 'LINEAR GEOMETRIC SOLVING SCHEME'
ENDIF
READ(5,'(A7)') CH_FLAG
IF(CH_FLAG.EQ.'DB_FLAG'.OR.CH_FLAG.EQ.'db_flag') THEN
    DB_FLAG=.TRUE.
    write(*,*) 'OUTPUT DEBUG INFORMATION'
    write(7,*) 'OUTPUT DEBUG INFORMATION'
ELSE
    DB_FLAG=.FALSE.
    write(*,*) 'DO NOT OUTPUT DEBUG INFORMATION'
    write(7,*) 'DO NOT OUTPUT DEBUG INFORMATION'
ENDIF
READ(5,'(A7)') CH_FLAG
IF(CH_FLAG.EQ.'MA_FLAG'.OR.CH_FLAG.EQ.'ma_flag') THEN
    MA_FLAG=.TRUE.
    write(*,*) 'NON-LINEAR MATERIAL SOLVING SCHEME'
    write(7,*) 'NON-LINEAR MATERIAL SOLVING SCHEME'
ELSE
    MA_FLAG=.FALSE.
    write(*,*) 'LINEAR MATERIAL SOLVING SCHEME'
    write(7,*) 'LINEAR MATERIAL SOLVING SCHEME'
ENDIF
READ(5,'(A7)') CH_FLAG
IF(CH_FLAG.EQ.'UL_FLAG'.OR.CH_FLAG.EQ.'ul_flag') THEN
    UL_FLAG=.TRUE.
    write(*,*) 'UPDATED LAGRAGIAN SOLVING SCHEME'
    write(7,*) 'UPDATED LAGRAGIAN SOLVING SCHEME'
ELSE
```

```
            UL_FLAG=.FALSE.
            write(*,*) 'TOTAL LAGRAGIAN SOLVING SCHEME'
            write(7,*) 'TOTAL LAGRAGIAN SOLVING SCHEME'
         ENDIF
         READ(5,'(A7)') CH_FLAG
         IF(CH_FLAG.EQ.'ST_FLAG'.OR.CH_FLAG.EQ.'st_flag') THEN
            ST_FLAG=.TRUE.
            write(*,*) 'CONSIDERING TENSILE FAILURE'
            write(7,*) 'CONSIDERING TENSILE FAILURE'
         ELSE
            ST_FLAG=.FALSE.
            write(*,*) 'NOT CONSIDERING TENSILE FAILURE'
            write(7,*) 'NOT CONSIDERING TENSILE FAILURE'
         ENDIF
         READ(5,'(A7)') CH_FLAG
         IF(CH_FLAG.EQ.'SC_FLAG'.OR.CH_FLAG.EQ.'sc_flag') THEN
            SC_FLAG=.TRUE.
            write(*,*) 'INFORMATION SHOWING ON SCREEN'
            write(7,*) 'INFORMATION SHOWING ON SCREEN'
         ELSE
            SC_FLAG=.FALSE.
            write(*,*) 'NO INFORMATION SHOWING ON SCREEN'
            write(7,*) 'NO INFORMATION SHOWING ON SCREEN'
         ENDIF
C.....INTEGRATION PARAMETERS
C.....N_W=0,NEWMARK METHOD; N_W=1, WILSON METHOD:
         IF(DY_FLAG) THEN
C      IF(N_W.EQ.0) THEN
          THITA=1.0
            BATA=0.25
            GAMA=0.50
            A0=GAMA*DT
            A1=1.0/(DT*DT*BATA)
            A2=-1.0/(BATA*DT)
            A3=-1.0/(2.0*BATA)
            A4=A0*A1
            A5=A0*A2
            A6=DT+A0*A3
            A7=A3+1.0
         A8=DT-A0
C      ELSE
C      THITA=1.4
C      A1=6./(THITA*DT)**2.
C      A0=A1/THITA
C      A2=-6.0/(THITA*DT)
```

```
C       A3=-3.0
C       A4=3.0/(THITA*DT)
C       A5=A3
C       A6=-THITA*DT/2.0
C       A7=-6.0/(THITA*THITA*DT)
C       A8=1.0-3.0/THITA
C    ENDIF
C    ELSE
C     THITA=1.0
     ENDIF
C-------------------------------------------------------------------------
C                 VARIABLES
C U -- TOTAL DISPLACEMENT VECTOR, GLOBAL, ARRANGED BY
ACTIVATED D.O.F.
C UR -- INCREMENTAL DISPL. VECTOR, GLOBAL, ARRANGED BY
ACTIVATED D.O.F.
C UUR -- DISPL. INCREMENT IN ITERATION, GLOBAL, ARRANGE BY
ACTIVATED D.O.F.
C UL -- ELEMENT TOTAL DISPL. VECTOR.   URL -- ELEMENT INCREMENTAL
DISPL. VECTOR.
C F -- TOTAL FORCE VECTOR, GLOBAL, ARRANGED BY TOTAL D.O.F.
C FR -- INCREMENT FORCE VECTOR, GLOBAL, ARRANGE BY ACTIVATED
D.O.F.
C XC -- TOTAL NODE COORDINATE, GLOBAL, ARRANGED BY ACTIVATED
D.O.F.
C XL -- ELEMENT NODAL COORDINATE,
C PF -- INCREMENTAL NODAL REACTION FORCE, ARRANGED BY TOTAL
D.O.F.
C TPF -- TOTAL NODAL REACTION FORCE, ARRANGED BY TOTAL D.O.F.
C TF -- REFERENCE FORCE FOR ITERATION AT NITEM=I
C ID -- GLOBAL IDENTIFICATION,
C      ID>0, NON-CONSTRAINT, KNOWN-FORCE; ID NUMBER=NUMBER OF
ACTIVATED D.O.F.
C      ID<0, CONSTRAINT, KNOWN-DISPLACEMENT
C LD -- ELEMENT IDENTIFICATION
C      ISW=6,        LD=TOTAL D.O.F NUMBER
C      OTHERS,       LD=ID NUMBER ARRANGED BY ACTIVATED D.O.F.FOR
REAL NODES
C                 LD=0          ,FOR EMPTY NODES
C-------------------------------------------------------------------------
C                 FLOWCHART
C
C    form mass matrix, M <--
C    TPF <-- 0
C    DO 30 II=1,NSTEP
```

```
C     form stiffness matrix, A <--
C     TF <-- 0, UR <-- 0
C     DO 40 III=1,NITEM
C     FR <-- 0, UUR <-- 0
C     FR  <-- F (external load)
C     FR  <-- FR+specified displacement+element load
C     FR <-- FR+dynamic factor(V1,W1)
C     UUR <-- FR+TF
C     solve
C     UR <-- UR+UUR
C      (display TF,FR,UUR,UR for debug)
C     calculate TF <--
C     calculate PF <--
C 40   continue
C     U <-- U+UR
C     W2 <--, V2 <--
C     calculate incremental reaction force, PF <--
C     TPF <-- TPF+PF
C     calculate stresses, update modulus
C     V1 <-- V2, W1 <-- W2
C     update coordinate, XC <--
C 30   continue
C
C----------------------------------------------
C.....FORM MASS MATRIX
4    CALL PZERO(R(NSM),NNEQ)
     CALL PFORM(R(NF),R(NFR),M(NLD),R(NUL),R(NURL),R(NXL),R(NXLO),
    1 R(NS),R(NP),R(NPF),R(NTF),R(NU),R(NUR),R(NXC),R(NXCO),M(NIX)
    2 ,R(ND),M(NID),M(NJP),R(NSM),R(NV2),R(NVL),NST,NEN1,5)
     CALL PZERO(R(NTPF),NNEQ)
     CALL PZERO(R(NU),NNEQ)


C--------------------------------------------------------------
C.....INITIALIZE U, U. , U..  (STARTS FROM STATIC STATE)

     CALL PZERO(R(NV1),NNEQ)
     CALL PZERO(R(NW1),NNEQ)
C-----------------------------------------------------


C----------------Beginning of Increment Analysis----------------
     DO 30 II=1,NSTEP
     write(*,*) 'TOTAL LOADING STEPS=', nstep
     write(7,*) 'TOTAL LOADING STEPS=', nstep
C.....FORM ELEMENT STIFFNESS
```

```
      CALL PZERO(A,NK)
      ASEM=.TRUE.
      CALL PFORM(R(NF),R(NFR),M(NLD),R(NUL),R(NURL),R(NXL),R(NXLO),
     1 R(NS),R(NP),R(NPF),R(NTF),R(NU), R(NUR),R(NXC),R(NXCO),M(NIX)
     2 ,R(ND),M(NID),M(NJP),R(NSM),R(NV2),R(NVL),NST,NEN1,3)
      ASEM=.FALSE.
      DO 10 I=1,NEQ
      NN=M(NJP+I-1)
      IF(DB_FLAG) WRITE(83,*) 'EQ.NUM=',I,'NN=',NN,'OLD A(NN)=',A(NN)
      IF(DY_FLAG) A(NN)=A(NN)+A1*R(NSM+I-1)
      IF(DB_FLAG) WRITE(83,*) 'A(NN)=',A(NN),'R(NSM)=',R(NSM+I-1)
10    CONTINUE
C.....LDLT TRIANGULAR DECOMPOSITION
      CALL LDLT(A,M(NJP),NEQ)
C.....NODAL FORCE INPUT
      CALL PZERO(R(NUR),NNEQ)
      CALL PZERO(R(NFR),NNEQ)
      CALL PLOAD (M(NID),R(NF),R(NFR),NNEQ,NPROP,III,THITA)
      CALL PFORM(R(NF),R(NFR),M(NLD),R(NUL),R(NURL),R(NXL),R(NXLO),
     1 R(NS),R(NP),R(NPF),R(NTF),R(NU),R(NUR),R(NXC),R(NXCO),M(NIX),
     2 R(ND),M(NID),M(NJP),R(NSM),R(NV2),R(NVL),NST,NEN1,3)
      DO 16 I=1,NEQ
      IF(DB_FLAG) WRITE(83,*) 'EQ.NUM=',I,'OLD NFR=',R(NFR+I-1)
C--------------------------------------------------------------
C......KEY POINT: IF THE FOLLOWING EQUATION IS INCLUDED IN THE
ALGORITHM,
C......THE STABILITY IS NOT GOOD. THEREFORE, WE OMIT IT. THIS MEANS
THE FIRST
C......STEP WE GET THE STATIC SOLUTION AND USE THIS SOLUTION AS THE
INITIAL
C......VALUE FOR THE ITERATIONS TO GET THE EXACT DYNAMIC
SOLUTION. IN THIS
C......WAY, THE STABILITY CAN BE ALWAYS GARRANTEED.
C

C......NEWMARK , BATHE PAGE 352
C......FULL EFFECTIVE LOAD VECTOR
C......
      R(NFR+I-1)=R(NFR+I-1)-R(NSM+I-1)*(A2*R(NV1+I-1)+(A3)*R(NW1+I-1))
C--------------------------------------------------------------
      IF(DB_FLAG) WRITE(83,*) 'NEW NFR=',R(NFR+I-1)
      R(NUR+I-1)=R(NFR+I-1)
16    CONTINUE
```

```
C.....FORWARD ELIMINATION AND BACKWARD SUBSTITUTION
      CALL FORBACK(A,R(NUR),M(NJP),NEQ)
C.....FORBACK DOESN'T CHANGE THE CONTENT IN MATRIX A
C.....ITERATION DURING EACH LOADING STEP: NSTEP
C.....COMPUTE THE REACTION
      IF(DB_FLAG) THEN
         CALL PZERO(R(NPF),NNEQ)
         CALL PFORM(R(NF),R(NFR),M(NLD),R(NUL),R(NURL),R(NXL),R(NXLO),
     1   R(NS),R(NP),R(NPF),R(NTF),R(NU),R(NUR),R(NXC),R(NXCO),M(NIX)
     2   ,R(ND),M(NID),M(NJP),R(NSM),R(NV2),R(NVL),NST,NEN1,6)
         CALL PRTREAC(R(NPF),R(NF),M(NID),RDB,II,2)
         CALL PRTDIS(M(NID),R(NUR),R(NF),R(NV2),R(NW2),2)
      ENDIF
C
C--------------Beginning of Iteration-----------------------
      DO 40 III=1,NITEM
      write(*,*) 'ITERATION STEP=',III,'   LOADING STEP=',II
      write(6,*) 'ITERATION STEP=',III,'   LOADING STEP=',II
      IF(DB_FLAG) THEN
       write(7,*) 'ITERATION STEP=',III,'   LOADING STEP=',II
      ENDIF
      DO 31 I=1,NEQ
      IF(.NOT.DY_FLAG) THEN
        R(NWW+I-1)=0.0
      ELSE
         R(NWW+I-1)=A1*R(NUR+I-1)+A2*R(NV1+I-1)+(A3)*R(NW1+I-1)
      ENDIF
31    CONTINUE
C.....CALCULATE REFERENCE FORCE VECTOR TF
      CALL PZERO(R(NTF),NNEQ)
      CALL PFORM(R(NF),R(NFR),M(NLD),R(NUL),R(NURL),R(NXL),R(NXLO),
     1 R(NS),R(NP),R(NPF),R(NTF),R(NU),R(NUR),R(NXC),R(NXCO),M(NIX),
     2 R(ND),M(NID),M(NJP),R(NSM),R(NV2),R(NVL),NST,NEN1,7)
      DO 32 I=1,NEQ
      R(NUUR+I-1)=R(NFR+I-1)-R(NSM+I-1)*R(NWW+I-1)+R(NTF+I-1)

32    CONTINUE
      WRITE(*,*) 'F,A',R(NUUR+85-1),A(85)

C.....FORWARD ELIMINATION AND BACKWARD SUBSTITUTION
      CALL FORBACK(A,R(NUUR),M(NJP),NEQ)
C.....UPDATE INCREMENTAL DISPLACEMENT VECTOR
C.....CONVERGENCE CRITERIA - EULERIAN VECTOR NORM

      TOLRUUR=0.
```

```fortran
      TOLRUR=0.
      TOLC=0.

      DO 17 I=1,NEQ

        R(NUR+I-1)=R(NUR+I-1)+R(NUUR+I-1)

      TOLRUUR=TOLRUUR+R(NUUR+I-1)*R(NUUR+I-1)
      TOLRUR=TOLRUR+R(NUR+I-1)*R(NUR+I-1)


17    CONTINUE


C     WRITE(*,*) 'UUR,UR',85,R(NUUR+85-1),R(NUR+85-1)

      TOLC=SQRT(TOLRUUR)/SQRT(TOLRUR)
      WRITE(6,*) III,' ','TOLC = ',TOLC
      WRITE(*,*) III,' ','TOLC = ',TOLC

C.......
      IF(DB_FLAG) THEN
         DO 6 MM=1,NEQ
         WRITE(83,*) 'N=',MM,'FR+M*W=',R(NFR+MM-1)-R(NSM+MM-1)*
     1   R(NWW+MM-1),'TF=',R(NTF+MM-1)
6        WRITE(7,*) 'N=',MM,'NUR=',R(NUR+MM-1),'NUUR=',R(NUUR+MM-1)
         DO 7 MM=NEQ+1,NNEQ
         WRITE(83,*) 'n=',MM,'FR+M*W=',R(NFR+MM-1)-R(NSM+MM-1)*
     1   R(NWW+MM-1),'TF=',R(NTF+MM-1)
7        WRITE(7,*) 'n=',MM,'NUR=',R(NUR+MM-1),'NUUR=',R(NUUR+MM-1)
      ENDIF
C...........
C.....COMPUTE THE REACTION
         CALL PZERO(R(NPF),NNEQ)
         CALL PFORM(R(NF),R(NFR),M(NLD),R(NUL),R(NURL),R(NXL),R(NXLO),
     1   R(NS),R(NP),R(NPF),R(NTF),R(NU),R(NUR),R(NXC),R(NXCO),M(NIX)
     2   ,R(ND),M(NID),M(NJP),R(NSM),R(NV2),R(NVL),NST,NEN1,6)
c------------------------------------------------------------
      DO 33 I=1,NJ
      DO 33 J=1,NDF
      K1=(I-1)*NDF+J
      K2=M(NID+K1-1)
c        IF(K2.GT.0) R(NPF+K1-1)=-R(NSM+K2-1)*R(NWW+K2-1)+R(NPF+K1-1)
33    CONTINUE
c------------------------------------------------------------
      IF(DB_FLAG) THEN
```

```fortran
      CALL PRTREAC(R(NPF),R(NF),M(NID),RDB,II,2)
      CALL PRTDIS(M(NID),R(NUR),R(NF),R(NV2),R(NW2),2)
      ENDIF


c..... UAR .. Tolerance for the (Daht,1985?) Euclidian Vector norm=1%
      IF (TOLC.LT.0.01) GOTO 140
c     UAR


40    CONTINUE

140   WRITE(*,*) 'END OF INTERNAL ITER= ', III, ' TOLC=',TOLC
      WRITE(6,*) 'END OF INTERNAL ITER= ', III, ' TOLC=',TOLC
C-------------End of Iteration------------------------
      DO 18 I=1,NEQ
      IF(.NOT.DY_FLAG) THEN
          R(NU+I-1)=R(NU+I-1)+R(NUR+I-1)
      ELSE
        IF(N_W.EQ.0) THEN
            R(NU+I-1)=R(NU+I-1)+R(NUR+I-1)
            R(NW2+I-1)=A1*R(NUR+I-1)+A2*R(NV1+I-1)+A7*R(NW1+I-1)
            R(NV2+I-1)=R(NV1+I-1)+A8*R(NW1+I-1)+A0*R(NW2+I-1)
        ELSE
            R(NW2+I-1)=A0*R(NUR+I-1)+A7*R(NV1+I-1)+A8*R(NW1+I-1)
            R(NV2+I-1)=R(NV1+I-1)+0.5*DT*(R(NW2+I-1)+R(NW1+I-1))
            R(NU+I-1)=R(NU+I-1)+DT*R(NV1+I-1)+(DT*DT/6.0)*(R(NW2+I-1)
     *      +2.*R(NW1+I-1))
            R(NUR+I-1)=DT*R(NV1+I-1)+(DT*DT/6.0)*(R(NW2+I-1)
     *      +2.*R(NW1+I-1))
        ENDIF
      ENDIF
18    CONTINUE
      CALL PRTDIS(M(NID),R(NU),R(NF),R(NV2),R(NW2),1)
      CALL PLTDIS(R(NXC),R(NUR),M(NID),R(NF),R(NUXC),II,RDB)
C     CALL PLTVEL(R(NV2),M(NID),R(NF),R(NUXC),II,SPEED,RDB)
C     CALL PLTACL(R(NW2),M(NID),R(NF),R(NUXC),II,RDB)
C.....COMPUTE THE INCREMENTAL REACTION PERTICLUARLY FOR WILSON
METHOD
C     CALL PZERO(R(NPF),NNEQ)
C     CALL PFORM(R(NF),R(NFR),M(NLD),R(NUL),R(NURL),R(NXL),R(NXLO),
C   1 R(NS),R(NP),R(NPF),R(NTF),R(NU),R(NUR),R(NXC),R(NXCO),M(NIX)
C   2 ,R(ND),M(NID),M(NJP),R(NSM),R(NV2),R(NVL),NST,NEN1,6)
C     CALL PRTREAC(R(NPF),R(NF),M(NID),RDB,II,2)
C     CALL PRTDIS(M(NID),R(NUR),R(NF),R(NV2),R(NW2),2)
      DO 19 I=1,NNEQ
19    R(NTPF+I-1)=R(NTPF+I-1)+R(NPF+I-1)
```

```
      CALL PRTREAC(R(NTPF),R(NF),M(NID),RDB,II,1)
C.....COMPUTE ELEMENT STRESSES
      CALL PFORM(R(NF),R(NFR),M(NLD),R(NUL),R(NURL),R(NXL),R(NXLO),
     1 R(NS),R(NP),R(NPF),R(NTF),R(NU),R(NUR),R(NXC),R(NXCO),M(NIX)
     2 ,R(ND),M(NID),M(NJP),R(NSM),R(NV2),R(NVL),NST,NEN1,4)
c.....AVERAGE TANGENTIAL MODULUS IN EACH ELEMENT
      CALL PZERO(R(NV1),2*NNEQ)
      IF(.NOT.DY_FLAG) GOTO 24
      DO 22 I=1,NEQ
      R(NV1+I-1)=R(NV2+I-1)
22    R(NW1+I-1)=R(NW2+I-1)
24    CONTINUE
      CALL CUPDATE(R(NXC),R(NUR),M(NID),R(NF),M(NIX),NEN1)
C     CALL PLTFAL(M(NIX),M(NTEN),M(NSHE),NEN1,II,RDB)
      NPROP=NPROP+1
30    CONTINUE
C-----------------End of Increment Analysis--------------------
20    WRITE(*,2200) FO
c     WRITE(81,*) 'F'
      RETURN
2000  FORMAT(' NUMBER OF NODAL POINTS         =',I5/
     1      ' NUMBER OF ELEMENTS         =',I5/
     1      ' NUMBER OF MATERIALS        =',I5/
     1      ' NUMBER OF DEGREES/NODE       =',I5/
     1      ' NUMBER OF DIMENSION SPACE     =',I5/
     1      ' NUMBER OF NODES/ELEMENT      =',I5/)
2200  FORMAT(/' ** END OF FINITE ELEMENT PROGRAM **/
     1      '   THE RESULTS ARE STORED IN FILE : ',A9)
3000  FORMAT(' **PROBLEM SIZE TOO LARGE (INTEGER ARRAY)**')
3001  FORMAT(' **PROBLEM SIZE TOO LARGE (REAL ARRAY)**')
3500  FORMAT(' **FATAL ERROR** GLOBAL STIFFNESS MATRIX TOO BIG'/)
      END


C.........................................
      SUBROUTINE PFORM(F,FR,LD,UL,URL,XL,XLO,S,P,PF,TF,U,UR,X,XCO
     1 ,IX,D,ID,JP,SM,V2,VL,NST,NEN1,ISW)
      IMPLICIT REAL*8 (A-H,O-Z)
      LOGICAL ASEM,IT_FLAG
      COMMON/ASEM/ASEM
      COMMON/CDATA/NDF,NDM,NEN,NJ,NE,NEQ
      COMMON/ELDATA/LM,N,MA,MCT,IEL,NEL
      COMMON/INTERFACE/NINTR,CS,SN,H
      COMMON/PROCESS/NPROP,NITEM,IT_FLAG
      COMMON/DYNAMICS/SPEED,DT,THITA,BATA,GAMA
      DIMENSION UL(NDF,*),URL(NDF,*),U(*),UR(*),F(NDF,*),FR(*)
```

```
1 ,TF(*),S(NST,*),P(*),XL(NDM,*),X(NDM,*),D(20,*),IX(NEN1,*),
2 ID(NDF,*),LD(NDF,*),JP(*),SM(*),VL(NDF,*),V2(*),PF(NDF,*)
3 ,XCO(NDM,*),XLO(NDM,*)
  IEL=0
  MCT=0
  DO 110 N=1,NE
C.....ZEROLIZE UL,URL,S,P
  CALL PZERO(UL,NST*(NST+5))
  CALL PZERO(VL,NST)
  MA=IX(NEN1,N)
  DO 108 I=1,NEN
  II=IX(I,N)
  IF(II.NE.0) GO TO 105
  DO 102 J=1,NDF
102  LD(J,I)=0
  GO TO 108
105  IID=II*NDF-NDF
  NEL=I
  DO 106 J1=1,NDM
  XLO(J1,I)=XCO(J1,II)
106  XL(J1,I)=X(J1,II)
  DO 107 J=1,NDF
  K=ID(J,II)
  IF(K.GT.0) then
      URL(J,I)=UR(K)
      VL(j,I)=V2(K)
  endif
  INEN=I+NEN
  IF(K.LT.0) then
C.....REMEMBER THAT ONLY THE CALCULATION OF ELEMENT NODAL
REACTION FORCE TF
C.....DO NOT REQUIRE THE SPECIFIED DISPLACEMENT. IN OTHER CASES,
SUCH AS
C.....THE CALCULATION OF TOTAL REACTION NODAL REACTION FORCE
AND ELEMENT
C.....STRESS DO REQUIRE INCLUDING THE SPECIFIED DISPLACEMENTS.
      IF(ISW.EQ.6.OR.ISW.EQ.4) URL(J,I)=F(J,II)
      IF(ISW.EQ.7) URL(J,I)=0.0
      URL(J,INEN)=F(J,II)
       IF(ABS(F(J,II)).GT.1.0E-5) THEN
         VL(J,I)=F(J,II)/DT
       ELSE
         VL(J,I)=0.0
       ENDIF
   ENDIF
```

```fortran
      IF(ISW.EQ.6) K= IID+J
107   LD(J,I)=K
108   CONTINUE
      IE20=D(20,MA)
      IF(IE20.NE.IEL) MCT=0
      IEL=IE20
      CALL
ELEMLIB(D(1,MA),UL,URL,XL,XLO,IX(1,N),S,P,VL,NDF,NDM,NST,ISW)
      IF(ASEM.AND.ISW.EQ.3) CALL ADDSTF(LD,JP,S,NST)
      IF(ISW.EQ.7) CALL BASBLY(TF,P,LD,NST)
130   IF(ISW.EQ.6) CALL BASBLY(PF,P,LD,NST)
      IF(.NOT.ASEM.AND.ISW.EQ.3) CALL MODIFY(FR,LD,S,URL(1,NEN+1)
     *   ,NST)
      IF(.NOT.ASEM.AND.ISW.EQ.3) CALL BASBLY(FR,P,LD,NST)
      IF(ISW.EQ.5) THEN
          DO 122 I=1,NEN
          DO 122 J=1,NDF
          K=LD(J,I)
          KK=(I-1)*NDF+J
          IF(K.GT.0) SM(K)=SM(K)+P(KK)
122   CONTINUE
      ENDIF
110   CONTINUE
      RETURN
      END


C...................................................
      SUBROUTINE PGAUSS(L,LINT,R,Z,W)
C.... GAUSS POINTS AND WEIGHTS FOR TWO DIMENSIONS
C
      IMPLICIT REAL*8 (A-H,O-Z)
      COMMON /ELDATA/ LM,N,MA,MCT,IEL,NEL
      DIMENSION LR(9),LZ(9),LW(9),R(3),Z(3),W(3),G4(4),H4(4)
      DATA LR/-1,1,1,-1,0,1,0,-1,0/,LZ/-1,-1,1,1,-1,0,1,0,0/
      DATA LW/4*25,4*40,64/
      LINT = L*L
      GO TO (1,2,3,4),L
C.... 1X1 INTEGRATION
1     R(1) = 0.0E0
      Z(1) = 0.0E0
      W(1) = 4.0E0
      IF(NEL.EQ.3) THEN
      Z(1) = -1.0E0/3.0E0
      W(1) = 3.0E0
      END IF
```

```
      RETURN
C.... 2X2 INTEGRATION
2     G = 1.0E0/SQRT(3.0E0)
      DO 21 I = 1,4
      R(I) = G*LR(I)
      Z(I) = G*LZ(I)
21    W(I) = 1.0E0
      RETURN
C.... 3X3 INTEGRATION
3     G = SQRT(0.6E0)
      H = 1.0E0/81.0E0
      DO 31 I = 1,9
      R(I) = G*LR(I)
      Z(I) = G*LZ(I)
31    W(I) = H*LW(I)
      RETURN
C.... 4X4 INTEGRATION
4     G = SQRT(4.8E0)
      H = SQRT(30.0E0)/36.0E0
      G4(1) = SQRT((3.0E0+G)/7.0E0)
      G4(4) = - G4(1)
      G4(2) = SQRT((3.0E0-G)/7.0E0)
      G4(3) = -G4(2)
      H4(1) = 0.50E0 - H
      H4(2) = 0.50E0 + H
      H4(3) = 0.50E0 + H
      H4(4) = 0.50E0 - H
      I = 0
      DO 41 J = 1,4
      DO 41 K = 1,4
      I = I + 1
      R(I) = G4(K)
      Z(I) = G4(J)
      W(I) = H4(J)*H4(K)
41    CONTINUE
      RETURN
      END


C.........................................
      SUBROUTINE PLOAD(ID,F,FR,NN,NPROP,III,THITA)
      IMPLICIT REAL*8 (A-H,O-Z)
      LOGICAL GE_FLAG,DY_FLAG,DB_FLAG,MA_FLAG,UL_FLAG,ST_FLAG,
     * SC_FLAG
      DIMENSION F(1),ID(1),FR(1)
      COMMON /FLAG_BLO/ GE_FLAG,DY_FLAG,DB_FLAG,MA_FLAG,UL_FLAG,
```

```
      *  ST_FLAG,SC_FLAG
         DO 50 I=1,NN
50    FR(I)=0.0
         DO 100 N=1,NN
         J=ID(N)
C     IF(.NOT.DY_FLAG) THEN
            IF(J.GT.0) THEN
               IF(NPROP.EQ.1) THEN
                  FR(J)=F(N)+FR(J)
               ENDIF
            ENDIF
C     ELSE
C         IF(J.GT.0) FR(J)=F(N)*(NPROP-1.)+F(N)*THITA+FR(J)
C     ENDIF
100   CONTINUE
         RETURN
         END


c.................................................
C.....GENERATE ACCELERA.FIL FILE FOR PLOT COMMAND TO
C.....PLOT THE ACCELERATION FIELD CONFIGURATION
         SUBROUTINE PLTACL(W,ID,F,D,NN,RDB)
         IMPLICIT REAL*8 (A-H,O-Z)
         LOGICAL IT_FLAG
         DIMENSION W(*),ID(NDF,*),F(NDF,*),D(NDM,*)
         COMMON/CDATA/NDF,NDM,NEN,NJ,NE,NEQ
         COMMON/PROCESS/NPROP,NITEM,IT_FLAG
         DO 110 N=1,NJ
         DO 110 I=1,NDM
         K=ID(I,N)
         IF(K.LT.0) D(I,N)=0.0
         IF(K.GT.0) D(I,N)=W(K)
110   CONTINUE
         DISPLACE=RDB*NPROP
         WRITE(85,*) NN,DISPLACE
         WRITE(85,1000) ((D(I,N),I=1,NDM),N=1,NJ)
         RETURN
1000  FORMAT(6E15.7)
         END


c.................................................
C.....GENERATE DISPLACE.FIL FILE FOR PLOT COMMAND TO
C.....PLOT THE DEFORMED MESH CONFIGURATION
         SUBROUTINE PLTDIS(X,UR,ID,F,D,NN,RDB)
         IMPLICIT REAL*8 (A-H,O-Z)
```

```
      LOGICAL IT_FLAG
      DIMENSION X(NDM,*),UR(*),ID(NDF,*),F(NDF,*),D(NDM,*)
      COMMON/PROCESS/NPROP,NITEM,IT_FLAG
      COMMON/CDATA/NDF,NDM,NEN,NJ,NE,NEQ
      DO 110 N=1,NJ
      DO 110 I=1,NDM
      K=ID(I,N)
      IF(K.LT.0) D(I,N)=X(I,N)+F(I,N)
      IF(K.GT.0) D(I,N)=X(I,N)+UR(K)
110   CONTINUE
      DISPLACE=RDB*NPROP
      WRITE(81,*) NN,DISPLACE
      WRITE(86,*) NN,DISPLACE
      WRITE(81,1000) ((D(I,N),I=1,NDM),N=1,NJ)
      WRITE(86,1000) ((D(I,N),I=1,NDM),N=1,NJ)
      RETURN
1000  FORMAT(3E23.15)
      END


C........................................................
C.....GENERATE DATA FILE TO PLOT THE FAILURE ZONE IN FRONT OF TOOL
      SUBROUTINE PLTFAL(IX,NTENSILE,NSHEAR,NEN1,NN,RDB)
      IMPLICIT REAL*8 (A-H,O-Z)
      LOGICAL IT_FLAG
      DIMENSION NTENSILE(NEN,*),NSHEAR(NEN,*),IX(NEN1,*)
      DIMENSION V(20)
      COMMON/CDATA/NDF,NDM,NEN,NJ,NE,NEQ
      COMMON/PROCESS/NPROP,NITEM,IT_FLAG
      DO 10 N=1,NE
      MA=IX(NEN1,N)
      NMA=ma+48
      LINT=4
      IF(NDM.EQ.3) LINT=8
      DO 12 L9 = 1,LINT
      NNN=(N-1)*LINT+L9
      IF(NDM.EQ.2) READ(NMA,REC=NNN) (V(I),I=1,14)
      IF(NDM.EQ.3) READ(NMA,REC=NNN) (V(I),I=1,20)
      NTENSILE(L9,N)=0
      NSHEAR(L9,N)=0
      IF(NDM.EQ.2) THEN
        IF(V(14).GE.0.5) NTENSILE(L9,N)=1
        IF(V(13).GE.0.5) NSHEAR(L9,N)=1
      ENDIF
      IF(NDM.EQ.3) THEN
        IF(V(19).GE.0.5) NSHEAR(L9,N)=1
```

```
      IF(V(20).GE.0.5) NTENSILE(L9,N)=1
      ENDIF
12    CONTINUE
10    CONTINUE
      DISPLACE=RDB*NPROP
      WRITE(82,*) NN,DISPLACE
      WRITE(82,1000) ((NTENSILE(I,J),NSHEAR(I,J),I=1,LINT),J=1,NE)
      RETURN
1000  FORMAT(10(2X,I4,2X,I4))
      END


c..............................................
C.....GENERATE VELOCITY.FIL FILE FOR PLOT COMMAND TO
C.....PLOT THE VELOCITY FIELD CONFIGURATION
      SUBROUTINE PLTVEL(V,ID,F,D,NN,SPEED,RDB)
      IMPLICIT REAL*8 (A-H,O-Z)
      LOGICAL IT_FLAG
      DIMENSION V(*),ID(NDF,*),F(NDF,*),D(NDM,*)
      COMMON/CDATA/NDF,NDM,NEN,NJ,NE,NEQ
      COMMON/PROCESS/NPROP,NITEM,IT_FLAG
      DO 110 N=1,NJ
      DO 110 I=1,NDM
      K=ID(I,N)
      IF(K.LT.0) THEN
         D(I,N)=0.0
         IF(F(I,N).GE.1.E-05) D(I,N)=SPEED
      ENDIF
      IF(K.GT.0) D(I,N)=V(K)
110   CONTINUE
      DISPLACE=RDB*NPROP
      WRITE(84,*) NN,DISPLACE
      WRITE(84,1000) ((D(I,N),I=1,NDM),N=1,NJ)
      RETURN
1000  FORMAT(6E15.7)
      END


c....Uriel A. Rosa  June 6,96
c....Uriel A. Rosa  June 1,96
C....................................................
      SUBROUTINE PMESH(XC,XLO,IX,ID,D,UL,URL,S,P,NEN1,NST)
C.....DATA INPUT AND GENERATION ROUTINE
      IMPLICIT REAL*8 (A-H,O-Z)
      CHARACTER COOR*6,XX*18
      COMMON/CDATA/NDF,NDM,NEN,NJ,NE,NEQ
      COMMON/MDATA/NUMMAT
```

```
      COMMON/ELDATA/LM,N,MA,MCT,IEL,NEL
      COMMON /FLAG_BLO/ GE_FLAG,DY_FLAG.DB_FLAG.MA_FLAG.UL_FLAG.
     * ST_FLAG,SC_FLAG
      DIMENSION XC(NDM,*),XLO(NDM,*),IX(NEN1.*),ID(NDF.*),D(20,*)
      LOGICAL ERR,GE_FLAG,DY_FLAG,DB_FLAG,MA_FLAG,UL_FLAG,
     * ST_FLAG,SC_FLAG
      DATA XX/' NODAL COORDINATES'/COOR/' COOR '/

C.....GENERATE PLOTMESH.FIL DATA FILE
      INQUIRE(FILE='PLOTMESH.FIL',EXIST=ERR)
      IF(ERR) THEN
          OPEN(80,FILE='PLOTMESH.FIL',status='old')
          CLOSE(80,STATUS='DELETE')
      ENDIF
      OPEN(80,FILE='PLOTMESH.FIL',status='new')

C.....GENERATE MSH.DAT DATA FILE
      INQUIRE(FILE='MSH.DAT',EXIST=ERR)
      IF(ERR) THEN
          OPEN(88,FILE='MSH.DAT',status='old')
          CLOSE(88,STATUS='DELETE')
      ENDIF
      OPEN(88,FILE='MSH.DAT',status='new')

C.....NODAL COORDINATES DATA INPUT
1     CALL GENVEC(NDM,XC,XX,COOR,NJ,ERR)
      IF(ERR) WRITE(*,3000)
      IF(ERR) STOP
C.....ELEMENT DATA INPUT
2     CALL ELDAT(IX,NEN1)
C.....GENERATE PLOTMESH.FIL
      WRITE(80,*) 'T'
      WRITE(80,*) NJ,NE,NDF,NEN,NDM
      WRITE(80,1000) ((XC(I,J),I=1,NDM),J=1,NJ)
      WRITE(80,1100) ((IX(I,J),I=1,NEN),J=1,NE)
      WRITE(80,*) 'F'

C.....GENERATE MSH.DAT
      WRITE(88,*) '/PREP7'
      WRITE(88,*) '/TITLE,Title,Dynat8'
      WRITE(88,*) 'ET,1,45'
      WRITE(88,*) 'EX,1,10'
      WRITE(88,*) 'EY,1,10'
      WRITE(88,*) 'EZ,1,10'
      WRITE(88,*) ' '
```

```
      WRITE(88,1088) (J,(XC(I,J),I=1,NDM),J=1,NJ)
      WRITE(88,1188) ((IX(I,J),I=1,NEN),J=1,NE)

c     WRITE(88,*) ' '
c     WRITE(88,*) 'NPLOT'
c     WRITE(88,*) 'EPLOT'
c     WRITE(88,*) 'ITER,1,1'
c     WRITE(88,*) 'AFWRITE'
c     WRITE(88,*) 'FINISH'
c     WRITE(88,*) '/INPUT,27'
c     WRITE(88,*) 'FINISH'

C.....MATERIAL DATA INPUT
3     DO 304 N=1,NUMMAT
      READ(5,*) MA,IEL
      IF(DB_FLAG) WRITE(6,2000) MA,IEL
      IF(SC_FLAG) WRITE(*,2000) MA,IEL
      IF(MA.EQ.0) GO TO 4
      CALL PZERO(D(1,MA),20)
      D(20,MA)=IEL
      CALL ELEMLIB(D(1,MA),UL,URL,XC,XLO,IX,S,P,VL,NDF,NDM,NST,1)
304   CONTINUE
C.....BOUNDARY CONDITIONS INPUT
c1000  FORMAT(10E15.7)
c1100  FORMAT(16(4X,I5))
1000  format(3e15.7)
1100  format(4(4x,i5))

C.....FORMAT FOR MSH.DAT
1088  FORMAT ((((' N,',I5,3(',',E15.7))))
1188  FORMAT ((((' E',8(',',I5))))

1200  format(4x,A1)
2000  FORMAT(/' MATERIAL TYPE ',I4,' ELEMENT TYPE ',I4/)
4     CALL BOUN(ID)
      WRITE(*,*) ' END OF MESH GENERATION'
3000  FORMAT(' **FATAL ERROR** IN MESH GENERATION')
      RETURN
      END

C..................................................
      SUBROUTINE PROFIL(JP,ID,IX,NEN1,NK)
      IMPLICIT REAL*8 (A-H,O-Z)
      COMMON/CDATA/NDF,NDM,NEN,NJ,NE,NEQ
```

```fortran
      DIMENSION JP(1),ID(NDF,1),IX(NEN1,*)
C.....SET UP EQUATION NUMBERS
      NEQ=0
      NAD=0
      DO 50 N=1,NJ
      DO 40 I=1,NDF
      J=ID(I,N)
      IF(J) 30,20,30
20    NEQ=NEQ+1
      ID(I,N)=NEQ
      JP(NEQ)=0
      GO TO 40
30    NAD=NAD-1
      ID(I,N)=NAD
C     WRITE(6,*) 'N=',N,'NAD=',NAD
40    CONTINUE
50    CONTINUE
C.....COMPUTE ROW BANDWIDTH
      DO 500 N=1,NE
      DO 400 I=1,NEN
      II=IX(I,N)
      IF(II.EQ.0) GO TO 400
      DO 300 K=1,NDF
      KK=ID(K,II)
      IF(KK.LE.0) GO TO 300
      DO 200 J=1,NEN
      JJ=IX(J,N)
      IF(JJ.EQ.0) GO TO 200
      DO 100 L=1,NDF
      LL=ID(L,JJ)
      IF(LL.LE.0) GO TO 100
      M=MAX0(KK,LL)
      JP(M)=MAX0(JP(M),IABS(KK-LL))
100   CONTINUE
200   CONTINUE
300   CONTINUE
400   CONTINUE
500   CONTINUE
C.....COMPUTE DIAGONAL POINTERS FOR PROFIL
      NK=1
      JP(1)=1
      IF(NEQ.EQ.1) RETURN
      DO 600 N=2,NEQ
600   JP(N)=JP(N)+JP(N-1)+1
      NK=JP(NEQ)
```

```
      WRITE(*,2000)NK
2000  FORMAT(' THE MAXIMUM STORAGE OF GLOBAL STIFFNESS =',I6/)
      RETURN
      END


C.............................................................
C.....NSIGN=1, TO OUTPUT TOTAL DISPLACEMENT
C.....NSIGN=2, TO OUTPUT INCREMENTAL DISPLACEMENT
      SUBROUTINE PRTDIS(ID,U,F,V2,W2,NSIGN)
      IMPLICIT REAL*8 (A-H,O-Z)
      LOGICAL DB_FLAG,GE_FLAG,DY_FLAG,MA_FLAG,UL_FLAG,ST_FLAG
     * ,SC_FLAG
      COMMON/CDATA/NDF,NDM,NEN,NJ,NE,NEQ
      COMMON/PROCESS/NPROP,NITEM
      COMMON /FLAG_BLO/GE_FLAG,DY_FLAG,DB_FLAG,MA_FLAG,UL_FLAG,
     * ST_FLAG,SC_FLAG
      DIMENSION ID(NDF,*),U(*),F(NDF,*),UL(6),V2(*),W2(*),VL(6),WL(6)
      DO 102 II=1,NJ,50
      IF(DB_FLAG) THEN
         IF(NSIGN.EQ.1) WRITE(6,2000)(K,K=1,NDF)
         IF(NSIGN.EQ.2) WRITE(6,2002)(K,K=1,NDF)
      ENDIF
      JJ=MIN0(NJ,II+49)
      DO 102 N=II,JJ
      NOUT=0
      DO 100 I=1,NDF
      K=ID(I,N)
C     IF(K.LT.0) U(NEQ-K)=F(I,N)*NPROP
      IF(K.LT.0) THEN
         IF(NSIGN.EQ.1) UL(I)=F(I,N)*NPROP
         IF(NSIGN.EQ.2) UL(I)=F(I,N)
         VL(I)=V2(NEQ-K)
         WL(I)=W2(NEQ-K)
      ENDIF
      IF(K.GT.0) THEN
         UL(I)=U(K)
         VL(I)=V2(K)
         WL(I)=W2(K)
      ENDIF
      IF(ABS(F(I,N)).GT.1.E-6) NOUT=1
100   CONTINUE
      IF(DB_FLAG) THEN
         IF(NOUT.EQ.1) WRITE(6,2001) N,(UL(I),I=1,NDF)
      ENDIF
102   CONTINUE
```

```
      RETURN
2000  FORMAT(///1X,'NODAL DISPLACEMENTS'/2X,'NODE',6(I8,'DISP'))
2001  FORMAT(I6,6E12.4)
2002  FORMAT(///1X,'INCREMENT DISPLACE'/2X,'NODE',6(I8,'DISP'))
      END


C.....Modified........Uriel A. Rosa   Feb 01/96 & May 11/96
C.....................................
      SUBROUTINE PRTREAC(R,F,ID,RDB,II,NSort)
      IMPLICIT REAL*8 (A-H,O-Z)
      LOGICAL  GE_FLAG,DY_FLAG,DB_FLAG,MA_FLAG,UL_FLAG,ST_FLAG
     * ,SC_FLAG
      COMMON/CDATA/NDF,NDM,NEN,NJ,NE,NEQ
      COMMON/PROCESS/NPROP,NITEM
      COMMON /FLAG_BLO/ GE_FLAG,DY_FLAG,DB_FLAG,MA_FLAG,UL_FLAG,
     * ST_FLAG,SC_FLAG
      DIMENSION F(NDF,*),ID(NDF,*)
      REAL*8 R(NDF,*),RSUM(6),FORC(6)
      NNEQ=NDF*NJ
      DO 50 K=1,NDF
      RSUM(K)=0.0
      FORC(K)=0.0
50    CONTINUE
      disp=RDB*NPROP
      WRITE(7,*) 'N=',II,'     DISP=',DISP
      WRITE(*,*) 'DISP=',DISP
      WRITE(6,*) 'DISP=',DISP
      IF(.NOT.DB_FLAG) THEN
          IF(NSort.EQ.1) THEN
        WRITE(6,2004) (K,K=1,NDF)
        WRITE(7,2004) (K,K=1,NDF)
      ENDIF
      IF(NSort.EQ.2) THEN
        WRITE(6,2000) (K,K=1,NDF)
        WRITE(7,2000) (K,K=1,NDF)
        ENDIF
      ENDIF
      DO 100 N=1,NJ,50
      J=MIN0(NJ,N+49)
      IF(DB_FLAG) THEN
        IF(NSort.EQ.1) THEN
          WRITE(6,2004) (K,K=1,NDF)
          WRITE(7,2004) (K,K=1,NDF)
        ENDIF
        IF(NSort.EQ.2) THEN
```

292

```
          WRITE(6,2000) (K,K=1,NDF)
          WRITE(7,2000) (K,K=1,NDF)
            ENDIF
        ENDIF
        DO 100 I=N,J
        DO 75 K=1,NDF
C     R(K,I)=-R(K,I)
        RSUM(K)=RSUM(K)-R(K,I)
75    CONTINUE
        DO 76 K=1,NDF
76    IF(ABS(R(K,I)).GT.1.0E-3) GO TO 77
        GO TO 100
77    IF(DB_FLAG) WRITE(6,2001) I,(-R(K,I),K=1,NDF)
100   CONTINUE
c********************************************
        DO 120 N=1,NJ
        NSIGN=0
        DO 110 I=1,NDF
        K=ID(I,N)
        IF(K.LT.0) THEN
            IF(ABS(F(I,N)).GT.1.E-6) THEN
              NSIGN=1
            ENDIF
        ENDIF
110   CONTINUE
        IF(NSIGN.EQ.1) THEN
            DO 115 I=1,NDF
115   FORC(I)=FORC(I)-R(I,N)
C       WRITE(6,2001) N,(-R(K,N),K=1,NDF)
C       WRITE(7,2001) N,(-R(K,N),K=1,NDF)
        ENDIF
120   CONTINUE
        WRITE(7,2003)(FORC(K),K=1,NDF)
        WRITE(*,2003)(FORC(K),K=1,NDF)
        WRITE(6,2003)(FORC(K),K=1,NDF)
        WRITE(6,2002)(RSUM(K),K=1,NDF)
        WRITE(7,2002)(RSUM(K),K=1,NDF)
        WRITE(*,2002)(RSUM(K),K=1,NDF)

        WRITE(89,5000) II,(',',FORC(K),K=1,NDF)
C       WRITE(*,5000) II,(',',FORC(K),K=1,NDF)


c********************************************
        RETURN
2000  FORMAT(/5X,'INCREM. REACTIONS'/2X,'NODE',6(I8,' DOF'))
```

293

```
2001  FORMAT(I6,6E12.4)
2002  FORMAT(3X,'TOTAL SUM',6E12.4)
2003  FORMAT(3X,'LOCAL SUM',6E12.4)
2004  FORMAT(/5X,'TOTAL REACTIONS'/2X,'NODE',6(I8,' DOF'))
5000  FORMAT(I6,3(A1,E12.4))
      END


C.........................................................
      SUBROUTINE PSTRES(SIG,P1,P2,P3)
      IMPLICIT REAL*8 (A-H,O-Z)
C.... COMPUTE PRINCIPAL STRESSES (2 DIMENSIONS)
C
      DIMENSION SIG(3)
C.... STRESSES MUST BE STORED IN ARRAY SIG(3) IN THE ORDER
C    TAU-XX,TAU-XY,TAU-YY
      XI1 = (SIG(1) + SIG(3))/2.0E0
      XI2 = (SIG(1) - SIG(3))/2.0E0
      RHO = SQRT(XI2*XI2 + SIG(2)*SIG(2))
      P1 = XI1 + RHO
      P2 = XI1 - RHO
      P3 = 45.0E0
      IF(XI2.NE.0.0) P3 = 22.5E0*ATAN2(SIG(2),XI2)/ATAN(1.0)
      RETURN
      END


C.........................................................
      SUBROUTINE PZERO(P,N)
      IMPLICIT REAL*8 (A-H,O-Z)
      DIMENSION P(N)
      DO 100 I=1,N
100   P(I)=0.0
      RETURN
      END


C.........................................................
      SUBROUTINE ROTATE(S,CS,SN,NST,NDF,FLAG)
      IMPLICIT REAL*8 (A-H,O-Z)
      LOGICAL FLAG
      DIMENSION S(NST,NST)
C.....ROTATE TO GLOBAL FRAME
      IF(CS.EQ.1.) RETURN
      DO 13 I=1,NST,NDF
      J=I+1
      DO 11 N=1,NST
      T     =S(N,I)*CS-S(N,J)*SN
```

```fortran
      S(N,J) =S(N,I)*SN+S(N,J)*CS
11    S(N,I) = T
13    CONTINUE
      IF(.NOT.FLAG) RETURN
      DO 14 I =1,NST,NDF
      J= I+1
      DO 12 N=1,NST
      T     =S(I,N)*CS-S(J,N)*SN
      S(J,N) =S(I,N)*SN+S(J,N)*CS
12    S(I,N)=T
14    CONTINUE
      RETURN
      END


c Function to determine lapsed time from BASE
* This version works for any period up to 24 hours.
c A.E. Krause
c
      REAL FUNCTION SECNDS(BASE)
      implicit none
      include 'definiti.fd'
      REAL BASE,TIME
      INTEGER IHR,IMIN,ISEC,I100TH,IYR,IMON,IDAY,DAY_START,year_start,
     +    month_start,day_of_year_start,sum,i,day_of_year
      integer days(12),tdays(12)
      logical leap_year,leap_year_start
      SAVE DAY_START,month_start,year_start,days,tdays,
     +  day_of_year_start
      data days/31,28,31,30,31,30,31,31,30,31,30,31/
      CALL GETDAT(IYR,IMON,IDAY)
      IF(BASE.EQ.0.0)THEN
         sum=0
         leap_year_start=FALSE
         do i=1,12
            tdays(i)=sum
            if(i.eq.2.AND.leap_year(IYR))then
               sum=sum+1
               leap_year_start=TRUE
            endif
            sum=sum+days(i)
         enddo
         year_start=IYR
         month_start=IMON
         day_start=IDAY
         day_of_year_start=tdays(month_start)+day_start
```

```fortran
      ENDIF
      CALL GETTIM(IHR,IMIN,ISEC,I100TH)
      TIME=(100*(60*(IMIN+60*IHR)+ISEC)+I100TH)/100.0
      IF(IDAY.NE.DAY_START.OR.IMON.NE.month_start)THEN
        day_of_year=tdays(IMON)+IDAY
        TIME=TIME+(day_of_year-day_of_year_start)*86400.0
      ENDIF
      SECNDS=TIME-BASE
      RETURN
      END
    logical function leap_year(year)
    implicit none
    integer year
    leap_year=((mod(year,4).eq.0.AND.mod(year,100).ne.0).OR.
   +  (mod(year,400).eq.0))
    return
    end


C......................................................
      SUBROUTINE SETMEM(N,M,ERR)
C.....MONITOR AVAILABLE MEMORY
      IMPLICIT REAL*8 (A-H,O-Z)
      LOGICAL ERR
      ERR=.FALSE.
      IF(N.LE.M) RETURN
      ERR=.TRUE.
      WRITE(*,2000) N,M
      WRITE(6,2000) N,M
      RETURN
2000  FORMAT(5X,'**INSUFFICIENT STORAGE**',5X,'REQUIRED =',I8,5X,
   1      'AVAILABLE =',I8/)
      END


C......................................................
      SUBROUTINE SHAP2(S,T,SHP,IX,NEL)
C.... ADD QUADRATIC FUNCTIONS AS NECESSARY
      IMPLICIT REAL*8 (A-H,O-Z)
      DIMENSION IX(*),SHP(3,*)
      S2 = (1.0E0-S*S)/2.0E0
      T2 = (1.0E0-T*T)/2.0E0
      DO 100 I=5,9
      DO 100 J = 1,3
100   SHP(J,I) = 0.0
C.... MIDSIDE NODES (SERENDIPITY)
      IF(IX(5).EQ.0) GO TO 101
```

```
      SHP(1,5) = -S*(1.0E0-T)
      SHP(2,5) = -S2
      SHP(3,5) = S2*(1.0E0-T)
101   IF(NEL.LT.6) GO TO 107
      IF(IX(6).EQ.0) GO TO 102
      SHP(1,6) = T2
      SHP(2,6) = -T*(1.0E0+S)
      SHP(3,6) = T2*(1.0E0+S)
102   IF(NEL.LT.7) GO TO 107
      IF(IX(7).EQ.0) GO TO 103
      SHP(1,7) = -S*(1.0E0+T)
      SHP(2,7) = S2
      SHP(3,7) = S2*(1.0E0+T)
103   IF(NEL.LT.8) GO TO 107
      IF(IX(8).EQ.0) GO TO 104
      SHP(1,8) = -T2
      SHP(2,8) = -T*(1.0E0-S)
      SHP(3,8) = T2*(1.0E0-S)
C.... INTERIOR NODE (LAGRANGIAN)
104   IF(NEL.LT.9) GO TO 107
      IF(IX(9).EQ.0) GO TO 107
      SHP(1,9) = -4.0E0*S*T2
      SHP(2,9) = -4.0E0*T*S2
      SHP(3,9) = 4.0E0*S2*T2
C.... CORRECT EDGE NODES FOR INTERIOR NODE (LAGRANGIAN)
      DO 106 J= 1,3
      DO 105 I = 1,4
105   SHP(J,I) = SHP(J,I) - 0.25E0*SHP(J,9)
      DO 106 I = 5,8
106   IF(IX(I).NE.0) SHP(J,I) = SHP(J,I) - .5E0*SHP(J,9)
C.... CORRECT CORNER NODES FOR PRESENSE OF MIDSIDE NODES
107   K = 8
      DO 109 I = 1,4
      L = I + 4
      DO 108 J = 1,3
108   SHP(J,I) = SHP(J,I) - 0.5E0*(SHP(J,K)+SHP(J,L))
109   K = L
      RETURN
      END


C................................................
      SUBROUTINE SHAPE(SS,TT,X,SHP,XSJ,NDM,NEL,IX,FLG)
      IMPLICIT REAL*8 (A-H,O-Z)
      LOGICAL FLG
      DIMENSION SHP(3,*),X(NDM,1),S(4),T(4),XS(2,2),SX(2,2),IX(*)
```

```fortran
      DATA S/-0.5E0,0.5E0,0.5E0,-0.5E0/,T/-0.5E0,-0.5E0,0.5E0,0.5E0/
C.... FORM 4-NODE QUADRILATERAL SHAPE FUNCTIONS
      DO 100 I = 1,4
      SHP(3,I) = (0.5e0+S(I)*SS)*(0.5e0+T(I)*TT)
      SHP(1,I) = S(I)*(0.5e0+T(I)*TT)
100   SHP(2,I) = T(I)*(0.5e0+S(I)*SS)
      IF(NEL.GE.4) GO TO 120
C.... FORM TRIANGLE BY ADDING THIRD AND FOURTH TOGETHER
      DO 110 I=1,3
110   SHP(I,3) = SHP(I,3)+SHP(I,4)
C.... ADD QUADRATIC TERMS IF NECESSARY
120   IF(NEL.GT.4) CALL SHAP2(SS,TT,SHP,IX,NEL)
C.... CONSTRUCT JACOBIAN AND ITS INVERSE
      DO 130 I = 1,NDM
      DO 130 J = 1,2
      XS(I,J) = 0.0
      DO 130 K = 1,NEL
130   XS(I,J) = XS(I,J) + X(I,K)*SHP(J,K)
      XSJ = XS(1,1)*XS(2,2)-XS(1,2)*XS(2,1)
      IF(FLG) RETURN
      SX(1,1) = XS(2,2)/XSJ
      SX(2,2) = XS(1,1)/XSJ
      SX(1,2) =-XS(1,2)/XSJ
      SX(2,1) =-XS(2,1)/XSJ
C.... FORM GLOBAL DERIVATIVES
      DO 140 I = 1,NEL
      TP      = SHP(1,I)*SX(1,1)+SHP(2,I)*SX(2,1)
      SHP(2,I) = SHP(1,I)*SX(1,2)+SHP(2,I)*SX(2,2)
140   SHP(1,I) = TP
      RETURN
      END


C.....Uriel A.Rosa...June 03,96
C.....Uriel A.Rosa...May 30,96
C..................................................
c.....DETERMINE THE VALUE OF KNOWN DISPLACEMENT RDB AND SEND
C.....IT TO UPPER-LEVEL SUBROUTINE
      SUBROUTINE VALBOUN(F,ID,RDB)
      IMPLICIT REAL*8 (A-H,O-Z)
      DIMENSION ID(NDF,*),F(NDF,*)
      COMMON/CDATA/NDF,NDM,NEN,NJ,NE,NEQ
      DO 120 N=1,NJ
      DO 110 I=1,NDM
      K=ID(I,N)
C     UAR
```

```fortran
C     WRITE(88,*) 'ID(I,N)',ID(I,N)
C     UAR
      IF(K.LT.0) THEN
          IF(F(I,N).GT.1.E-6) RDB=F(I,N)
          END IF

110   CONTINUE

C     UAR - Restr.

      IF(ID(1,N).LT.0.0) THEN
       WRITE(88,428) N,F(1,N)
      END IF
      IF(ID(2,N).LT.0.0) THEN
       WRITE(88,429) N,F(2,N)
      END IF
      IF(ID(3,N).LT.0.0) THEN
       WRITE(88,430) N,F(3,N)
      END IF


C     UAR - Forces

      IF(ID(1,N).GT.0) THEN
        WRITE(88,501) N,F(1,N)
      END IF

      IF(ID(2,N).GT.0) THEN
       WRITE(88,502) N,F(2,N)
      END IF

       IF(ID(3,N).GT.0) THEN
       WRITE(88,503) N,F(3,N)
      END IF

C     UAR

120   CONTINUE

      WRITE(88,*) ' '
      WRITE(88,*) 'FINISH'

C     UAR
428   FORMAT ('D,',I5,',UX,',E15.7)
429   FORMAT ('D,',I5,',UY,',E15.7)
```

```
430   FORMAT ('D,',I5,',UZ,',E15.7)

501   FORMAT ('F,',I5,',FX,',E15.7)
502   FORMAT ('F,',I5,',FY,',E15.7)
503   FORMAT ('F,',I5,',FZ,',E15.7)

C     UAR

      RETURN
      END
```

Dyntool-2

Obs: **Dyntool-2 uses same subroutines from Dyntool except those ones listed as follows:**

```
c.....Uriel A.Rosa .... June 4,96
c.....Uriel A.Rosa .... June 2,96
c.....Modified   Uriel A. Rosa   Feb 10/96 ; May-18-96 (Poisson) UAR
c
      SUBROUTINE ELMT26(D,UL,URL,XL,XLO,IX,S,P,VL,NDF,NDM,NST,ISW)
      IMPLICIT REAL*8 (A-H,O-Z)
      CHARACTER  HEAD*50,WD*11,WDD*10,FILENAME(12),fi*12
C.....THREE-DIMENSIONAL, ISOTROPIC, NON-LINEAR, STRAIN RATE-
DEPENDENT
C.....ELASTICITY ELEMENT WITH 8 NODES. THE TANGENT MODULUS Es IS
EXPRESSED
C.....ON THE BASIS OF DUNCAN-CHANG MODEL (1970).
C.....DESIGNED BY JIE SHEN
C.....NOV. 14, 1993
      REAL*8 D(*),XL(NDM,*),XLO(NDM,*)
      COMMON /ELDATA/ LM,N,MA,MCT,IEL,NEL
      COMMON /HEAD/HEAD
      COMMON /CDATA/ N1,N2,NEN,NJ,NE,NEQ
      COMMON /DYNAMICS/ SPEED,DT,THITA,BATA,GAMA
      COMMON /FLAG_BLO/
GE_FLAG,DY_FLAG,DB_FLAG,MA_FLAG,UL_FLAG,
    *  ST_FLAG,SC_FLAG
      DIMENSION UL(NDF,*),URL(NDF,*),IX(*),S(NST,NST),P(NST),
    * VL(NDF,*),SHP(4,8),SHPO(4,8),XG(8),YG(8),ZG(8),WG(8),SIG(9)
    * ,EPS(6)
C     Grefe(I4) UAR
      DIMENSION GREFE(3)

      DIMENSION DEPS(6),DEPSR(3),DSIG(6),WDD(2),V(20),G(4),GG(3)
    * ,SIGN(3)
      LOGICAL
FLAG,GE_FLAG,DY_FLAG,DB_FLAG,MA_FLAG,UL_FLAG,ST_FLAG,
    * SC_FLAG
      EQUIVALENCE (FI,FILENAME(1))
      DATA WD/'3-D PROBLEM'/
      DATA WDD/'SHEAR FAILURE','TENSILE FAILURE'/
      data fi /'middata .fil'/
C
C.... GO TO CORRECT ARRAY PROCESSOR
      GO TO(1,2,3,4,5,4,4), ISW
```

```fortran
C.... INPUT MATERIAL PROPERTIES
1     NMA=ma+48
      filename(8)=char(NMA)
      INQUIRE(FILE=fi,EXIST=FLAG)
      IF(FLAG) THEN
          OPEN(NMA,FILE=fi,status='old')
          CLOSE(NMA,STATUS='DELETE')
      END IF
      OPEN(NMA,FILE=fi,ACCESS='DIRECT',status='new',RECL=160,
     * FORM='UNFORMATTED')
c.....D(1)=Ks(-);D(2)=ns(-);D(3)=Xun(-);D(4)=Rho(kN/m^3);D(5)=L(-)
c.....D(6)=K(-);D(7)=Cohn(kPa);D(8)=Fai(Degree);D(9)=Rsf(-);D(10)=Bs(-)
c.....D(11)=dEpsn(0)(1/s);D(12)=St(-);D(13)=Sc(-);D(14)=Ms(-)
      READ(5,*) D(1),D(2),D(3),D(4),D(5),D(6),D(7),D(8),D(9),D(10)
     * ,D(11),D(12),D(13),D(14)
      Es=D(1)*100.
      XUN=D(3)
      L=int(D(5))
      K=int(D(6))
      IF(L.EQ.0) L=2
      IF(K.EQ.0) K=1
      L = MIN0(4,L)
      D(5) = L
      K = MIN0(4,MAX0(1,K))
      D(6) = K
      G(1)=Es*(1.-XUN)/(1.+XUN)/(1.-2.*XUN)
      G(2)=XUN*G(1)/(1.0E0-XUN)
      G(3)=Es/2.0E0/(1.0E0+XUN)
C.....SET INITIAL STRESSES AND STRAINS TO ZERO AND ELASTIC MATRIC G
      DO 12 I1=1,20
12    V(I1)=0.0
      DO 14 I=1,3
      NN1=15+I
      V(NN1)=G(I)
14    CONTINUE
      MMM=NE*8
      DO 16 I2=1,MMM
16    WRITE (NMA,REC=I2) (V(I),I=1,20)
      LINT=0
      WRITE(*,2000) D(1),D(2),D(3),D(4),L,K,D(7),D(8),D(9),D(10)
     * ,D(11),D(12),D(13),D(14)
      WRITE(6,2000) D(1),D(2),D(3),D(4),L,K,D(7),D(8),D(9),D(10)
     * ,D(11),D(12),D(13),D(14)
      WRITE(7,2000) D(1),D(2),D(3),D(4),L,K,D(7),D(8),D(9),D(10)
     * ,D(11),D(12),D(13),D(14)
```

```
      WRITE(*,2050) (G(I),I=1,3)
      WRITE(6,2050) (G(I),I=1,3)
      WRITE(7,2050) (G(I),I=1,3)
      WRITE(6,2001) HEAD
         RETURN
C.....  WRITE INFORMATION ON SCREEN
2      RETURN
c.............................................................
3    NMA=MA+48
     L = int(D(5))
     L=2
C    IF(L*L*L.NE.LINT) CALL PGAUSS3(L,LINT,XG,YG,ZG,WG)
     CALL PGAUSS3(L,LINT,XG,YG,ZG,WG)
     DO 36 L9 = 1,LINT
     NNN=(N-1)*8+L9
     READ(NMA,REC=NNN) (V(I),I=1,20)
     DO 32 I=1,3
32    G(I)=V(I+15)
     CALL SHP3 (XG(L9),YG(L9),ZG(L9),XL,SHP,XSJ,NDM,NEL,IX,.FALSE.)
C.............................................................
     XXSJ = XSJ*WG(L9)
C.............................................................
C.....CALCULATE THE ELEMENT STIFFNESS MATRIX S
     GG(1)=G(1)*XXSJ
     GG(2)=G(2)*XXSJ
     GG(3)=G(3)*XXSJ
     NSL=NEL*NDF
     DO 34 J=1,NEL
     J1=(J-1)*NDF
     DO 34 K=J,NEL
     K1=(K-1)*NDF
     S(J1+1,K1+1)=S(J1+1,K1+1)+SHP(1,J)*SHP(1,K)*GG(1)+SHP(2,J)*
    1 SHP(2,K)*GG(3)+SHP(3,J)*SHP(3,K)*GG(3)
     S(J1+1,K1+2)=S(J1+1,K1+2)+SHP(1,J)*SHP(2,K)*GG(2)+SHP(2,J)*
    1 SHP(1,K)*GG(3)
     S(J1+1,K1+3)=S(J1+1,K1+3)+SHP(1,J)*SHP(3,K)*GG(2)+SHP(3,J)*
    1 SHP(1,K)*GG(3)
     S(J1+2,K1+1)=S(J1+2,K1+1)+SHP(2,J)*SHP(1,K)*GG(2)+SHP(1,J)*
    1 SHP(2,K)*GG(3)
     S(J1+2,K1+2)=S(J1+2,K1+2)+SHP(2,J)*SHP(2,K)*GG(1)+SHP(1,J)*
    1 SHP(1,K)*GG(3)+SHP(3,J)*SHP(3,K)*GG(3)
     S(J1+2,K1+3)=S(J1+2,K1+3)+SHP(2,J)*SHP(3,K)*GG(2)+SHP(3,J)*
    1 SHP(2,K)*GG(3)
     S(J1+3,K1+1)=S(J1+3,K1+1)+SHP(3,J)*SHP(1,K)*GG(2)+SHP(1,J)*
    1 SHP(3,K)*GG(3)
```

```
      S(J1+3,K1+2)=S(J1+3,K1+2)+SHP(3,J)*SHP(2,K)*GG(2)+SHP(2,J)*
     1 SHP(3,K)*GG(3)
      S(J1+3,K1+3)=S(J1+3,K1+3)+SHP(3,J)*SHP(3,K)*GG(1)+SHP(2,J)*
     1 SHP(2,K)*GG(3)+SHP(1,J)*SHP(1,K)*GG(3)
C....FORM LOWER PART BY SYMMETRY
      S(K1+1,J1+1)=S(J1+1,K1+1)
      S(K1+2,J1+1)=S(J1+1,K1+2)
      S(K1+3,J1+1)=S(J1+1,K1+3)
      S(K1+1,J1+2)=S(J1+2,K1+1)
      S(K1+2,J1+2)=S(J1+2,K1+2)
      S(K1+3,J1+2)=S(J1+2,K1+3)
      S(K1+1,J1+3)=S(J1+3,K1+1)
      S(K1+2,J1+3)=S(J1+3,K1+2)
      S(K1+3,J1+3)=S(J1+3,K1+3)
34    CONTINUE
36    CONTINUE
      RETURN
C..............................................
C.....MODIFY TANGENT MODULUS,OUTPUT RESULTS AND CALCULATE
FORCE RESIDUE
C... SET STRESS HISTORY
4     NMA=MA+48
      L=int(D(5))
      Ess=D(1)*100.
      XUN=D(3)
      FAI=D(8)*3.1415926/180.0
      Rsf=D(9)
      C=D(7)
C     IF(L*L*L.NE.LINT) CALL PGAUSS3(L,LINT,XG,YG,ZG,WG)
      L=2
      CALL PGAUSS3(L,LINT,XG,YG,ZG,WG)
      DO 430 L9 = 1,LINT
      NNN=(N-1)*8+L9
      READ(NMA,REC=NNN) (V(I),I=1,20)
      do 402 I=1,3
402   G(I)=V(I+15)
      DO 404 I=1,6
404   EPS(I)=V(I)
      DO 406 I=1,9
      SIG(I)=V(I+6)
406   CONTINUE
C.... COMPUTE ELEMENT STRESSES, STRAINS, AND FORCES
C.....COMPUTE ELEMENT SHAPE FUNCTIONS
      CALL SHP3 (XG(L9),YG(L9),ZG(L9),XL,SHP,XSJ,NDM,NEL,IX,.FALSE.)
C.................................................
```

```
C.... COMPUTE STRAINS AND COORDINATES
      DO 408 I = 1,6
408   DEPS(I) = 0.0
      XX = 0.0
      YY = 0.0
      ZZ = 0.0
      VX = 0.0
      VY = 0.0
      VZ = 0.0
      DO 410 JK = 1,NEL
      XX = XX + SHP(4,JK)*XL(1,JK)
      YY = YY + SHP(4,JK)*XL(2,JK)
      ZZ= ZZ + SHP(4,JK)*XL(3,JK)
      VX = VX + SHP(4,JK)*VL(1,JK)
      VY = VY + SHP(4,JK)*VL(2,JK)
      VZ = VZ + SHP(4,JK)*VL(3,JK)
C.....COMPUTE INCREMENTAL STRAINS
      DEPS(1) = DEPS(1) + SHP(1,JK)*URL(1,JK)
      DEPS(2)=DEPS(2)+SHP(2,JK)*URL(2,JK)
      DEPS(3) = DEPS(3) + SHP(3,JK)*URL(3,JK)
      DEPS(4)=DEPS(4)+SHP(2,JK)*URL(1,JK)+SHP(1,JK)*URL(2,JK)
      DEPS(5)=DEPS(5)+SHP(3,JK)*URL(2,JK)+SHP(2,JK)*URL(3,JK)
410   DEPS(6)=DEPS(6)+SHP(3,JK)*URL(1,JK)+SHP(1,JK)*URL(3,JK)
      DO 411 I=1,3
411   DEPSR(I)=DEPS(I)/DT
      SRXYZ=SQRT(DEPSR(1)**2.+DEPSR(2)**2.+DEPSR(3)**2.)
      VXYZ=SQRT(VX*VX+VY*VY+VZ*VZ)
C.... COMPUTE STRESS
      DSIG(1) =G(1)*DEPS(1)+G(2)*DEPS(2)+G(2)*DEPS(3)
      DSIG(2) =G(2)*DEPS(1)+G(1)*DEPS(2)+G(2)*DEPS(3)
      DSIG(3) =G(2)*DEPS(1)+G(2)*DEPS(2)+G(1)*DEPS(3)
      DSIG(4)=G(3)*DEPS(4)
      DSIG(5)=G(3)*DEPS(5)
      DSIG(6)=G(3)*DEPS(6)
C.....COMPUTE TOTAL STRESSES AND STRAINS
      DO 412 II=1,6
412   SIG(II)=SIG(II)+DSIG(II)
      DO 413 I=1,6
413   EPS(I)=EPS(I)+DEPS(I)
      IF(ISW.EQ.6.OR.ISW.EQ.7) GO TO 426
      CALL PSTRES3(SIG,SIG(7),SIG(8),SIG(9))
C.............................................
C.....SAVE PRESENT STRESS DATA
      DO 414 I=1,6
      V(I)=EPS(I)
```

```fortran
414 CONTINUE
    DO 416 I=1,9
416 V(I+6)=SIG(I)

c     WRITE(6,2060) L9,N
c       WRITE(6,*) 'SIGMA7=',SIG(7),'SIGMA8',SIG(8),'SIGMA9',SIG(9)
c       WRITE(89,3333) 'SIGMA7,8,9=',SIG(7),SIG(8),SIG(9)


C.................................................................
C.....CHECK THE STATE OF STRESS OF EACH UNIT
c*******************************************
C....ISIG(7)I<ISIG(9)I WHEN BOTH SIG(7) AND SIG(9) ARE LE 0.
C....THEREFORE, SIGMA 3 SHOULD BE -SIG(7)
C
C....INITIALIZATION

C......tt --> strain rate difference
    TT=SRXYZ-D(11)
c    IF(D(14).GT.0.001) THEN
c        IF(TT.GT.1.0.AND.DY_FLAG) Ess=Ess*TT**D(14)
c    END IF
    IF(D(2).LT.1E-6.OR.SIG(7).GT.0.0) THEN
        XX=1.0
    ELSE
      IF(D(2).GT.0.001) THEN
          XX=(-SIG(7)/100.)**D(2)
        ELSE
        XX=1.0
      END IF
    END IF
C    IF(DB_FLAG) WRITE(6,*) 'TT=',TT**D(16),'XX=',XX
C.....TREATMENT OF FAILED ELEMENTS
    IF(V(19).GE.0.5.OR.V(20).GE.0.5) THEN


c ----------------------------------------------------------------
c   May 18/96 UAR  If tension or shear failure -> then Poisson ratio is
c     set to xun=0.49 or 0.499 according to Duncan&Chang (1976-thesis)
c     for a occurance of no volume change at failure; (Jose H.F.Pereira).
c ----------------------------------------------------------------
    Xun=0.499
    Es=Ess*XX/D(12)


C    UAR
c      WRITE(*,*) "L9 N",L9,N
c      WRITE(*,*) "Es",Es
```

```
C     UAR

         GO TO 420
      END IF
C.....TENSILE FAILURE CRITERION ( WHEN SIG(7)>0 )
      IF(SIG(7).GT.0.) THEN
         TC=C*D(13)
         IF(SIG(7).GE.TC) THEN
          IF(ST_FLAG) THEN
            Es=Ess/D(12)
            V(20)=1.0
          ELSE
            Es=Ess
         END IF
           GO TO 420
          ELSE
           SIGMAF=2.0*C*COS(FAI)/(1.0-SIN(FAI))
           GO TO 419
          END IF
      END IF
C.....SHEAR FAILURE CRITERION ( WHEN SIG(7)<0 )
      SIGMAF=(2.0*C*COS(FAI)-2.0*SIG(7)*SIN(FAI))/
     * (1.0-SIN(FAI))
      IF(DB_FLAG) WRITE(6,*) ' OLD SIGMAF=',SIGMAF

c.....criteria tt>0 ---> incorporate strain rate effects in sigmaf
418   IF(TT.GT.0.0.AND.DY_FLAG) SIGMAF=SIGMAF+d(10)*TT
      IF(DB_FLAG) WRITE(6,*) ' NEW SIGMAF=',SIGMAF
C
C.....SHEAR FAILURE (sigma1-sigma3)>sigmaf
419   QQ13=(SIG(7)-SIG(9))-SIGMAF
      IF(QQ13.GT.1.0E-6) THEN
c     WRITE(6,2010) N,WDD(1)
C     WRITE(*,2010) N,WDD(1)
         Es=Ess*XX/D(12)
         V(19)=1.0
         GOTO 420
      END IF
C.....NO SHEAR FAILURE
      DNG=D(9)*(SIG(7)-SIG(9))/SIGMAF
      IF (DNG.GE.0.99) DNG=0.99
      Es=Ess*XX*(1.-DNG)*(1.-DNG)

c......UAR
c......Chi's triaxial parameters to correct Poisson's ratio
```

```
c......for UAR triaxial test soil DH00-90.
      CHIA=0.4287
      CHIB=0.0658

      RSP=(SIG(7)-SIG(9))/SIGMAF
c......RSP (Poisson's strength ratio) <=1.0 => Poisson=CHIA+CHIB*RSP
c..................... > 1.0 => Poisson=0.499
      XUN=CHIA+CHIB*RSP

      IF (RSP.GT.1.0) THEN
       WRITE(*,*) 'RSP>1.0'
       XUN=0.499
      END IF

c     WRITE(*,*) 'Poisson=',XUN
c......UAR

C.....FORM ELASTIC MATRIC DD
420   G(1)=Es*(1.-XUN)/(1.+XUN)/(1.-2.*XUN)
      G(2)=XUN*Es/(1.+XUN)/(1.-2.*XUN)
      G(3)=Es/(2.0*(1.0+XUN))

c     WRITE(89,*) 'Es',Es

c.....................    IF(DB_FLAG) THEN
C.........Failured elements...............
C      WRITE(6,*) 'G(1)=',G(1),'G(2)=',G(2),'G(3)=',G(3)
C      IF(V(19).GT.0.5) WRITE(7,*) L9,' OF ',N,' IS SHEAR FAILED'
c      IF(V(19).GT.0.5) WRITE(*,*) L9,' OF ',N,' IS SHEAR FAILED'

C      IF(V(20).GT.0.5) WRITE(7,*) L9,' OF ',N,' IS TENSILE FAILED'
c      IF(V(20).GT.0.5) WRITE(*,*) L9,' OF ',N,' IS TENSILE FAILED'
c.....................    ENDIF


      IF(MA_FLAG) THEN
        DO 422 I4=1,3
422   V(I4+15)=G(I4)
      END IF
C.............................................
      WRITE(NMA,REC=NNN) (V(I),I=1,20)
C.............................................
C.... OUTPUT STRESSES AND STRAINS
      IF(MCT.GT.0) GO TO 424
c     WRITE(6,2001) HEAD
```

```fortran
      MCT = 50
424   MCT=MCT-2
C.....ONLY OUTPUT INFORMATION AT GAUSSAN POINT 1
c     IF(L9.EQ.1) THEN
c     WRITE(6,2002) L9,N,MA,(SIG(II),II=1,5),XX,YY,EPS,SIG(6)
c     ENDIF
      GOTO 430
C.................................................
426   XXSJ = XSJ*WG(L9)
      J1 = 1
      DO 428 J9 = 1,NEL
      IF(ISW.EQ.7.OR.ISW.EQ.6) THEN
        P(J1)=P(J1)-(SHP(1,J9)*DSIG(1)+SHP(2,J9)*DSIG(4)+
     *  SHP(3,J9)*DSIG(6))*XXSJ
        P(J1+1)=P(J1+1)-(SHP(2,J9)*DSIG(2)+SHP(1,J9)*DSIG(4)+
     *  SHP(3,J9)*DSIG(5))*XXSJ
        P(J1+2)=P(J1+2)-(SHP(3,J9)*DSIG(3)+SHP(2,J9)*DSIG(5)+
     *  SHP(1,J9)*DSIG(6))*XXSJ
          GOTO 428
      END IF
         P(J1)=P(J1)-(SHP(1,J9)*SIG(1)+SHP(2,J9)*SIG(4)+
     *  SHP(3,J9)*SIG(6))*XXSJ
        P(J1+1)=P(J1+1)-(SHP(2,J9)*SIG(2)+SHP(1,J9)*SIG(4)+
     *  SHP(3,J9)*SIG(5))*XXSJ
        P(J1+2)=P(J1+2)-(SHP(3,J9)*SIG(3)+SHP(2,J9)*SIG(5)+
     *  SHP(1,J9)*SIG(6))*XXSJ
428   J1 = J1 + NDF
430   CONTINUE
C.....AVERAGE TANGENTIAL MODULUS IN EACH ELEMENT
      IF(ISW.EQ.4.AND.MA_FLAG) THEN
          DO 432 I=1,3
      SIGN(I)=0.0
432     G(I)=0.0
      DO 436 L9 = 1,LINT
      NNN=(N-1)*8+L9
      READ(NMA,REC=NNN) (V(I),I=1,20)
         DO 434 I=1,3
         IF(V(19).GT.0.5.OR.V(20).GT.0.5) SIGN(I)=1.0
434     G(I)=G(I)+V(I+15)/8.0
436     CONTINUE
         DO 440 L9=1,LINT
      NNN=(N-1)*8+L9
         READ(NMA,REC=NNN) (V(I),I=1,20)

c       UAR
```

309

```
c       minimum value for residual elastic modulus=0.50 kPa
        GREFE(16)=1.0*(1.-XUN)/(1.+XUN)/(1.-2.*XUN)
        GREFE(17)=1.0*XUN/(1.+XUN)/(1.-2.*XUN)
        GREFE(18)=1.0/(2.0*(1.0+XUN))
c       UAR
c       gdivi = value to divide Et after failure
        GDIVI=1000.0
c       UAR

        DO 438 I4=1,3
        IF(SIGN(I4).GE.0.5) THEN
c          V(I4+15)=1.E-6
c       UAR  G()/1000 means "Es"/1000
        V(I4+15)=V(I4+15)/GDIVI
c          minimum value for residual elastic modulus=0.50 kPa
        IF(V(I4+15).LT.GREFE(I4+15)) THEN
           V(I4+15)=GREFE(I4+15)
        END IF
c       UAR
c       Write(*,*) 'G(i)=',V(16),V(17),V(18)
           GOTO 438
        END IF
        V(I4+15)=G(I4)
438     CONTINUE
        WRITE(NMA,REC=NNN) (V(I),I=1,20)
440     CONTINUE
        END IF
C...........
        RETURN
C.....ISOPARAMETRIC ELEMENT MASS MATRIX FOR PLANE PROBLEMS
C    P=DIAGONAL (LUMPED) MASS ARRAY (IN VECTOR)
C.....COMPUTE MATRIX AT EACH INTEGRATION POINT
5       L=int(D(5))
        L=2
C    IF(L*L*L.NE.LINT) CALL PGAUSS3(L,LINT,XG,YG,ZG,WG)
        CALL PGAUSS3(L,LINT,XG,YG,ZG,WG)
        DO 504 L9 = 1,LINT
        CALL SHP3 (XG(L9),YG(L9),ZG(L9),XL,SHP,XSJ,NDM,NEL,IX,.FALSE.)
        DMASS=D(4)*XSJ*WG(L9)
        DO 502 I=1,NEL
           P(3*I-2)=P(3*I-2)+DMASS*SHP(4,I)
           P(3*I-1)=P(3*I-2)
           P(3*I)=P(3*I-2)
502     CONTINUE
504     CONTINUE
```

310

```
      RETURN
C........................................................
C.... FORMATS FOR INPUT-OUTPUT
2000  FORMAT(/5X,43H 3-D, ISOTROPIC, NON-LINEAR, RATE-DEPENDENT /
     * 5X,49HELASTICITY ELEMENT WITH EIGHT NODES(DUNCAN-CHANG) //
     1 10X,3HKs=,E15.5,3H(-)/
     2 10X,3Hns=,E15.5,3H(-)/
     3 10X,4HXUN=,E15.5,3H(-)/
     4 10X,4HRho=,E15.5,8H(kN/m^3)/
     5 10X,2HL=,I4/
     6 10X,2HK=,I4/
     7 10X,2HC=,E15.5,5H(kPa)/
     8 10X,4HFai=,E15.5,8H(Degree)/
     9 10X,4HRsf=,E15.5,3H(-)/
     * 10X,3HBs=,E15.5,3H(-)/
     1 10X,8HdEps(0)=,E15.5,5H(1/s)/
     2 10X,3HSt=,E15.5,3H(-)/
     3 10X,3HSc=,E15.5,3H(-) /
     4 10X,3HMs=,E15.5,3H(-) /)
2001  FORMAT(/A50/5X,16HELEMENT STRESSES/2X,15HGAUSS POINT----,
     * //1X,18H ELEMENT MATERIAL,
     1 3X,9H11-STRESS,3X,9H12-STRESS,3X9H22-STRESS,4X,
     2 8H1-STRESS,4X,8H2-STRESS/2X,7H1-COORD,2X,7H2-COORD,3X,
     3 9H11-STRAIN,3X,9H12-STRAIN,3X,9H22-STRAIN,12X,5HANGLE)
2002  FORMAT(2x,I3,/2I9,5E12.3/2F9.3,3E12.3,F18.2/1X)
C     FORMAT(/5X,18HELEMENT NO. & MATE,3X,9H11-STRESS,11H 12-
STRESS,
C     * 12H---22-STRESS,4X,8H1-STRESS,4X,8H2-STRESS/5X,10H-----STATE,
C     & 2X,11HOF THE UNIT,/5X,2I9,5E12.3,5X,A10)
2010  FORMAT(/2X,12HELEMENT NO.=,I7,2X,10H----STATE=,A30)
2020  FORMAT(/5X,8(6F9.4)/)
2040  FORMAT(2x,18HRATIO OF BRAKING= ,F12.9,4H ET=,F7.3/)
2050  FORMAT(/5X,28HINITIAL ELASTIC MATRIC VALUE/,'G(1)=',F18.7,
     1 'G(2)=',F18.7,'G(3)=',F18.7)
2060  FORMAT(/5X,15HGAUSS POINT----,I2,12H NO. OF ELEM,2X,I3)
3333  format(a14,3f12.4)
      END


      SUBROUTINE SHP3 (SS,TT,YY,X,SHP,XSJ,NDM,NEL,IX,FLG)
      IMPLICIT REAL*8 (A-H,O-Z)
      REAL*8 X
      LOGICAL FLG
      DIMENSION SHP(4,*),X(NDM,*),QS(8),QT(8),QY(8),XS(3,3)
     1 ,SX(3,3),IX(*)
      DATA QS/0.5E0,-0.5E0,-0.5E0,0.5E0,0.5E0,-0.5E0,-0.5E0,
```

```
     1 0.5E0/,QT/-0.5E0,-0.5E0,-0.5E0,-0.5E0,0.5E0,0.5E0,
     1 0.5E0,0.5E0/,QY/-0.5E0,-0.5E0,0.5E0,0.5E0,-0.5E0,-0.5E0,
     1 0.5E0,0.5E0/
C.... FORM 8-NODE ISOPARAMETER ELEMENT SHAPE FUNCTIONS
      DO 100 I = 1,8
      PS=0.5E0+QS(I)*SS
      PT=0.5e0+QT(I)*TT
      PY=0.5e0+QY(I)*YY
      SHP(1,I) = QS(I)*PT*PY
      SHP(2,I) = PS*QT(I)*PY
      SHP(3,I) = PS*PT*QY(I)
100   SHP(4,I)= PS*PT*PY
C     do 101 i=1,8
C101     write(*,*) 'shp(1,i)',shp(1,i),'shp(4,i)',shp(4,i)
C.... CONSTRUCT JACOBIAN AND ITS INVERSE
      DO 130 I = 1,NDM
      DO 130 J = 1,3
      XS(I,J) = 0.0
      DO 130 K = 1,NEL
130   XS(I,J) = XS(I,J) + X(J,K)*SHP(I,K)
C     write(*,*) 'xs(1,1)',xs(1,1),'xs(2,2)',xs(2,2),'xs(3,3)',xs(3,3)
C...FORM JACOBIAN DETERMINANT
      XSJ=XS(1,1)*XS(2,2)*XS(3,3)+XS(2,1)*XS(3,2)*XS(1,3)
     1 +XS(3,1)*XS(1,2)*XS(2,3)-XS(1,3)*XS(2,2)*XS(3,1)
     1 -XS(2,1)*XS(1,2)*XS(3,3)-XS(1,1)*XS(3,2)*XS(2,3)
C     write(*,*) 'xsj=',xsj
      IF(FLG) RETURN
      SX(1,1)=(XS(2,2)*XS(3,3)-XS(2,3)*XS(3,2))/XSJ
      SX(1,2)=(XS(1,3)*XS(3,2)-XS(3,3)*XS(1,2))/XSJ
      SX(1,3)=(XS(2,3)*XS(1,2)-XS(1,3)*XS(2,2))/XSJ
      SX(2,1)=(XS(3,1)*XS(2,3)-XS(3,3)*XS(2,1))/XSJ
      SX(2,2)=(XS(1,1)*XS(3,3)-XS(1,3)*XS(3,1))/XSJ
      SX(2,3)=(XS(2,1)*XS(1,3)-XS(1,1)*XS(2,3))/XSJ
      SX(3,1)=(XS(2,1)*XS(3,2)-XS(2,2)*XS(3,1))/XSJ
      SX(3,2)=(XS(3,1)*XS(1,2)-XS(1,1)*XS(3,2))/XSJ
      SX(3,3)=(XS(1,1)*XS(2,2)-XS(2,1)*XS(1,2))/XSJ
C.... FORM GLOBAL DERIVATIVES
      DO 140 I = 1,NEL
      TP=SHP(1,I)*SX(1,1)+SHP(2,I)*SX(1,2)+SX(1,3)*SHP(3,I)
      TQ=SHP(1,I)*SX(2,1)+SHP(2,I)*SX(2,2)+SX(2,3)*SHP(3,I)
      SHP(3,I)=SHP(1,I)*SX(3,1)+SHP(2,I)*SX(3,2)+SX(3,3)*SHP(3,I)
      SHP(2,I)=TQ
140   SHP(1,I)=TP
      K=IX(1)
      RETURN
```

```
      END


      SUBROUTINE PGAUSS3(L,LINT,X,Y,Z,W)
C.... GAUSS POINTS AND WEIGHTS FOR TWO DIMENSIONS
C
      IMPLICIT REAL*8 (A-H,O-Z)
      COMMON /ELDATA/ LM,N,MA,MCT,IEL,NEL
      DIMENSION QX(8),QY(8),QZ(8),X(*),Y(*),Z(*),W(*)
      DATA QX/1.,-1.,-1.,1.,1.,-1.,-1.,1./,
     1 QY/-1.,-1.,-1.,-1.,1.,1.,1.,1./
      DATA QZ/-1.,-1.,1.,1.,-1.,-1.,1.,1./
      LINT = L*L*L
C.... 2X2X2 INTEGRATION
      G=1.0E0/SQRT(3.0E0)
      DO 21 I=1,8
      X(I)=G*QX(I)
      Y(I)=G*QY(I)
      Z(I)=G*QZ(I)
21    W(I)=1.0E0
      RETURN
      END


      SUBROUTINE PSTRES3(SIG,P1,P2,P3)
C.... COMPUTE PRINCIPAL STRESSES (3 DIMENSIONS)
C
      IMPLICIT REAL*8 (A-H,O-Z)
      DIMENSION SIG(6),A(4),RT1(2),RT2(2),RT3(2)
C.... STRESSES MUST BE STORED IN ARRAY SIG(6) IN THE ORDER
C     TAU-XX,TAU-YY,TAU-ZZ,TAU-XY,TAU-YZ,TAU-XZ
      AI1=SIG(1)+SIG(2)+SIG(3)
      AI2=SIG(1)*SIG(2)+SIG(2)*SIG(3)+SIG(1)*SIG(3)-SIG(4)*SIG(4)
     1 -SIG(5)*SIG(5)-SIG(6)*SIG(6)
      AI3=SIG(1)*SIG(2)*SIG(3)+2.*SIG(4)*SIG(5)
     1 *SIG(6)-SIG(1)*SIG(5)*SIG(5)-SIG(2)
     1 *SIG(6)*SIG(6)-SIG(3)*SIG(4)*SIG(4)
      A(1)=1.
      A(2)=-AI1
      A(3)=AI2
      A(4)=-AI3
      TOL=0.001
      CALL CUBIC(A,RT1,RT2,RT3,TOL,NOROOT)
      P1=RT1(1)
      P2=RT2(1)
      P3=RT3(1)
```

```
      IF(P1.LT.P2) THEN
      P=P1
      P1=P2
      P2=P
      END IF
      IF(P1.LT.P3) THEN
      P=P1
      PP=P2
      P1=P3
      P2=P
      P3=PP
      END IF
      IF(P2.LT.P3) THEN
      P=P2
      P2=P3
      P3=P
      END IF
      RETURN
      END


      SUBROUTINE CUBIC(A,RT1,RT2,RT3,TOL,NOROOT)
C
C    THIS SUBROUTINE FINDS THE ROOTS (REAL OR REAL AND
C    COMPLEX) TO ANY CUBIC EQUATION.
C
      IMPLICIT REAL*8 (A-H,O-Z)
      DIMENSION A(4),C(4),RT1(2),RT2(2),RT3(2), B(2)
      ZERO = TOL/10.
      IF(ABS(A(1) ) - ZERO) 7,7,12
  7   CALL QUADRT(A(2), RT1,RT2,TOL,NOROOT)
      RETURN
 12   NOROOT = 3
      IT = 0
      DO 1 I = 2,4
  1   A(I) = A(I)/A(1)
      A(1) = 1.0
      IF(ABS(A(2)).LE.ZERO) GO TO 2
      NDA = 3
      B(1) = 1.0
      B(2) = -(A(2)*.333333)
      CALL LINCNG(A,NDA,B,C)
      IT = 1
      GO TO 4
  2   DO 3 I = 1,4
  3   C(I) = A(I)
```

314

```fortran
4   X = (C(4)*C(4))*.25 + (C(3)**3) *.037037
    IF(X.LT.0.0) GO TO 9
    X = SQRT(X)
    Y = -(C(4)*.5)
    I = 1
    RT1(I) = Y + X
5   N = 0
    IF(RT1(I).LT.0.0) N = 1
    IF(ABS(RT1(I)).LE.ZERO) GO TO 6
    RT1(I) = EXP((ALOG(ABS(RT1(I))))*.333333)
    IF(N.EQ.1) RT1(I) = -RT1(I)
6   IF(I.EQ.2) GO TO 8
    I = 2
    RT1(I) = Y - X
    GO TO 5
8   RT2(2) = ((RT1(1) - RT1(2))*.5)*1.732051
    RT1(1) = RT1(1) + RT1(2)
    RT1(2) = 0.0
    RT2(1) = - RT1(1) * .5
    RT3(1) = RT2(1)
    RT3(2) = -RT2(2)
    GO TO 11
9   ZZ = ABS(C(3))
    X = -(C(4)*.5)/SQRT((ZZ**3)*.037037)
    ANG= ACOS(X)
    Y = 2.0*(SQRT(ZZ*.333333))
    ANG = ANG*.333333
    RT1(1) = Y*COS(ANG)
    RT2(1) = Y*COS(ANG + 2.09440)
    RT3(1) = Y * COS(ANG + 4.18879)
    RT1(2) = 0.0
    RT2(2) = 0.0
    RT3(2) = 0.0
11  IF(IT.EQ.0) RETURN
    RT1(1) = RT1(1) + B(2)
    RT2(1) = RT2(1) + B(2)
    RT3(1) = RT3(1) + B(2)
    RETURN
    END
    SUBROUTINE QUADRT(A,ROOT1,ROOT2,TOL,NOROOT)
C
C   THIS SUBROUTINE SOLVES ANY QUADRATIC EQUATION OF THE FORM
C   A(1)X**2 + A(2)X + A(3) FOR REAL OR IMAGINARY ROOTS.
C
    IMPLICIT REAL*8 (A-H,O-Z)
```

```
      DIMENSION A(3), ROOT1(2), ROOT2(2)
      ZERO = TOL/10.
      IF(ABS(A(1)) - ZERO) 2,2,1
   2  IF(ABS(A(2)) - ZERO) 3,3,4
   3  NOROOT = 0
      RETURN
   1  NOROOT = 2
      X = A(2)*A(2) - 4.0 *A(1) * A(3)
      Y = A(1) + A(1)
      Z = SQRT(ABS(X))/Y
      W = -A(2)/Y
      IF(X.LT.0.0) GO TO 7
      ROOT1(1) = W + Z
      ROOT1(2) = 0.0
      ROOT2(1) = W - Z
      ROOT2(2) = 0.0
      RETURN
   7  ROOT1(1) = W
      ROOT1(2) = Z
      ROOT2(1) = W
      ROOT2(2) = -Z
      RETURN
   4  NOROOT = 1
      ROOT1(1) = -A(3)/A(2)
      ROOT1(2) = 0.
      RETURN
      END


      SUBROUTINE LINCNG(A,NDA,B,C)
C
C     SUBROUTINE TO MAKE A LINEAR CHANGE OF VARIABLES
C     IN A GIVEN POLYNOMIAL.
C
      IMPLICIT REAL*8 (A-H,O-Z)
      DIMENSION A(1), B(2), C(1)
      B1PWR = 1.0
      NZ = NDA + 1
      DO 4 I = 1,NZ
   4  C(I) = A(I)
   6  DO 8 I = 2,NZ
   8  C(I) = C(I) + C(I-1)*B(2)
      C(NZ) = C(NZ)*B1PWR
      NZ = NZ - 1
      B1PWR = B1PWR*B(1)
      IF (NZ.GT.1) GO TO 6
```

```fortran
      C(1) = C(1) * B1PWR
      RETURN
      END


C.....INCREMENTAL ANALYSIS VERSION 1.0 FOR VAX 3100 with iteration
C.....and with constant time step (Bathe algorithm)
      PROGRAM FEP2
C.....FEM SOFTWARE FOR MACHINE-SOIL SYSTEM
C.....VERSION 1.0
C.....WRITTEN BY JIE SHEN.
C.....DEC.19, 1993
C.....FORTRAN COLUMN MAJOR
      IMPLICIT REAL*8 (A-H,O-Z)
      LOGICAL EXFIL
      REAL T0,DT,SECNDS
      CHARACTER*9 FI,FO
      CHARACTER NAMINP(9),NAMOUT(9),HEAD*50,HEAD1*50
      COMMON/HEAD/HEAD1
      EQUIVALENCE (FI,NAMINP(1)),(FO,NAMOUT(1))
      DATA FI,FO/'    .DAT','    .OUT'/
      DATA HEAD/' FEM SOFTWARE FOR MACHINE-SOIL SYSTEM 1.0 '/
      HEAD1=HEAD
      WRITE(*,1000)
      WRITE(*,*) ' INPUT FILE NAME (5 LETTERS ONLY) :'
      READ (*,'(5A1)') (NAMINP(I),I=1,5)
      DO I=1,5
        NAMOUT(I)=NAMINP(I)
      END DO
      INQUIRE(FILE=FO,EXIST=EXFIL)
      IF(EXFIL)THEN
        OPEN(6,FILE=FO,STATUS='OLD')
      ELSE
        OPEN(6,FILE=FO,STATUS='NEW')
      END IF
      OPEN(5,FILE=FI,STATUS='OLD')
c****************************
      inquire(file='output.fil',exist=exfil)
      if(exfil) then
           open(7,file='output.fil',status='old')
           close(7,status='delete')
      endif
      open(7,file='output.fil',status='new')
C.........................
      inquire(file='disp.fil',exist=exfil)
      if(exfil) then
```

```
            open(81,file='disp.fil',status='old')
            close(81,status='delete')
      endif
      open(81,file='disp.fil',status='new')
C..........................
      inquire(file='VELO.fil',exist=exfil)
      if(exfil) then
            open(84,file='VELO.fil',status='old')
            close(84,status='delete')
      endif
      open(84,file='VELO.fil',status='new')
C..........................
      inquire(file='ACCE.fil',exist=exfil)
      if(exfil) then
            open(85,file='ACCE.fil',status='old')
            close(85,status='delete')
      endif
      open(85,file='ACCE.fil',status='new')
C..........................
      inquire(file='fail.fil',exist=exfil)
      if(exfil) then
            open(82,file='fail.fil',status='old')
            close(82,status='delete')
      endif
      open(82,file='fail.fil',status='new')
C..........................
      inquire(file='gaus.fil',exist=exfil)
      if(exfil) then
            open(83,file='gaus.fil',status='old')
            close(83,status='delete')
      endif
      open(83,file='gaus.fil',status='new')
C..........................
      inquire(file='PLOTDISP.fil',exist=exfil)
      if(exfil) then
            open(86,file='PLOTDISP.fil',status='old')
            close(86,status='delete')
      endif
      open(86,file='PLOTDISP.fil',status='new')

C..........................
      inquire(file='LREAC.FIL',exist=exfil)
      if(exfil) then
            open(89,file='LREAC.FIL',status='old')
            close(89,status='delete')
```

318

```
        endif
        open(89,file='LREAC.FIL',status='new')

        WRITE(89,*) 'LREAC.FIL - NDF, TOOL LOCAL REAC: X,Y,Z'

C.........................
c    MAXM=30000  ------>  35000
c    MAXR=50000  ------>  85000
c    MAXA=500000 ------> 910000
     WRITE(6,1000)HEAD
     T0=SECNDS(0.0)
     CALL PCONTR(FO)
     DT=SECNDS(T0)
     WRITE(*,600)DT
600  FORMAT(' ','   Lapsed time = ',F10.1,' sec.')
1000 FORMAT(/A50/)
     END


c.....(Dynat10) UAR Jun-29-96  UAR CX. CHANGES
c.....(Dynat7) UAR May-30-96
c    (Dynat6) UAR May-24-96
C.....Modified...Uriel A. Rosa  Feb 10/96
C............................................
     SUBROUTINE PCONTR(FO)
     IMPLICIT REAL*8 (A-H,O-Z)
     REAL*8 TOLRUUR,TOLRUR,TOLC
     PARAMETER (MAXM=35000,MAXR=85000,MAXA=910000)
C.....IN SUBROUTINE ADDSTF, THERE IS ANOTHER PARAMETER
STATEMENT TO
C.....DEFINE MAXA WHICH ALSO NEED BE CHAGED, IF CHANGE HAPPENS
TO THE ABOVE
C.....MAXA. NOTE MAXM FOR INTEGER ARRAY, MAXR FOR REAL ARRAY,
AND MAXA FOR
C.....TOTAL STIFFNESS ARRAY
     CHARACTER FO*9,CFLAG*5,CH_FLAG*7
     LOGICAL ERR,ASEM,GE_FLAG,DY_FLAG,DB_FLAG,MA_FLAG,UL_FLAG,
    * ST_FLAG,IT_FLAG,SC_FLAG
     COMMON/M/M(MAXM)
     COMMON/R/R(MAXR)
     COMMON/A/A(MAXA)
     COMMON/CDATA/NDF,NDM,NEN,NJ,NE,NEQ
     COMMON/MDATA/NUMMAT
     CHARACTER FD*25,FORC*6,P
     COMMON/PRINT/P
     COMMON/ASEM/ASEM
```

```
C.....NPROP DENOTES NUMBER OF TOTAL INCREMENT STEPS
C.....NITEM DENOTES NUMBER OF TOTAL ITERATION STEPS DURING EACH
LOADING STEP
      COMMON/PROCESS/NPROP,NITEM,IT_FLAG
      COMMON/DYNAMICS/SPEED,DT,THITA,BATA,GAMA
C    GE_FLAG FOR IDENTIFING LINEAR OR NON-LINEAR GEOMETRIC
ANALYSIS
C    DY_FLAG FOR IDENTIFING STATIC OR DYNAMIC ANALYSIS
C    DB_FLAG FOR IDENTIFING OUTPUT STATUS FOR DEBUG OR NOT
C    MA_FLAG FOR IDENTIFING VARIABLE OR CONSTAT STIFFNESS
C    UL_FLAG FOR IDENTIFING UPDATED OR TOTAL LAGRANGINA METHOD
C    ST_FLAG FOR CONSIDERING TENSILE FAILURE INFLUENCE ON SHEAR
STRENGTH
C    SC_FLAG FOR SHOWING THE INFORMATION ON SCREEN
      COMMON /FLAG_BLO/ GE_FLAG,DY_FLAG,DB_FLAG,MA_FLAG,UL_FLAG,
     * ST_FLAG,SC_FLAG
      DATA FORC/' FORC '/FD/' NODAL FORCE/DISPL'/
C.....READ IN CONTROL DATA

      I=0
2     READ(5,'(A5)') CFLAG
      IF(CFLAG.EQ.'MSFEM'.OR.CFLAG.EQ.'msfem') I=1
      IF(I.EQ.0) GO TO 2
      READ(5,*)   NJ,NE,NUMMAT,NDF,NDM,NEN
      WRITE(*,2000) NJ,NE,NUMMAT,NDF,NDM,NEN
      WRITE(6,2000) NJ,NE,NUMMAT,NDF,NDM,NEN
      NEN1=NEN+1
      NNEQ=NJ*NDF
      NST=NDF*NEN
      NSW=NE*NEN
C.....INTEGER ARRAY POINTERS
      NIX=1
      NID=NIX+NEN1*NE
      NLD=NID+NNEQ
      NJP=NLD+NST
      NTEN=NJP+NNEQ
      NSHE=NTEN+NSW
      NENDI=NSHE+NSW
C.....REAL ARRAY POINTERS
      NXC=1
      NUXC=NXC+NJ*NDM
      NXCO=NUXC+NJ*NDM
      ND=NXCO+NJ*NDM
C.....LIMITTED TO 19 PARAMETERS FOR EACH KIND OF MATERIAL.
C.....THE 20TH IS THE ELEMENT TYPE NUMBER.
```

```
         NXL=ND+20*NUMMAT
         NXLO=NXL+NEN*NDM
         NUL=NXLO+NEN*NDM
         NURL=NUL+2*NST
         NS=NURL+NST*2
         NP=NS+NST*NST
         NF=NP+NST
         NPF=NF+NNEQ
         NTF=NPF+NNEQ
         NTPF=NTF+NNEQ
         NU=NTPF+NNEQ
         NFR=NU+NNEQ
         NUR=NFR+NNEQ
         NUUR=NUR+NNEQ
         NSM=NUUR+NNEQ
         NU1=NSM+NNEQ
         NV1=NU1+NNEQ
         NW1=NV1+NNEQ
         NU2=NW1+NNEQ
         NV2=NU2+NNEQ
         NW2=NV2+NNEQ
         NWW=NW2+NNEQ
         NUI=NWW+NNEQ
         NVL=NUI+NNEQ
         NENDR=NVL+NST
C
C    NWW -- INCREMENTAL ACCELERATION;
C
C
      CALL SETMEM(NENDI,MAXM,ERR)
      IF(ERR) THEN
      WRITE(*,3000)
      WRITE(6,3000)
      STOP
      END IF
      CALL SETMEM(NENDR,MAXR,ERR)
      IF(ERR) THEN
      WRITE(*,3001)
      WRITE(6,3001)
      STOP
      END IF
      CALL MZERO(M(1),NENDI)
      CALL PZERO(R(1),NENDR)
C.....MESH GENERATION
      CALL PMESH(R(NXC),R(NXLO),M(NIX),M(NID),R(ND),R(NUL),R(NURL)
```

```fortran
      * ,R(NS),R(NP),NEN1,NST)
        CALL GENVEC(NDF,R(NF),FD,FORC,NJ,ERR)
        IF(ERR) GO TO 20


c     UAR
c     DO 800 I1=1,NDM*NJ
c800   WRITE(88,*) R(NID+I1-1)


C       WRITE(88,1088) (J,(XC(I,J),I=1,NDM),J=1,NJ)
C       1088  FORMAT ((('N,',I5,3(',',E15.7))))
c     UAR

      DO 3 I1=1,NDM*NJ
3     R(NXCO+I1-1)=R(NXC+I1-1)
C.....DEFINE THE PROFIL FOR GLOBAL STIFFNESS MATRIX STORAGE
      CALL PROFIL(M(NJP),M(NID),M(NIX),NEN1,NK)
      CALL SETMEM(NK,MAXA,ERR)
      IF(ERR) THEN
      WRITE(*,3500)
      STOP
      ENDIF
c     WRITE(*,*)' DO YOU WANT TO OUTPUT ELEMENT STIFFNESS (Y/N)?'
c     READ (*,'(A)') P
      P='N'
C.....DETERMINE NON-ZERO DISPLACEMENT BOUNDARY CONDITION
MAGNITUDE
      CALL VALBOUN(R(NF),M(NID),RDB)
C.....DETERMINE COORDINATES OF GAUSS POINTS
c     CALL GAUSS(R(NXC),R(NXL),M(NIX),NEN1)
C.....INITIAL PARAMETERS(SPEED(M/S))
      NPROP=1
      WRITE(*,*)'INPUT SPEED(M/S):2.5, 5.0, 10.0 OR 15.0:'
      READ(5,*) SPEED,NSTEP,NITEM,N_W
      write(7,*) 'speed(m/s)=',speed
      write(*,*) 'speed(m/s)=',speed
      write(81,*) speed
      WRITE(84,*) SPEED
      WRITE(85,*) SPEED
      WRITE(82,*) SPEED
      WRITE(86,*) SPEED
      WRITE(*,*)'INPUT TOTAL STEPS:'
C     READ(*,*) NSTEP
      write(7,*) 'TOTAL STEPS=',NSTEP
      write(*,*) 'TOTAL STEPS=',NSTEP
```

```
      write(81,*) nstep
      WRITE(84,*) NSTEP
      WRITE(85,*) NSTEP
      WRITE(82,*) NSTEP
      WRITE(86,*) NSTEP
      write(7,*) 'ITERATION STEPS=',NITEM
      write(*,*) 'ITERATION STEPS=',NITEM
      write(*,*) 'interval(m)=',RDB
      write(7,*) 'interval(m)=',RDB
      IF(RDB.LE.1.E-6) RDB=1

c     UAR
      IF(RDB.LE.1.E-6) write(*,*) 'Warning: RDB=1'
      IF(RDB.LE.1.E-6) write(7,*) 'Warning: RDB=1'
c     UAR

      DT=RDB/SPEED
      IF(N_W.EQ.0) THEN
         write(*,*) 'NEWMARK METHOD'
         write(7,*) 'NEWMARK METHOD'
      ELSE
         write(*,*) 'WILSON METHOD'
         write(7,*) 'WILSON METHOD'
      ENDIF
      READ(5,'(A7)') CH_FLAG
      IF(CH_FLAG.EQ.'DY_FLAG'.OR.CH_FLAG.EQ.'dy_flag') THEN
         DY_FLAG=.TRUE.
         write(*,*) 'DYNAMIC SOLVING SCHEME'
         write(7,*) 'DYNAMIC SOLVING SCHEME'
      ELSE
         DY_FLAG=.FALSE.
         write(*,*) 'STATIC SOLVING SCHEME'
         write(7,*) 'STATIC SOLVING SCHEME'
      ENDIF
      READ(5,'(A7)') CH_FLAG
      IF(CH_FLAG.EQ.'GE_FLAG'.OR.CH_FLAG.EQ.'ge_flag') THEN
         GE_FLAG=.TRUE.
         write(*,*) 'NON-LINEAR GEOMETRIC SOLVING SCHEME'
         write(7,*) 'NON-LINEAR GEOMETRIC SOLVING SCHEME'
      ELSE
         GE_FLAG=.FALSE.
         write(*,*) 'LINEAR GEOMETRIC SOLVING SCHEME'
         write(7,*) 'LINEAR GEOMETRIC SOLVING SCHEME'
      ENDIF
      READ(5,'(A7)') CH_FLAG
```

```fortran
IF(CH_FLAG.EQ.'DB_FLAG'.OR.CH_FLAG.EQ.'db_flag') THEN
    DB_FLAG=.TRUE.
    write(*,*) 'OUTPUT DEBUG INFORMATION'
    write(7,*) 'OUTPUT DEBUG INFORMATION'
ELSE
    DB_FLAG=.FALSE.
    write(*,*) 'DO NOT OUTPUT DEBUG INFORMATION'
    write(7,*) 'DO NOT OUTPUT DEBUG INFORMATION'
ENDIF
READ(5,'(A7)') CH_FLAG
IF(CH_FLAG.EQ.'MA_FLAG'.OR.CH_FLAG.EQ.'ma_flag') THEN
    MA_FLAG=.TRUE.
    write(*,*) 'NON-LINEAR MATERIAL SOLVING SCHEME'
    write(7,*) 'NON-LINEAR MATERIAL SOLVING SCHEME'
ELSE
    MA_FLAG=.FALSE.
    write(*,*) 'LINEAR MATERIAL SOLVING SCHEME'
    write(7,*) 'LINEAR MATERIAL SOLVING SCHEME'
ENDIF
READ(5,'(A7)') CH_FLAG
IF(CH_FLAG.EQ.'UL_FLAG'.OR.CH_FLAG.EQ.'ul_flag') THEN
    UL_FLAG=.TRUE.
    write(*,*) 'UPDATED LAGRAGIAN SOLVING SCHEME'
    write(7,*) 'UPDATED LAGRAGIAN SOLVING SCHEME'
ELSE
    UL_FLAG=.FALSE.
    write(*,*) 'TOTAL LAGRAGIAN SOLVING SCHEME'
    write(7,*) 'TOTAL LAGRAGIAN SOLVING SCHEME'
ENDIF
READ(5,'(A7)') CH_FLAG
IF(CH_FLAG.EQ.'ST_FLAG'.OR.CH_FLAG.EQ.'st_flag') THEN
    ST_FLAG=.TRUE.
    write(*,*) 'CONSIDERING TENSILE FAILURE'
    write(7,*) 'CONSIDERING TENSILE FAILURE'
ELSE
    ST_FLAG=.FALSE.
    write(*,*) 'NOT CONSIDERING TENSILE FAILURE'
    write(7,*) 'NOT CONSIDERING TENSILE FAILURE'
ENDIF
READ(5,'(A7)') CH_FLAG
IF(CH_FLAG.EQ.'SC_FLAG'.OR.CH_FLAG.EQ.'sc_flag') THEN
    SC_FLAG=.TRUE.
    write(*,*) 'INFORMATION SHOWING ON SCREEN'
    write(7,*) 'INFORMATION SHOWING ON SCREEN'
ELSE
```

```fortran
      SC_FLAG=.FALSE.
      write(*,*) 'NO INFORMATION SHOWING ON SCREEN'
      write(7,*) 'NO INFORMATION SHOWING ON SCREEN'
      ENDIF
C.....INTEGRATION PARAMETERS
C.....N_W=0,NEWMARK METHOD; N_W=1, WILSON METHOD;
      IF(DY_FLAG) THEN
C     IF(N_W.EQ.0) THEN
      THITA=1.0
        BATA=0.25
        GAMA=0.50
        A0=GAMA*DT
        A1=1.0/(DT*DT*BATA)
        A2=-1.0/(BATA*DT)
        A3=-1.0/(2.0*BATA)
        A4=A0*A1
        A5=A0*A2
        A6=DT+A0*A3
        A7=A3+1.0
      A8=DT-A0
C     ELSE
C       THITA=1.4
C       A1=6./(THITA*DT)**2.
C       A0=A1/THITA
C       A2=-6.0/(THITA*DT)
C       A3=-3.0
C       A4=3.0/(THITA*DT)
C       A5=A3
C       A6=-THITA*DT/2.0
C       A7=-6.0/(THITA*THITA*DT)
C       A8=1.0-3.0/THITA
C     ENDIF
C     ELSE
C       THITA=1.0
      ENDIF
C------------------------------------------------------------------
C                 VARIABLES
C U -- TOTAL DISPLACEMENT VECTOR, GLOBAL, ARRANGED BY
ACTIVATED D.O.F.
C UR -- INCREMENTAL DISPL. VECTOR, GLOBAL, ARRANGED BY
ACTIVATED D.O.F.
C UUR -- DISPL. INCREMENT IN ITERATION, GLOBAL, ARRANGE BY
ACTIVATED D.O.F.
C UL -- ELEMENT TOTAL DISPL. VECTOR.  URL -- ELEMENT INCREMENTAL
DISPL. VECTOR.
```

```
C F -- TOTAL FORCE VECTOR, GLOBAL, ARRANGED BY TOTAL D.O.F.
C FR -- INCREMENT FORCE VECTOR, GLOBAL, ARRANGE BY ACTIVATED
D.O.F.
C XC -- TOTAL NODE COORDINATE, GLOBAL, ARRANGED BY ACTIVATED
D.O.F.
C XL -- ELEMENT NODAL COORDINATE,
C PF -- INCREMENTAL NODAL REACTION FORCE, ARRANGED BY TOTAL
D.O.F.
C TPF -- TOTAL NODAL REACTION FORCE, ARRANGED BY TOTAL D.O.F.
C TF -- REFERENCE FORCE FOR ITERATION AT NITEM=I
C ID -- GLOBAL IDENTIFICATION,
C      ID>0, NON-CONSTRAINT, KNOWN-FORCE; ID NUMBER=NUMBER OF
ACTIVATED D.O.F.
C      ID<0, CONSTRAINT, KNOWN-DISPLACEMENT
C LD -- ELEMENT IDENTIFICATION
C      ISW=6,      LD=TOTAL D.O.F NUMBER
C      OTHERS,     LD=ID NUMBER ARRANGED BY ACTIVATED D.O.F.FOR
REAL NODES
C                LD=0        ,FOR EMPTY NODES
C---------------------------------------------------------------------------
C                 FLOWCHART
C
C    form mass matrix, M <--
C    TPF <-- 0
C    DO 30 II=1,NSTEP
C    form stiffness matrix, A <--
C    TF <-- 0, UR <-- 0
C    DO 40 III=1,NITEM
C    FR <-- 0, UUR <-- 0
C    FR  <-- F (external load)
C    FR  <-- FR+specified displacement+element load
C    FR <-- FR+dynamic factor(V1,W1)
C    UUR <-- FR+TF
C    solve
C    UR <-- UR+UUR
C     (display TF,FR,UUR,UR for debug)
C    calculate TF <--
C    calculate PF <--
C 40   continue
C    U <-- U+UR
C    W2 <--, V2 <--
C    calculate incremental reaction force, PF <--
C    TPF <-- TPF+PF
C    calculate stresses, update modulus
C    V1 <-- V2, W1 <-- W2
```

```
C    update coordinate, XC <--
C 30   continue
C
C---------------------------------------------------
C.....FORM MASS MATRIX
4     CALL PZERO(R(NSM),NNEQ)
      CALL PFORM(R(NF),R(NFR),M(NLD),R(NUL),R(NURL),R(NXL),R(NXLO),
     1 R(NS),R(NP),R(NPF),R(NTF),R(NU),R(NUR),R(NXC),R(NXCO),M(NIX)
     2 ,R(ND),M(NID),M(NJP),R(NSM),R(NV2),R(NVL),NST,NEN1,5)
      CALL PZERO(R(NTPF),NNEQ)
      CALL PZERO(R(NU),NNEQ)


C---------------------------------------------------------------
C.....INITIALIZE U, U. , U.. (STARTS FROM STATIC STATE)

      CALL PZERO(R(NV1),NNEQ)
      CALL PZERO(R(NW1),NNEQ)
C---------------------------------------------------------------


C----------------Beginning of Increment Analysis---------------
      DO 30 II=1,NSTEP
      write(*,*) 'TOTAL LOADING STEPS=', nstep
      write(7,*) 'TOTAL LOADING STEPS=', nstep
C.....FORM ELEMENT STIFFNESS
      CALL PZERO(A,NK)
      ASEM=.TRUE.
      CALL PFORM(R(NF),R(NFR),M(NLD),R(NUL),R(NURL),R(NXL),R(NXLO),
     1 R(NS),R(NP),R(NPF),R(NTF),R(NU), R(NUR),R(NXC),R(NXCO),M(NIX)
     2 ,R(ND),M(NID),M(NJP),R(NSM),R(NV2),R(NVL),NST,NEN1,3)
      ASEM=.FALSE.
      DO 10 I=1,NEQ
      NN=M(NJP+I-1)
      IF(DB_FLAG) WRITE(83,*) 'EQ.NUM=',I,'NN=',NN,'OLD A(NN)=',A(NN)

C     UAR CX. CHANGES
      IF(DY_FLAG) A(NN)=A(NN)+A4*R(NSM+I-1)

      IF(DB_FLAG) WRITE(83,*) 'A(NN)=',A(NN),'R(NSM)=',R(NSM+I-1)
10       CONTINUE
C.....LDLT TRIANGULAR DECOMPOSITION
      CALL LDLT(A,M(NJP),NEQ)
C.....NODAL FORCE INPUT
      CALL PZERO(R(NUR),NNEQ)
      CALL PZERO(R(NFR),NNEQ)
```

```
      CALL PLOAD (M(NID),R(NF),R(NFR),NNEQ,NPROP,III,THITA)
      CALL PFORM(R(NF),R(NFR),M(NLD),R(NUL),R(NURL),R(NXL),R(NXLO),
     1 R(NS),R(NP),R(NPF),R(NTF),R(NU),R(NUR),R(NXC),R(NXCO),M(NIX),
     2 R(ND),M(NID),M(NJP),R(NSM),R(NV2),R(NVL),NST,NEN1,3)
      DO 16 I=1,NEQ
      IF(DB_FLAG) WRITE(83,*) 'EQ.NUM=',I,'OLD NFR=',R(NFR+I-1)
C------------------------------------------------------------
C......KEY POINT: IF THE FOLLOWING EQUATION IS INCLUDED IN THE
ALGORITHM,
C......THE STABILITY IS NOT GOOD. THEREFORE, WE OMIT IT. THIS MEANS
THE FIRST
C......STEP WE GET THE STATIC SOLUTION AND USE THIS SOLUTION AS THE
INITIAL
C......VALUE FOR THE ITERATIONS TO GET THE EXACT DYNAMIC
SOLUTION. IN THIS
C......WAY, THE STABILITY CAN BE ALWAYS GARRANTEED.
C

C......NEWMARK , BATHE PAGE 512  (?)
C......FULL EFFECTIVE LOAD VECTOR
C......

C   UAR CX.CHANGES
      R(NFR+I-1)=R(NFR+I-1)-R(NSM+I-1)*(A5*R(NV1+I-1)+(A6)*R(NW1+I-1))
C------------------------------------------------------------

      IF(DB_FLAG) WRITE(83,*) 'NEW NFR=',R(NFR+I-1)
      R(NUR+I-1)=R(NFR+I-1)
16    CONTINUE


C.....FORWARD ELIMINATION AND BACKWARD SUBSTITUTION
      CALL FORBACK(A,R(NUR),M(NJP),NEQ)
C.....FORBACK DOESN'T CHANGE THE CONTENT IN MATRIX A
C.....ITERATION DURING EACH LOADING STEP: NSTEP
C.....COMPUTE THE REACTION
      IF(DB_FLAG) THEN
         CALL PZERO(R(NPF),NNEQ)
         CALL PFORM(R(NF),R(NFR),M(NLD),R(NUL),R(NURL),R(NXL),R(NXLO),
     1 R(NS),R(NP),R(NPF),R(NTF),R(NU),R(NUR),R(NXC),R(NXCO),M(NIX)
     2 ,R(ND),M(NID),M(NJP),R(NSM),R(NV2),R(NVL),NST,NEN1,6)
         CALL PRTREAC(R(NPF),R(NF),M(NID),RDB,II,2)
         CALL PRTDIS(M(NID),R(NUR),R(NF),R(NV2),R(NW2),2)
      ENDIF
C
```

```
C----------------Beginning of Iteration----------------------
      DO 40 III=1,NITEM
      write(*,*) 'ITERATION STEP=',III,'   LOADING STEP=',II
      write(6,*) 'ITERATION STEP=',III,'   LOADING STEP=',II
      IF(DB_FLAG) THEN
       write(7,*) 'ITERATION STEP=',III,'   LOADING STEP=',II
      ENDIF
      DO 31 I=1,NEQ
      IF(.NOT.DY_FLAG) THEN
       R(NWW+I-1)=0.0
      ELSE

C     UAR  VEL.VECTOR
C     UAR CX. CHANGES
          R(NWW+I-1)=A0*(A1*R(NUR+I-1)+A2*R(NV1+I-1)+(A3)*R(NW1+I-1))
          R(NWW+I-1)=R(NWW+I-1)+DT*R(NW1+I-1)
C    WRITE(*,*) 'DT',DT

      ENDIF
31    CONTINUE
C.....CALCULATE REFERENCE FORCE VECTOR TF
      CALL PZERO(R(NTF),NNEQ)
      CALL PFORM(R(NF),R(NFR),M(NLD),R(NUL),R(NURL),R(NXL),R(NXLO),
     1 R(NS),R(NP),R(NPF),R(NTF),R(NU),R(NUR),R(NXC),R(NXCO),M(NIX),
     2 R(ND),M(NID),M(NJP),R(NSM),R(NV2),R(NVL),NST,NEN1,7)
      DO 32 I=1,NEQ
      R(NUUR+I-1)=R(NFR+I-1)-R(NSM+I-1)*R(NWW+I-1)+R(NTF+I-1)

32    CONTINUE
      WRITE(*,*) 'F,A',R(NUUR+85-1),A(85)


C.....FORWARD ELIMINATION AND BACKWARD SUBSTITUTION
      CALL FORBACK(A,R(NUUR),M(NJP),NEQ)
C.....UPDATE INCREMENTAL DISPLACEMENT VECTOR
C.....CONVERGENCE CRITERIA - EULERIAN VECTOR NORM

      TOLRUUR=0.
      TOLRUR=0.
      TOLC=0.

      DO 17 I=1,NEQ

         R(NUR+I-1)=R(NUR+I-1)+R(NUUR+I-1)

      TOLRUUR=TOLRUUR+R(NUUR+I-1)*R(NUUR+I-1)
```

```
      TOLRUR=TOLRUR+R(NUR+I-1)*R(NUR+I-1)

17    CONTINUE


C     WRITE(*,*) 'UUR,UR',85,R(NUUR+85-1),R(NUR+85-1)

      TOLC=SQRT(TOLRUUR)/SQRT(TOLRUR)
      WRITE(6,*) III,' ','TOLC = ',TOLC
      WRITE(*,*) III,' ','TOLC = ',TOLC

C.......
      IF(DB_FLAG) THEN
         DO 6 MM=1,NEQ
         WRITE(83,*) 'N=',MM,'FR+M*W=',R(NFR+MM-1)-R(NSM+MM-1)*
     1   R(NWW+MM-1),'TF=',R(NTF+MM-1)
6        WRITE(7,*) 'N=',MM,'NUR=',R(NUR+MM-1),'NUUR=',R(NUUR+MM-1)
         DO 7 MM=NEQ+1,NNEQ
         WRITE(83,*) 'n=',MM,'FR+M*W=',R(NFR+MM-1)-R(NSM+MM-1)*
     1   R(NWW+MM-1),'TF=',R(NTF+MM-1)
7        WRITE(7,*) 'n=',MM,'NUR=',R(NUR+MM-1),'NUUR=',R(NUUR+MM-1)
      ENDIF
C...........
C.....COMPUTE THE REACTION
         CALL PZERO(R(NPF),NNEQ)
         CALL PFORM(R(NF),R(NFR),M(NLD),R(NUL),R(NURL),R(NXL),R(NXLO),
     1   R(NS),R(NP),R(NPF),R(NTF),R(NU),R(NUR),R(NXC),R(NXCO),M(NIX)
     2   ,R(ND),M(NID),M(NJP),R(NSM),R(NV2),R(NVL),NST,NEN1,6)
c---------------------------------------------------------------
      DO 33 I=1,NJ
      DO 33 J=1,NDF
      K1=(I-1)*NDF+J
      K2=M(NID+K1-1)
c        IF(K2.GT.0) R(NPF+K1-1)=-R(NSM+K2-1)*R(NWW+K2-1)+R(NPF+K1-1)
33    CONTINUE
c---------------------------------------------------------------
      IF(DB_FLAG) THEN
         CALL PRTREAC(R(NPF),R(NF),M(NID),RDB,II,2)
         CALL PRTDIS(M(NID),R(NUR),R(NF),R(NV2),R(NW2),2)
      ENDIF

c..... UAR .. Tolerance for the (Daht,1985?) Euclidian Vector norm=1%
      IF (TOLC.LT.0.01) GOTO 140
c     UAR
```

```
40  CONTINUE

140  WRITE(*,*) 'END OF INTERNAL ITER= ', III, ' TOLC=',TOLC
     WRITE(6,*) 'END OF INTERNAL ITER= ', III, ' TOLC=',TOLC
C-------------End of Iteration-------------------------
     DO 18 I=1,NEQ
     IF(.NOT.DY_FLAG) THEN
        R(NU+I-1)=R(NU+I-1)+R(NUR+I-1)
     ELSE
      IF(N_W.EQ.0) THEN
         R(NU+I-1)=R(NU+I-1)+R(NUR+I-1)
         R(NW2+I-1)=A1*R(NUR+I-1)+A2*R(NV1+I-1)+A7*R(NW1+I-1)
         R(NV2+I-1)=R(NV1+I-1)+A8*R(NW1+I-1)+A0*R(NW2+I-1)
      ELSE
         R(NW2+I-1)=A0*R(NUR+I-1)+A7*R(NV1+I-1)+A8*R(NW1+I-1)
         R(NV2+I-1)=R(NV1+I-1)+0.5*DT*(R(NW2+I-1)+R(NW1+I-1))
         R(NU+I-1)=R(NU+I-1)+DT*R(NV1+I-1)+(DT*DT/6.0)*(R(NW2+I-1)
     *    +2.*R(NW1+I-1))
         R(NUR+I-1)=DT*R(NV1+I-1)+(DT*DT/6.0)*(R(NW2+I-1)
     *    +2.*R(NW1+I-1))
      ENDIF
     ENDIF
18   CONTINUE
     CALL PRTDIS(M(NID),R(NU),R(NF),R(NV2),R(NW2),1)
     CALL PLTDIS(R(NXC),R(NUR),M(NID),R(NF),R(NUXC),II,RDB)
C    CALL PLTVEL(R(NV2),M(NID),R(NF),R(NUXC),II,SPEED,RDB)
C    CALL PLTACL(R(NW2),M(NID),R(NF),R(NUXC),II,RDB)
C.....COMPUTE THE INCREMENTAL REACTION PERTICLUARLY FOR WILSON
METHOD
C       CALL PZERO(R(NPF),NNEQ)
C       CALL PFORM(R(NF),R(NFR),M(NLD),R(NUL),R(NURL),R(NXL),R(NXLO),
C    1  R(NS),R(NP),R(NPF),R(NTF),R(NU),R(NUR),R(NXC),R(NXCO),M(NIX)
C    2  ,R(ND),M(NID),M(NJP),R(NSM),R(NV2),R(NVL),NST,NEN1,6)
C       CALL PRTREAC(R(NPF),R(NF),M(NID),RDB,II,2)
C       CALL PRTDIS(M(NID),R(NUR),R(NF),R(NV2),R(NW2),2)
     DO 19 I=1,NNEQ
19   R(NTPF+I-1)=R(NTPF+I-1)+R(NPF+I-1)
     CALL PRTREAC(R(NTPF),R(NF),M(NID),RDB,II,1)
C.....COMPUTE ELEMENT STRESSES
     CALL PFORM(R(NF),R(NFR),M(NLD),R(NUL),R(NURL),R(NXL),R(NXLO),
     1 R(NS),R(NP),R(NPF),R(NTF),R(NU),R(NUR),R(NXC),R(NXCO),M(NIX)
     2 ,R(ND),M(NID),M(NJP),R(NSM),R(NV2),R(NVL),NST,NEN1,4)
c.....AVERAGE TANGENTIAL MODULUS IN EACH ELEMENT
     CALL PZERO(R(NV1),2*NNEQ)
     IF(.NOT.DY_FLAG) GOTO 24
```

```
      DO 22 I=1,NEQ
      R(NV1+I-1)=R(NV2+I-1)
22    R(NW1+I-1)=R(NW2+I-1)
24    CONTINUE
      CALL CUPDATE(R(NXC),R(NUR),M(NID),R(NF),M(NIX),NEN1)
C     CALL PLTFAL(M(NIX),M(NTEN),M(NSHE),NEN1,II,RDB)
      NPROP=NPROP+1
30    CONTINUE
C--------------------End of Increment Analysis--------------------
20    WRITE(*,2200) FO
c     WRITE(81,*) 'F'
      RETURN
2000  FORMAT(' NUMBER OF NODAL POINTS        =',I5/
     1        ' NUMBER OF ELEMENTS           =',I5/
     1        ' NUMBER OF MATERIALS          =',I5/
     1        ' NUMBER OF DEGREES/NODE       =',I5/
     1        ' NUMBER OF DIMENSION SPACE    =',I5/
     1        ' NUMBER OF NODES/ELEMENT      =',I5/)
2200  FORMAT(/' ** END OF FINITE ELEMENT PROGRAM **'/
     1        '   THE RESULTS ARE STORED IN FILE : ',A9)
3000  FORMAT(' **PROBLEM SIZE TOO LARGE (INTEGER ARRAY)**')
3001  FORMAT(' **PROBLEM SIZE TOO LARGE (REAL ARRAY)**')
3500  FORMAT(' **FATAL ERROR** GLOBAL STIFFNESS MATRIX TOO BIG'/)
      END

c....Uriel A. Rosa  June 29,96
c....Uriel A. Rosa  June 6,96
c....Uriel A. Rosa  June 1,96
C.....................................................
      SUBROUTINE PMESH(XC,XLO,IX,ID,D,UL,URL,S,P,NEN1,NST)
C.....DATA INPUT AND GENERATION ROUTINE
      IMPLICIT REAL*8 (A-H,O-Z)
      CHARACTER COOR*6,XX*18
      COMMON/CDATA/NDF,NDM,NEN,NJ,NE,NEQ
      COMMON/MDATA/NUMMAT
      COMMON/ELDATA/LM,N,MA,MCT,IEL,NEL
      COMMON /FLAG_BLO/ GE_FLAG,DY_FLAG,DB_FLAG,MA_FLAG,UL_FLAG,
     * ST_FLAG,SC_FLAG
      DIMENSION XC(NDM,*),XLO(NDM,*),IX(NEN1,*),ID(NDF,*),D(20,*)
      LOGICAL ERR,GE_FLAG,DY_FLAG,DB_FLAG,MA_FLAG,UL_FLAG,
     * ST_FLAG,SC_FLAG
      DATA XX/' NODAL COORDINATES'/COOR/' COOR '/

C.....GENERATE PLOTMESH.FIL DATA FILE
      INQUIRE(FILE='PLOTMESH.FIL',EXIST=ERR)
```

```fortran
      IF(ERR) THEN
          OPEN(80,FILE='PLOTMESH.FIL'.status='old')
          CLOSE(80,STATUS='DELETE')
      ENDIF
      OPEN(80,FILE='PLOTMESH.FIL',status='new')

C.....GENERATE MSH.DAT DATA FILE
      INQUIRE(FILE='MSH.DAT',EXIST=ERR)
      IF(ERR) THEN
          OPEN(88,FILE='MSH.DAT',status='old')
          CLOSE(88,STATUS='DELETE')
      ENDIF
      OPEN(88,FILE='MSH.DAT',status='new')

C.....NODAL COORDINATES DATA INPUT
1     CALL GENVEC(NDM,XC,XX,COOR,NJ,ERR)
      IF(ERR) WRITE(*,3000)
      IF(ERR) STOP
C.....ELEMENT DATA INPUT
2     CALL ELDAT(IX,NEN1)
C.....GENERATE PLOTMESH.FIL
      WRITE(80,*) 'T'
      WRITE(80,*) NJ,NE,NDF,NEN,NDM
      WRITE(80,1000) ((XC(I,J),I=1,NDM),J=1,NJ)
      WRITE(80,1100) ((IX(I,J),I=1,NEN),J=1,NE)
      WRITE(80,*) 'F'

C.....GENERATE MSH.DAT
      WRITE(88,*) '/PREP7'
      WRITE(88,*) '/TITLE,Title,Dynat10'
      WRITE(88,*) 'ET,1,45'
      WRITE(88,*) 'EX,1,10'
      WRITE(88,*) 'EY,1,10'
      WRITE(88,*) 'EZ,1,10'
      WRITE(88,*) ' '

      WRITE(88,1088) (J,(XC(I,J),I=1,NDM),J=1,NJ)
      WRITE(88,1188) ((IX(I,J),I=1,NEN),J=1,NE)

c     WRITE(88,*) ' '
c     WRITE(88,*) 'NPLOT'
c     WRITE(88,*) 'EPLOT'
c     WRITE(88,*) 'ITER,1,1'
c     WRITE(88,*) 'AFWRITE'
c     WRITE(88,*) 'FINISH'
```

```
c     WRITE(88,*) '/INPUT,27'
c     WRITE(88,*) 'FINISH'

C.....MATERIAL DATA INPUT
3     DO 304 N=1,NUMMAT
      READ(5,*) MA,IEL
      IF(DB_FLAG) WRITE(6,2000) MA,IEL
      IF(SC_FLAG) WRITE(*,2000) MA,IEL
      IF(MA.EQ.0) GO TO 4
      CALL PZERO(D(1,MA),20)
      D(20,MA)=IEL
      CALL ELEMLIB(D(1,MA),UL,URL,XC,XLO,IX,S,P,VL,NDF,NDM,NST,1)
304   CONTINUE
C.....BOUNDARY CONDITIONS INPUT
c1000  FORMAT(10E15.7)
c1100  FORMAT(16(4X,I5))
1000  format(3e15.7)
1100  format(4(4x,i5))

C.....FORMAT FOR MSH.DAT
1088  FORMAT ((('  N,',I5,3(',',E15.7))))
1188  FORMAT ((('  E',8(',',I5))))

1200  format(4x,A1)
2000  FORMAT(/' MATERIAL TYPE ',I4,' ELEMENT TYPE ',I4/)
4     CALL BOUN(ID)
      WRITE(*,*) ' END OF MESH GENERATION'
3000  FORMAT(' **FATAL ERROR** IN MESH GENERATION')
      RETURN
      END
```

Appendix C

Dyntool program tree

```
| MAIN
| | SECNDS[2]
| | | GETDAT?
| | | LEAP_YEAR
| | | GETTIM?
| | PCONTR
| | | SETMEM[3]
| | | MZERO
| | | PZERO[11]
| | | PMESH
| | | | GENVEC
| | | | ELDAT
| | | | PZERO...
| | | | ELEMLIB
| | | | | ELMT16 (not used)
| | | | | | PGAUSS[3]
| | | | | | SHAPE[5]
| | | | | | | SHAP2
| | | | | | PSTRES
| | | | | ELMT26
| | | | | | PGAUSS3[3]
| | | | | | SHP3[3]
| | | | | | PSTRES3
| | | | | | | CUBIC
| | | | | | | | QUADRT
| | | | | | | | | LINCNG
| | | | BOUN
| | | GENVEC...
| | | PROFIL
| | | VALBOUN
| | | PFORM[7]
| | | | PZERO[2]...
| | | | ELEMLIB...
| | | | ADDSTF
| | | | BASBLY[3]
| | | | MODIFY
| | | LDLT
| | | PLOAD
| | | FORBACK[2]
| | | PRTREAC[3]
```

| | | PRTDIS[3]
| | | PLTDIS
| | | CUPDATE

Appendix D

Dyntool flat tool input sample data: 171 nodes , 92 brick elements (flt84.dat)

3-d,depth=100mm,width=9o4mm,elemt 26
msfem
171,92,1,3,3,8
1,1,0,0.0047,0.2
4,0,0,0.15,0.2
5,1,0,0.0047,0.15
8,0,0,0.15,0.15
9,0,0,0,0.1
10,1,0,0.0047,0.1
13,0,0,0.15,0.1
14,0,0,0,0.05
15,1,0,0.0047,0.05
18,0,0,0.15,0.05
19,0,0,0,0
20,1,0,0.0047,0
23,0,0,0.15,0
24,1,0.05,0.0047,0.2
27,0,0.05,0.15,0.2
28,1,0.05,0.0047,0.15
31,0,0.05,0.15,0.15
32,0,0.05,0,0.1
33,1,0.05,0.0047,0.1
36,0,0.05,0.15,0.1
37,0,0.05,0,0.05
38,1,0.05,0.0047,0.05
41,0,0.05,0.15,0.05
42,0,0.05,0,0
43,1,0.05,0.0047,0
46,0,0.05,0.15,0
47,0,0.1,0,0.2
48,1,0.1,0.0047,0.2
51,0,0.1,0.15,0.2
52,0,0.1,0,0.15
53,1,0.1,0.0047,0.15
56,0,0.1,0.15,0.15
57,0,0.1,0,0.1
58,1,0.1,0.0047,0.1
61,0,0.1,0.15,0.1
62,0,0.1,0,0.05
63,1,0.1,0.0047,0.05
66,0,0.1,0.15,0.05

67,0,0.1,0,0
68,1,0.1,0.0047,0
71,0,0.1,0.15,0
72,0,0.2,0,0.2
73,1,0.2,0.0047,0.2
76,0,0.2,0.15,0.2
77,0,0.2,0,0.15
78,1,0.2,0.0047,0.15
81,0,0.2,0.15,0.15
82,0,0.2,0,0.1
83,1,0.2,0.0047,0.1
86,0,0.2,0.15,0.1
87,0,0.2,0,0.05
88,1,0.2,0.0047,0.05
91,0,0.2,0.15,0.05
92,0,0.2,0,0
93,1,0.2,0.0047,0
96,0,0.2,0.15,0
97,0,0.3,0,0.2
98,1,0.3,0.0047,0.2
101,0,0.3,0.15,0.2
102,0,0.3,0,0.15
103,1,0.3,0.0047,0.15
106,0,0.3,0.15,0.15
107,0,0.3,0,0.1
108,1,0.3,0.0047,0.1
111,0,0.3,0.15,0.1
112,0,0.3,0,0.05
113,1,0.3,0.0047,0.05
116,0,0.3,0.15,0.05
117,0,0.3,0,0
118,1,0.3,0.0047,0
121,0,0.3,0.15,0
122,0,0.4,0,0.2
123,1,0.4,0.0047,0.2
126,0,0.4,0.15,0.2
127,0,0.4,0,0.15
128,1,0.4,0.0047,0.15
131,0,0.4,0.15,0.15
132,0,0.4,0,0.1
133,1,0.4,0.0047,0.1
136,0,0.4,0.15,0.1
137,0,0.4,0,0.05
138,1,0.4,0.0047,0.05
141,0,0.4,0.15,0.05

142,0,0.4,0,0
143,1,0.4,0.0047,0
146,0,0.4,0.15,0
147,0,0.5,0,0.2
148,1,0.5,0.0047,0.2
151,0,0.5,0.15,0.2
152,0,0.5,0,0.15
153,1,0.5,0.0047,0.15
156,0,0.5,0.15,0.15
157,0,0.5,0,0.1
158,1,0.5,0.0047,0.1
161,0,0.5,0.15,0.1
162,0,0.5,0,0.05
163,1,0.5,0.0047,0.05
166,0,0.5,0.15,0.05
167,0,0.5,0,0
168,1,0.5,0.0047,0
171,0,0.5,0.15,0
0,0,0,0,0
1,1,1,28,5,1,24,29,6,2,25,0
4,1,1,33,10,5,28,34,11,6,29,0
7,1,1,37,14,9,32,38,15,10,33,0
11,1,1,42,19,14,37,43,20,15,38
15,1,1,53,28,24,48,54,29,25,49
18,1,1,58,33,28,53,59,34,29,54
21,1,1,62,37,32,57,63,38,33,58
25,1,1,67,42,37,62,68,43,38,63
28,0,1,70,45,40,65,71,46,41,66
29,1,1,77,52,47,72,78,53,48,73
33,1,1,82,57,52,77,83,58,53,78
37,1,1,87,62,57,82,88,63,58,83
41,1,1,92,67,62,87,93,68,63,88
44,0,1,95,70,65,90,96,71,66,91
45,1,1,102,77,72,97,103,78,73,98
49,1,1,107,82,77,102,108,83,78,103
53,1,1,112,87,82,107,113,88,83,108
57,1,1,117,92,87,112,118,93,88,113
61,1,1,127,102,97,122,128,103,98,123
65,1,1,132,107,102,127,133,108,103,128
69,1,1,137,112,107,132,138,113,108,133
73,1,1,142,117,112,137,143,118,113,138
77,1,1,152,127,122,147,153,128,123,148
81,1,1,157,132,127,152,158,133,128,153
85,1,1,162,137,132,157,163,138,133,158
89,1,1,167,142,137,162,168,143,138,163

92,0,1,170,145,140,165,171,146,141,166
1,26
24.54,0,0.4287,1.32,2,1,6.7,39.3,0.7,2.00,0.0005,1.1
0,0,0,0,0
1,0,1,1,0
5,0,1,1,0
10,0,1,1,0
24,0,0,1,0
28,0,0,1,0
33,0,0,1,0
48,5,-1,0,0
58,0,1,0,0
47,5,-1,-1,0
57,0,1,1,0
9,5,-1,-1,0
19,0,1,1,1
15,0,1,0,0
20,0,1,0,1
2,1,-1,0,0
4,0,1,1,0
6,1,-1,0,0
8,0,1,1,0
11,5,-1,0,0
21,0,1,0,1
12,5,-1,0,0
22,0,1,0,1
13,5,-1,-1,0
23,0,1,1,1
32,5,0,-1,0
42,0,0,1,1
62,0,0,1,0
67,0,0,1,1
72,5,0,-1,0
92,0,0,1,1
97,5,0,-1,0
117,0,0,1,1
122,5,0,-1,0
142,0,0,1,1
147,5,-1,-1,0
167,0,1,1,1
27,0,0,1,0
31,0,0,1,0
36,5,0,-1,0
46,0,0,1,1
51,25,0,-1,0

151,0,1,1,0
56,25,0,-1,0
156,0,1,1,0
61,25,0,-1,0
161,0,1,1,0
66,25,0,-1,0
166,0,1,1,0
71,25,0,-1,-1
171,0,1,1,1
150,5,-1,0,0
170,0,1,0,1
149,5,-1,0,0
169,0,1,0,1
148,5,-1,0,0
168,0,1,0,1
43,1,0,0,-1
45,0,0,0,1
68,1,0,0,-1
70,0,0,0,1
93,1,0,0,-1
95,0,0,0,1
118,1,0,0,-1
120,0,0,0,1
143,1,0,0,-1
145,0,0,0,1
0,0,0,0,0
47,5,0.0001,0,0
57,0,0.0001,0,0
48,5,0.0001,0,0
58,0,0.0001,0,0
0,0,0,0,0
8.4,100,10000,0
dy_flag
no_ge_flag
nodb_flag
ma_flag
UL_FLAG
ST_FLAG

* UL_Flag should be used in order to make the out-of-balance
force vector to be zero *

Appendix E

Monorail hydraulic circuit

DIRECTIONAL CONTROL VALVE
WITH SOLENOID (DENINSON)
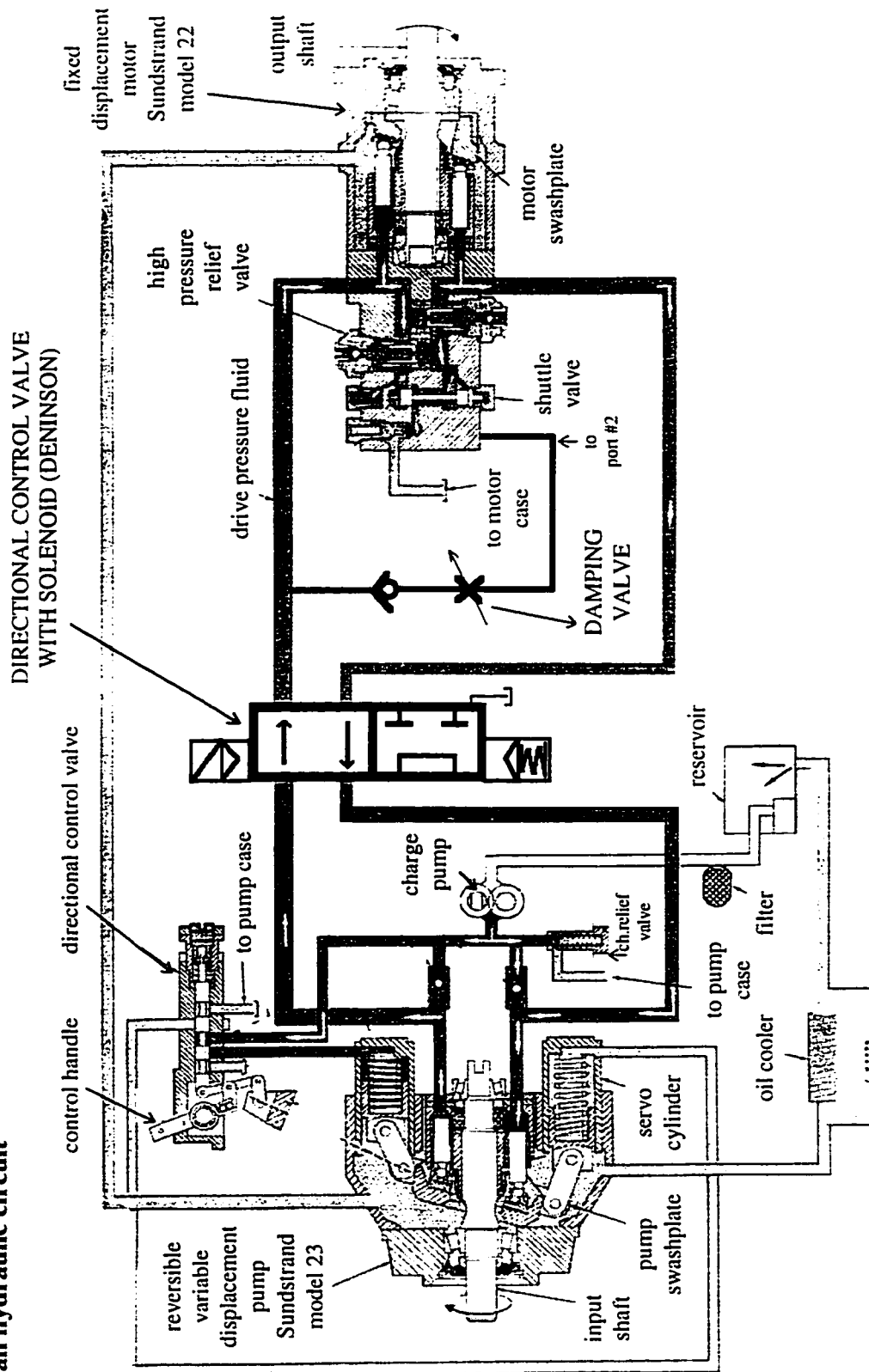
Appendix F

SAS input sample data (fas12.dat) and sample program (fas12.sas)

(fas12.dat)

1	1	1	1	1	112.8443
2	1	1	1	1	75.54804
3	1	1	1	1	78.12469
1	2	1	1	1	86.79357
2	2	1	1	1	82.93132
3	2	1	1	1	89.82632
1	3	1	1	1	89.79578
2	3	1	1	1	74.94781
3	3	1	1	1	92.57247
1	1	2	1	1	302.4878
2	1	2	1	1	243.644
3	1	2	1	1	307.2182
1	2	2	1	1	302.8063
2	2	2	1	1	416.5212
3	2	2	1	1	332.7686
1	3	2	1	1	219.1866
2	3	2	1	1	214.2041
3	3	2	1	1	184.3478
1	1	1	2	1	97.41201
2	1	1	2	1	117.4224
3	1	1	2	1	112.6954
1	2	1	2	1	55.27967
2	2	1	2	1	59.61629
3	2	1	2	1	69.79965
1	3	1	2	1	65.35588
2	3	1	2	1	56.54833
3	3	1	2	1	68.10781
1	1	2	2	1	516.313
2	1	2	2	1	428.5753
3	1	2	2	1	387.8103
1	2	2	2	1	475.3628
2	2	2	2	1	397.4427
3	2	2	2	1	394.7133
1	3	2	2	1	605.5133
2	3	2	2	1	417.6347
3	3	2	2	1	405.0501
1	1	1	1	2	159.5643
2	1	1	1	2	146.7866
3	1	1	1	2	86.12796

1	2	1	1	2	147.5684
2	2	1	1	2	137.3299
3	2	1	1	2	157.3672
1	3	1	1	2	93.15495
2	3	1	1	2	114.888
3	3	1	1	2	124.042
1	1	2	1	2	455.4154
2	1	2	1	2	447.0275
3	1	2	1	2	582.9299
1	2	2	1	2	393.5803
2	2	2	1	2	332.5111
3	2	2	1	2	380.2815
1	3	2	1	2	345.1109
2	3	2	1	2	345.4502
3	3	2	1	2	349.0776
1	1	1	2	2	188.7182
2	1	1	2	2	215.1753
3	1	1	2	2	213.9772
1	2	1	2	2	156.546
2	2	1	2	2	141.7306
3	2	1	2	2	168.9808
1	3	1	2	2	150.1857
2	3	1	2	2	157.8476
3	3	1	2	2	135.3325
1	1	2	2	2	808.9184
2	1	2	2	2	878.361
3	1	2	2	2	700.1122
1	2	2	2	2	802.5185
2	2	2	2	2	710.0367
3	2	2	2	2	724.7673
1	3	2	2	2	585.9609
2	3	2	2	2	551.3072
3	3	2	2	2	473.5855
1	1	1	1	3	170.2468
2	1	1	1	3	179.394
3	1	1	1	3	238.6844
1	2	1	1	3	131.1066
2	2	1	1	3	201.2552
3	2	1	1	3	222.8507
1	3	1	1	3	154.0701
2	3	1	1	3	161.1639
3	3	1	1	3	180.6284
1	1	2	1	3	600.3785
2	1	2	1	3	684.3849
3	1	2	1	3	803.6665

1	2	2	1	3	764.1842
2	2	2	1	3	539.207
3	2	2	1	3	603.3104
1	3	2	1	3	540.3384
2	3	2	1	3	458.0001
3	3	2	1	3	385.7683
1	1	1	2	3	310.9212
2	1	1	2	3	278.9322
3	1	1	2	3	313.6726
1	2	1	2	3	292.4151
2	2	1	2	3	276.0797
3	2	1	2	3	297.6855
1	3	1	2	3	210.1539
2	3	1	2	3	173.0109
3	3	1	2	3	201.1526
1	1	2	2	3	1063.546
2	1	2	2	3	1290.739
3	1	2	2	3	1044.293
1	2	2	2	3	832.1966
2	2	2	2	3	1116.344
3	2	2	2	3	868.9687
1	3	2	2	3	716.2232
2	3	2	2	3	756.3283
3	3	2	2	3	655.84

(fas12.sas)

```
title 'effect of R T D B S on draft F';
option ls=78;
data;
infile 'fas12.dat';
input R T D B S F;
proc glm;
class R T D B S;
model F = T D T*D B(D) T*B(D) S T*S D*S T*D*S S*B(D) T*S*B(D);
run;
```

Appendix G

Steady state draft vs. speed data shown on Figure 5.1

Time (s)	Speed (m/s)	Draft (N)
1.005	5.3	-432
1.011	5.3	-47
1.017	5.3	20
1.022	5.3	3
1.028	5.3	33
1.034	5.3	58
1.039	5.3	-168
1.045	5.3	363
1.051	5.3	-723
1.057	5.4	74
1.062	5.3	-151
1.068	5.3	-88
1.074	5.3	70
1.079	5.4	188
1.085	5.3	-219
1.091	5.3	330
1.097	5.3	-18
1.102	5.4	-302
1.108	5.4	-39
1.114	5.3	-126
1.119	5.4	397
1.125	5.4	-577
1.131	5.3	116
1.136	5.3	-118
1.142	5.4	180
1.148	5.3	-9
1.154	5.4	383
1.159	5.4	-401
1.165	5.4	-5
1.171	5.4	12
1.176	5.4	-101
1.182	5.4	-43
1.188	5.3	37
1.194	5.4	-59
1.199	5.4	619
1.205	5.4	3
1.211	5.4	-93
1.216	5.4	191
1.222	5.5	29
1.228	5.3	-59
1.234	5.4	58
1.239	5.4	-323
1.245	5.4	16

1.251	5.4	154
1.256	5.4	-18
1.262	5.4	-17
1.268	5.5	91
1.274	5.4	-134
1.279	5.4	387
1.285	5.4	-130
1.291	5.4	-1

average	5.4 m/s	-12 N
stdev	0.04 m/s	239 N